“Structure, tectonic processes and deformation of the South Aegean Sea”

Konstantina Tsampouraki-Kraounaki

The Emigrants of William McTaggart (1883–9)

Doctoral Dissertation 2021

Geology Department, University of Patras

"Structure, tectonic processes and deformation of the South Aegean Sea © 2021 by Konstantina tsampouraki-Kraounaki is licensed under CC BY-NC 4.0. To view a copy of this license, visit http://creativecommons.org/licenses/by-nc/4.0/

Advisory committee:

Dimitris Sakellariou (Supervisor): Research Director, Hellenic Centre for Marine Research, Athens, Greece

George Papatheodorou: Professor, Department of Geology, University of Patras, Greece

Jean Mascle: Emeritus Professor, Université de Nice Sophia-Antipolis, CNRS, Observatoire de la Côte d'Azur, France

Examining Committee:

D. Sakellariou (Supervisor): Research Director, Hellenic Centre for Marine Research, Athens, Greece

G. Papatheodorou: Professor, Department of Geology, University of Patras, Greece

G. Rousakis: Research Director, Hellenic Centre for Marine Research, Athens, Greece

P. Xypolias: Professor, Department of Geology, University of Patras, Greece

M. Geraga: Professor, Department of Geology, University of Patras, Greece

S. Kokkalas: Associate Professor, Department of Geology, University of Patras, Greece

A. Chatzipetros: Associate Professor, Department of Geology, Aristotle University of Thessaloniki, Greece

"The approval of the present thesis by the Examining Committee and the Department does not
presuppose the acceptance of the author's views."
(**Law 5343/1932, Article 202**)

Στον Οδυσσέα, στον Σέργιο και
σε όλα εκείνα τα παιδιά με τα
λαμπερά μάτια που αναζητούν
αλήθειες και ονειρεύονται με
πολύχρωμα πινέλα

Acknowledgments

Δε μου αρέσουν τα σοβαρά λόγια. Ποτέ δε μου άρεσαν. Καταλαβαίνω πως ως υποψήφιοι διδάκτορες οφείλουμε να ακολουθήσουμε κάποιες νόρμες και κανόνες ενός ορισμένου συγγραφικού πλαισίου. Προσπάθησα να το εφαρμόσω στο κυρίως κείμενο της διδακτορικής μου διατριβής. Αν μη τι άλλο οφείλει να είναι ένα ολοκληρωμένο κείμενο λεπτομερούς αποτύπωσης του ερευνητικού μας έργου. Μια εργασία αξιολογείται κυρίως εκ των αποτελεσμάτων της, της δομής της, της καινοτομίας της και της επιστημονικής της επάρκειας. Όμως η ολοκλήρωση της είναι μία ανθρώπινη συνθήκη, που φέρει συναισθήματα, σκέψεις, απογοητεύσεις και μικρές νίκες. Σα να χτίζεις ένα σπίτι από την αρχή ένα πράγμα. Θέλεις να είναι κατασκευαστικά άρτιο, να μη σου πέσει στο κεφάλι, θέλεις να χρησιμοποιήσεις καινούριες τεχνολογίες, καινούρια υλικά, όμως στο τέλος τέλος αυτό που θέλεις είναι να έχει ένα όμορφο κηπάκο με μια ανθισμένη γαρδένια να σου αρωματίζει την ατμόσφαιρά. Για αυτό στις ευχαριστίες θα ήθελα να ακολουθήσω ένα λίγο διαφορετικό δρόμο. Πιο δικό μου. Ξεδιπλώνοντας σταδιακά ένα ταξίδι στιγμών που με έφτασαν στο σήμερα. Ένα ταξίδι αναμνήσεων και ανθρωπων που ξεκινά τον Μαρτη του 2015 .

Μάρτης 2015. Ή μήπως να ήταν λίγο πιο νωρίς; Επίσημα πάντως ήταν σίγουρα πιο μετά. Δεν έχει όμως και μεγάλη σημασία για την ιστορία μας. Για μένα όλα τότε ξεκινούν. Σε ένα ταξίδι Παρίσι-Μαδρίτη. Τότε ήταν η αρχή. Ως επίσημα πλέον PhD candidate έκανα το πρώτο μου επαγγελματικό ταξίδι. Στην πραγματικότητα δεν πιστεύω πως είχα και πολλά να προσφέρω σε εκείνο το ταξίδι σίγουρα όμως είχα πολλά να μάθω. Ένα βαλιτσάκι γεμάτο κούπες και τσουρέκια και ένα μυαλουδάκι γεμάτο απορίες ήταν η αρχή. Και ήταν ο τρόπος του κύριου Δημήτρη να μου πει καλή αρχή. Συγγνώμη Δημήτρη για την προσφώνηση ¨κύριε¨, ξέρω πως δεν είναι η αγαπημένη σου. Όμως ξέρεις σε μια σωστή ιστορική αναδρομή δε θα μπορούσα να το παραλείψω. Οπότε κύριε Δημήτρη Σακελλαρίου , υπεύθυνε, supervisor, ψυχαναλυτή και φίλε πρώτα από όλους θέλω να ευχαριστήσω εσένα. Θέλω να σε ευχαριστήσω για όλα και για ακόμη περισσότερα. Θέλω να σε ευχαριστήσω που με δέχτηκες. Δεν είμαι και ο πιο εύκολος άνθρωπος του κόσμου άλλωστε. Θέλω να σε ευχαριστήσω που πίστεψες πως μπορώ να τα καταφέρω. Ακόμη και όλες εκείνες τις στιγμές που εγώ δεν το πίστευα. Θέλω να σε ευχαριστήσω για όσα μου δίδαξες και συνεχίζεις να μου διδάσκεις. Θέλω να σε ευχαριστήσω για εκείνα τα τεκτονικά σκαριφήματα σε χαρτοπετσέτες και τραπεζομάντηλα. Θέλω να σε ευχαριστήσω για εκείνες τις διαθέσιμες ρακές σε κάθε στιγμή κρίσης. Θέλω να σε ευχαριστήσω για εκείνες τις άτυπες διαφωνίες μας. Δεν ξέρω αν κάτι σου άφησαν, εμένα όμως ακόμη κ αυτές με έκαναν καλύτερη. Θέλω να σε ευχαριστήσω για την ευγένεια σου. Έχεις έναν μοναδικό τρόπο να με παροτρύνεις να κάνω παρουσιάσεις που ξέρεις πόσο ντρέπομαι και πόσο δυσκολεύομαι να κάνω. Θέλω να σε ευχαριστήσω για όλα εκείνα τα ταξίδια και για όλες εκείνες τις απαντήσεις σε κάθε είδους απορία. Θέλω να σε ευχαριστήσω γιατί μου έμαθες πως η ενασχόληση με την έρευνα δεν είναι μια απλή εργασιακή σχέση αλλά κάποιου είδους χόμπι και εμείς γουστάρουμε να είμαστε χομπίστες.

Θα μπορούσα να γράψω πολλά ακόμη, αλλά δε χρειάζεται θαρρώ. Σε ευχαριστώ για το εδώ που είμαι σήμερα.

Ένα σπιτάκι για να χτιστεί και να αντέξει στο χρόνο, χρειάζεται θεμέλια. Αν δεν έχεις μια γερή βάση να σε κρατάει το οικοδόμημα σου θα πέσει. Μπορεί να μη φαίνονται, μπορεί να είναι κρυμμένα, χωμένα βαθιά στη λάσπη και στο χώμα, μπορεί να σκουριάζουν, μπορεί να πιάνουν υγρασίες, αλλά χωρίς αυτά το σπιτάκι σου θα πέσει. Αυτά το κρατάνε να αντέξει. Θέλω λοιπόν εδώ να ευχαριστήσω ένα από τα πιο σημαντικά κεφάλαια της ζωής μου. Τον Στέφανο. Χωρίς εκείνον και τη βοήθεια του, αυτή η εργασία δε θα είχε ολοκληρωθεί ποτέ. Στέφανε σε ευχαριστώ για όλα. Σε ευχαριστώ γιατί αν δεν ήσουν εσύ εγώ δε θα ήμουν εγώ. Σε ευχαριστώ για τότε που ήθελα να εγκαταλείψω τη γεωλογία και να κάνω σχέδιο και εσύ το δέχτηκες ακόμη και αν ήξερες πως θα πεινάσουμε. Σε ευχαριστώ που με έσπρωξες να κάνω το μεταπτυχιακό. Σε ευχαριστώ για όλα εκείνα που δεν έκανες για να κάνω εγώ αυτά που κάνω σήμερα. Σε ευχαριστώ που θυσίασες τις δικές σου ευκαιρίες για να ζω με άνεση εγώ τις δικές μου. Σε ευχαριστώ για το νησί μας που ελπίζω να μην ξέχασες. Σε ευχαριστώ για εκείνη την καλύβα που προσπάθησες να μου φτιάξεις. Σε ευχαριστώ για όλες εκείνες τις γκρι μέρες που στέκεσαι πλάι μου. Σε ευχαριστώ που μου φωνάζεις όταν εγώ τα παρατάω. Σε ευχαριστώ για τις αξίες σου. Σε ευχαριστώ για τα δυο ταλιμπανάκια μας. Σε ευχαριστώ για όλα εκείνα τα «κάντε ησυχία, η μαμά δουλεύει». Σε ευχαριστώ που ξενυχτας δουλεύοντας τη νύχτα για να μπορώ με άνεση εγώ να δουλεύω τη μέρα. Σε ευχαριστώ για όλα εκείνα τα πρωινά, μεσημεριανά, τοστακια και πιτουλες που μου έφτιαξες. Σε ευχαριστώ για όλες εκείνες τις φορές που ήθελα να τα παρατήσω και δε με άφησες. Σε ευχαριστώ που πιστεύεις σε μένα ακόμη και όταν κανείς δεν το κάνει. Σε ευχαριστώ που είσαι ακόμη εδώ.

Στη συνέχεια θα ήθελα να ευχαριστήσω τα δύο αγοράκια μου, Οδυσσέα και Σέργιο. Για όλη εκείνη την υπομονή που δείχνουν στη μη φυσιολογική μαμά τους. Για όλες εκείνες τις φορές που θυσίασαν το παιχνίδι τους και την ανεμελιά τους για να μπορέσω εγώ να συγκεντρωθώ. Τους ευχαριστώ για εκείνη την απεριόριστη αγάπη. Τους ευχαριστώ για την ελπίδα που νιώθω κοιτάζοντας τους, πως αυτός ο κόσμος μπορεί και να αλλάξει τελικά. Τους ευχαριστώ για εκείνες τις ομαδικές αγκαλιές και εκείνα τα ρουφηχτά καθημερινά μας φιλιά. Όμως θέλω να τους ζητήσω και συγγνώμη γιατί άφησα τη ρουτίνα της καθημερινότητας μου να επιδράσει στις ευχάριστες στιγμές μας. Για όλα εκείνα τα όχι που έχουν ακούσει. Για τις μέρες που δεν παίξαμε και δε γελάσαμε όσο τους άξιζε γιατί εγώ έπρεπε να δουλέψω. Για τις διακοπές που δεν πήγαμε. Για εκείνες τις τρομακτικές βιντεοκλήσεις τις φορές που ήμουν στο πλοίο και χανόταν το σήμα και νόμιζαν πως η μαμά βούλιαξε. Δε βουλιάζουν έτσι εύκολα τα πλοία βρε τενεκέδες. Και να ξέρετε, είμαι πολύ τυχερή που με διαλέξατε για μαμά σας.

Ένα μεγάλο ευχαριστώ οφείλω στους γονείς μου Νότα και Πέτρο. Εσείς με μάθατε να είμαι αυτή που είμαι και να μην τα παρατάω στα δύσκολα. Σε ευχαριστώ μπαμπά που με έκανες να αγαπήσω τη θάλασσα. Δεν ήξερα τότε, σε εκείνες μας τις βουτιές με τις μάσκες πως έμπαινε ένας σπόρος έτοιμος να ανθίσει πολύ αργότερα. Σε ευχαριστώ γιατί όταν πίστεψα πως απέτυχα εσύ μου έμαθες πως μια σημερινή αποτυχημένη στιγμή μπορεί να είναι η αρχή για κάτι σπουδαίο αύριο. Σε ευχαριστώ μαμά που στερήθηκες τον χρόνο σου για να μεγαλώνεις τα δικά μου παιδιά όσο εγώ δουλεύω. Σε ευχαριστώ για εκείνα τα καθημερινά τηλεφωνήματα. Και εκείνους τους καφέδες όταν με πιάνουν οι μοναξιές μου.

Σας ευχαριστώ και τους δυο που με μάθατε να παλεύω κόντρα στο ρεύμα για να γίνει ο κόσμος μας καλύτερος. Φυσικά θέλω να ευχαριστήσω και τον αδερφό μου Άγγελο, τη Μαρία και τον μικρούλη Ορφέα για όλη εκείνη την υπομονή που δείχνουν καθημερινά.

Ευχαριστώ πάρα πολύ και τους γονείς τους Στέφανου, Γιώτα και Τάκη που με συντρόφευσαν από την αρχή σε τούτο το ταξίδι. Σύντροφε μου Τάκη σε ευχαριστώ για το ενδιαφέρον που δείχνεις πάντα για αυτό που κάνω. Ξέρεις, μου είναι δύσκολα τα λόγια, συνήθως με κερδίζουν οι ντροπές μου, όμως μαζί σου νιώθω πως οι σιωπές μας μεταφράζονται σε λέξεις. Μαμά του Στέφανου, Γιώτα, πόσο δύσκολο μου είναι να μιλήσω στον ενικό δε φαντάζεσαι. Σε ευχαριστώ για όλα. Σε ευχαριστώ για την αγάπη που δείχνεις για τα παιδάκια μου. Σε ευχαριστώ για όλες εκείνες τις εβδομάδες που χρειάζεται να έρχεσαι σπίτι μας για να τα προσέχεις. Συγγνώμη που δε νιώθεις τόσο άνετα εκεί, ελπίζω να αλλάξει αυτό. Και κυρίως σε ευχαριστώ που είσαι τόσο σπουδαία μαμά και με κάνεις να θέλω να γίνομαι καλύτερη.

Θέλω φυσικά να ευχαριστήσω και τα παιδιά που δουλεύουμε μαζί. Σύντροφοι στους ωκεανογραφικούς πλόες και στα πρωινά τσιγάρα. Κική μου σε ευχαριστώ για εκείνες τις ατελείωτες συζητήσεις μας. Σε ευχαριστώ για εκείνη την ώθηση που μου δίνεις όταν εγώ απογοητεύομαι. Για εκείνα τα κοκτέιλ στον Στυλίτη. Για την παρέα στο μεσημεριανό, μα κυρίως για τη φιλία σου. Ισίδωρε, σε ευχαριστώ που μου φτιάχνεις τη διάθεση. Σε ευχαριστώ για τις κόντρες μας, σε ευχαριστώ για τα γέλια μας και φυσικά σε ευχαριστώ που αποφάσισες να κάνεις το εμβόλιο. Γιάννη, παρεακι μου στα πηγαινελα, σε ευχαριστώ που από τα πρώτα μου βήματα στο χώρο ένιωσα πως υπάρχει ένας άνθρωπος που μπορώ να εμπιστευτώ και να μιλήσω. Σε ευχαριστώ για όλες εκείνες τις συμβουλές σου και για την υπομονή σου να ακούσεις τους προβληματισμούς μου. Σε ευχαριστώ για τις «ήσυχες» διαφωνίες μας και φυσικά σε ευχαριστώ γιατί η εμπειρία της ηλικίας σου με έκανε σοφότερη. Φρατζέσκα σε ευχαριστώ γιατί αν και η γνωριμία μας είναι πρόσφατη, έδειξες από την αρχή την πρόθεση σου να με βοηθήσεις και να συζητήσεις τους προβληματισμούς μου. Μαργαρίτα μου σε ευχαριστώ για όλη τη θετική σου ενεργεια και για όλες τις χρήσιμες συμβουλές σου.

Πολύ σημαντικό ρόλο σε αυτή μου την προσπάθεια, ακόμη και αν η ίδια δεν το ξέρει, έχει παίξει η φίλη μου Λύδία. Λυδιάκι μου, μπορεί να μην έχεις ίδέα τι ακριβώς κάνω, μα πάντα ήσουν εδώ. Σε ολές εκείνες τις απογοητεύσεις και τα άγχη που μπορεί να συνόδευαν αυτό το ταξίδι, σε ένιωθα πάντα κοντά μου. Για εκείνα τα κρίσιμα τηλεφωνήματα, που ήθελα απλά να σου πω πως θα τα παρατήσω, είχες τον τρόπο σου μέσα από τις συζητήσεις μας να με πείθεις να μην το κάνω. Και να μη φοβάμαι. Και ας μην το ξέρεις.

Ευχαριστώ επίσης τη φίλη μου Βιβή. Το αδερφάκι μου. Για όλες εκείνες τις καταιγίδες που τις αντιμετωπίζουμε παρέα. Για εκείνα τα τηλεφωνήματα που δε χωρούν μέσα τους καμία απόσταση.

Φυσικά θέλω να ευχαριστήσω τον Καθηγητή Γιώργο Παπαθεοδώρου, καθηγητή μου στο προπτυχιακό και μέλος της τριμελούς συμβουλευτικής επιτροπής του διδακτορικού μου. Κύριε Παπαθεοδώρου σας ευχαριστώ που με τη μεταδοτικότητα σας με κάνατε, πολλά χρόνια πριν να επιλέξω τη θαλάσσια γεωλογία και για όλες τις χρήσιμες συμβουλές σας στο πέρασμα των χρόνων.

Θα ήθελα να ευχαριστήσω τον Jean Mascle, που αν και με γνώριζε πολύ λίγο δέχτηκε με όλη του τη χαρά να είναι μέλος της τριμελούς μου. Κυρίως όμως τον ευχαριστώ γιατί η δουλειά του και το συγγραφικό του έργο, αποτέλεσε πηγή έμπνευσης για την ολοκλήρωση αυτής της εργασίας.

Ευχαριστώ επίσης όλα τα μέλη της επταμελούς εξεταστικής επιτροπης. Αρχικά θα ήθελα να ευχαριστήσω τον κύριο Γρηγόρη Ρουσάκη που αν δεν ήταν εκείνος μπορεί να μην είχα έρθει ποτέ σε επαφή με την ομάδα του ΕΛΚΕΘΕ. Σε ευχαριστώ για εκείνο το πρώτο μου ωκεανογραφικό ταξίδι στο Ιόνιο. Άλλωστε τότε δεν ξεκίνησαν όλα; Σε ευχαριστώ επίσης για τη στήριξη σου όλα αυτά τα χρόνια στο γραφείο και στα ταξίδια μας. Ευχαριστώ επίσης τους Π. Ξυπολιά και Σ. Κοκκάλα, ήταν οι πρώτοι που ως καθηγητές μου στο προπτυχιακό, με ενέπνευσαν να ασχοληθώ με την τεκτονική. Σας ευχαριστώ επίσης για τις όμορφες στιγμές που είχαμε περάσει στη γεωλογική χαρτογράφηση στην Κάρυστο. Επίσης κύριε Ξυπολιά, αν και φαντάζομαι δε θα το θυμάστε, θα ήθελα να σας ευχαριστήσω γιατι σε μια παρουσίαση της Επιτροπής Τεκτονικής της Ελληνικής Γεωλογικής Εταιρείας, μου εξηγήσατε, μια ερώτηση που είχα δεχτεί στα αγγλικά και την οποία δεν είχα καταλάβει, με αποτέλεσμα να γλιτώσω την συναισθηματική κατάρρευση μπροστά σε τόσο κόσμο. Ευχαριστώ την Μ. Γεραγά, όχι μόνο γιατί συμμέτέχει στην εξεταστική επιτροπή, αλλά και γιατί θυμάμαι σε μία εξέταση τότε στο μάθημα ¨Βιοδείκτες¨ αν το λέω καλά, που ήμουν έτοιμη να τα παρατήσω, με προέτρεψε να μην το κάνω. Τέλος, θα ήθελα να ευχαριστήσω τον κύριο Α. Χατζηπέτρο με το οποίο αν και δε γνωριζόμαστε προσωπικά, έχει αποτελέσει πολλές φορές πηγή έμπνευσης και συμβουλευτικής καθοδήγησης μέσα από το επιστημονικό του έργο. Δυσκολεύομαι να μη διατηρήσω ένα πιο αυστηρό επίπεδο γραφής στις ευχαριστίες που αφορούν την εξεταστική επιτροπή. Θα ήθελα όμως να τονίσω, πως τώρα, καθώς σκαλίζω το μυαλό μου συνειδητοποιώ, πως ο καθένας από εσάς, λίγο περισσότερο ή λίγο λιγότερο, δεν έχει σημασία, αφήσατε ένα προσωπικό στίγμα και μια ομορφη αναμνηση στην μέχρι τώρα πορεία μου. Η γεωλογία, είναι μια πανέμορφη επιστήμη, πλήρως υποτιμημένη στη χώρα μας. Ως δάσκαλοι έχετε αναλάβει το μεγάλο βάρος να πείσετε τους νέους ανθρώπους, να μην την εγκαταλείψουν, παρά την εργασιακή αβεβαιότητα που τη συντροφεύει. Με εμένα τα καταφέρατε. Οπότε έυχομαι και ελπίζω, να συνεχίσετε να μας καθοδηγείται και να μας εμπνέετε. Σας ευχαριστώ πολύ για όλα.

Ευχαριστώ επίσης τον Γιάννη Παναγιωτόπουλο για τις αμέτρητες συμβουλές του και για τις ευχάριστες στιγμές που μας παρέχει. Ευχαριστώ και όλο το πλήρωμα του ΑΙΓΑΙΟ που χωρίς εκείνους κανένα ταξίδι δεν θα μπορούσε να είχε συμβεί. Κυρίως όμως τον καπετάνιο του Θοδωρή και τον Γιάννη Κ. Καπετάνιε σε ευχαριστώ για όλες εκείνες τις όμορφες ιστορίες που συντροφεύουν τα ταξίδια μας. Γιάννη σε ευχαριστώ για τις πολύτιμες συμβουλές σου και για τις υπέροχες ρακές σου.

Είναι πολύ δύσκολο να χωρέσεις σε λέξεις τα ευχαριστώ που χρωστάς για ένα ταξίδι που διήρκησε τουλάχιστον 6 χρόνια. Σας ευχαριστω πολύ όλους που σταθήκατε πλάι μου. Στους περίεργους καιρούς που ζούμε, μακάρι να μπορέσουμε ο καθένας με τον δικό του ιδιαίτερο τρόπο, να συνεχίσει να αγωνίζεται, να ελπίζει, να ονειρεύεται και να διεκδικεί ένα καλύτερο μέλλον.

Funding

This work has been made possible because of the funding I have receiced throughout the implementation of this Thesis from the Institute of Oceanography of the Hellenic Centre for Marine Research.

Abstract

The PhD thesis explores the long-term deformation and active tectonic mechanisms that contributed to the geological evolution and the formation of the complex relief of the South Aegean Sea. Despite the geological surveys that have been conducted on the Aegean, the current state of knowledge is still in its infancy. Although it is widely accepted that the geotectonic evolution of the Aegean microplate is dominated by extension in a back-arc setting, recent geological, seismological and geodetic studies have shown that overall extension may evolve in combination with transpression or transtention. This dissertation summarizes the preexisting literature and the main deformation models that have been proposed for the Aegean and through the presentation of new bathymetric and seismic data aims to improve our understanding of the tectonic processes and deformation prevailing on the South Aegean Sea. In order to develop a geodynamic model that will explain the kinematic processes and deformation mechanisms that took place in the area, the main axis of the dissertation is structured by three main research papers, the results of which provide up-to-date information about the geodynamic evolution of the South Aegean.

Table of Contents

Acknowledgments 5

Funding 9

Abstract 10

Chapter description 15

Chapter 1: Introduction 17

1.1 Aegean domain 17

1.2 South Aegean Sea 23

Chapter 2: Aim-Objectives 26

Chapter 3: Methodology 28

Chapter 4: Main study 31

4.1 Seismic stratigraphy and geodynamic evolution of Christiana Basin, South Aegean Arc 31

4.1.1. Abstract *31*

4.1.2. Introduction *32*

4.1.3. Geological setting *34*

4.1.4. Materials and methods *35*

4.1.5. Results *37*

4.1.5.1. Seismic stratigraphy *37*

4.1.5.2. Basin's structure *44*

4.1.5.3. Volcanic deposits in Christiana Basin sedimentary archive *47*

4.1.6. Discussion *50*

4.1.6.1. Basin's stratigraphy *50*

4.1.6.2. Implications for the geodynamic evolution of the South Aegean Arc *52*

4.1.7. Conclusions *55*

Acknowledgements *57*

References *57*

4.2. The Santorini-Amorgos Shear Zone: Evidence for Dextral Transtension in the South Aegean Back-Arc Region, Greece 62

4.2.1 Abstract *62*

4.2.2 Introduction *62*

4.2.3 Geological setting *66*

4.2.3.1 Regional Geological Setting *66*

4.2.3.2 Seismostratigraphy of the Area *67*

4.2.3.3 Tectonic Setting *69*

4.2.3.4 The 1956 Amorgos Earthquake *72*

4.2.4 Materials and Methods *72*

4.2.5 Results *74*

4.2.5.1 Bathymetry-Geomorphology *74*

4.2.5.2 Seismic Stratigraphy: Basins *77*

4.2.5.2.1 Anafi Basin (AnB) 82

4.2.5.2.2 Anydros Basin (AdB) 83

4.2.5.2.3 Amorgos North (ANB) and Amorgos South (ASB) Basins 86

4.2.5.2.4 Astypalea North Basin (AsNB) 87

4.2.5.2.5 Astypalea South Basin (AsSB) 88

4.2.5.2.6 Kinairos Basin (KB) 88

4.2.5.3 Seismic Stratigraphy: Ridges *89*

4.2.5.3.1 Anydros Ridge (AdRa, AdRb) 89

4.2.5.3.2 Astypalea Ridge (AsRa, AsRb) 90

4.2.5.3.3 Akrotiri Ridge (AkR) 90

4.2.5.3.4 Anafi Ridge (AnR) 91

4.2.5.4 Faulting *91*

4.2.5.4.1 Ios Fault Zone (IFZ) and Amorgos South Relay Fault (ASRF) 92

4.2.5.4.2 Akrotiri Fault (AkdF) and Anydros Ridge North Fault Zone (AdRNFZ) 94

4.2.5.4.3 Perissa Fault (PF) and Anydros Ridge South Fault Zone (AdRSFZ) 95

4.2.5.4.4 Amorgos Fault (AF) and Amorgos North Relay Fault (ANRF) 96

4.2.5.4.5 Kinairos Fault (KF) 97

4.2.5.4.6 Anafi Fault Zone (AnFZ) and Astypalea Faulted Margin 98

4.2.5.4.7 Astypalea Ridge Fault Zone (AsRFZ) 98

4.2.5.4.8 Astypalea South Basin Faults 99

4.2.6 Discussion and Synthesis *100*

4.2.6.1 Basin evolution *100*

4.2.6.2 Deformation and Kinematics *105*

4.2.6.3 The Amorgos 1956 Earthquake *108*

4.2.6.4 Implications for the Plio-Quaternary Evolution of the South Aegean bak-arc *109*

4.2.7 Conclusions *112*

Acknowledgments 113

References 114

4.3. Plio-Quaternary extension and strike-slip tectonics in the Aegean 123

4.3.1 Abstract *123*

4.3.2. Introduction *123*

4.3.3. North Aegean Sea / North Aegean Trough (NAT) / North Anatolian Fault (NAF) *129*

4.3.3.1. Seafloor Morphology - Sedimentary Basins - Fault Network *129*

4.3.3.2 Seismological and Geodetic Constraints *134*

4.3.4. South Aegean Sea/Volcanic Arc *137*

4.3.4.1 Seafloor Morphology—Sedimentary Basins—Fault Network *137*

4.3.4.2. Seismological and Geodetic Constrains *141*

4.3.5. The Hellenic Arc and Trench *143*

4.3.4.1. Seafloor Morphology—Fault Network *143*

4.3.4.2 Seismological and Geodetic Constraints *146*

4.3.6. New Offshore Morphology and Fault Network *148*

4.3.7. Geodynamic Synthesis and Open Questions *155*

References 162

5. Conclusions-Discussion 174

6. Strategy Plan for Future Research 180

References 183

Chapter description

The present thesis is developed in 6 main chapters. **Chapter 1** is the introductory chapter. It includes a brief description of the models and hypotheses that have been proposed until now for the kinematic and geodynamic evolution of the Aegean. **Subchapter 1.1** summarizes the results obtained from previous studies for the South Aegean region. **Chapter 2** describes the main objectives of the current study. **Chapter 3** presents the methodology that has been followed for the accomplishment of this dissertation. **Chapter 4** presents the results that emerged in the context of the completion of this dissertation. It is divided into three subchapters each of which is a fully published work in scientific journals. Specifically, **subchapter 4.1** presents the full published study in the journal Marine Geology with the title "Seismic stratigraphy and geodynamic evolution of Christiana Basin, South Aegean Arc" (https://doi.org/10.1016/j.margeo.2018.02.012). This study analyzes the tectonic and volcano-sedimentary processes that have played a dominant role in the geodynamic evolution of Christiana Basin which has been formed at the central part of the Hellenic Volcanic Arc, between the volcanic groups of Milos to the west and Santorini to the east. **Subchapter 4.2** presents the work entitled as "The Santorini-Amorgos Shear Zone: Evidence for Dextral Transtension in the South Aegean Back-Arc Region, Greece", which has been published in the journal Geosciences (https://doi.org/10.3390/geosciences11050216). This study focuses on the offshore area between the islands of Santorini, Amorgos, Kinairos, Anafi and Astypalea named as Santorini-Amorgos Shear Zone (SASZ). Through the presentation of the morphotectonic characteristics which have been developed in the area, this work aims to understand the prevailing geotectonic regime and its relation with the deformation pattern that governs the Aegean domain. **Subchapter 4.3** includes the study entitled as "Plio-Quaternary extension and strike-slip tectonics in the Aegean" which has been published in book Transform Plate Boundaries and Fracture Zones (https://doi.org/10.1016/B978-0-12-812064-4.00014-1). This study provides an overview of the current state of knowledge on the geological structure, active tectonics, and the seismological regime in the Aegean, in order to argue about the different kinematic models proposed so far and to highlight the long-standing questions that remain unanswered. Furthermore, through the re-interpretation of geological, seismological and geodetic data and the presentation of recently acquired bathymetric and seismic data, aims to

understand the configuration principles of the dominant geological regime which evolved on the deformation of the Aegean during Plio-Quaternary. **Chapter 5**, which follows the presentation of the results, presents the synthesis of the main conclusions that emerged from the 3 published works. Finally, **Chapter 6** proposes future research goals, which may provide useful information for the geodynamic evolution of the southern Aegean.

Chapter 1: Introduction

1.1 Aegean domain

The complex geotectonic history of the Aegean aroused the global interest of the scientific community for decades. Its position on the southern edge of the overriding Eurasian plate, above the northward subducting slab of the East Mediterranean crust and the African plate (Figure 1.1), leads to the formation of a particular evolutionary tectonic framework which even today is not fully understood. The great technological progress of the recent years allowed the improvement of our knowledge on the kinematic regime and deformation pattern of the Aegean. The advance of GPS technology, the systematic recording and analysis of seismic events in recent years, and the ever-increasing acquisition of seismic and bathymetric data of the offshore Aegean have greatly contributed to the understanding of the basic kinematic principles governing the Aegean.

The collision of the Arabian and African plate with Eurasia sets the tectonic framework of the broader Aegean ((McKenzie, 1972, 1978; Jackson and McKenzie, 1988; Jackson, 1994; Papazachos and Kiratzi, 1996; Papazachos et al., 1998; McClusky et al., 2000). The determinant for the configuration of the evolution of the Aegean is the motion of two other smaller plates: the Anatolian plate and the Aegean plate. Anatolian and Aegean plates were first described by McKenzie (1972, 1978) and later by Jackson and McKenzie (1988), Papazachos et al. (1998), Papazachos (1999), and McClusky et al. (2000). The idea that the extension occurred in the Aegean domain is the result of the slab retreat and the westward displacement of Anatolia came already on 70's as suggested from the first plate kinematic models (McKenzie 1972, 1978; Le Pichon and Angelier 1979, 1981).

Taymaz et al, 1991 examined the relationship between the westward motion of eastern Turkey and the extension on the Aegean. They concluded that the extension on the Aegean Sea was initiated due to the failure of the western seaboard of Greece and Albania to rotate rapidly enough to accommodate the westward motion of Turkey which led to the change of deformation from strike-slip in the east to normal faulting in the west. Armijo et al (1996) argued that the kinematic model proposed by Taymaz et al (1991) fails to explain the difference in the slip rates between the

Greek and Anatolian sides of the Aegean, particularly the fast slip rate in the Corinth Rift and that doesn't include the N-S observed extension. They proposed a geodynamic model for the evo--lution of the Aegean by taking into account their results arising from their study of the Corinth Rift and as well as the constraints on the timing of major regional event: the geometry and kinematics of the major fault systems such as the North Anatolian Fault, the known palaeomagnetic rotations, and the current overall motion deduced from the geodesy (GPS and

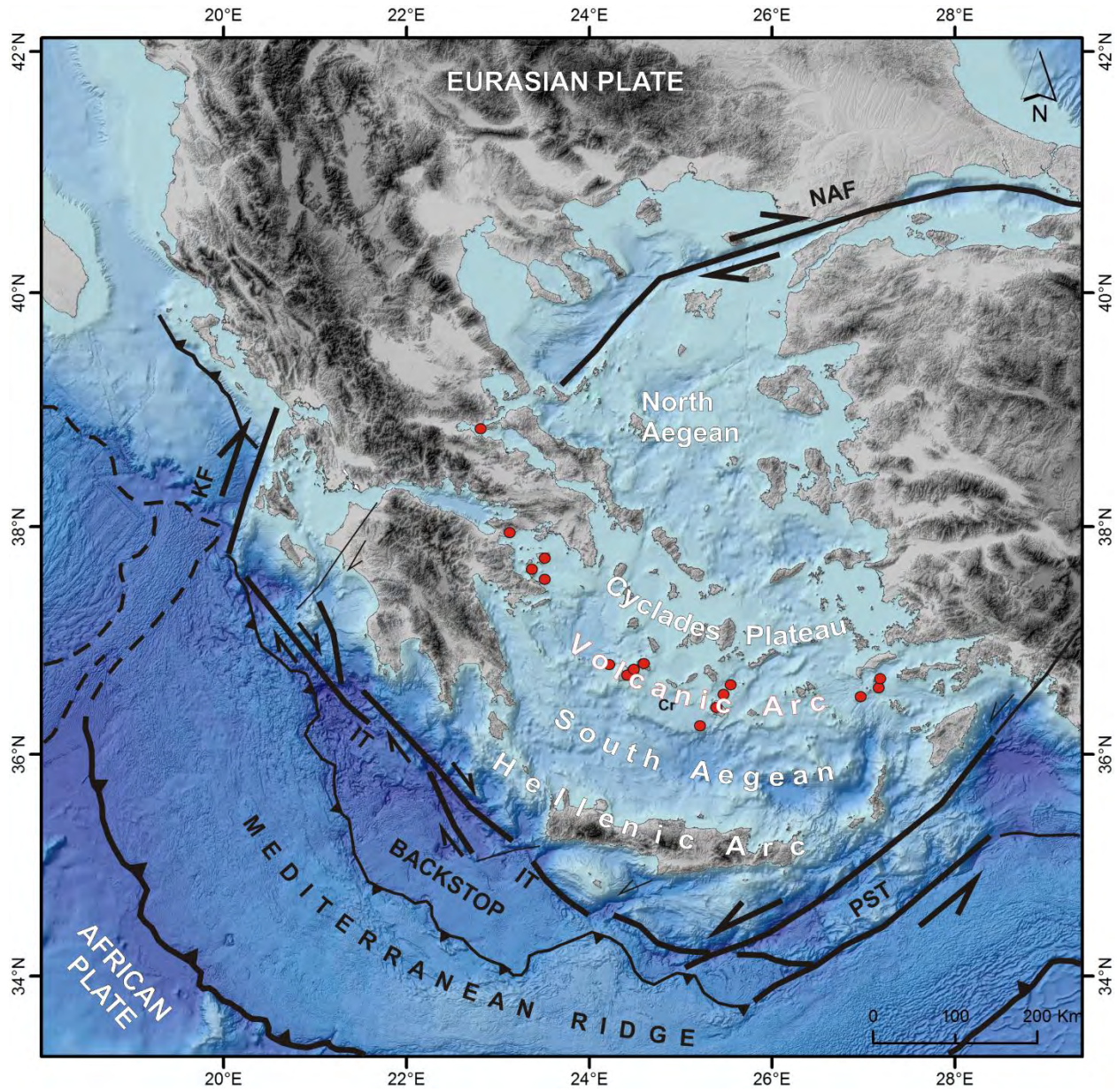

Figure 1.1: Major geodynamic elements of the Aegean. The red circles indicate the volcanoes of the Volcanic Arc. NAF: North Anatolian Fault, IT: Ionian Trench; KF: Kephallinia fault, PST: Pliny and Strabo Trenches (Sakellariou & Tsampouraki-Kraounaki, 2019)

SLR). This model foresees an onset of the regional extension at about 15 Ma or earlier and the propagation of the North Anatolian Fault at about 5 Myr ago. At the same time, the rift zones have opened and extension occurred mainly on the Central Aegean while decreases towards the western and eastern margins producing respectively clockwise and counterclockwise rotation and creating arc parallel extensional zones.

A few years later Gautier et al., (1999) argued that the extension on the Aegean domain is active before the onset of Arabian indentation into Eurasia so the initiation of the extension cannot be the result of the lateral extrusion of the Anatolia. They suggested that the extension has started during the Lower Miocene at ~21 Ma (in some parts of the Aegean such as the Cyclades it could have started earlier), as a result of the gravity spreading of the thickened continental lithosphere on its southern boundary. Then and not earlier than 16 Ma the Arabic indentation has started and the Anatolia escapes westwards along the North Anatolian Fault. As summarized by Brun and Sokoutis (2007), SW-NE extension started in Mid- Eocene times in the Southern Rhodope core complex as well as in surrounding regions of the Rhodope (Burchfiel et al. 2003; Kounov et al. 2004; Bonev et al. 2006).

Jolivet & Brun (2010) presented a summary of the Cenozoic evolution of the Aegean domain that started with the subduction of the northern margin of Tethys at the end of Cretaceous, below the southern margin of Eurasia. Extension resulted from the closure of two oceanic domains of Vardar and Pindos, leading to the stacking of three continental blocks that are from top to base: Rhodopia, Pelagonia and Adria in Cretaceous-Eocene. Considering the Eocene extension of the Rhodope as a part of the history of the Aegean Sea, the extension has started during the Middle Eocene (Brun and Sokoutis, 2010) and accommodated approximately 700 km of trench retreat (Jolivet and Brun, 2010; Jolivet et al., 2013). According to Ring et al. (2010) the earliest possible date for extension is the base of the Miocene. The interaction between back-arc extension and westward displacement of Anatolia explains the Neogene tectonic history of the Aegean. This interaction between two strongly oblique components of boundary displacement started during Middle Miocene (Dewey and Sengör 1979; Sengör et al., 2005; Philippon et al., 2014).

Philippon et al (2014) modelled the interaction between back-arc extension and Anatolia escape and divide the Aegean extension into two main stages. On the first stage, from middle

Eocene to middle Miocene, the extension was only driven by the southward retreat of the Hellenic trench at a rate lower than 1 $cm \cdot y^{-1}$. On the second stage, which lasts the last 13 Ma years, the interaction of trench retreat with Anatolia escape resulted in the southwest direction of trench retreat, with an accelerating rate of up to 3 $cm \cdot y^{-1}$. This discontinuity of the extension in space and time is also confirmed by Brun et al. (2015, 2016). The two-stage scenario is evidenced by a striking difference in the distribution of Paleogene and Neogene sedimentary basins in the Aegean region (Beniest et al, 2016 and references therein).

From the early '70s until today, several studies have tried to explain the geodynamic framework of the Aegean domain (Mc Kenzie, 1978; Dewey and Sengor, 1979; Le Pichon and Angelier, 1979, 1981), combining onshore and offshore data. Already from 1982, Angelier et al., realized that offshore research is necessary to understand the fault system that governs the Aegean. Mascle and Martin (1990) were the first who provide a comprehensive map of the offshore faulting for the entire Aegean. Until then very few systematic marine geological surveys were conducted, thus the state of knowledge is still far from complete. In addition, the tectonic models that have been proposed until then were based mainly on estimates of fault slip rates made on geological time scales and historical seismicity spanning up to 2000 years (Kahle et al., 2000 and references therein). Most of the data on the active continental deformation came mainly from the earthquake seismology and satellite imagery (Billiris et al.,1991). The development of new geodetic techniques made possible the measurement of the crustal motion rates and the estimation of the continental deformation (Billiris et al., 1991; Kahle et al., 2000).

One of the first attempts to compare geodetic and seismic data in Greece was made by Billiris et al., (1991). They re-occupied data from a first-order triangulation network of 1890-1900 to determine the relative displacements within an interval of ninety years and to correlate them with the seismological estimates. Early satellite laser ranging (SLR) observations show that the kinematic field in the eastern Mediterranean and Asia Minor is characterized by the westward motion of Anatolia and the SW motion of the Aegean Sea, with rates ranging between 20 and 35 mm yr^{-1}. (Kahle et al., 2000 and references therein). Reilinger et al. (1997) proposed that the motion of the Anatolia-Aegean region may be best described in terms of a single plate that is deforming internally (N-S extension) in the Aegean region. McClusky et al., (2000) argued for a

two-plate model as has been proposed previously (McKenzie, 1972) on the basis of seismic and neotectonics evidence. They also recognized SSW movement of the southwestern Aegean (south of latitude 39^0) and Peloponnesus at 30±2 mm/yr with low internal deformation(<2mm/yr) and counterclockwise rotation of the southeastern Aegean with increasing velocities towards the trench. They assumed that the latter represents a response to particularly rapid sinking of the downgoing plate below this section of the arc, possibly associated with complex bending/breaking of the subducted plate at the Hellenic-Cyprus arc junction.

Reilinger et al. (2006), mention that the comparison between fault slip rates estimates and geodetic rates, show uncertainties as the geodetic determination likely integrates deformation over a substantially wider area than the single geologic fault estimate. The GPS slip rates are mostly comparable to geologic estimates, and geologically active faults account for present-day block motions and regional deformation. In 2010, Reilinger et al. dissected the reason for the inconsistencies between the geodetic observations of the southern Aegean and Peloponnesus showing SW motion with little internal deformation (McClusky et al., 2000; Kahle et al., 2000; Reilinger et al., 2006), with the geophysical and geological evidence for widespread post-Pliocene extension throughout this area. They concluded that during the last ~1-4 Ma, the deformation of the main structures in the NW Turkey, the N Aegean, and central Greece (including the Marmara Sea pull-apart basin, the Gulfs of Corinth and Evia rift structures, and the right-lateral Kephalinia Fault) as has been developed sequentially from west to east is consistent with the GPS motion estimates and basin structures and total fault offsets. They suggested that the sequantial formation of these structures resulted from the propagation of the NAF on the North Aegean and that this change in tectonic configuration resulted in the concentration of extensional deformation associated with Africa slab retreat in the N Aegean allowing the S Aegean and Peloponnisos to translate SW with little internal deformation. Shortly after, Perouse et al., (2012) proposed a contrasting view to previous studies (e.g. Armijo et al., 1996; Goldsworthy et al., 2002; Reilinger et al., 2010; Shaw and Jackson, 2010) according to which the propagation of the NAF throughout continental Greece or Peloponnesus is not required, the NAF did not propagate westward of the Thessaloniki peninsula as the relative motion between stable Eurasia and the south Aegean was

gradually accommodated by widespread N-S extension from the Southern Balkans to the eastern Gulf of Corinth.

During the last 40 years, several studies and marine and geophysical cruises have been conducted for the improvement of our knowledge about the kinematic characteristics and the tectonic framework that governs the Aegean domain. (Angelier et al., 1982; Le Pichon, 1982; Le Pichon et al., 1982; McKenzie & Jackson, 1986; Jackson and McKenzie, 1988; Mascle and Martin, 1990; Billiris et al., 1991;Taymaz et al., 1991; Noomen et al., 1993; Straub & Kahle, 1994; Jackson, 1994; Kahle et al., 1995; Le Pichon et al., 1995; Armijo et al., 1996; Papazachos and Kiratzi, 1996; Davies et al., 1997; Reilinger et al., 1997; Clarke et al., 1998; Papazachos et al., 1998; Armijo et al., 1999; Cocard et al., 1999; Briole et al., 2000; Kahle et al., 2000; McClusky et al., 2000; Goldsworthy et al., 2002; Kiratzi & Louvari, 2003; Kreemer & Chamot-Rooke, 2004; Nyst & Thatcher, 2004; Kokkalas et al., 2006; Reilinger et al., 2006, 2010; Perouse et al., 2012; Chatzipetros et al., 2013). Most of them try to evaluate the observed kinematic characteristics in order to propose a tectonic model which could explain the present deformation pattern of the entire Aegean domain and the extensional regime of the eastern Mediterranean. As the propagation of the NAF across the North Aegean resulted decisively in the present-day displacement and on the deformation pattern, much of the previous studies focus on the northern Aegean and/or on the areas where tectonic changes resulted from the deformation associated with the NAF.

Even today there are still areas either not surveyed or poorly explored with the result what we know to be less compared to those required to know for obtaining a clear picture for the geodynamic processes that led to the present complex structure of the Aegean. The broader southern Aegean is one such area. Although several studies were conducted, throughout recent years on the offshore area between western Peloponnesus and eastern Anatolia, the surveys focused mainly on the understanding of the prevailing geological regime of specific areas rather than concerning the entire geological setting of South Aegean. The results arising from the marine geophysical cruises concerning wider areas are based on low-quality analog data (e.g Bartole et al., 1983, Mascle and Martin, 1990) and need to be further supported with high-quality data in order to better understand the geological processes that led to the formation of the South Aegean. A brief summary of the literature concerning the South Aegean Sea follows at the next chapter.

1.2 South Aegean Sea

The first information about the offshore area of the South Aegean Sea is coming from the interpretation of seismic data acquired in the 80s (Jongsma et al., 1977; Angelier et al., 1982; Lyberis et al., 1981, 1982; Bartole et al., 1983; Rossi et al.,1986). It is characterized by Bartole et al., (1983) as a U-shaped region between the Aegean Volcanic Arc and the outer island arc (Peloponnesus, Kithira, Antikythira, Crete, Karpathos, Kasos and Rhodes). A few years later, Mascle and Martin (1990) referred to South Aegean as the Cretan Sea which is bounded to the north by the Southern Cyclades Islands and to the south by Crete, Karpathos and Rhodes. The geotectonic structure of the South Aegean represents the subduction zone due to the collision of the northeastern part of the African Plate to the southeastern part of the European Plate. The zone has a big sharp curve trajectory expressed most clearly near the region of Crete Island (Ranguelov, 2005). Many authors have shown the existence of a Benioff Zone dipping beneath the South Aegean at an angle of about 35^0 from SSW to NNE (Papazachos and Comninakis, 1969, 1971; Caputo et al., 1970; Kárník, 1972; Papadopoulos, 1982. For detailed literature see Papadopoulos et al 1986 and references therein).

The Hellenic Volcanic Arc (Methana, Milos, Santorini, Kolumbo and Nisyros) is part of the South Aegean Sea and resulting from the subduction of the African plate beneath the Aegean–Anatolian plate. Today, the active volcanic activity in Greece is located on the Hellenic Volcanic Arc of the South Aegean which crosses the southern Aegean from the western Peloponnesus to the eastern South Aegean. Its volcanic activity is represented by four main volcanic groups (Pe-Piper and Piper, 2002): the Methana-Poros-Egina group in the Saronikos Gulf at the western edge of the volcanic arc, the Milos and Santorini groups in the south Aegean and the Nisyros-Kos group at the eastern edge of the volcanic arc. Magmatism is not limited to onshore outcrops of volcanic rocks and volcanoes but also to submarine volcanic edifices (e.g., Kolumbo and Paphsanias volcanoes). A thorough description of submarine volcanoes can be found in Nomikou et al. (2013). The volcanic arc comprises many islands and islets, most of which lie in the central part of the arc. The study of volcanic rocks in the entire Aegean region has shown that north of the present-day volcanic arc volcanic rocks of similar chemical composition to the rocks associated with current volcanic activity have been found, indicating southwards migration of

the volcanism. From Late Eocene (35–30 Ma) to the present, the magmatic arc migrated toward the south to reach its present-day position (Fytikas et al. 1984; Pe-Piper and Piper 2002, 2006, 2007). Kokkalas and Aydin (2013) related the linear arrangements of the volcanic centers along the active South Aegean Volcanic Arc with the activity of NE-trending and secondarily of NW-trending faults.

Angelier et al. (1982), based on offshore and onshore data in combination with studies of orbital imagery and aerial photographs, examined the neotectonic deformation of the South Aegean. They described two apparently normal fault systems that control the deformation in the Cretan Sea: a roughly longitudinal relative to the axis of the arc system (almost NNW-SSE to the west and NE-SW to the east) and an oblique system trending N-S, with distributed as en-echelon faults (dextral west of Crete, in the Kythira-Antikythira strait, and sinistral east of Crete, in the Kassos-Karpathos strait). They also relate the geometry of the faults and the extension to Late Pliocene and Quaternary movements and they suggest an Early Pleistocene change on the stress trajectories which led to a clock-wise rotation of extension in the southwestern segments of the arc.

Mascle and Martin (1990) recognized three structural areas within the Cretan Sea with deepening of the depressions from west to east. The western Cretan Sea, east of Peloponnesus with SSE-NNW trending depressions referred to as the Argolide basin. The Central Cretan Sea, with the E-W trending Cretan trough and the eastern Cretan Sea, between eastern Crete and Rhodes Island where depressions have evolved in a N-S trending axis. Papadopoulos and Pavlides (1992) who studied the offshore area of Amorgos Island through the prism of the seismotectonic activity suggest that the Amorgos region is characterized by extensional NW-SE to NNW-SSE stress pattern with significant NE-SW right-lateral strike-slip components and proposed that the complex structure of the South Aegean domain deviates from the pure extension regime in back-arc conditions. Perissoratis, (1995) through the processing and interpretation of seismic profiles acquired from Santorini and the surrounding area recognized NE-SW trending normal faults superimposed on previous E-W normal faults. The change in the fault trending may be related to the initiation of the Santorini volcanic activity during the Early Pleistocene. In 2003, Piper and Perissoratis have also recognized older E-W trending faults and

younger active faults, trending NNW to the western part of the arc and ENE to the eastern with observed sinistral strike-slip motion parallel to the convergence direction of the Aegean-Anatolian and African plates. The transition from the E-W faults to the NNW and ENE trending faults occurred during the Quaternary.

Le Pichon and Angelier (1979) have proposed that the formation of the Hellenic Trough and the subduction of the Mediterranean lithosphere happened around 13 My BP (Late Serravalian). Angelier et al. (1982) agreed with this assumption, but by understanding that there can be a large estimation error, they recognize that further research is required to obtain reliable conclusions. Bartole et al. (1983) suggest that the basins formation may be dated back to Tortonian or even later to Late Serravalian times. Mascle and Martin (1990) proposed also that rifting processes started during Late Miocene (probably Serravalian) and resulted to the formation of E-W extensional features. They also set a chronological framework for the geodynamic evolution of the South Aegean. They proposed that N-S extension characterizes Crete in the Late Miocene. A brief compressional event has followed, and then the extension oriented at NE-SW and NW-SE and became more active along the western and eastern borders (Peloponnesus and Dodekanisa). During the Pleistocene a second general and short compressional event due to the southern subduction reduces the extensional regime and the extension is concentrated on the southwestern and south eastern borders of the South Aegean. Lykousis et al. (1995) also discussed a Late Quaternary extension in the North Ikarian Basin which has followed an earlier compressive deformation. The current structural pattern with prevailing NW-SE direction in the Peloponnesus and NE-SW direction in Anatolia and in western and eastern Crete resulted from the interaction of different oriented extensional features. Piper and Perissoratis (2003) suggested that a major change in the tectonic style occurred in the Early Pliocene which chronologically coincides with the propagation of the NAF into the Aegean according to Armijo et al. (1999).

Chapter 2: Aim-Objectives

The key issues being addressed in this study relate to the understanding of the geodynamic processes that contributed to the formation of the South Aegean. The main axis of the present doctoral thesis consists of three papers. The papers are listed below and are referred to as **Paper I-III**.

Paper I: "**Seismic stratigraphy and geodynamic evolution of Christiana Basin, South Aegean Arc.**" (Tsampouraki-Kraounaki, K.; Sakellariou, D. Seismic stratigraphy and geodynamic evolution of Christiana Basin, South Aegean Arc. Mar. Geol. 2018, 399, 135–147. https://doi.org/10.1016/j.margeo.2018.02.012)

Paper II: "**The Santorini-Amorgos Shear Zone: Evidence for Dextral Transtension in the South Aegean Back-Arc Region, Greece.**" (Tsampouraki-Kraounaki, K.; Sakellariou, D.; Rousakis, G.; Morfis, I.; Panagiotopoulos, I.; Livanos, I.; Manta, K.; Paraschos, F.; Papatheodorou, G. The Santorini-Amorgos Shear Zone: Evidence for Dextral Transtension in the South Aegean Back-Arc Region, Greece.Geosciences 2021, 11, 216. https://doi.org/10.3390/geosciences11050216)

Paper III: "**Plio-Quaternary extension and strike-slip tectonics in the Aegean.**" (Sakellariou, D.; Tsampouraki-Kraounaki, K. Plio-Quaternary Extension and Strike-Slip Tectonics in the Aegean. In Transform Plate Boundaries and Fracture Zones; Elsevier: Amsterdam, The Netherlands, 2019; pp. 339–374. https://doi.org/10.1016/B978-0-12-812064-4.00014-1)

Papers I and **II** analyse and discuss the development of two neighboring selected areas of the South Aegean Sea (Christiana Basin and the offshore area south of Amorgos Island) which seem to be subject to similar deformation mechanisms which are related to their position on the South Aegean back arc area. **Paper III** aims to set the general framework of evolutionary deformation that prevails in the wider Aegean domain and summarizes the preexisting literature and the main deformation models that have been proposed for the Aegean.

The research leading to this dissertation attempts to extract results of geodynamic development characteristics of specific South Aegean areas (**Figure 2.1**) and to integrate them into the broader evolutionary pattern not only of the South Aegean but of the wider Aegean as whole. The utilization of the results arising from older studies and the interpretation of older and

recently acquired seismic profiles from the South Aegean Sea and from the Cretan Basin, contributes to the understanding of the geological processes prevailing in back-arc areas and identify open questions and challenges for future research.

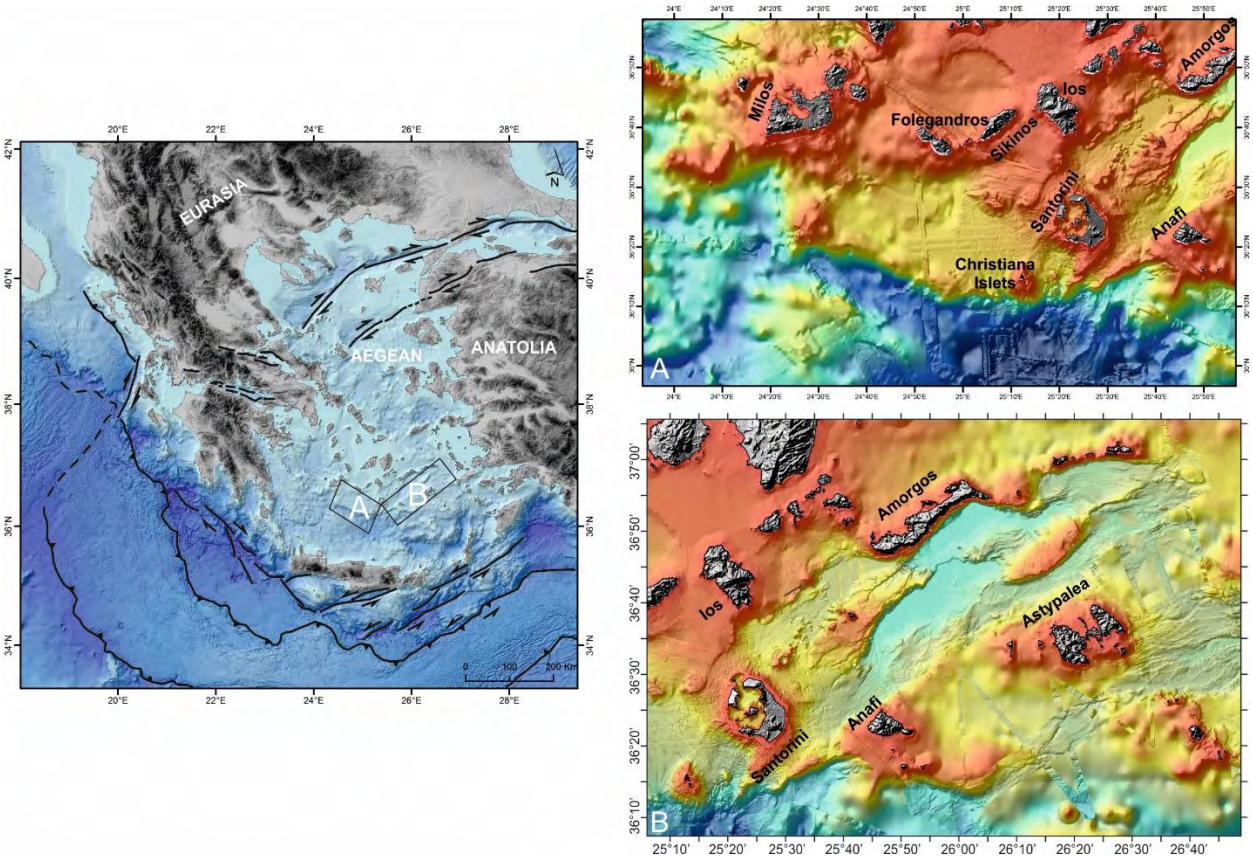

Figure 2.1: Left: Morpological map showing the main tectonic elements bounding the Aegean domain. The black squares indicate the study areas in the Central part of the South Aegean. (**A**): Bathymetric map of Christiana Basin, (**B**): Bathymetric map of Santorini-Amorgos Shear Zone.

Chapter 3: Methodology

The present thesis was based both, on the processing and interpretation of recently acquired seismic and bathymetric data, and on the reprocessing of older analog seismic profiles and the analysis of the results which have been emerged from previous studies. Initially, to understand the geological and kinematic characteristics that formed the Southern Aegean, two adjacent areas were selected (Figure 2.1): (1) Christiana basin and (2) the offshore area between Santorini, Amorgos and Astypalea Islands (Santorini-Amorgos Shear Zone). The selection of these areas was made due to the adequacy of the data for detailed research coverage and due to their special geographical location in the central southern Aegean and the Hellenic volcanic arc. The results of the surveys in these two areas as well as the methodology followed are described also in **subchapters 4.1** and **4.2**. However, it is worth noting that for both areas seismic and swath bathymetry data were processed and interpreted. Subsequently, as the southern Aegean is affected by the geodynamic deformation that controls the entire Aegean, the general framework of evolutionary deformation that prevails in the wider Aegean domain was defined. A more detailed description of the methodology followed is presented in the following paragraphs.

The data used for Christiana Basin were acquired during several oceanographic cruises (years 1986-1992, 2006, and 2017) (Figure 3.1). A detailed description of the instruments used for the data acquisition is given in **Chapter 4.1.4**. The seismic data collected during the years 1986-1992, with the research vessels ***AEGAEO*** and ***SONNE***, are old, analog seismic profiles, acquired on thermal paper. For this reason, they first needed to be digitized. After being scanned, their exact location was determined based on the geospatial data (latitude and longitude) recorded on the ship. Then, for the analysis of the seismic stratigraphy, the design program ***CorelDRAW*** was used to map the different seismic units within the sedimentary sequence, highlight the main acoustic reflectors and identify the dominant fault network which deforms Christiana Basin. The seismic data collected on the years 2006 and 2017, with the research vessel ***AEGAEO***, are new digital seismic profiles recorded by using ***Triton Imaging, Inc.*** acquisition software and hardware at 2 s shooting rate and by ***CodaOctopus DA4G™ 2000*** acquisition software and hardware at 3 s shooting rate respectively. The 2016 SEG-Y data have been processed with ***Triton Imaging, Inc.*** software for their improvement and the 2017 data have been improved, when needed, with ***CodaOctapus***

Survey Engine software. For the final processing and interpretation of the seismic data was used the ***CorelDRAW*** program.

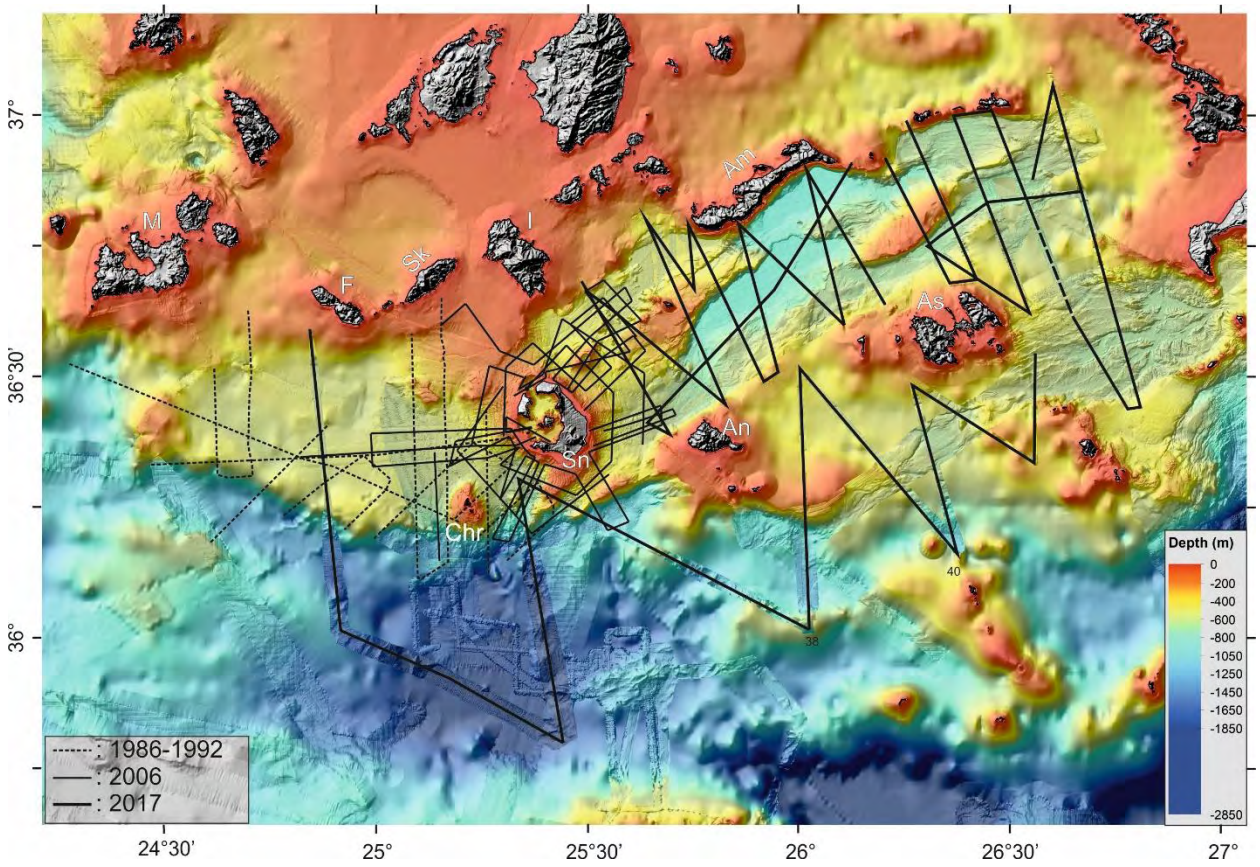

Figure 3.1: Bathymetric map showing the location of the seismic profiles described in the text

Swath bathymetry and seismic data have been used and interpreted for Santorini-Amorgos Shear Zone. The bathymetric data provide information on the geomorphological features of the area (basins, ridges). The seismic profiles led to new insights into the seismic stratigraphy and the dominant fault network prevailing in the area. Swath bathymetry data were collected in the years 2001, 2006, 2007, 2008, 2016, and 2017 and seismic data were collected in the years 2006, 2016, and 2017. A detailed description of the instruments used for the data acquisition is given in Chapter 4.2.4. The bathymetric data have been processed using the ***MB-System***, ***PDS 2000***, and ***Global Mapper*** software and reprocessed at 20 m resolution in ***Arc-GIS***. These data have been used for the creation of the bathymetric map as presented in Chapter 4 (Figures 4.2.2A, 4.2.3, 4.2.9). The acquired seismic profiles have been processed with the ***CodaOctapus Survey Engine*** software

and have been exported as jpeg images to make their geological processing and interpretation in the ***CorelDRAW*** design program.

Finally, in order to understand the wider geodynamic framework of the Aegean, it was necessary to gather the results of previous studies conducted for the Aegean and to review them in the light of more recent data. The results of this effort are presented in **subchapter 4.3**. In an attempt to present in the best possible way both the results that have emerged from the pre-existing literature and the results that have emerged based on the latest data, the study was divided into three main axes. Firstly, the Aegean Sea has been divided into three sub-regions: The North Aegean Sea, the South Aegean Sea/Volcanic Arc and the Hellenic Arc and Trench. For each of them, are summarized the main results concerning its morphological characteristics, the dominant fault network as well as the results that have been obtained from geodetic and seismological surveys. A detailed review of the results arising from the interpretation and re-interpretation of old and recent multi- and single-channel profiles, through the presentation of the most recent bathymetric map of the Aegean Sea, follows next. The last part of the study concerns the presentation of the main conclusions that have been emerged by the analysis of the new offshore morphology and the reprocessing and interpretation of old and recent seismic data and highlights the necessity of further research to better understand the precise geological mechanisms that have activated during the Aegean evolution.

Chapter 4: Main study

4.1 Seismic stratigraphy and geodynamic evolution of Christiana Basin, South Aegean Arc

https://doi.org/10.1016/j.margeo.2018.02.012

4.1.1. Abstract

The analysis and interpretation of vintage and recent seismic profiles across Christiana Basin in the South Aegean arc provided information on the seismic stratigraphy and chrono-stratigraphy of the basin, the occurrence of volcanic deposits within the sedimentary basin infill, and its post-Miocene geodynamic evolution. Plio- Quaternary sediments overlie a Messinian erosion surface on the basin's margins, while in the basin, they have been deposited above the Messinian evaporites. The basin evolved in two stages. During the early stage, subsidence of the three main depocenters in the NW, W and SE part of the basin has been controlled by E-W to ESE- WNW trending faults. The end of the early stage is marked by the cessation of activity on the southern marginal fault and the migration of the northern faults towards north where the basin expanded significantly towards south and north. The seismic stratigraphy of the younger stage deposits is characterized by the presence of three thick, pyroclastic flows. They occur only in the eastern part of the basin and have therefore derived from Santorini volcanic center since Middle Pleistocene. The youngest one is associated with the Minoan eruption while the next one is slightly younger than 0.42 Ma and may be linked with activity in Peristeria volcano. The lower pyroclastic flow has deposited shortly after 1.2 Ma and is the thickest (100 msec) and widest distributed pyroclastic flow deposit in the basin. It is most probably the biggest pyroclastic flow known in the South Aegean Sea. It may be associated with an eruption of the early volcanic centers of Akrotiri. No evidence of volcanic or volcano-clastic deposits derived from west, i.e. from Milos volcanic center has been found in Christiana Basin. By taking into consideration the similar, two stage structural evolution of the Santorini-to-Amorgos area proposed in the literature, it is suggested here that since Early to Middle Quaternary, the E-W trending Christiana Basin may be considered as an area of extension developed on the right side of the southwestern termination of the NE- SW trending, dextral Santorini-Amorgos fault zone.

4.1.2. Introduction

The Aegean Sea is located on the northern margin of the East Mediterranean Sea, between the Southern Balkan Peninsula (Greece) and Anatolia (Turkey). It is a geologically complex area with very specific characteristics due to its position on the southern edge of the overriding Eurasian plate, above the northward subducting slab of the East Mediterranean crust and the African plate. As a result of the convergence between the two plates, a series of structural features has been developed, named from the south to the north as: the accretionary prism of the East Mediterranean Ridge, the backstop, the series of long troughs and deep depressions known as Hellenic Trench, the Hellenic Island Arc, the South Aegean Back-Arc Basin and the Hellenic Volcanic Arc (Figure 4.1.1).

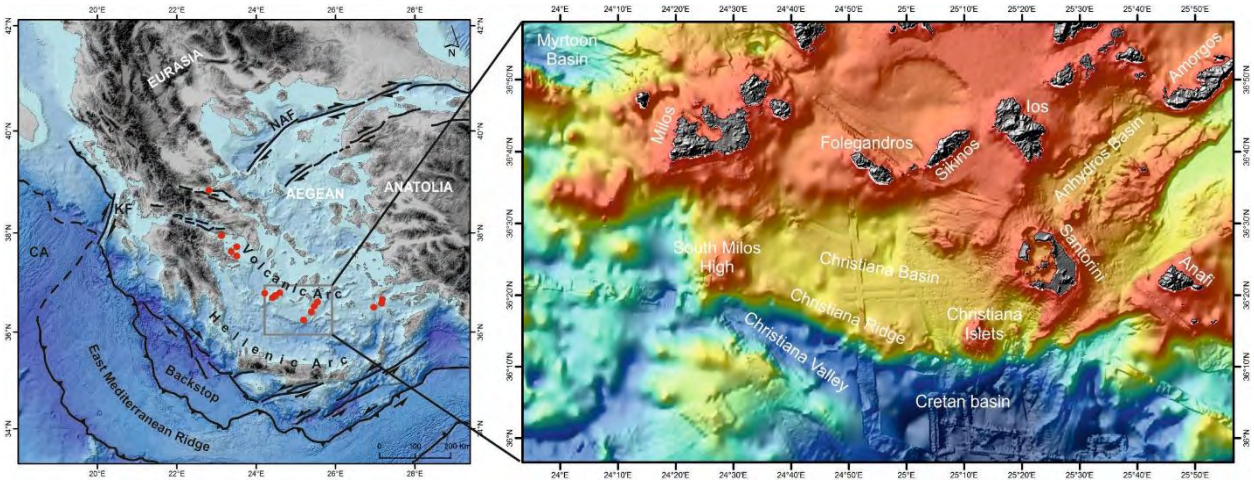

Figure 4.1.1: Left: Morphological map of the Aegean Sea, showing the main structural features and tectonic elements and the location of the survey area in the central part of the Hellenic Volcanic Arc. Red dots mark active volcanic centers. NAF: North Anatolian Fault, KF: Kephallonia Fault, CA: Calabrian Arc. Bathymetry from EMODNET Bathymetry 250m resolution, processed by HCMR. Right: Bathymetric map of the survey area with the main morphological features mentioned in the text. Bathymetry: (a) EMODNET Bathymetry 250m resolution, processed by HCMR; (b) swath bathymetry 50m resolution, HCMR courtesy.

The Hellenic Volcanic Arc, also known as South Aegean Arc, includes four main volcanic groups (Pe-Piper and Piper, 2002): the Methana-Poros-Egina group in the Saronikos Gulf at the western edge of the volcanic arc, the Milos and Santorini groups in the south Aegean and the Nisyros-Kos group at the eastern edge of the volcanic arc. The most recent volcanic activity occurs in Santorini with at least nine eruptions during the last 600 years (Papazachos, 1989; Fytikas et al., 1990).

This paper focuses on the results arising from the geological study of Christiana Basin (Figure 4.1.1.), also known as Milos (Bartole et al., 1983) or Christiani Basin (Piper and Perissoratis, 2003). It has been named after Christiana islets, a group of three volcanic islets at the southeastern edge of the basin, southwest of Santorini. Along with Santorini and Kolumbo volcanic centers, Christiana islets are aligned on the "Kameni- Kolumbo Line", a SW-NE trending strike-slip fracture zone (Sakellariou et al., 2010). The Christiana Basin is an elongated basin, located on the northern margin of the Cretan Basin. Due to the position of the basin, at the central sector of the Hellenic Volcanic arc, between the volcanic groups of Milos to the west and Santorini to the east, is expected that the volcanic activity of these two volcanic groups may have been recorded in its sedimentary sequence. Therefore, a brief summary of the volcanic history of these two islands, as has been discussed and has become widely known by previous authors appears necessary and is given below.

According to Anastasakis and Piper (2005), Milos shows the longest record of volcanism in the arc since Mid-Pliocene. Fytikas et al. (1986) gave a comprehensive overview of the volcanic history of the island. The volcanic activity started with submarine eruptions in the western part of the island. The oldest records for volcanism are from Late Pliocene about 3.4–3.0 Ma BP. At 2.0 Ma BP the volcanic activity at the western part of the island has ceased and the volcanism has migrated eastwards. At 0.5 Ma BP, the volcanic activity was localized in the central part of the island. Subsequently, a quiescent period has fol- lowed, which lasted until 0.4 Ma BP, with the building up of the Trachilas cone and later on the one of the Fyriplaka complex. The latest volcanism dates at about 0.1 Ma BP.

Santorini, Christiana and Kolumbo volcanic structures form the Santorini volcanic group which has spatially developed along a NE–SW trending zone, marked by deep seismic activity (Papazachos and Panagiotopoulos, 1993). The volcanic activity started about 2 million years ago with the extrusion of dacitic lavas from vents in the area of the present-day Akrotiri peninsula and continued to produce different kinds of lavas and pyroclasts (Friedrich, 2000). Druitt et al. (1989) divided the volcanic evolution of Santorini into the following stages: i) Akrotiri volcanoes (approx. 2 Ma–600 ka years ago); ii) Cinder cones of the Akrotiri peninsula (around 600–300 ka); iii) Peristeria Volcano (530–300 ka); iv) Thera Pyroclastic Formation and v) Kameni shield (1613

BCE–present). The cyclic construction of shield volcanoes interrupted by large explosive and destructive events like the Minoan eruption is the most characteristic type of activity over the last 200.000 years. The oldest recognized volcanic unit related to one of Santorini's eruptive events (Akrotiri), is of Early Pleistocene age and evolved submarine (Druitt et al., 1999). West of Santorini there is no evidence for thick pyroclastic deposits derived from the major felsic eruptions of the Thera Pyroclastic Formation over the past 250 ka. Thick marine pyroclastic deposits of the Thera Pyroclastic Formation have been mapped to the south of Santorini (Sparks et al., 1983; Anastasakis, 2007).

4.1.3. Geological setting

Despite the geographical position of Christiana Basin between the volcanic centers of Milos and Santorini, extensive researches, describing the special geodynamics of the formation of the basin, have not been presented yet, through the preexisting literature. However, the following paragraphs describe the main results arising from extensive studies of the wider South Aegean region including Christiana Basin.

According to Piper et al. (2007) the Christiana Basin, along with the Cretan Basin has been developed as a result of Miocene extension, in contrast to the Myrtoon basin (NW of Milos Island), which was already a deep basin in Late Miocene (Anastasakis and Piper, 2005). Although Piper and Perissoratis (2003) have recognized a deactivation of faults north and south of Milos Island at about 0.7 Ma, they also recognize subsidence in the northern margin of the Cretan Basin. A major active normal fault clearly defines the northern margin of Christiana Basin. The general fault pattern in the area shows E-W trending, including buried faults. (Piper et al., 2007). The Plio-Quaternary sediments of the basin overlie the Messinian erosion surface near the basin margins (Bartole et al., 1983; Martin, 1987). Anastasakis and Piper (2005), following the interpretation of Piper and Perissoratis (2003), have defined three key reflectors A, B and C, of latest Pliocene to Quaternary age. They assigned ages to these reflectors, based 1) on the sedimentation rates in the South Aegean Sea, 2) on the identification of volcanic rocks and their correlation with well-known dated volcanic events and 3) on the chronology of stacked coastal progradation sequences. Reflector A seems to correspond to MIS 12 (0.45 Ma) while the age of the reflectors B and C have been estimated at about 1.0 Ma and 2.0 Ma respectively.

Piper et al. (2007), relying on limited penetration sparker seismic profiles, suggested that the main volcanism of Akrotiri and Christiana was triggered by NE-SW trending strike-slip faults initiated in Late Pliocene or Early Quaternary. The volcanic horizons of Santorini have been correlated with the younger (0,65–0,55 Ma) and older Akrotiri (1.6 ka) eruption respectively (Piper et al., 2007). According to Piper et al. (2007), the upper volcanic rocks of Christiana Island have a similar age with the younger Akrotiri episode, while the age of the lower ones compared to the age of the lower volcanic rocks of Santorini appears to be older and comparable to the age of Reflector C, a fact that implies latest Pliocene age. Pyroclastic deposits related to the major felsic eruptions of the Thera Pyroclastic Formation have not been found in the area west of Santorini. The most prominent pyroclastic units predate the Thera Pyroclastic Formation (Piper et al., 2007). This is a suggestion, that will be further examined in the current study. Thick marine pyroclastic deposits of the Thera Pyroclastic Formation have been mapped to the south of Santorini (Sparks et al., 1983; Anastasakis, 2007). NW of Santorini, submarine pyroclastic flows related to younger Akrotiri and Peristeria volcano have been mapped (Piper et al., 2007).

Based on the interpretation of seismic reflection profiles, this paper intends to present a detailed map of the prevailing fault network, suggest a chronological approach of the stratigraphy and reveal the tectonic and volcano-sedimentary processes that played a dominant role in the geodynamic evolution of Christiana Basin.

4.1.4. Materials and methods

Two data sets have been used in the present study. The first one includes analog, single-channel seismic profiles acquired across the entire Christiana basin, while the second one includes recently acquired, digital, seismic profiles from the eastern part of the basin (Figure 4.1.2). The analog seismic data were acquired during several oceanographic cruises aboard the research vessels ***AEGAEO*** and ***SONNE*** in the years 1986–1992. These profiles were acquired on thermal paper, using a ***BOLT'S Air-Gun*** acoustic source of 40 ci and/or 10 ci and a ***SIG'S*** hydrophone STREAMER with incorporated preamplifier. The new, digital profiles were acquired in 2006 and 2017 during two oceanographic cruises with the R/V ***AEGAEO***. The vintage data provide valuable information on the structure of the basin and allow a fairly comprehensive interpretation of the seismic stratigraphy. The new, digital seismic profiles acquired with a ***BOLT'S Air-Gun*** of 10 ci

and 40 ci allow a detailed interpretation of the seismic stratigraphy of the basin. Re-interpretation of the old profiles under the light of the information provided by the new seismic profiles, has led to a significantly improved interpretation of the seismic stratigraphy and structure of Christiana Basin.

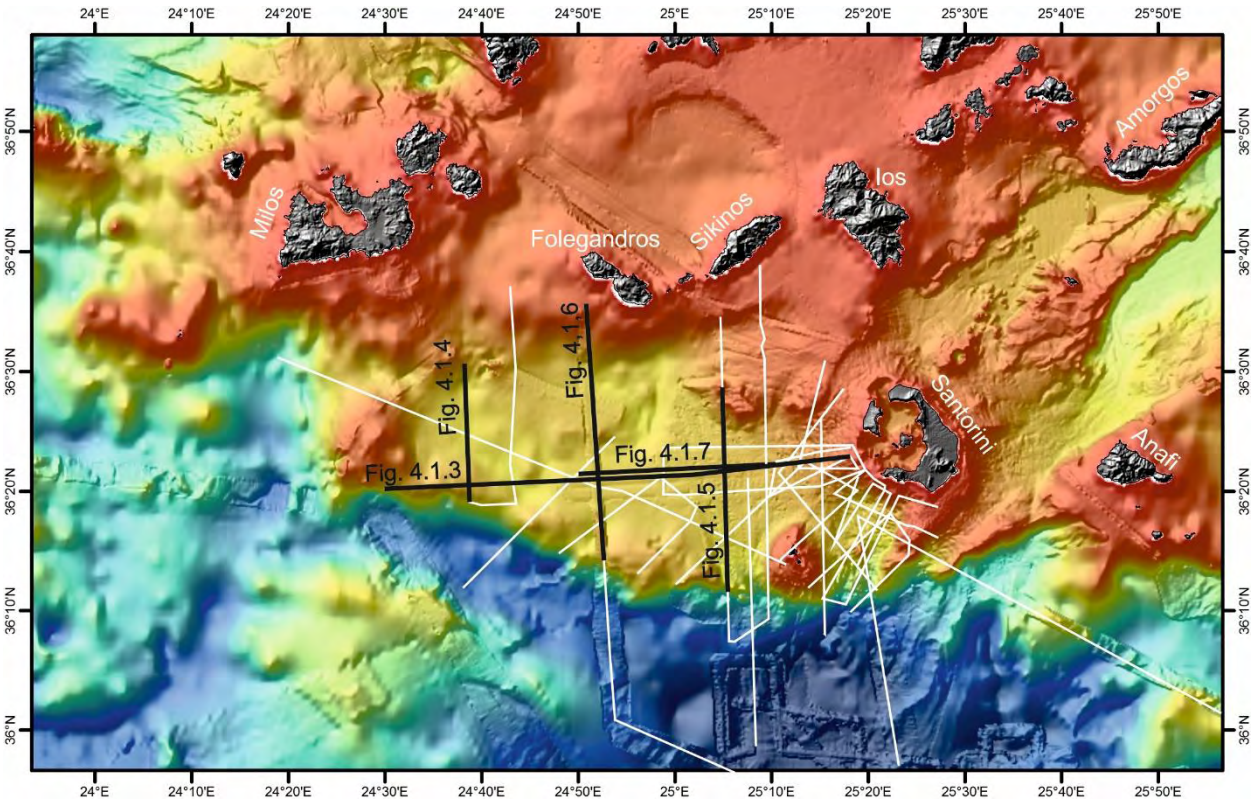

Figure 4.1.2: Bathymetric map of Christiana Basin showing the location of the seismic profiles described in the text

During the interpretation of the seismic profiles, the main reflectors were identified and the main acoustic units were determined based on their geometrical relationship with the overlying and underlying layers and their acoustic character. The results were correlated with the seismic stratigraphy and litho-stratigraphy of adjacent basins (i.e. Piper and Perissoratis, 2003; Anastasakis and Piper, 2005) with the aim to take advantage of the available indirect chronological constrains and provide approximate ages of the prominent seismic reflectors and sequences of the basin and the temporal distribution of the fault activity.

4.1.5. Results

The interpretation of the seismic profiles reveals new information on the seismic stratigraphy, the structure and the volcano-sedimentary processes in Christiana Basin. The results have been grouped into three main sections as presented in more detail below.

4.1.5.1. Seismic stratigraphy

Seven main, distinct seismic units have been recognized in Christiana Basin's infill, including the basin's margins as shown in Table 4.1.1. The results of the seismic stratigraphy of Christiana (Figures 4.1.3, 4.1.4, 4.1.5, 4.1.6 and 4.1.7) are being compared with the seismic stratigraphy of the Myrtoon basin as presented by Anastasakis and Piper (2005), in order to enable a chrono-stratigraphic approach of the volcano-sedimentary processes in the basin. The chrono-stratigraphically defined reflectors A, B and C of Anastasakis and Piper (2005) along with their seismic stratigraphic criteria have been used here for the interpretation of the Christiana Basin's infill.

Table 4.1.1: Description of the different seismic units recognized in Christiana Basin.

Unit	Illustration	Seismic Character	Description	Thickness
1	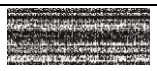	Intense, parallel, high amplitude, closely spaced reflectors	Highest unit, basinwide occurrence	40-60 msec
2		Parallel, closely spaced, medium amplitude reflectors, showing a more transparent character at the eastern part of the basin	Basinwide unit, thinning out towards the margins	Max.300 msec in the center of the basin
3	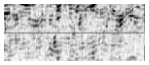	Chaotic, undulating, high to low amplitude, discontinuous reflectors	Wedge-shaped unit (II, II, III) thinning out towards West. Correspond to pyroclastic flow from Santorini	I ≈ 40-50 msec II ≈ 20 msec III ≈ 100 msec
4	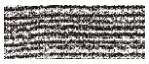	Parallel, closely spaced, semi-continuous, medium amplitude reflectors become stronger towards the margins	A uniformly spread unit	Max. 100 msec
5		Low amplitude, semi-transparent, sub-parallel, widely spaced reflectors	A great thickness unit at the lower part of the sedimentary sequence	Exceeds 200 msec
6		Incoherent, discontinuous, high amplitude, irregular reflectors	Is correlated with the Messinian evaporites	30-50 msec
7		High amplitude, irregular surface above a reflection free unit	Acoustic basement	-

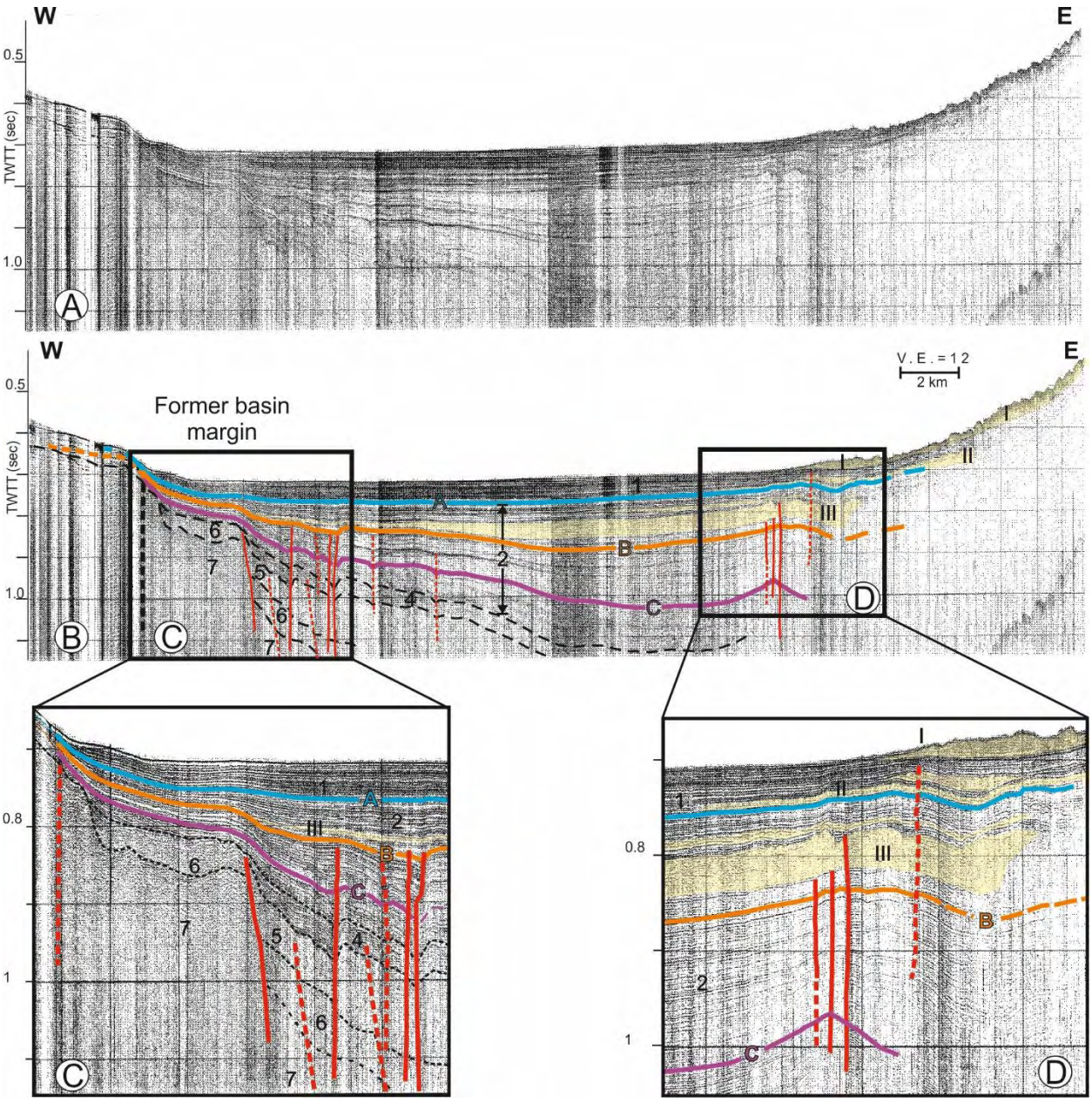

Figure 4.1.3: (**A**) Uninterpreted, analog, single channel seismic profile crossing Christiana Basin in W-E direction. (B**)** Interpreted profile showing seismic stratigraphic interpretation. (**C**) Detail of the western part of the profile showing the faulted, older margin. (**D**) Detail of the eastern part of the profile focusing on the pyroclastic flows. Numbers 1 to 7 correspond to seismic units described in the text. I, II, III show the pyroclastic flows. A, B and C correspond to Anastasakis and Piper (2005) chronostratigraphic horizons.

Unit 1(Figure 4.1.3) is the uppermost stratigraphic unit, occupies the greatest part of the basin, with an average thickness of approximately 50 msec in the center of the basin. It is characterized by continuous, closely spaced, high amplitude reflectors, resting conformably on the underlying sedimentary sequence in the basin but with an angular unconformity (onlap relationship) on the

basin's margin (Figures 4.1.3, 4.1.4 and 4.1.5). Based on the similarities of the acoustic character and stratigraphic position, we correlate Unit 1 with the uppermost unit observed by Piper and Perissoratis (2003) in the Eastern Myrtoon Basin and the Folegandros Basins and by Anastasakis and Piper (2005) in the Mirtoon Basin. According to Piper and Perissoratis (2003), the high-

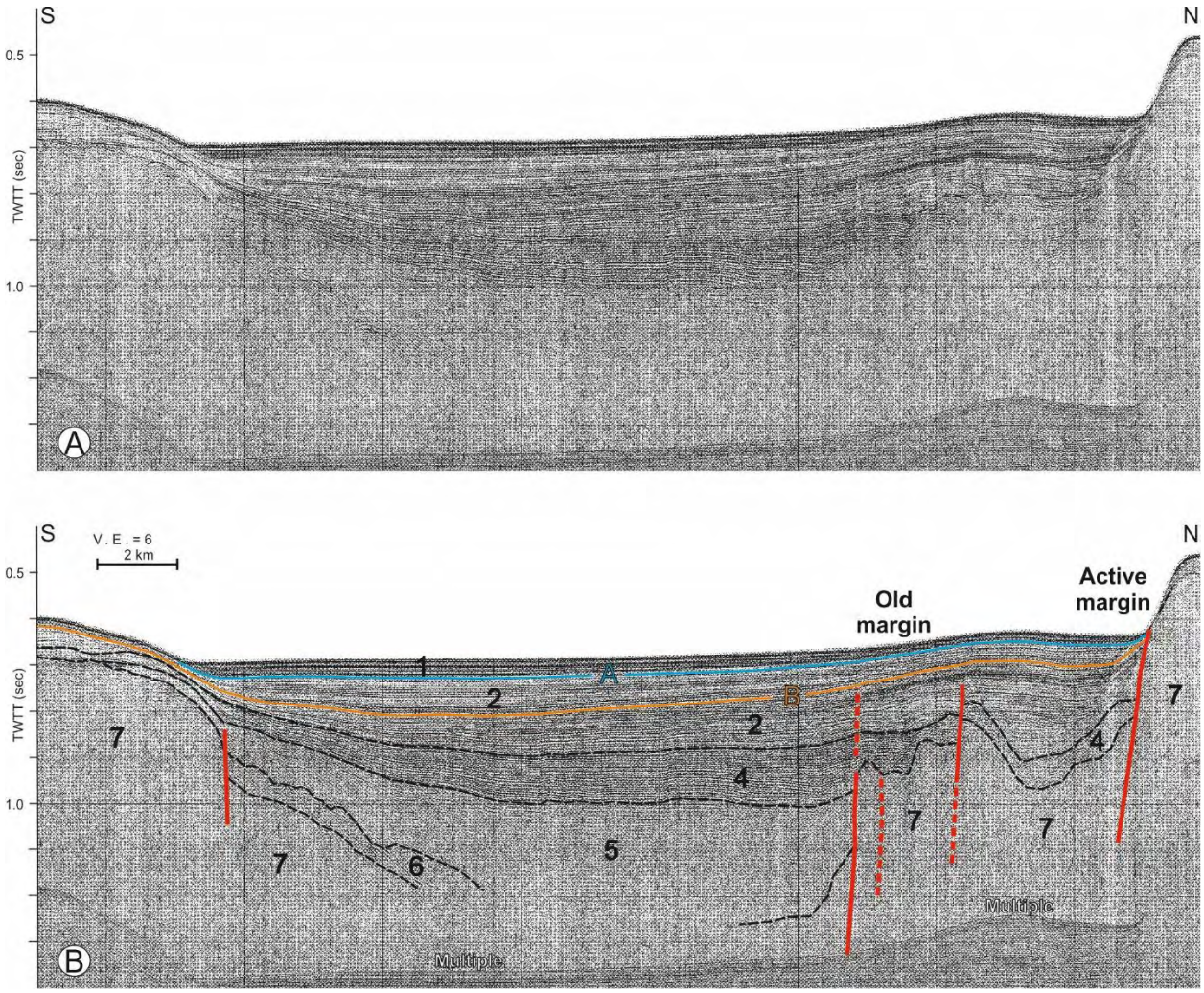

Fig. 4.1.4:(**A**) Uninterpreted, analog, single channel seismic profile crossing the western part of Christiana Basin in S-N direction. (**B**) Interpreted profile showing seismic stratigraphy interpretation. Explanation of symbols as in Fig. 4.1.3.

amplitude reflectors result from the deposition of volcanic tephra derived from the late rhyolitic centres of Milos, dated from 0.49 Ma to 0.09 Ma. The reflector A marks the bottom of Unit 1. We consider Reflector A as equivalent to the Reflector A of Anastasakis and Piper (2005) and to the UF1 unconformity observed by Piper and Perissoratis (2003). Following Anastasakis and Piper (2005), reflector A correlates laterally with MIS 12 progradational deposits and may therefore date

to about 0.42 Ma. At least 2 chaotic layers (I, II) with undulating, high amplitude, dis- continuous character, representative of seismic Unit 3 lie at the seabed and at the base of Unit 1, in the eastern part of the basin, as illustrated on Figures 4.1.3 and 4.1.5**.** Their seismic character, the decrease of their thickness away from Santorini and the irregular morphology of their boundaries with the underlying and overlying strata suggest that they are volcanogenic deposits derived from Santorini volcanic center and they will be discussed in detail below.

Unit 2 underlies Unit 1, its thickness reaches 300 msec in the center of the basin and it thins out towards the margins. Although its general acoustic character is mainly characterized by parallel, closely spaced, continuous, medium-amplitude reflectors, some differences are observed between the eastern and western part of the basin. In the eastern part (Figures 4.1.3 and 4.1.4), Unit 2 displays a more transparent character and thin chaotic layers alternate with the continuous, closely spaced reflectors. Reflector B, as defined by Anastasakis and Piper (2005), can be traced in the entire basin, at a mean depth of roughly 140 msec below the seafloor, while Reflector C can be imaged at a mean depth of approximately 300 msec below the seafloor. Both of them fall within Unit 2. While reflector B do not mark any particular event or change in the sedimentary sequence, Reflector C displays locally an erosional character. Truncation of the underlying reflectors below C is evident at the western part and possibly at the center of the profile on Figure 4.1.7**.** Between the Reflectors B and C, a high amplitude basinwide reflector can be observed on the profiles on Figures 4.1.5 and 4.1.7. Its acoustic character indicates coarse-grained deposits and probably represents a sandy turbidite. Similar to Unit 1, in the eastern part of Christiana Basin (Figure 4.1.5), an up to 100 msec thick unit (III) representative of seismic Unit 3 (Table 4.1.1), with chaotic, incoherent undulating, discontinuous, high amplitude reflectors can be outlined within Unit 2. Due to its seismic character, it can be reasonably associated with volcanogenic deposits generated from one of Santorini's early volcanic events. The differences between the seismic stratigraphy of the western and eastern parts of the basin are very well illustrated on Figure 4.1.3**.**

In the basinal area (Figure 4.1.4) Unit 4 underlies Unit 2. It is characterized by closely spaced, semi-continuous, medium amplitude reflectors and is a uniformly spread unit, with thickness reaching 100 msec, that shows high amplitude character towards the south and western margins. Unit 5 underlies Unit 4 and displays a low amplitude seismic character, with semi-transparent, sub-parallel, widely spaced, continuous to discontinuous reflectors. Its thickness exceeds 200 msec in some parts of the basin. Unit 5 is the lowermost unit in the seismic stratigraphy of Christiana Basin's infill. Due to the attenuation of the seismic signal, its bottom is not imaged in the center of the basin. The disparities on the seismic character of unit 4 and 5, with unit 4 displaying more enhanced reflectors, indicate that terrigenous sediment supply occurs during the deposition of unit 4, in contrast to the less reflective character of unit 5 which suggests hemipelagic deposition (Figure 4.1.7).

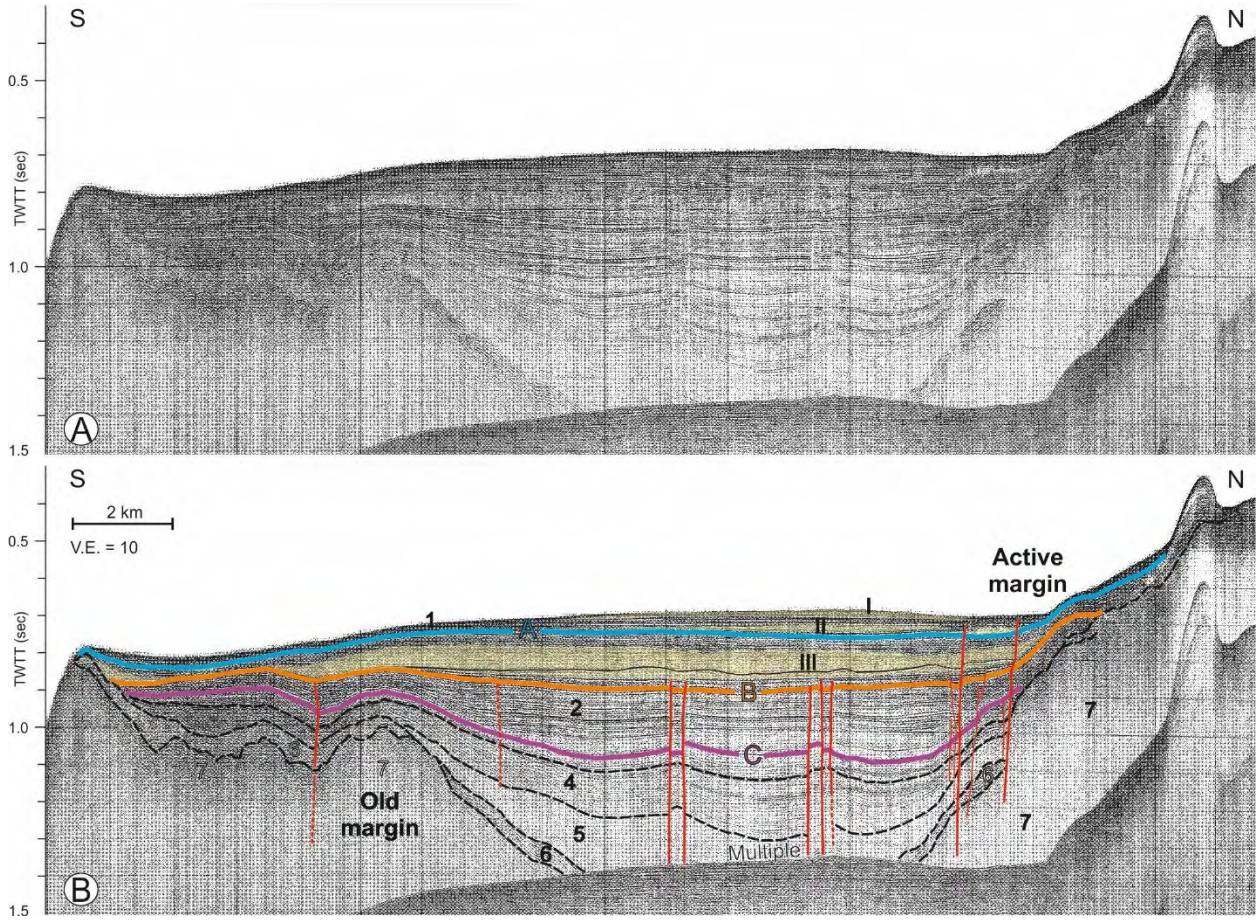

Figure 4.1.5: (**A**) Uninterpreted, analog, single channel seismic profile crossing the eastern part of Christiana Basin in S-N direction (**B**) Interpreted profile showing stratigraphy interpretation. Explanation of figures as in Fig. 4.1.3.

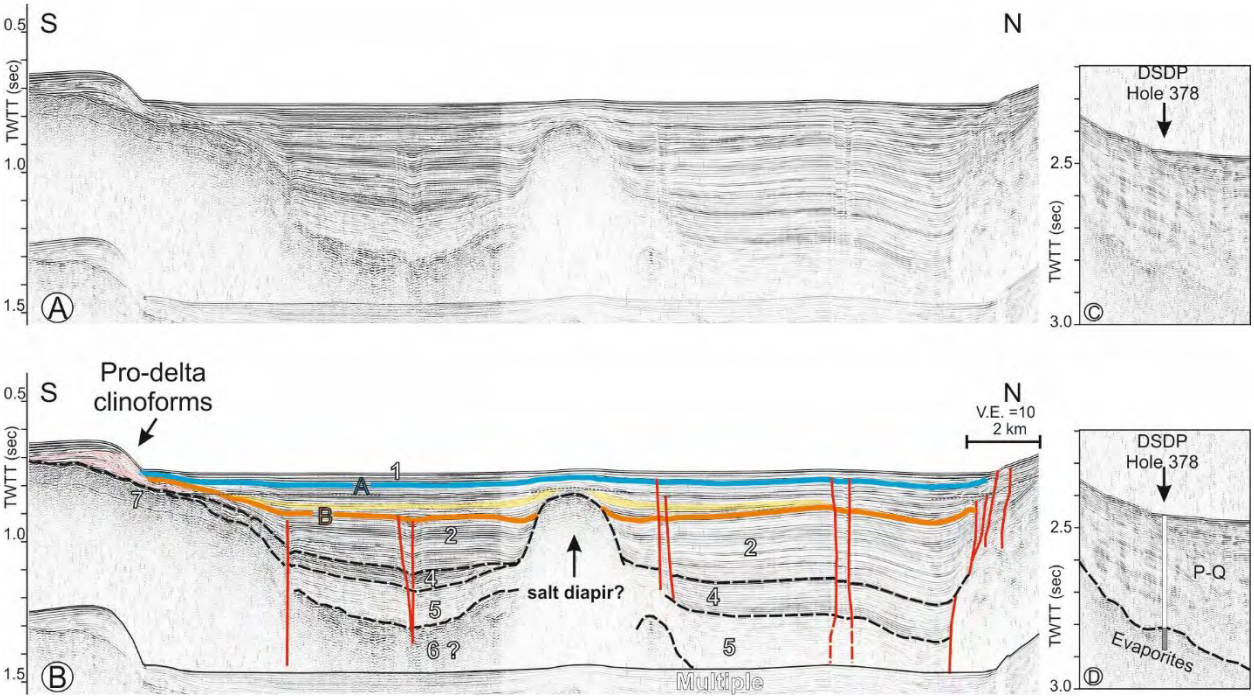

Figure 4.1.6: (**A**) Uninterpreted, single channel seismic profile crossing the center of Christiana Basin in S-N direction. (**B**) Interpreted profile showing seismic stratigraphy interpretation. (**C**) Uninterpreted section of a seismic profile passing from the DSDP Hole 378 in the Cretan Basin. (**D**) Section of a profile with the boundary between Messinian.

A well-imaged, high amplitude, irregular reflector separates Unit 5 above, from Unit 6 below. The latter is characterized by incoherent, discontinuous, high amplitude, irregular reflectors. Contrary to the well-developed and well stratified seismic character within the basin, this unit displays a more disturbed seismic character close to the flanks, probably due to slope failures. The seismic character and the irregular morphology of this interface along with the seismic character of Unit 6, are good arguments to suggest that it represents the Messinian marker as observed by Anastasakis and Piper (2005) below Milos Basin. Furthermore, this is in good agreement with the results of the Deep Sea Drilling Project (DSDP), Hole 378, in the Cretan Basin (Hsu et al., 1978). The Figure 4.1.6D illustrates a section of seismic profile passing from DSDP 378 site. The profile was acquired during the same cruise (2017) and with the same sound source (Airgun 40 ci) and settings as the profile on Figure 4.1.6A. It is evident that the seismic character of the top and the internal reflectors of unit 6 in Figure 4.1.6A is identical with the ones of the unit which corresponds to the Messinian evaporite deposits in Figure 4.1.6D. In that case, the low-

reflective Unit 5 which overlies the Unit 6, may correspond stratigraphically to the Zanclean - Early Pliocene marls of the Trubi or Argille Azzure Formations (Roveri et al., 1998, 2008, 2014).

The presence of salt diapirs as mentioned by Bartole et al. (1983) in the center of Christiana Basin, supports the assumption that the interface between unit 5 and unit 6 is the Messinian marker separating the Pliocene sediments from the evaporites. The data presented here are in favor of this interpretation: the profiles of Figures 4.1.6 and 4.1.7 show two dome-like structures which emanate from unit 6. The seismic reflectors of unit 5 in Figure 4.1.7 are dragged upwards at their contact with the dome, while the seismic reflectors of the basin's infill above the dome are fractured. In Figure 4.1.6 the dome penetrates Units 5, 4 and the lower half of Unit 2 while the

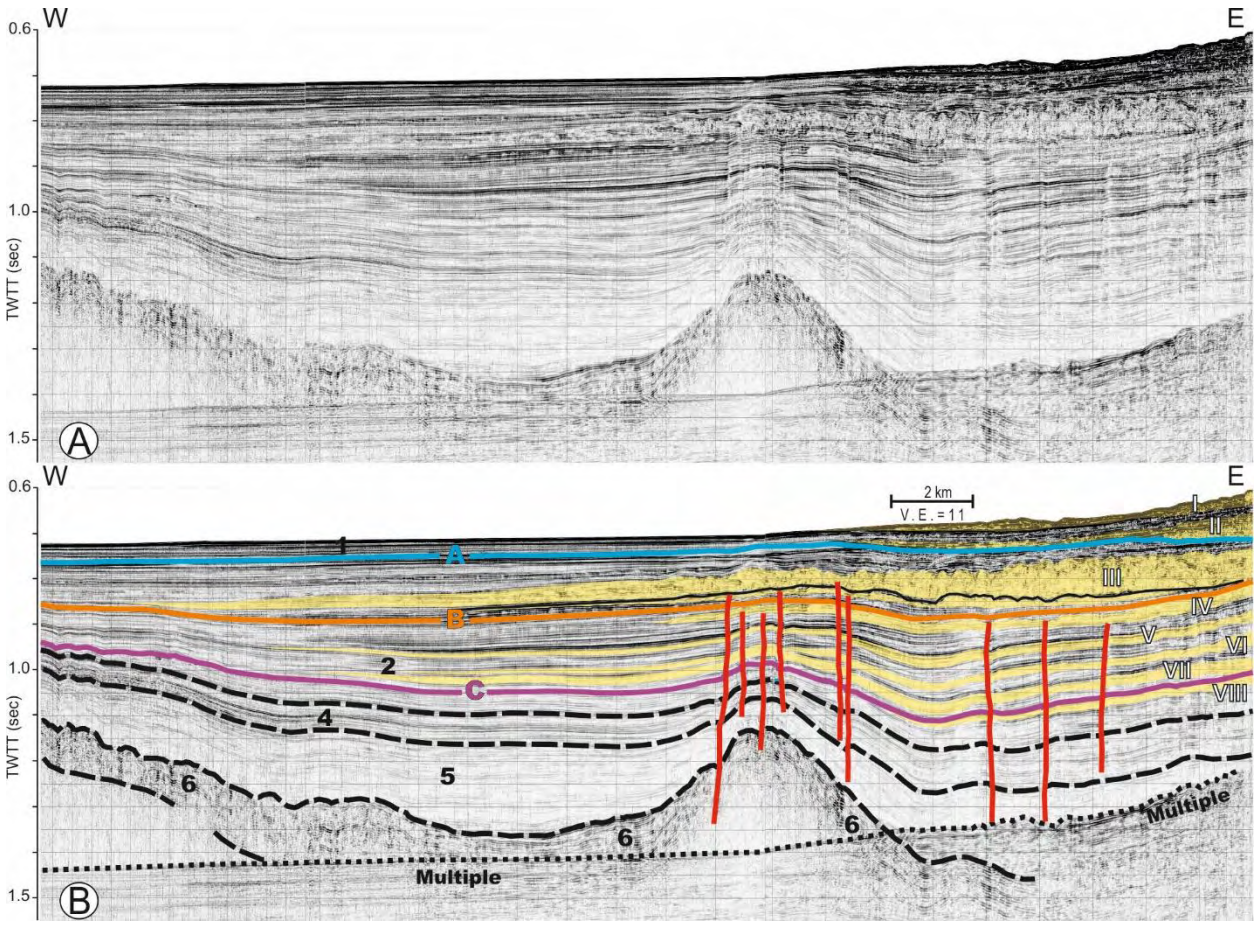

Fig. 4.1.7: (**A**) Uninterpreted, single channel seismic profile crossing the central-eastern part of Christiana Basin in W-E direction. (**B**) Interpreted profile showing seismic stratigraphy interpretation. The Roman numerals from I to III show pyroclastic flows as described in detail in the text. IV to VIII indicate probable, older pyroclastic flows. Explanation of the rest symbols as in Fig. 4.1.3.

upper internal reflectors of these units have been dragged upwards at the contact with the dome. The dome is characterized by transparent seismic character, without internal reflectors. The weakening and thinning of the overlying strata in Figures 4.1.6 and 4.1.7 indicate the vertical development of the domes that have intruded into the reflection geometry of the upper sediments by forcing them upwards. The fact that the domes of Figures 4.1.6 and 4.1.7 are very close on the map suggests that probably the seismic profiles have recorded the same structure from a different spatial angle. The available data and the results described so far are in favor of an evaporitic origin of the domes, in accordance with the interpretation of Bartole et al. (1983).

An incoherent, high amplitude, thick and morphologically irregular reflector marks the interface between Unit 5 or Unit 6 and the underlying acoustic basement of the basin indicating a hard substrate. This reflector occurs at shallow depths below the seafloor at the southern margin of Christiana Basin and is exposed at the northern margin. The seismic character, as well as the nature of the acoustic basement (Unit 7) underneath, coincides very well with the interface which represents the eroded surface of the alpine basement, initially exposed, before the onset of the basin's subsidence.

Finally, poorly preserved prograding deposits have been observed locally on the basin's margins. A northward prograding clinoform occurs on the southern margin, with the inflection point at roughly 650 msec (450–500 m) bpsl (Figure 4.1.6), indicating that Christiana Ridge was exposed above sea level. Prodelta deposits have also been mapped on the northern margin. One clinoform west of Folegandros displays topset to foreset transition at ~330 msec, while a second one south of the edge of Sikinos shelf is poorly acquired.

4.1.5.2. Basin's structure

The processing and interpretation of seismic data provide information on the main processes which have dominated the formation of Christiana Basin during Plio-Quaternary. Extensional and strike-slip faulting control the development of the basin. The seismic stratigraphy portrait, as described in the previous section, shows that a well stratified sedimentary sequence (Units 1 to 5) has been deposited on top of the Messinian evaporates in the basin and above the Alpine acoustic basement at the basin's margins. Three main depocenters are distinguished in the NW, W and SE part of the basin, wherein the sediments' thickness exceeds 600, 500 and 700 msec

respectively (Figure 4.1.8). Since the basement below the depocenters has not been imaged, the above values should be considered as minimum for the thickness of the depocenters.

The most striking feature arising from the structural interpretation of the seismic profiles is that the post-Miocene evolution of the basin displays two main stages. The formation of the three main depocenters is associated with the early stage of the basin. Subsidence in these three depocenters has been controlled by E-W trending faults which are now buried below the upper half of Unit 2. Activity on the old, marginal faults has ceased before the deposition of Reflector B, i.e. before 1.2 Ma or even earlier (Figures 4.1.4, 4.1.5 and 4.1.6).

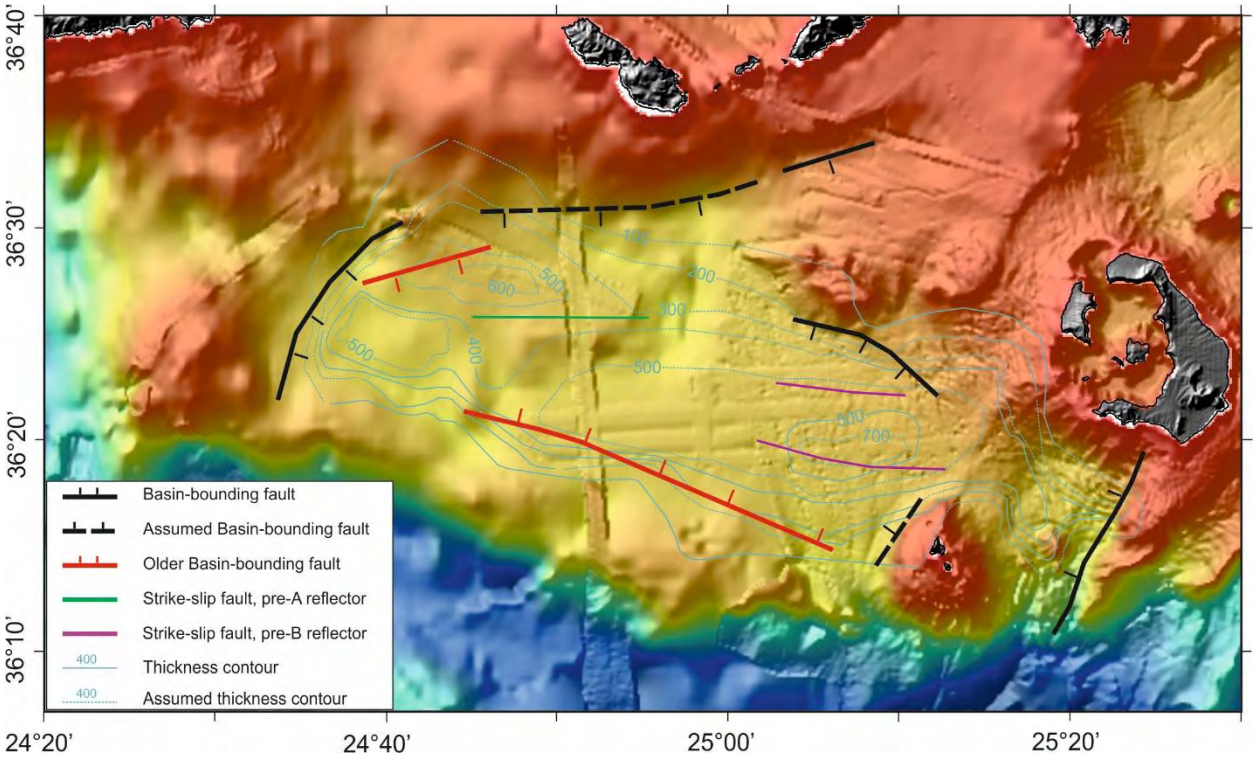

Fig. 4.1.8: Fault and sediment thickness map of Christiana Basin. Sediment thickness in milliseconds twtt.

During the early stage of the basin's evolution, the southern margin is controlled by one or more, WNW-ESE trending, north-facing faults (Figures 4.1.3, 4.1.4 and 4.1.6), which separate the lower part of the basin's infill (Units 5 and 4) to the north from the alpine basement of Christiana Ridge. The latter separates Christiana Basin to the north from Christiana Valley and the Cretan Basin to the south and extends from the South Milos High to the west to the volcanic dome of Christiana Islets to the east (Figure 4.1.1). Activity on the south marginal faults terminates either

at the end of the deposition of Unit 4 or shortly after. The greatest part of Unit 2 onlaps the irregular top surface of the alpine basement of Christiana Ridge.

In contrast to the other margins of the basin, the southern margin highlights the transition from the early, fault-controlled basin boundary to the present, not faulted margin which is unconformably overlain by the younger strata. The uplifted acoustic basement of Christiana Ridge forms a horst that separates Christiana Basin from the Cretan Basin. The ridge has undergone southward tilting, which is evident from the southward slopping of the top of the alpine basement and its sedimentary cover. Interestingly, the stratigraphic relationship of the sedimentary cover of the ridge to the basin infill indicates that southward tilting has continued for a long time after the termination of the activity on the south, basin-bounding faults.

The western and northern margins of the basin have migrated towards west and north respectively (Figure 4.1.4). The older faults run roughly E-W and control the northern boundaries of the depocenters. Similar to the southern marginal faults, they cease by the end of the deposition of Unit 4 or during the early parts of Unit 2. The present margin is defined by new faults which cut and downthrow the older margin. The seismic reflectors of Unit 2 onlap the alpine basement of the former margin (Figures 4.1.4, 4.1.5 and 4.1.6).

Narrow zones of deformation have been mapped between undeformed, well-stratified sediments. A group of near vertical (700–850) and deep-seated faults run through the basin in E-W direction, crosscutting its sedimentary infill. There is a considerable change in sediments reflectivity across these faults, with reflectors dragging downwards at both sides of the faults with a similar sense of vertical movement. In addition, splay faults branching from a main one, create local fault networks comparable to positive and/or negative flower structures. The aforementioned characteristics indicate significant strike-slip component (Figures 4.1.5 and 4.1.6). The intra-basinal faults remain active throughout the early stage of the basin's evolution and cease before the deposition of Reflector B, i.e. before 1.2 Ma.

The transition from the first (early) to the second (present) stage of development comes with a recognizable widening of the basinal area. The deposition of Unit 1 and of the upper half of Unit 2 takes place during the second stage. The main volcanogenic deposits (to be described in detail in the following section) occur in this stage too and are younger than Reflector B. Towards East,

Christiana Basin terminates at the large, composite volcanic mount of Santorini (Thera). It is the one that separates Christiana Basin from Anydhros and Amorgos Basins. At the SE border of the basin, east of Christiana islets, an apparently normal fault, trending NE-SW, follows the irregular morphology of the southern shelf of Santorini. The northwestern slope of Christiana islets coincides with an active, apparently normal fault trending NE-SW. It may probably be associated with the formation of the Christiana volcanic dome. The position and the orientation of these two faults are in line with the Kameni-Kolumbo fault zone, as described by Sakellariou et al. (2010).

The current picture of Christiana Basin suggests that it continues to be at the second phase of development, while the first stage probably lasted until Lower or Middle Pleistocene. The tectonic map (Figure 4.1.8) shows the main, basin-bounding and intra-basin faults and the sediment thickness (in milli-seconds two-way travel-time) above the alpine basement or above the Messinian.

4.1.5.3. Volcanic deposits in Christiana Basin sedimentary archive

The huge volume of volcanogenic material produced by the volcanic activity of Santorini during the late Quaternary can be mapped in the Eastern Mediterranean (Anastasakis, 2007) and particularly over a large area of the Aegean Sea, so unsurprisingly has also affected the deposition processes in Christiana Basin. The description of the seismic character and the reasons suggesting volcanic origin of the layers I, II and III has been given in **Section 4.1.5.1.** The soundest observation worth of repeating here is that these deposits can be mapped only in the eastern part of the basin. Their thickness decreases gradually with the distance from Santorini and consequently, their origin should be associated with Santorini's eruptive events. Notwithstanding the seismic character of I, II and III has been niched and described as Unit 3, there are some differences between them which will be discussed further below. In addition to the three major volcanogenic layers mentioned above, at least five layers, 20–30 msec thick, displaying chaotic seismic character and representing probable pyroclastic flows have been recognized in the lower half of Unit 2, below Reflector B, in the eastern part of the basin (Figure 4.1.7). If these layers do represent pyroclastic flows derived from Santorini volcanic center, they may constitute evidence of volcanic activity as early as Lower Pleistocene or Upper Pliocene. This paper focuses on the three most highly distinguished volcanogenic layers of the uppermost sedimentary sequence

above Reflector B, as they have been mapped on the seismic profiles acquired from the area. From the younger to the older they are named with the Roman numerals I, II and III.

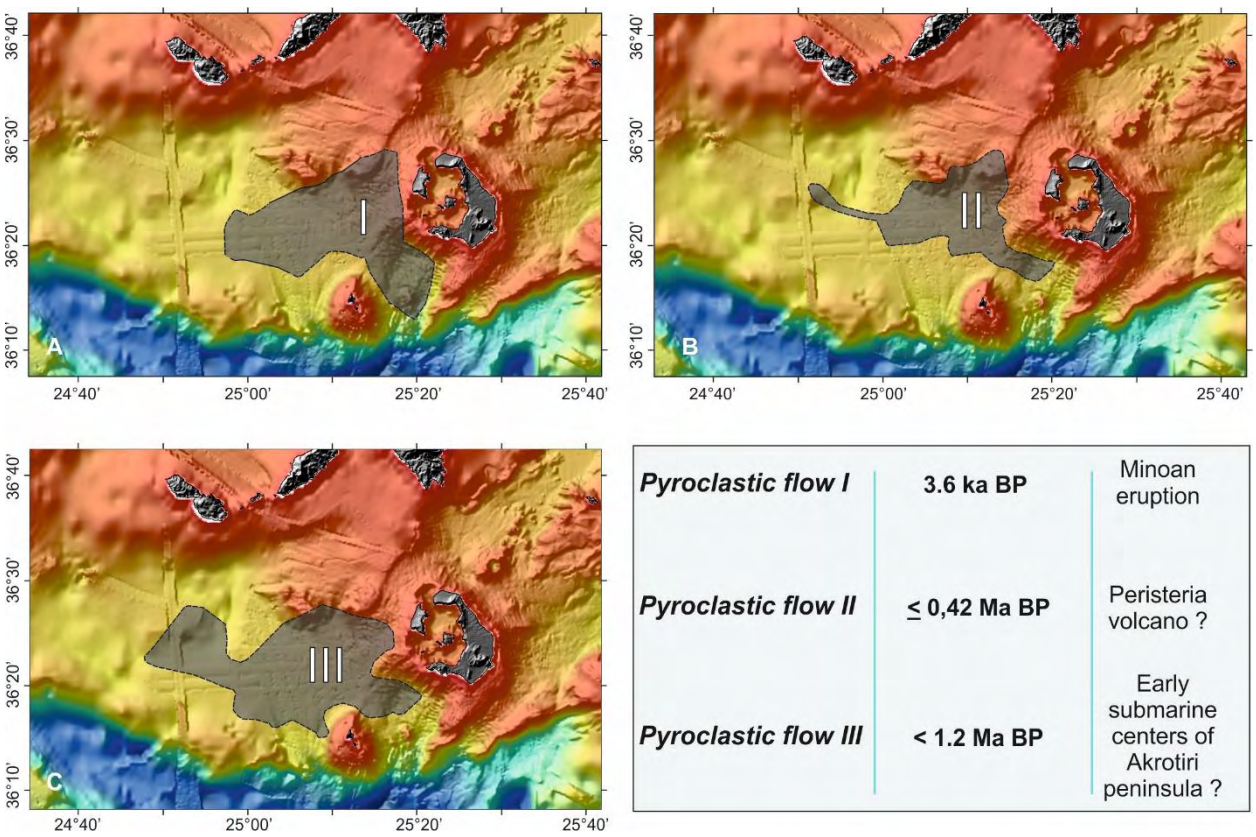

Fig. 4.1.9: Spatial distribution of pyroclastic flows in Christiana Basin. Pyroclastic flow I, (B) Pyroclastic flow II, (C) Pyroclastic flow III.

Layer I occurs on the seafloor, displays high relief and has a maximum thickness of 40–50 msec close to Santorini island. The available and studied seismic profiles do not provide sufficiently high-resolution information in order to identify sedimentary deposits covering the top of Layer I. The stratigraphic position of the latter on the very top of the basin's infill indicates that it has been emplaced during the last, large eruption of Santorini, the Minoan eruption. This is in agreement with the observations of Sigurdsson et al. (2006) for massive and chaotic layers of submarine pyroclastic flow deposits around Santorini. On the western slopes of Santorini, the Minoan pyroclastic flow deposits display a peculiar morphology with block-rich deposits forming a very irregular surface, an evidence of extensive instability. Slope failure processes affecting the submarine Minoan pyroclastic flow are known from the eastern flank of Santorini Island too (Bell et al., 2013). Towards west the top of the flow deposit becomes smoother and dis-

continuous, indicating that the greatest volume of the pyroclastic material has been deposited close to the islands. Figure 4.1.9A illustrates the spatial distribution of the Minoan pyroclastic flow deposits in Christiana Basin. Note that the area covered by the Minoan pyroclastic deposit is slightly larger than the one presented by Sigurdsson et al. (2006).

Layer II is considerably thinner than the previous one. It is observed at about 50 msec depth below the seafloor and is limited to the NE part of the Christiana Basin (Figure 4.1.9B). The Reflector A of Anastasakis and Piper (2005) coincides with the base of this layer, thus its age may be comparable to or slightly younger than ~0.42 Ma. Following this observation, we can reasonably assume that the volcanogenic layer II may be the result of an early eruption of Santorini, possibly associated with the Peristeria volcano, which is located in the northern part of the present caldera.

The Minoan eruption is one of the largest volcanic events known in historical time, comparable in size to the enormous eruption of Tambora, Indonesia in 1815 (Sigurdsson and Carey, 1989; Sigurdsson et al., 2006). Nevertheless, the related to the Minoan eruption layer I, compared to the layer III, looks small. The latter is the most widespread volcanogenic deposit occurring in Christiana Basin (Figure 4.1.9C). It is a major, thick flow, with thickness reaching 100 msec. The great thickness of this deposit, along with its extensive areal distribution in the basin, suggest that it has been generated by a very large eruptive event, possibly much larger than any other, known eruption of Santorini volcanic province. As described in the section on the Seismic stratigraphy, the pyroclastic flow III is embedded within unit 2. High amplitude, wavy and undulating reflectors characterize the upper part of the flow, while the lower part shows a more chaotic character. The internal structure of this layer displays hyperbolic echo prints indicating the presence of large blocks within the deposit. A high amplitude continuous reflector can be recognized at about 20 msec above the bottom, separating a lower and thinner part from an upper, considerably thicker one. This is probably an indication that the layer III may comprise multiple volcanic deposits. The stratigraphic position of III is between Reflectors A and B of Anastasakis and Piper (2005), which is between 0,42 and 1,25 Ma. Actually, in several parts of the basin Reflector B roughly coincides with the base of layer III, therefore, its emplacement may have taken place 1,25 Ma ago or shortly after. Consequently, layer III may be associated with one of

the early eruptions that took place in the Santorini volcanic field, probably with an eruption related with the Akrotiri volcanoes.

4.1.6. Discussion

4.1.6.1. Basin's stratigraphy

The geodynamic evolution of Christiana basin, the seismic stratigraphy and chrono-stratigraphy of its infill and the effect of multiple volcanic events on the sedimentary archive have been revealed through the processing and interpretation of the acquired seismic profiles.

Seven seismic units (1 to 7), with different seismic character and spatial distribution, have been mapped within Christiana Basin. The current study cautiously infers that Units 1, 2, 4 and 5 represent the Plio-Quaternary sediments overlying an erosional surface which corresponds to the Messinian Margin Erosion Surface (Roveri et al., 2014) at the basin's margin, while in the basin they have been deposited above the Messinian evaporites (Unit 6). The seismic characteristics of the surface and of the internal reflectors of Unit 6, as mentioned in **Section 4.1.5.1.** coincides very well with the results of DSDP Hole 378, in the Cretan Basin (Hsu et al., 1978). If this assumption is correct, then Unit 6 constitutes the selenite facies similar to the onshore Primary Lower Gypsum deposits (Lugli et al., 2010).

A dome in the central part of the basin has been interpreted as a probable salt dome formed due to mobilization or diapirism of the evaporite deposits. Still, the poor network of seismic reflection profiles adjacent to the dome and the attenuation of the seismic signal at the lowermost parts of the sedimentary sequence do not allow a confident adoption of a definitive interpretation and alternative interpretations for the origin of the dome cannot be excluded. Multiple working hypotheses have been applied to the best approach to the origin of the dome. One of the alternative interpretations is that compressional stress associated with strike-slip faulting cause the formation of pop up like structures. Nevertheless, no faults have been mapped in the vicinity of this structure which could explain the formation of the dome. Another alternative approach to the origin of the domes can be inferred from the findings of Hooft et al. (2017). These authors have mapped on the seafloor a shallow seamount, which they called Proteus Knoll. The geographic location of Proteus Knoll coincides roughly with the location of the dome observed in this paper (Figures 4.1.6 and 4.1.7). Hooft et al. (2017) assigned to the knoll a volcanic character

because of its shape, high magnetization and the steep sides. Since the basin of Christiana is located right on the volcanic arc, and even if the data presented here do not show evidence of volcanic activity below the basin, the volcanic origin of the domes can't be explicitly ruled out. However, any possible interpretation will still be a hypothesis if it cannot be confirmed by a dense network of high-resolution seismic profiles and/or by deep drillings.

Low sea-level delta progradation sequences, displaying the characteristic sigmoidal pattern of internal reflectors, have been observed along the northern and southern margin of the basin. At the southern margin the inflection point of the clinoform has been observed at around 450–500m bpsl. The prograding deposits on the northern margin occur at 240–250 m. Anastasakis and Piper (2005) identified the MIS 12 at 230m below sea level NW of Folegandros Island and estimated a mean subsidence rate of 0.23 m/ky. In the absence of any other chronological constrains it is reasonable to assume that the prograding deposits on the northern margin of Christiana Basin correspond to MIS 12 too. If the subsidence rate of the southern margin is comparable to the one of the northern margin, the sigmoidal deposits observed at 450–500m bpsl on the southern margin of the basin (northern flank of Christiana Ridge) should be significantly older than MIS 12. Consequently, Christiana Ridge must have been exposed and subjected to subaerial erosion during the formation of these clinoforms.

The seismic stratigraphy of the younger stage deposits is characterized by the presence of at least three chaotic layers (I, II, III, representative of unit 3) with irregular tops (Figures 4.1.3, 4.1.5, 4.1.7). They occur in the eastern part of the basin and their thickness diminishes towards west (Figure 4.1.9). They have been interpreted as volcanogenic deposits derived from Santorini volcanic center since Middle Pleistocene. The seismic characteristics of layers I, II, III as arise from the processing of the acquired profiles do not allow a clear interpretation and description of their volcanic origin and of the deposition mechanisms. However, the information extracted from the data are adequate to reach a potential interpretation. The seismic character and configuration of these deposits results in two possible interpretations about their emplacement mechanisms either as pyroclastic flows or as mass transport deposits related to volcanic activity, in particular as debris avalanche deposits. No clear distinguishing criteria are available in the literature regarding their different seismic characteristics that may allow their segregation. Systematic surveys from

other volcanoes, including Stromboli and Montserrat, did not provide decisive criteria to differentiate submarine pyroclastic flow from debris avalanche deposits (Sparks et al., 1980; Hayashi and Self, 1992; Legros and Druitt, 2000; Chiocci et al., 2008; Romagnoli et al., 2009; Crutchley et al., 2013; Karstens et al., 2013). Bell et al. (2013) have studied the hummocky seafloor features on the eastern submarine flank of Santorini volcano and concluded that they belong to 6 km wide, 20 km long and up to 75m thick, multi-stage debris avalanche deposit which is composed of pyroclastic flow deposits produced during the Minoan eruption. This composite landslide was caused by one of the several large earthquakes or volcanic eruptions that have occurred in or close to the Santorini volcano since the Minoan eruption. The Layer I has been mapped and studied by Sigurdsson et al. (2006) all around Santorini and has been interpreted as pyroclastic flow deposit related to the Minoan eruption. The Layers II and III display similar seismic characteristics to Layer I. Distinct concave-down reflection within layer III and adjacent to Santorini Island, indicate the existence of transported blocks. A similar to Layer III, chaotic deposit occurs at similar stratigraphic level on seismic profiles acquired east of Santorini and has been interpreted by Sakellariou et al. (2012) as pyroclastic flow deposit. Therefore, although the debris avalanche as deposition mechanism can't be excluded, the widespread distribution of layers I, II and III within Christiana Basin, their occurrence all around Santorini, the similarities of the seismic character of layers II and III with layer I which is confirmed as pyroclastic flow, and the absence of mapped scars associated with large volume landslides support their interpretation as pyroclastic flows.

4.1.6.2. Implications for the geodynamic evolution of the South Aegean Arc

The major conclusion on the structure of Christiana Basin derived from this study is the two-stage evolution with deactivation of the older basin-bounding faults, migration of the northern margin towards north and enlargement of the basin after Early to Middle Pleistocene. Similar observations have been reported from several other basins in the South Aegean Sea. Jongsma et al. (1977) report two post-Messinian unconformities observed in several basins of the South Aegean Sea, a first one in Middle Pliocene (around 3 Ma) and a second one in Late Pliocene (roughly 1.5 Ma). Bartole et al. (1983) state that among the various seismic unconformities in the South Aegean Sea, the most widespread one corresponds to the Lower-Middle Quaternary

unconformity (Q) found at DSDP 378 site, which dates the last significant tectonic event of the area. They have observed this unconformity in the basins of Heraklion, Akrotiri (north of Chania, Crete), Kamilonissi, east of Antikythera, east of Maleas and in Christiana Basin. Mascle and Martin (1990) have observed that in the South Aegean basins the Pliocene sediments are affected by extensional faulting and are overlain unconformably by Quaternary deposits.

Piper and Perissoratis (2003) have recognized major unconformities in the basins of the western South Aegean Sea at about 1 Ma, whereas they appear to become younger in the eastern part of the arc. They state that in the central part of the volcanic arc a pronounced change in fault pattern occurred at about 0.7 Ma, although E-W faults appear to have accommodated subsidence on the northern margin of the Christiana basin. This later hypothesis is slightly different from the results presented here, according to which the main, early, basin bounding faults ceased at or before 1.2 Ma.

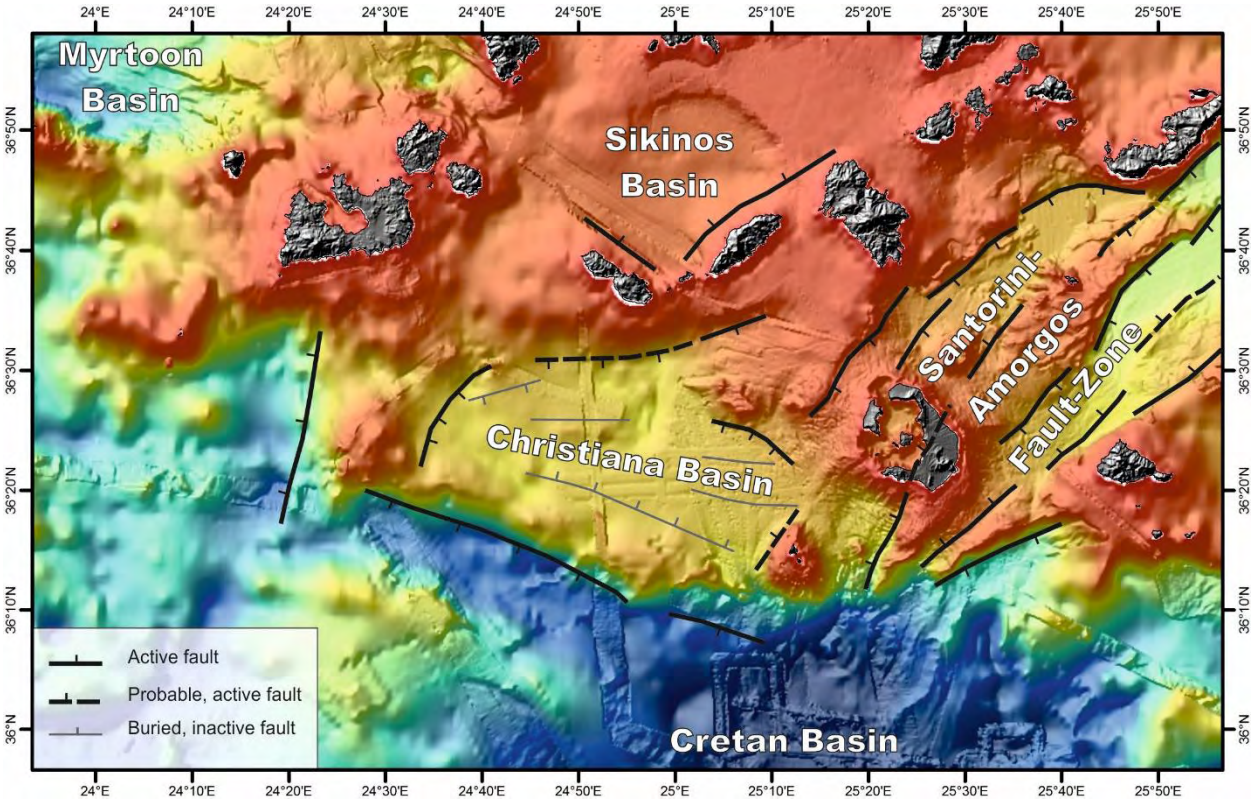

Fig. 4.1.10. Fault pattern in the central part of the Hellenic Volcanic Arc. Faults in Christiana Basin are from this study. Faults in the others areas have been drawn and modified after Mascle and Martin (1990), Piper and Perissoratis (2003), Piper et al. (2007), Sakellariou et al. (2010), Nomikou et al. (2016), Sakellariou and Tsampouraki-Kraounaki (2016), Tsampouraki- Kraounaki and Sakellariou (2017).

Ten Veen and Meijer (1998) state that the Pliocene-Messinian unconformity in Crete marks a change in tectonic style, from Late Miocene extension to Pliocene sinistral shear on a N75E shear. Similarly, Piper and Perissoratis (2003) have observed that in the eastern part of the South Aegean Arc, from Santorini through Amorgos to Kos, a pronounced NE-SW trending set of faults has been initiated in Middle Pleistocene while the general style of the faults, with narrow basement ridges and abrupt basin inversions, strongly suggests a strike slip regime. Piper et al. (2007) proposed a structural evolution of the area surrounding Santorini, according to which, predominantly E-W Pliocene faulting in Christiana Basin and Santorini to Amorgos area has been followed by NE-SW trending faults interpreted as dextral strike slip on the basis of seismicity data (Bohnhoff et al., 2006). These faults should have been initiated in the Early to Middle Quaternary (Piper and Perissoratis, 2003) as regional crustal-scale strike slip faults and thus potentially provide pathways for the ascent of magma.

Mascle and Martin (1990) had already recognized in the eastern part of the South Aegean Arc a deformation pattern consisting of NE-SW trending, elongated half grabens indicating active intense tectonism in the form of shearing associated with transcurrent faults. In accordance to that, Sakellariou et al. (2010) have proposed that the spatial distribution of the volcanic centers of Santorini volcanic group (Santorini and Kolumbo submarine chain) coincides with the NE-SW trending Anydros graben which constitutes a negative flower structure of a 40 km, possibly dextral, strike-slip zone, the Kameni-Kolumbo strike- slip and can be prolonged SW-wards to Christiana volcanic island. Recently, Tsampouraki-Kraounaki and Sakellariou (2017) mapped in detail, by means of systematic swath bathymetry and seismic profiling, the fault network of the NE-SW trending, morphologically complex area northeast of Thera till Amorgos, Astypalea and Kalymnos Islands, including the Anydhros Basin and the six sub-basins of Amorgos Basin. They concluded that this area undergoes dextral transtensional deformation accommodated by NE-SW strike-slip to oblique faults and E- W normal, step-over faults. The dextral sense of movement along the Santorini-Amorgos area inferred by geological criteria coincides with the seismological observations of Bohnhoff et al. (2006) who analyzed over 2000 earthquakes between 2002 and 2004 and concluded that the highest activity was identified along the SW–NE striking Santorini (Thera) - Amorgos zone which is present in the state of right-lateral transtension. Opposite to the

strike-slip character of deformation east of Santorini suggested by the previous authors, Hübscher et al. (2015), Nomikou et al. (2016, 2018) and Hooft et al. (2017) infer that normal faulting is the superior tectonic mechanism for the formation of Anydhros Basin and Santorini-Amorgos Ridge, while strike slip faulting is of local character with insignificant effect.

The data presented here on the two-stage structural evolution of Christiana Basin are in line with the observations from many other basins of the South Aegean Sea as described above. It is worth noting that the direction of the main, basin-bounding faults remains E-W throughout its evolution, during both the early and later stage. This is in contrast with the change of the fault trend and kinematics in the Santorini to Amorgos area from E-W normal faulting in Pliocene to NE- SW strike slip (or oblique) faulting since Early or Middle Quaternary (Piper et al., 2007; Tsampouraki-Kraounaki and Sakellariou, 2017). This apparent discrepancy may be explained by the change of the kinematic regime and the subsequent change of deformation style in the various areas. Thus, the general, extensional deformation accommodated by E-W trending faults prevailing throughout Pliocene over Christiana basin to Santorini, Amorgos, Astypalea and Kos area (Piper and Perissoratis, 2003) has been replaced in Early to Middle Quaternary in the area east of Santorini by NE-SW trending, dextral strike slip (or oblique slip with significant horizontal component) fault zone. The latter can be considered as a composite, dextral strike slip zone, the Santorini-Amorgos Fault zone (Figure 4.1.10) (Tsampouraki-Kraounaki and Sakellariou, 2017). Consequently, the E-W trending Christiana Basin, during its later stage of evolution, should be considered as an area of enhanced, localized extension developed on the right side of the southwestern termination of the NE-SW trending, dextral Santorini- Amorgos fault zone, similar to what would be expected in a “horsetail structure”.

4.1.7. Conclusions

The processing and interpretation of seismic profiles acquired from Christiana Basin provide evidence that the basin has been evolved in two stages. During the early stage, subsidence has been controlled by E- W to ESE-WNW trending faults with a significant horizontal component of movement. The formation of three main depocenters in the NW, W and SE part of the basin, with thickness of more than 600, 500 and 700 msec respectively, is associated with the early stage. The seismic units 5, 4 and the lower half of unit 2 have been deposited during the early stage. In the

eastern part of the basin, the lower half of unit 2, below reflector B, is characterized by the intercalation of at least five, 20–30 msec thick, chaotic layers (unit 3) with irregular tops (IV to VIII on Figure 4.1.7). They all thin out towards west, implying that they represent pyroclastic flow deposits originated from Santorini volcanic center in Late Pliocene to Early Pleistocene. The early stage of the evolution of the basin lasted until Early to Middle Pleistocene.

The end of the early stage is marked by the cessation of activity on the southern, basin bounding fault and the migration of the northern faults towards north. The upper half of the seismic unit 2 and the unit 1 have been deposited during the younger stage. The basin has expanded significantly towards south and north. The new deposits covered the old, southern tectonic margin of the basin and draped unconformably the Christiana Ridge. The originally horizontally deposited strata on the ridge include prodelta sequences and are now tilted towards south. The old northern margin has been covered too by the younger stage de- posits. The present northern tectonic margin is located much closer to Folegandros and Sikinos Islands and trends WSW-ENE.

On the basin's margins the Plio-Quaternary sedimentary formations overly the erosional surface of the Messinian, while in the basin, they have been deposited on the Messinian evaporites. A prominent dome observed in the central part of the basin has been interpreted as probable salt dome intruding the lower part of the basin infill.

The seismic stratigraphy of the younger stage deposits is characterized by the presence of three thick, chaotic layers (I, II, III, re- presentative of unit 3) with irregular tops (Figures 4.1.3, 4.1.5, 4.1.7). They occur in the eastern part of the basin and their thickness diminishes towards west (Figure 4.1.9). Their seismic configuration and spatial distribution in the Christiana Basin strongly suggest pyroclastic flow deposits derived from Santorini volcanic center since Middle Pleistocene. The youngest deposit I occurs on the seafloor, displays maximum thickness of about 50 msec and extensive slope failure structures on the eastern flank of Santorini and is associated with the Early Bronze Age (Minoan) eruption at 3.6 ka BP. The second deposit II, with a maximum thickness of 50 msec close to Santorini, is underlain by the Reflector A of 0.42 Ma suggested age (Anastasakis and Piper, 2005) and may be correlated with an eruption of the Peristeria volcano. Finally, the pyroclastic flow deposit III has been deposited on the seafloor of the eastern part of

Christiana Basin slightly after the Reflector B of 1.2 Ma suggested age (Anastasakis and Piper, 2005). It is the thickest (100 msec) and the widest distributed pyroclastic flow deposit in the basin and most probably the biggest known in the South Aegean Sea. As its presumed age is slightly younger than 1.2 Ma, it may be associated with an eruption of the early volcanic centers of Akrotiri. Note that the ages of II and III suggested here are slightly different from the ones observed by Piper et al. (2007).

All pyroclastic flow deposits observed and mapped on the seismic profiles of this study derive from the east, from the volcanic center of Santorini. Their ages span from the recent, 3.6 ka old Minoan flow (I) to the presumably Late Pliocene or Early Pleistocene flow deposits intercalated in the lower part of seismic unit 2. The seismic profiles studied here, as well as any other seismic profiles presented previously from Christiana Basin (Piper and Perissoratis, 2003; Anastasakis and Piper, 2005; Anastasakis, 2007) did not provide any evidence of volcanic deposits derived from west, i.e. from Milos volcanic center.

Acknowledgements

We are grateful to Ch. Anagnostou and E. Tripsanas for providing us with the old seismic profiles presented here and for the useful discus- sions. The first author would like to thank G. Anastasakis for the valuable and inspiring discussions during the supervision of her MSc thesis, parts of which have been used in this paper. The collection of the data presented here would not have been possible without the excellent collaboration with the captain and the crew of R/V Aegaeo. Their assistance and continuous support during the cruises in the South Aegean Sea have been extremely valuable. We thank David J.W. Piper and Laurent Jolivet for their valuable comments and critical reviews which significantly improved the final version of this work.

References

Anastasakis, G., 2007. The anatomy and provenance of thick volcaniclastic flows in the Cretan Basin, South Aegean Sea. Mar. Geol. 240, 113–135.

Anastasakis, G., Piper, D.J.W., 2005. Late Neogene evolution of the western South Aegean volcanic arc: sedimentary imprint of volcanicity around Milos. Mar. Geol. 215, 135–158.

Bartole, R., Catani, G., Lenardon, G., Vinci, A., 1983. Tectonics and sedimentation of the Southern Aegean Sea. Boll. Oceanol. Teor. Appl. 4, 319–340.

Bell, K.L.C., Carey, S., Nomikou, P., Sigurdsson, H., Sakellariou, D., 2013. Submarine evidence of a debris avalanche deposit on the eastern slope of Santorini volcano, Greece. Tectonophysics 597-598, 147–160.

Bohnhoff, M., Rische, M., Meier, T., Becker, D., Stavrakakis, G., Harjes, H.-P., 2006. Microseismic activity in the Hellenic Volcanic Arc, Greece, with emphasis on the seismotectonic setting of the Santorini–Amorgos zone. Tectonophysics 423, 17–33.

Chiocci, F., Romagnoli, C., Bosman, A., 2008. Morphologic resilience and depositional processes due to the rapid evolution of the submerged Sciara del Fuoco (Stromboli Island) after the December 2002 submarine slide and tsunami. Geomorphology 100 (3–4), 356–365.

Crutchley, G.J., Karstens, J., Berndt, C., Talling, P.J., Watt, S.F.L., Vardy, M.E., Hühnerbach, V., Urlaub, M., Sarkar, S., Klaeschen, D., Paulatto, M., Le Friant, A., Lebas, E., Maeno, F., 2013. Insights into the emplacement dynamics of volcanic landslides from high-resolution 3D seismic data acquired offshore Montserrat, Lesser Antilles. Mar. Geol. 335, 1–15.

Druitt, T.H., Mellors, R.A., Pyle, D.M., Sparks, R.S.J., 1989. Explosive volcanism on Santorini, Greece. Geol. Mag. 2, 95–126.

Druitt, T.H., et al., 1999. Santorini Volcano. J. Geol. Soc. Lond. Mem. 19 (Geological Society).

Friedrich, W., 2000. Fire in the Sea, The Santorini Volcano: Natural History and the Legend of Atlantis. Cambridge University Press, UK (ISBN 0521652901).

Fytikas, M., Innocenti, F., Kolios, N., Manetti, P., Mazzuoli, R., Poli, G., Rita, F., Villari, L., 1986. Volcanology and petrology of volcanic products from the island of Milos and neighbouring islets. J. Volcanol. Geotherm. Res. 28, 297–317.

Fytikas, M., Kolios, N., Vougioukalakis, G., 1990. Post-Minoan volcanic activity of the Santorini Volcano. Volcanic hazard and risk, forecasting possibilities. In: Hardy, D.A. (Ed.), Thera and the Aegean World III. 2. The Thera Foundation, London, pp. 183–198.

Hayashi, J., Self, S., 1992. A comparison of pyroclastic flow and debris avalanche mobility. J. Geophys. Res. 97 (B6), 9063.

Hooft, E.E.E., Nomikou, P., Toomey, T.R., Lampridou, D., Getz, C., Christopoulou, M.E., O'Hara, D., Arnoux, G.M., Bodmer, M., Gray, M., Heath, B.A., VanderBeek, B.P., 2017. Backarc tectonism, volcanism, and mass wasting shape seafloor morphology in the Santorini-Christiana-Amorgos region of the Hellenic Volcanic Arc. Tectonophysics 712–713, 396–414.

Hsu, K.J., Montadert, L., Bernouilli, D., Bizon, G., Cita, M., Erickson, A., Fabricius, F., Garrison, R.E., Kido, R.B., Mellieres, F., Muller, C., Wright, R.C., 1978. Site 378: Cretan basin. Init. Rep. Deep Sea Drill. Proj. 42 (1), 321–357.

Hübscher, C., Ruhnau, M., Nomikou, P., 2015. Volcano-tectonic evolution of the poly- genetic Kolumbo submarine volcano/Santorini (Aegean Sea). J. Volcanol. Geotherm. Res. 291, 101–111.

Jongsma, D., Wissman, G., Hinz, F., Garde, S., 1977. Seismic studies in the Cretan Sea. The southern Aegean Sea: an extensional marginal basin without sea floor spreading? Results of R.V. "Meteor" and R.R.S. "Shacleton" cruises. "Meteor" Forschungsergeb. Geol. Geophys. C 27, 3–30.

Karstens, J., Crutchley, G., Berndt, C., Talling, P., Watt, S., Hühnerbach, V., Friant, A., Lebas, E., Trofimovs, J., 2013. Emplacement of pyroclastic deposits offshore Montserrat: insights from 3D seismic data. J. Volcanol. Geotherm. Res. 257, 1–11.

Legros, F., Druitt, T., 2000. On the emplacement of ignimbrite in shallow-marine en- vironments. J. Volcanol. Geotherm. Res. 95 (1–4), 9–22.

Lugli, S., Manzi, V., Roveri, M., Schreiber, B.C., 2010. The Primary Lower Gypsum in the Mediterranean: a new facies interpretation for the first stage of the Messinian salinity crisis. Palaeogeogr. Palaeoclimatol. Palaeoecol. 297, 83–99.

Martin, L., 1987. Structure et evolution recente de la mere gee: apports d'une etude par seismique reflexion. These Doct. Univ, Paris VI.

Mascle, J., Martin, L., 1990. Shallow structure and recent evolution of the Aegean Sea: a synthesis based on continuous seismic reflection profiles. Mar. Geol. 94, 271–299.

Nomikou, P., Hübscher, C., Ruhnau, M., Bejelou, K., 2016. Tectono-stratigraphic evolu- tion through successive extensional events of the Anydros Basin, hosting Kolumbo volcanic field at the Aegean Sea, Greece. Tectonophysics 671 (2016), 202–217.

Nomikou, P., Hübscher, C., Papanikolaou, D., Farangitakis, G.P., Ruhnau, M., Lampridou, D., 2018. Expanding extension, subsidence and lateral segmentation within the Santorini - Amorgos basins during Quaternary: implications for the 1956 Amorgos events, central - south Aegean Sea, Greece. Tectonophysics 722, 138–153.

Papazachos, B.C., 1989. Long and short term prediction of the volcanic eruptions in Santorini. In: Proceedings of 3rd International Congress "Thera and the Aegean World III" 2, 125–129, September 4–8 1989, Santorini, Greece.

Papazachos, B.C., Panagiotopoulos, D.G., 1993. Normal faults associated with volcanic activity and deep rupture zones in the southern Aegean volcanic arc. Tectonophysics 220, 301–308.

Pe-Piper, G., Piper, D., 2002. The Igneous Rocks of Greece. Beitrage Zur Regionalen Geologie Der Erde. Vol. 30 Gebruder Borntraeger, Berlin-Stuttgart (573 pp.

Piper, D.J.W., Perissoratis, C., 2003. Quaternary neotectonics of the South Aegean arc. Mar. Geol. 198, 259–288.

Piper, D.J.W., Pe-Piper, G., Perissoratis, C., Anastasakis, G., 2007. Distribution and chronology of submarine volcanic rocks around Santorini and their relationship to faulting. Geol. Soc. Lond., Spec. Publ. 291, 99–111.

Romagnoli, C., Casalbore, D., Chiocci, F., Bosman, A., 2009. Offshore evidence of large- scale lateral collapses on the eastern flank of Stromboli, Italy, due to structurally- controlled, bilateral flank instability. Mar. Geol. 262 (1–4), 1–13.

Roveri, M., Manzi, V., Bassetti, M.A., Merini, M., Ricci Lucchi, F., 1998. Stratigraphy of the Messinian post-evaporitic stage in eastern-Romagna (northern Apennines, Italy). Giorn. Geol. 60, 119–142.

Roveri, M., Lugli, S., Manzi, V., Schreiber, B.C., 2008. The Messinian Sicilian stratigraphy revisited: toward a new scenario for the Messinian salinity crisis. Terra Nova 20, 483–488.

Roveri, M., Flecker, R., Krijgsman, W., Lofi, J., Lugli, S., Manzi, V., Sierro, F.J., Bertini, A., Camerlenghi, A., De Lange, G., Govers, R., Hilgen, F.J., Hübscher, C., Meijer, P.Th., Stoica, M., 2014. The Messinian Salinity Crisis: past and future of a great challenge for marine sciences. Mar. Geol. 349, 113–125.

Sakellariou, D., Tsampouraki-Kraounaki, K., 2016. Offshore faulting in the Aegean Sea: a synthesis based on bathymetric and seismic profiling data. Bull. Geol. Soc. Greece L/ 1, 124–133.

Sakellariou, D., Sigurdsson, H., Alexandri, M., Carey, S., Rousakis, G., Nomikou, P., Georgiou, P., Ballas, D., 2010. Active tectonics in the Hellenic Volcanic Arc: the Kolumbo submarine volcanic zone. Bull. Geol. Soc. Greece XLIII (2), 1056–1063.

Sakellariou, D., Rousakis, G., Nomikou, P., Bell, K.L.C., Carey, S., Sigurdsson, H., 2012. Tsunami triggering mechanisms associated with the 17th cent. BC Minoan eruption of Thera volcano, Greece. In: Proc., 22nd International Offshore and Polar Engineering Conference, Tsunami and Safety Symposium, pp. 61–67 (Rhodes, Greece, June 17–22, 2012).

Sigurdsson, H., Carey, S., 1989. Plinian and co-ignimbrite tephra fall from the 1815 eruption of Tambora volcano. Bull. Volcanol. 51 (4), 243–270.

Sigurdsson, H., Carey, S., Alexandri, M., Vougioukalakis, G., Croff, K.L., Roman, C., Sakellariou, D., Anagnostou, C., Rousakis, G., Ioakim, C., Gogou, A., Ballas, D., Misaridis, T., Nomikou, P., 2006. Marine investigations of Greece's Santorini volcanic field. Eos 87 (34), 337–339.

Sparks, R.S.J., Sigurdsson, H., Carey, S.N., 1980. The entrance of pyroclastic flows into the sea I. Oceanographic and geologic evidence from Dominica, Lesser Antilles. J. Volcanol. Geotherm. Res. 7 (1–2), 87–96.

Sparks, R.S.J., Brazier, S., Huang, T.C., Muerdter, D., 1983. Sedimentology of the Minoan deep-sea tephra layer in the Aegean and eastern Mediterranean. Mar. Geol. 54, 131–167.

Ten Veen, J.H., Meijer, P.Th., 1998. Late Miocene to Recent tectonic evolution of Crete (Greece): geological observations and model analysis. Tectonophysics 298, 191–208. Tsampouraki-Kraounaki, K., Sakellariou, D., 2017. Strike-slip deformation behind the Hellenic subduction: the Amorgos Shear Zone, South Aegean Sea. In: Proc. 8th Intern. INQUA Meeting on Paleoseismology, Active Tectonics and Archeoseismology, pp. 392–395

4.2. The Santorini-Amorgos Shear Zone: Evidence for Dextral Transtension in the South Aegean Back-Arc Region, Greece

https://doi.org/10.3390/geosciences11050216

4.2.1 Abstract

Bathymetric and seismic data provide insights into the geomorphological configuration, seismic stratigraphy, structure, and evolution of the area between Santorini, Amorgos, Astypalea, and Anafi islands. Santorini-Amorgos Shear Zone (SASZ) is a NE-SW striking feature that includes seven basins, two shallow ridges, and hosts the volcanic centers of Santorini and Kolumbo. The SASZ initiated in the Early Pliocene as a single, W-E oriented basin. A major reorganization of the geodynamic regime led to (i) reorientation of the older faults and initiation of NE-SW striking ones, (ii) disruption of the single basin and localized subsidence and uplift, (iii) creation of four basins out of the former single one (Anafi, Amorgos South, Amorgos North, and Kinairos basins), (iv) rifting of the northern and southern margins and creation of Anydros, Astypalea North, and Astypalea South basins, and (v) uplift of the ridges. Dextral shearing and oblique rifting are accommodated by NE-SW striking, dextral oblique to strike-slip faults and by roughly W-E striking, normal, transfer faults. It is suggested here that enhanced shearing in NE-SW direction and oblique rifting may be the dominant deformation mechanism in the South Aegean since Early Quaternary associated with the interaction of North Anatolian Fault with the slab roll-back.

4.2.2 Introduction

The Aegean back-arc domain displays a complicated, not yet fully understood, tectonic structure and has been developed on the southern edge of the overriding Eurasian plate, above the northward subducting slab of the East Mediterranean crust. The tectonic setting and the active deformation render the Aegean as a key area for the understanding of back-arc deformation processes. The post-Miocene history of the Aegean is characterized by back-arc extension already initiated in the Eocene (Brun et al., 2016; Jolivet et al., 2013 and references therein) and by the westward motion of Anatolia expressed through the dextral, strike-slip North Anatolian Fault (NAF) (Armijo et al., 1996; Armijo et al., 1999; Reilinger et al., 2010 and references therein). Several hypotheses have been proposed about the evolution of the complex deformation of the Aegean

(McKenzie, 1972; McKenzie, 1978; Le Pichon and Angelier, 1979; Dewey and Sengor, 1979; Le Pichon et al., 1981). Seismological and geological studies (Armijo et al., 1996; Armijo et al., 1999; Angelier et al., 1982; Le Pichon et al., 1982; Le Pichon, 1983; McKenzie and Jackson, 1986; Jackson and McKenzie, 2007; Taymaz et al., 1991; Jackson, 1994; Papazachos and Kiratzi, 1996; Papazachos et al., 1998; Goltsworthy et al., 2002; Kiratzi, 2003; Kokkalas et al., 2006; Chatzipetros et al., 2013) and GPS surveys (Billiris et al., 1991; Noomen et al., 1993; Straub and Kahle, 1994; Kahle et al., 1995; Le Pichon et al., 1995; Davies et al., 1997; Reilinger et al., 1997; Clarke et al., 1998; Cocard et al., 1999; Kahle et al., 2000; Briole et al., 2000; McClusky et al., 2000; Kreemer and Chamot-Rooke, 2004; Nyst and Thatcher, 2004; Reilinger et al., 2006; Reilinger et al., 2010; Perouse et al., 2012; Kassaras et al., 2020; Briole et al., 2021) have tried to define and explain the kinematic setting in the Aegean. However, comprehensive evidence on the geological evolution and the strain localization in the Aegean has not yet been revealed because there are still many areas that have either not been surveyed or have been with insufficient data (Sakellariou and Tsampouraki-Kraounaki, 2019).

The Aegean domain is characterized by Mascle and Martin, (1990) as a deforming microplate bounded to the north by the dextral North Anatolian Fault and to the south by the sinistral fault zones of Strabo and Pliny Trenches (Figure 4.2.1). The deformation in the northern part is mainly controlled by NE-SW trending strike-slip faulting (Sakellariou and Tsampouraki-Kraounaki, 2019). The active tectonic framework of the North Aegean, derived from geological and geophysical data and earthquake focal mechanisms, indicates a typical right-lateral strike-slip faulting regime (Taymaz et al., 1991; Kiratzi, 2003; Pavlides and Tranos, 1991) along the North Anatolian Fault and its southern branches. GPS data confirm the strike-slip motion across the NAF to about 23 mm/year (Kahle et al., 2000; McClusky et al., 2000; Kreemer and Chamot -Rooke, 2004; Nyst and Thatcher, 2004; Reilinger et al., 2006; Reilinger et al., 2010; Perouse et al., 2012; Müller et al., 2013). The central and western parts of the South Aegean Sea behave more or less like a rigid body, according to the kinematic model proposed by Kreemer and Chamot-Rooke, (2004). These authors suggest that the backstop of the Mediterranean Ridge (Figure 4.2.1) and the southern Aegean block exhibit insignificant internal deformation and move with 33–34 mm/year in the direction of S24° W ± 1° towards stable Africa, while the southeastern Aegean moves

moderately fast in an SSE direction, away from the rigid South Aegean (Kahle et al., 1999; Kiratzi, 2003; McClusky et al., 2000; Kreemer and Chamot -Rooke, 2004 references therein).

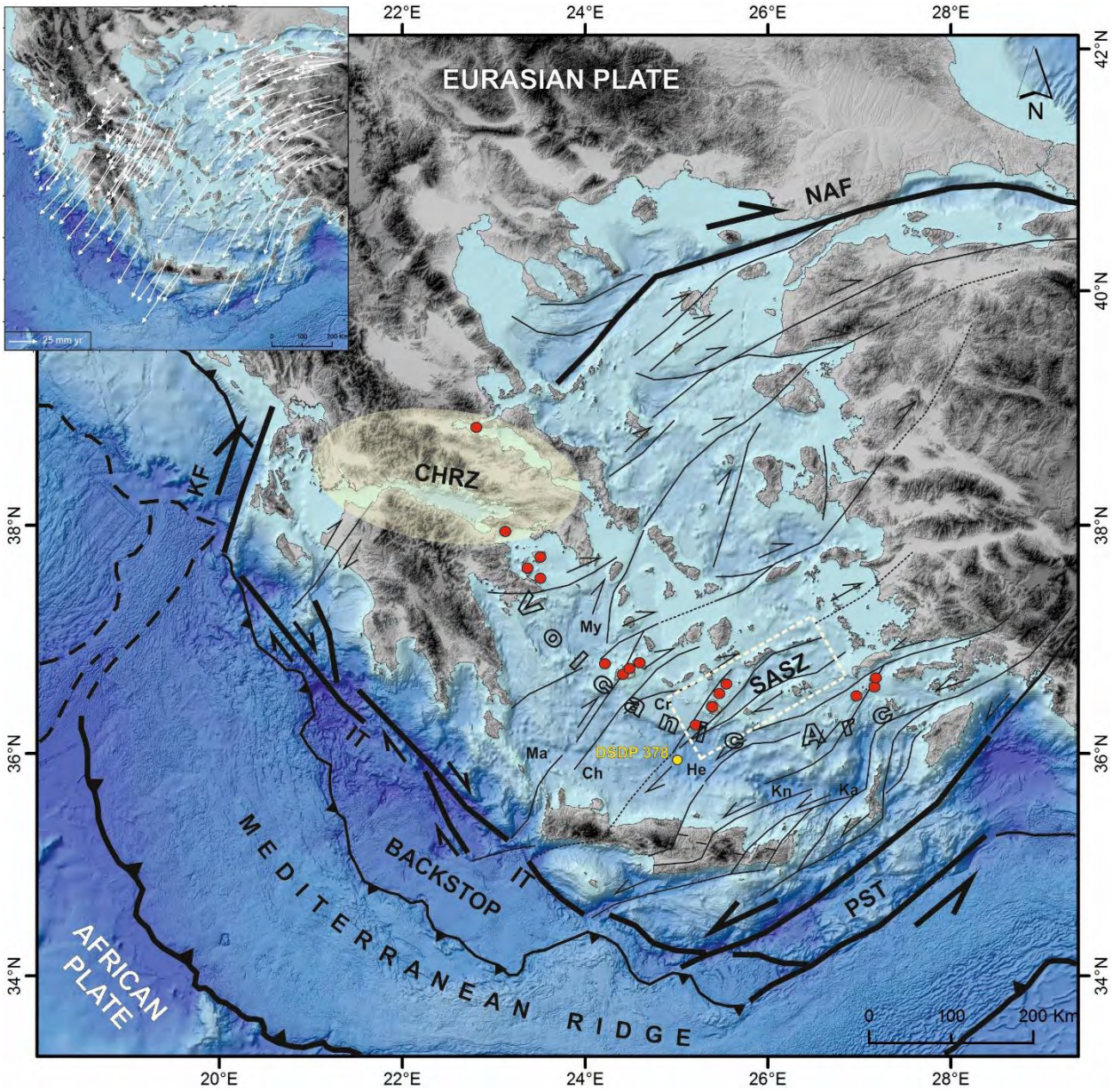

Figure 4.2.1: Major geodynamic elements of the broader Aegean Region, modified after Sakellariou and Tsampouraki-Kraounaki (Dimitriadis et al. 2009). The white parallelogram delineates the study area. Red dots represent the volcanoes on the Hellenic Volcanic Arc. NAF: North Anatolian Fault, KF: Kephallinia Fault, IT: Ionian Trench, PSF: Pliny-Strabo Trenches CHRZ: Central Hellenic Relay Zone, SASZ: Santorini-Amorgos Shear Zone. Basins: Cr: Christiana, He: Heraklion, Ka: Karpathos, Kn: Kamilonissi, Ma: Maleas, My: Myrtoon.

Although it is widely accepted that the geotectonic evolution of the Aegean microplate is dominated by extension in a back-arc setting, recent geological, seismological and geodetic studies have shown that overall extension may evolve in combination with transpression or transtention (Tur et al., 2015 and references therein). The uniqueness of this complex deformation developed in an active plate boundary zone, between two almost parallel but with opposite sense of movement strike-slip zones, demonstrates the distinctiveness of the area and explains the existence of multiple different kinematic models proposed so far (Figure 4.2.1). The style of deformation and kinematics changes from North to South across the Aegean. Dextral strike-slip tectonics along NE-SW major fault zones dominates in the North Aegean and as far south as the North Ikarian Basin (Kiratzi, 2003). Sakellariou and Tsampouraki-Kraounaki, (2019) propose that dextral-strike slip faulting prevails further to the South, with the Santorini-Amorgos (SA) Fault Zone being the last one towards the south, that displays a dextral sense of motion. This is in agreement with the results of the micro-seismicity research of Bohnhoff et al., (2006), who suggest right-lateral transtension along the SW–NE Santorini (Thera)-Amorgos zone with the direction of extension being NW–SE. They also propose that Santorini-Amorgos Zone is a major structural boundary of the Hellenic Volcanic Arc which is characterized by crustal weakness and divides the seismically and volcanically more active eastern part from the quiet western part.

The same area seems to be a transition zone between the northern and southern Aegean, as the change from dextral to sinistral sense of shear seems to occur south of the Santorini-Amorgos Fault Zone. Pe-Piper et al. (2005) related the volcanism at Kos and Nisyros islands with sinistral ENE–WSW trending strike-slip faults. Furthermore, recent studies of Uluğ et al., (2005) and İşcan et al., (2012) have shown that the Gulf of Gökova (GG), east of the island of Kos, undergoes deformation related to strike-slip tectonics. Ocakoğlu et al., (2018) also mapped a left-lateral NE-SW strike-slip fault zone with segments crossing the Gökova Gulf from its northern part to south of Kos. Tur et al., (2015) interpreted this area as part of a lazy-S shaped structure which includes the Kamilonisi Basin (KaB), the South and North Karpathos Basins (SK and NK), and the Gulf of Gökova. The aforementioned literature data verify the suggestion of Mascle and Martin, (1990) according to which, NE-SW trending shear zones control the Plio-Quaternary evolution of the Aegean. Further on, they support the observations of Sakellariou and Tsampouraki-Kraounaki,

(2019) on the change of the sense of shear, from dextral to sinistral, across the Aegean. According to Sakellariou and Tsampouraki-Kraounaki, (2019) the Santorini-Amorgos Fault coincides with the southeastern boundary of the "rigid "Central Aegean Block with the deforming Southeast Aegean Block as defined by Reilinger et al. (2010).

The present study focuses on the southeastern margin of the Central Aegean Sea (Figure 4.2.1), particularly in the area between Santorini, Amorgos, and Astypalea islands, referred to as Santorini-Amorgos Shear Zone (SASZ). The purpose of this study is divided into two main levels. The detailed mapping of the morphotectonic tissue of the area, through the presentation of the results concerning the seismic stratigraphy, the seabed morphology, and the dominant fault network of the area constitute the first level. The interpretation and understanding thereof, lead us to the second level and to the questions arising from its correlation with the deformation prevailing in the entire Aegean domain.

4.2.3 Geological setting

4.2.3.1 Regional Geological Setting

The study area is bounded by the islands of Central and southeastern Aegean and, more specifically, by Santorini Island to the west, Amorgos Island and Kinairos and Levitha Islets to the north, and Anafi and Astypalea Islands to the south (Figure 4.2.2). Metamorphic, volcanic and Neogene-Quaternary sediments constitute those islands (Bornovas and Rondoyanni, 1984). The central and western part of that area is described by Nomikou et al. (2018) as the Santorini-Amorgos Tectonic Zone (SATZ). Alpine formations, separated by the system of Miocene extensional detachments, form the basement of the area. Metamorphic rocks of the Attico-Cycladic complex constitute Santorini's basement (Kilias et al., 2013). The metamorphic formations of the Atticocycladic massif (gneisses, schists, marbles, and limestones) covering the greatest part of the island of Amorgos and the eastern part of Anafi (Melidonis, 1964) show a different stratigraphy, related to the external shallow-water carbonate platform of the Hellenides (Fytrolakis and Panikolaou, 1981; Papanikolaou, 2013). According to Papadopoulos and Pavlides (1992), Amorgos Island is constituted by rocks of the Triassic, post-Triassic-Eocene, and middle Eocene-Oligocene. Very few outcrops of Pleistocene and alluvial deposits can be found. The morphology of the Amorgos Island is the result of brittle deformation (mainly normal to right-

lateral oblique-slip faults) (Papadopoulos and Paviles, 1992 and references therein). Non- or low-grade metamorphic rocks of Late Cretaceous age crop out on Anafi (Soukis and Papanikolaou, 2004).

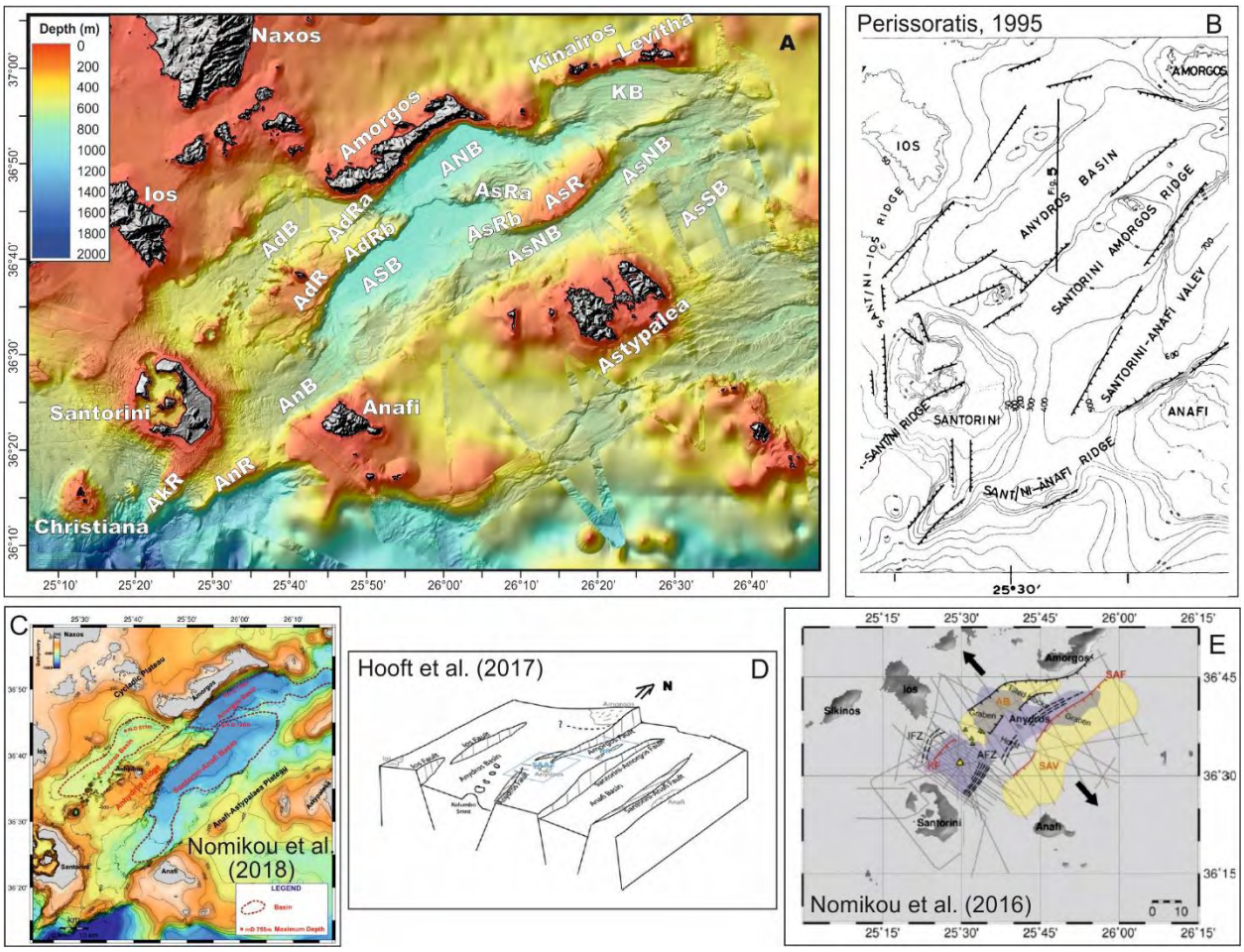

Figure 4.2.2: (**A**): Terminology of the main geomorphological elements used and discussed in the current work. AdB: Anydro Basin, AdR: Anydros Ridge, AnB: Anafi Basin, ANB: Amorgos North Basin, ASB: Amorgos South Basin, AsNB: Astypale North Basin, AsSB: Astypalea South Basin, AsR: Astypalea Ridge, KB: Kinairos Basin. Bathymetry: 25 m resolution swath bathymetry superimposed on 100 m resolution EMODNET Bathymetry. (**B**–**E**): Terminology used by Perissoratis (1995) Nomikou et al. (2018), Hooft et al. (2017), and Nomikou et al. (2016), respectively.

4.2.3.2 Seismostratigraphy of the Area

Several studies focusing on the seismic stratigraphy of the area, provide useful information on the sedimentary sequences deposited offshore. Perissoratis (1995) mapped the main morphological features of the area between Santorini and the southwestern edge of Amorgos (Figure 4.2.2) and named them as Anydros Basin, Santorini-Amorgos Ridge, Santorini-Anafi Valley, and Santorini-Anafi Ridge. The same designations were also adopted by Nomikou et al.

(2016). Afterwards, Hooft et al. (2017) renamed Santorini-Anafi Valley to Anafi Basin, and, one year later, Nomikou et al. (2018) expanded their field of research to the east (south of Amorgos Island) and recognized the existence of another basin, named as Amorgos Basin (Figure 4.2.2). The same study renamed the Anafi Basin to Santorini-Anafi Basin. The presentation of the results of the preexisting literature follows the naming of the morphological features as described in each work from which the specific results are taken.

Plio-Quaternary sediments of 600–700 m thickness maximum, intercalated with volcanoclastic material mainly in Anydros Basin, have been mapped in the offshore area (Perissoratis, 1995; Nomikou et al., 2016; Sakellariou et al., 2017; Hübscher et al., 2015). Three distinct seismo-stratigraphic units referred to as A, B, and C (from top to bottom) are recognized and described by Perissoratis (1995) within Anydros Basin and Santorini-Anafi Valley. Unit A is divided into two subunits, unit A1 and unit A2, by an erosional unconformity which is related to various sea-level changes that occurred during the Quaternary. Unit A1 shows high amplitude strong subparallel reflectors, while unit A2 displays a more regular and parallel seismic character. In some areas, subunit A1 lies conformably on A2, and it is not clearly distinguishable from A2 (Piper and Perissoratis, 2003). Syn-sedimentary faults mainly only affect subunit A2. Unit B is overlain unconformably by unit A2 (UR2) on ridges and on some basins and conformably in some basin areas (Piper and Perissoratis, 2003). Unit B is unconformably resting on unit C showing strong and continuous reflectors, such as those in subunit A2, although its reflectors display higher amplitude. The unconformity between Unit A and Unit B coincides with the Pliocene/Quaternary boundary of the drilling results of Site 378 (Hsu et al., 1978), indicating that Unit B is mainly of Pliocene age, while Unit A is assumed to be of Quaternary age (Perissoratis, 1995). According to Perissoratis (1995), the lowermost parts of unit B were deposited as a basin filling facies during and after the formation of the basins. Unit C marks the acoustic basement in the survey area and represents the alpine formations of the Atticocycladic Massif that crop out on the surrounding islands (Perissoratis, 1995; Nomikou et al., 2016). On the Santorini-Anafi Valley, Unit C can be mapped only in the shallow areas of the surrounding ridges. The Santorini-Amorgos Ridge is mainly formed by unit C that is locally covered by thin layers of sediments. Unit A is considered to be of Quaternary age, and unit B is mainly of Pliocene age (Perissoratis,

1995). Piper and Perissoratis (2003), following the interpretation of the seismic stratigraphy of Perissoratis (1995), named the unconformities within subunits A1–A2, and units B and C from top to bottom as UR1, UR2, and UR3 for the offshore area between the Santorini, Anafi, and Amorgos islands. UR1 is equivalent to the UK1 unconformity (west of Kalymnos) and the UN1 unconformity (between Kos and Nisyros). UN1 postdates the Kos Plateau Tuff that has a radiometric age of 161 ka [68]. Based on a mean sedimentation rate of 0.1 m/kyear, the estimated age of UR3 is 150–190 ka (Smith et al., 1996).

Within the sedimentary sequence of Anydros Basin, six basin-fill units have been mapped, from AB-1 to AB-6, and are separated by unconformities ab-1 to ab-6 (Nomikou et al., 2016; Nomikou et al., 2018). The same authors related units AB-6 and AB-5 with units A1 and A2 (volcanoclastics of Quaternary age) of Perissoratis (1995) and unit AB-4 with unit B (terrestrial or shallow water sediments of Pliocene age). Hübscher et al. (2015) related the five angular unconformities to rift pulses and suggested that they are associated with the five eruptive phases of the Kolumbo submarine volcano. Within the sedimentary sequence of Santorini-Anafi Basin (SAB), six different seismic units have been mapped and named from bottom to top as Sab-1 to Sab-6 [54], while Sab-0 corresponds to the acoustic basement. The interface between Sab-1 and Sab-0 displays a strong amplitude character with chaotic reflections beneath it. Nomikou et al. (2018), recognized seismic units Amb-6 to Amb-3 as equivalents of the four upper units of Santorini-Anafi Basin and suggested that the Amorgos Basin is younger than SAB and AB.

An attempt to define a chronological framework about the geodynamic evolution of the area was made by Nomikou et al. (2018), based on the work of Hinsbergen et al. (2007). They suggested that the older parts of the sedimentary sequence (named as Units 1–3 on their study) are related with the initiation of the Aegean strike-slip system around 5.3–3.8 Ma, and the upper observed unconformities are related to the Rhodos tilting on 2.5–1.8 Ma and on 0.8 Ma.

4.2.3.3 Tectonic Setting

Due to the complexity of the deformation in back-arc areas, the precise mechanisms dominating and affecting the formation of the main geomorphological features are not yet clear. The contradiction of the different theories, that have been suggested about the geodynamic processes that dominate the Aegean region and vary from the expected pure extension, that is

customary to occur on back-arc zones, to more complex zones of transpresion and transtention (Sakellariou and Tsampouraki-Kraounaki, 2019), seems to be imprinted in the Santorini Amorgos Shear Zone, as well. Mascle and Martin (1990) and Piper and Perissoratis (2003) provided tectonic maps of the offshore faulting in the South Aegean Sea. Mascle and Martin (1990) were the first to recognize NE-SW trending strike-slip faulting in the area. Papadopoulos and Pavlides (1992) characterized the master neotectonic fault of Amorgos as an oblique-normal fault with a significant right-lateral strike-slip component and suggested that the tectonic picture of the area is more complex than the pure extension expected in back-arc basins.

Perissoratis et al. (1993) suggested that the main faults controlling the deformation at the offshore area eastwards of Santorini Island trend NE-SW and were activated after the previous NW-SE trending faults. The predominant fault network that formed the Santorini-Anafi valley, the Anydros Basin, and the Santorini-Amorgos Ridge (Figure 4.2.2) trends NE-SW and has resulted from the offset of the preexisting E-W faults and, secondarily, from earlier N-S faults that formed the Santorini-Anafi Ridge (Perissoratis, 1995). The E-W and N-S faults affected the older parts of the sedimentary sequence (Unit C and the lower part of Unit B), while the NE-SW trending faults affected the younger parts (the uppermost part of Unit B and Unit A) of the sedimentary sequence (Perissoratis, 1995). From Kos through Amorgos to Santorini, the 650-trending strike-slip faulting initiated around 0.6–0.8 Ma near Amorgos, 0.4 Ma east of Astypalea, and 0.2 Ma around Nisyros, while the basinal areas between Amorgos and Santorini which were formed during the deposition of Unit B prior to 0.6 Ma, now form prominent ridges (Piper and Perissoratis, 2003). The shift of the tectonic regime from E-W to NE-SW led to basin inversion (Perissoratis et al., 1993; Piper and Perissoratis, 2003). The style of NE-SW faulting, the narrow basement ridges, and the basin inversions strongly suggest a strike-slip regime (Piper and Perissoratis, 2003; Piper et al., 2007).

Sakellariou et al. (2017) proposed that both Thera and Kolumbo volcanic centers occur within the NE-SW-trending Anydros graben, which constitutes a negative flower structure related to a 40-km long, possibly dextral, strike-slip zone, the Kameni-Kolumbo strike-slip, which can be extended SW-wards to the Christiana volcanic island. This is in agreement with the results of Heath et al. (2019), who found that the volcanic centers of Christiana-Santorini and Kolumbo lie

in a NE-SW trending basin-like structure, named as proto-Anydros Basin. They also confirm that volcanism initiated after the transition to NW-SE extension in the Pleistocene, as has been proposed also by previous models. Hübscher et al. (2015), although they do not recognize strike-slip indicators within Anydros Basin, do not exclude the possibility of their existence. Nomikou et al. (2016) proposed normal, NE-SW trending faulting as the main deformation mechanism. Secondary faults, showing remarkable steep dip angles, probably indicate a strike-slip component, which could explain the presence of right lateral transtensional stresses, expected by Bohnhoff et al. (2006) and Sakellariou et al. (2017). Tsampouraki-Kraounaki and Sakellariou (2017) suggest that the NE-SW-trending and morphologically complex area northeast of Thera until the Amorgos, Astypalea, and Kalymnos islands (which encompasses Anydhros Basin and the six subbasins of Amorgos Basin) undergoes dextral transtensional deformation accommodated by NE-SW strike-slip to oblique faults and E-W normal step-over faults. These results coincide very well with the microseismicity data of Bohnhoff et al. (2006), who observed the highest seismic activity along the SW–NE striking Santorini–Amorgos zone and proposed that the Santorini–Amorgos zone is presently in the state of right-lateral transtension, acting as a major structural boundary of the volcanic arc between a seismically and volcanically quite western and an active eastern part. The results of Dimitriadis et al. (2009, 2010) on the seismic activity of the Santorini-Kolumbo zone and of Papadimitriou et al. (2015) on the caldera of Santorini are in agreement with these observations.

On the other hand, the interpretation of the data of Nomikou et al. (2018) support normal faulting as the main deformation mechanism that forms the geomorphological features of the area.

The available GPS campaigns indicate that the central Aegean acts as a coherent block moving SW with little internal deformation. Geological and geodetic data indicate that, south of the Amorgos shear zone, the sense of shear changes from the dextral transtension of the Santorini to Amorgos area and the dextral oblique rifting along the Amorgos shear zone (Bohnhoff et al., 2006; Piper et al., 2007; Sakellariou et al., 2017; Tsampouraki-Kraounaki and Sakellariou, 2017; Tsampouraki -Kraounaki and Sakellariou, 2018), to sinistral towards the southeast. Tzanis et al. (2020) studied the kinematic regime of the Santorini area by using gravity, magnetotelluric, and

DGPS data. According to their interpretation, kinematics in that area is characterized by NW-SE dextral strike slip faults and NE-SW normal to sinistral faults generated by N-S oriented σ1 and E-W oriented σ3. Very recently, Briole et al. (2021), based on a dense network of GPS stations, analyzed the velocities of the period 2000–2020, and they quantified several characteristics of the deformation of the Aegean. They built a kinematic model comprising ten crustal blocks corresponding to areas where the velocities present homogeneous gradients. The major fault zones and zones of localized deformation constitute boundaries between the blocks. Amorgos basin fault zone is one of these boundaries where the authors recognize a dextral transtensional movement of 4.5 mm year-1 between the Amorgos and Astypalea islands.

4.2.3.4 The 1956 Amorgos Earthquake

The exceptional magnitude 7.8 of the 9 July 1956, Amorgos earthquake, and the tsunami that followed, have affected that area and caused several damages on the neighboring islands. A second seismic event, with a magnitude of M = 7.2, followed the first earthquake 13 min later in the same region. The focal mechanism of the Amorgos 1956 earthquake and the precise location of its epicenter are still debated. Papadopoulos and Pavlides (1992) noted that the 1956 mainshock, the epicenter of its largest aftershock, and the volcanic centers of Santorini, Christiana, and Columbo strike along the same structural line, indicating a possible geodynamic association between the seismotectonic and volcanotectonic processes in this part of the South Aegean. Various studies have been conducted in order to understand the focal mechanism of the Amorgos earthquake. The proposed focal mechanisms vary between dextral strike-slip and dip-slip movement on a NE-SW-trending SE dipping fault (Okal et al., 2009 and references therein). Okal et al. (2009) and Shirokova (1972) proposed a normal faulting geometry, while Papazachos and Delibassis (1961) and Ritsema (1974) suggested strike-slip as the focal mechanism. Brüstle et al. (2014) proposed a dextral SE dipping normal fault plane solution as the focal mechanism for the first event and a thrust fault mechanism for the second.

4.2.4 Materials and Methods

This study uses two data sets, swath bathymetry and seismic profiles, collected during various cruises of HCMR's research vessel ***AEGAEO***. Swath bathymetry data were collected with the use of a hull-mounted multibeam system ***ELAG SEABEAM 2120*** (20 kHz) and ***1180*** (180kHz) as

follows (Figure 4.2.3): (i) around Santorini Island in 2001 (Alexandri et al., 2003) and 2006 [THERA project (Sigurdsson et al., 2006)]; (ii) east and southeast of Astypalea in 2007–2008 (Nomikou and Papanikolaou, 2011); (iii) between Amorgos, Anafi, and Astypalea Islands in 2016 during the

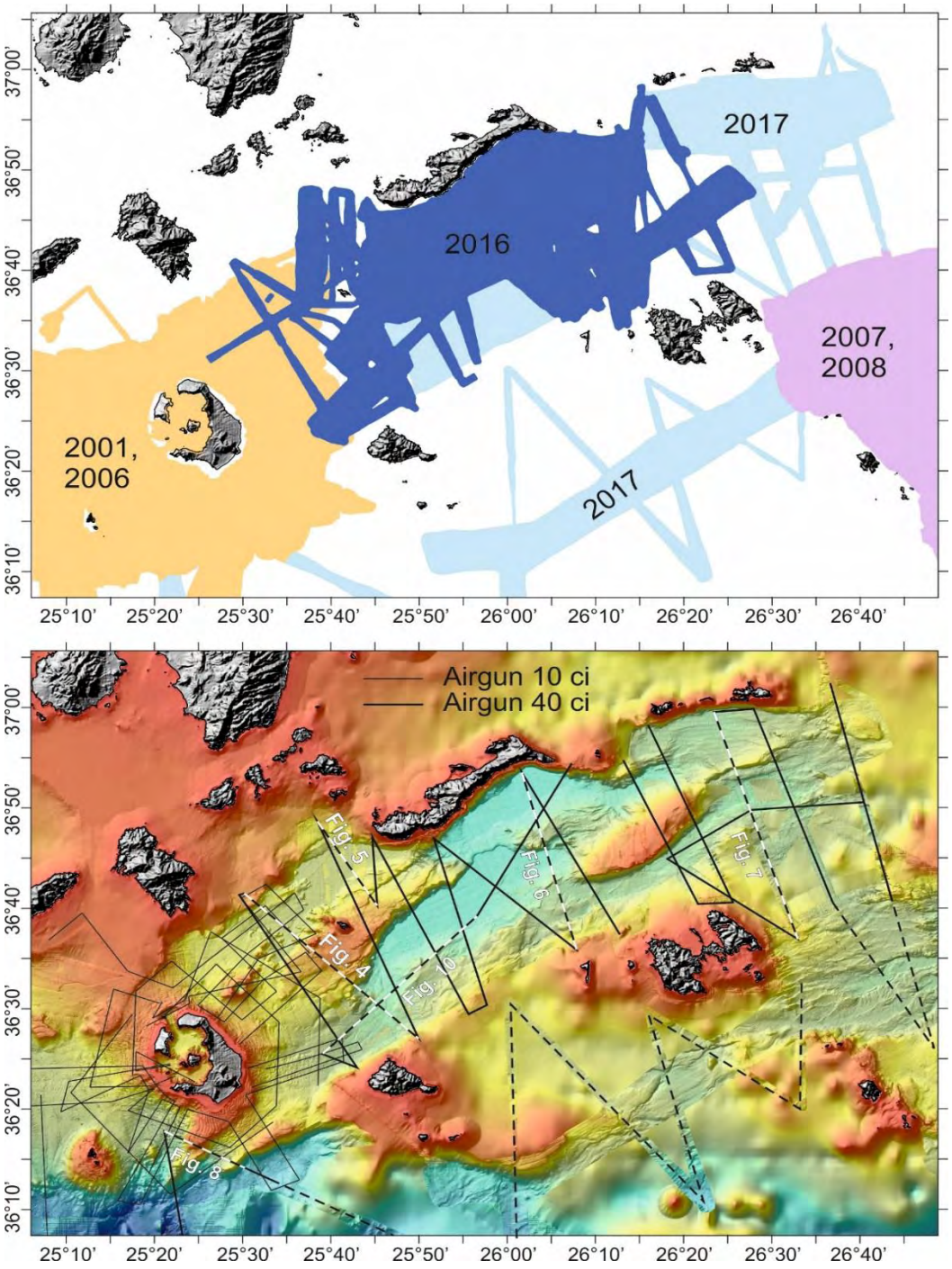

Figure 4.2.3: Left: Swath bathymetry coverage and year of acquisition. Right: Swath bathymetry map of the study area showing the location of the airgun 10 ci and 40 ci seismic lines acquired in the study area. Dashed white and black lines show the seismic lines described in the text.

Eurofleets2 LGT-AMORGOS-56 cruise; (iv) east of Amorgos Island and south of Anaphi and Astypalea Islands in 2017 (SOUTH AEGEAN cruise). All recent and older swath bathymetry data were integrated into one data set, processed using the MB-System, PDS 2000, and Global Mapper software and reprocessed at 20 m resolution in Arc-GIS.

Single channel seismic profiles were collected during the following three cruises (Figure 4.2.3): ***airgun 10 in³*** profiles in 2006 around Santorini (THERA project) and airgun 40 in³ in 2016 (Eurofleets2 LGT-AMORGOS-56 cruise) and in 2017 (SOUTH AEGEAN cruise). In all surveys, the sound source was towed at 2–5-3 m water depth behind the stern of the vessel. The 2006 profiles have been recorded on a surface towed SIG seismic streamer (65 m active length, 48 hydrophones at 1 m spacing) Triton Imaging, Inc. acquisition software and hardware at 2 s shooting rate. The 2016 and 2017 profiles have been recorded on ***CodaOctopus DA4G™ 2000*** acquisition software and hardware at 3 s shooting rate. The ***CodaOctapus Survey Engine*** software has been used for the processing of all profiles and the improvement of the signal-to-noise ratio when needed. Processing included adjustment of time varied gain (TVG), signal rectification (when necessary), across track smoothing, and pass-band frequency filtering between 100 Hz and 300 Hz.

4.2.5 Results

4.2.5.1 Bathymetry-Geomorphology

The Santorini Amorgos Shear Zone is a composite morphological feature that includes seven NE-SW trending, spindle-shaped or elongated basins and two uplifted, shallow ridges. The names of the basins, from the northwest to the southeast, are: Anydros (AdB), Anafi (AnB), Amorgos South (ASB), Amorgos North (ANB), Kinairos (KB), Astypalea North (AsNB), and Astypalea South Basins (AsSB). The ridges are named as Astypalea (AsR) and Anydros (AdR) Ridges, while both display two splays (Figure 4.2.2). Two more, smaller ridges, Akrotiri (AkR) and Anafi (AnR), occur in the southwestern part of the study area. Their main morphological characteristics are presented in Table 4.2.1**.**

Astypalea Ridge (AsR) is located on the NE part of the study area and separates Kinairos and Amorgos North basins from Astypalea North Basin. Its main body is located southeast of Amorgos Island and displays elongated, flat-topped shape. The ridge is extended approximately

19 km to the NE as a very narrow elevation of the seafloor which separates Kinairos Basin from the eastern part of Astypalea North Basin. To the SW, it is divided into two branches. The W-E trending northern branch (AsRa) splays out of the northwestern side of the main body and separates Amorgos North from Amorgos South basins. A series of SW dipping faulted escarpments separate it from the main body. Its prolongation towards the west is connected with the Anydros Ridge. The southern branch (AsRb) initiates in the southwestern tip of AsR and prolongs towards the SW. It separates the Amorgos South from the Astypalea North basin and merges with the steep slope NE of Anafi Island.

The NE-SW trending, elongated Anydros Ridge (AdR) is located at the western part of the study area. Its summit at the center of the ridge forms the Anydros islet. Towards the SW, the top of the ridge deepens gradually and smoothly, to form a roughly 400 m deep morphological saddle between Anydros Ridge and the steep eastern slopes of Santorini. Taking into consideration the main morphological direction prevailing in the study area, the Anydros Ridge is in line with the mountainous part (Profitis Elias Mt.) of southern Santorini and with the Akrotiri Ridge. The northeastern part is divided into two branches by the prolongation of the Amorgos escarpment. The northern branch (AdRa) connects with the steep, NE-SW trending slope off Amorgos, while the southern branch (AdRb) connects with AsRa.

Akrotiri Ridge (AkR) constitutes the underwater prolongation of the southern part of Santorini towards the SW. AkR extends roughly 20 km off the southwestern coast of Santorini and its top displays rugged morphology. It separates Christiana Basin to the NW (Tsampouraki-Kraounaki and Sakellariou, 2019) from the westernmost part of Anafi Basin to the SE.

Anafi Ridge (AnR) runs parallel to and south of Akrotiri Ridge. The island of Anafi marks the northeastern termination of the AnR. It separates the 400 m western part of Anafi Basin from the over 1000 m deep Cretan Basin to the south.

The narrow, elongated Anydros Basin is located NE of Santorini. It is bounded to the NW by the faulted slopes of the islands of Ios and Koufonisia and to the SE by Anydros Ridge. The floor of the SE part of the basin hosts more than 20 volcanic cones, including the submarine volcano Kolumbo (Nomikou et al., 2012). The cones display conical or sub-conical shape, and their NE-

SW linear distribution follows the direction of the long basin axis. Contrary to the SW part, the seafloor on the NE part of the basin is flat and free of volcanic structures.

Table 4.2.1. Morphological characteristics of SASZ basins and ridges.

Geomorphological feature	*Length (km)*	*Width (km)*	*Orientation*	*Margins / Slopes*	*Other Information*
Astypalea Ridge (AsR)	29	9	NE-SW	Steep faulted SE-dipping slope	Two branches (AsRa, AsRb)
Anydros Ridge (AdR)	37	11	NE-SW	Steep faulted SE-dipping slopes	Two branches (AdRa, AdRb)
Akrotiri Ridge (AkR)	17	< 5	NE-SW	Steep NW and SE slopes	SW of Santorini Island
Anafi Ridge (AnR)	30	< 6	NE-SW	Steep NW and SE slopes	Ends on Anafi Island
Anydros Basin (AdB)	> 42	< 10	NE-SW	Steep faulted NE margin, variably steep NW and SE margins	It hosts the Kolumbo volcanic chain. N-ward asymmetry of the NE part of the basin
Anafi Basin (AnB)	40	< 8	NE-SW	Variably steep SE and NW margins	S-ward asymmetry
Amorgos South Basin (ASB)	43	11	NE-SW	Steep faulted NW margin. Gently sloping S and SE margins.	N-ward asymmetry
Amorgos North Basin (ANB)	34	9	NE-SW	Steep faulted NW margin. Gently sloping S and SE margins.	N-ward asymmetry
Kinairos Basin (KB)	32	11	ENE-WSW	Steep northern margins	N-ward asymmetry
Astypalea North Basin (AsNB)	63	6	NE-SW	Steep, faulted northern margin	N-ward asymmetry
Astypalea South Basin (AsSb)	22	18	ENE-WSW		

Amorgos North (ANB) and Amorgos South (ASB) basins display similar morphological characteristics. Both basins display morphological asymmetry, with steep, faulted, northern

margins. ASB is a spindle shaped basin, bounded to the North by the Anydros Ridge and the northern branch of Astypalea Ridge (AsRa). The southern boundary is formed by the NE-SW trending slope of Anafi and the southern branch of Astypalea Ridge (AsRb). ANB is a triangular to lazy-S-shaped basin. The steep slopes of Amorgos Island form the northern margin of ANB, while the northern branch of Astypalea Ridge constitutes the southern margin.

Kinairos Basin has been developed south of the islands of Kinairos and Levitha. It displays northward asymmetry with a steep northern boundary and a smooth southern margin to the northeastern prolongation of Astypalea Ridge.

A gentle elevation of the seafloor divides Astypalea Basin into two sub-basins. The northern one (AsNB) is characterized by a very narrow and elongated shape, which shows a convex shape, following the curvature of Astypalea Ridge. The southern one (AsSB), east of Astypalea Island, displays more irregular and asymmetric shape. However, a thorough analysis and description of AsSB does not fall within the goals of the present work.

Anafi Basin is bounded to the north by Akrotiri Ridge, Santorini Island, and Anydros Ridge and to the South by Anafi Ridge, Anafi Island, and the shallow plateau between Anafi and Astypalea. Anafi Basin displays elongated shape in NE-SW direction and, opposite to the previously described basins, is characterized by southward asymmetry.

4.2.5.2 Seismic Stratigraphy: Basins

Seven basins (AdB, AnB, ASB, ANB, KB, AsSB, AsNB) separated by structurally uplifted ridges have been identified in the study area. Similarities and differences, observed in the seismic stratigraphy of the basins, provide insights into the Plio-Quaternary evolution of the Santorini-Amorgos Shear Zone. Despite some variations and differences in the seismic stratigraphy of each basin, a common designation was used to describe the seismic packages constituting their sedimentary infill. Six successive seismic units have been mapped within the sedimentary infill of the basins, named from top to bottom as Units 1, 2, 3, 4, 5, and 6.

Unit 1, the youngest one, is characterized by well stratified, closely spaced, high amplitude, coherent and continuous reflectors running parallel to the seafloor. Unit 2 displays a more complex seismic character and shows differences from basin to basin, which will be discussed in more detail in the analysis of the seismic stratigraphy of each basin. It is mostly characterized by

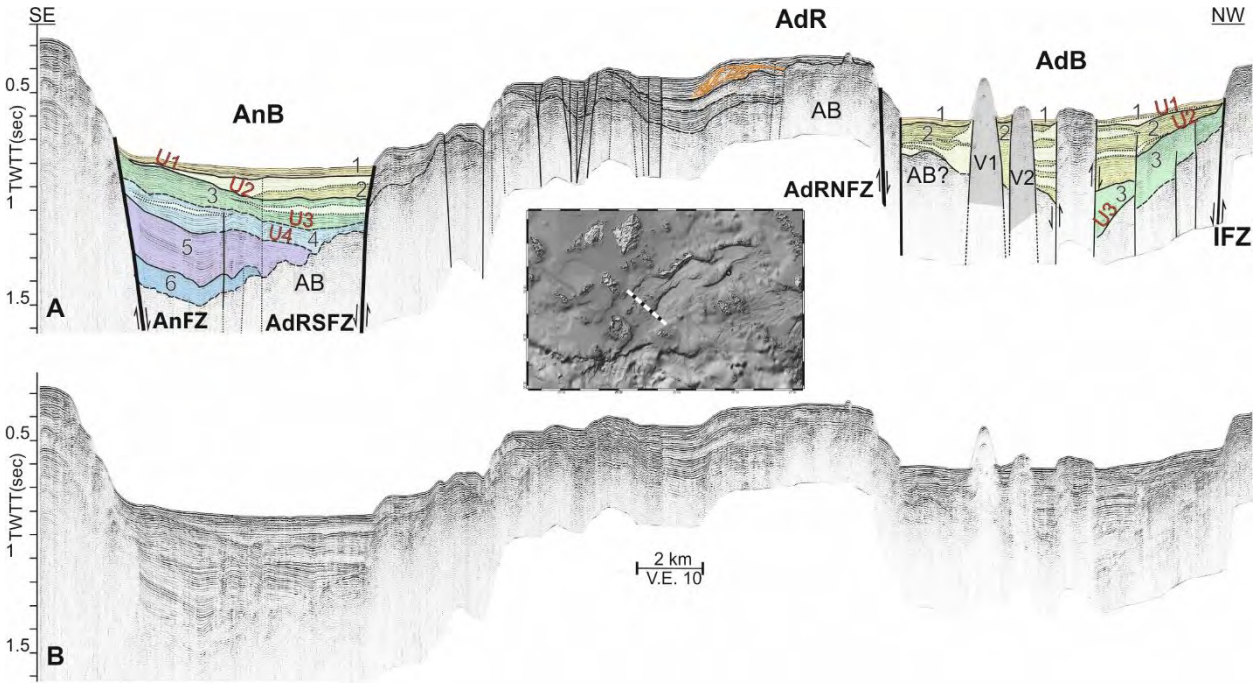

Figure 4.2.4: Air gun 40 ci seismic profile crossing the western part of Anydros Basin (AdB), Anydros Ridge (AdR), and Anafi Basin (AnB). The numbers 1 to 6 represent the six seismic units described in the text. U1, U2, U3, and U4 correspond to the observed, major unconformities. AB: Acoustic Basement, AdRNFZ: Anydros Ridge North Fault Zone, AdRSFZ: Anydros Ridge South Fault Zone, AnFZ: Anafi Fault Zone IFZ: Ios Fault Zone. V1 and V2: Submarine volcanic domes of Kolumbo chain.

high amplitude, semi-continuous, undulating, and medium coherent reflectors, alternating with low coherent energy and internal high amplitude, discontinuous and irregular reflectors. Unit 3 is defined by a rhythmic alternation of high amplitude, continuous and parallel reflections with transparent and semi-continuous reflections and/or incoherent, low amplitude discontinuous reflectors. Unit 4 is characterized mainly by high amplitude, continuous, parallel reflectors which, in some cases, become more undulating and discontinuous with depth. Unit 5 shows a rhythmic alternation of high amplitude, continuous and parallel reflectors with semi-continuous, medium amplitude and wavy reflectors Finally, Unit 6 is characterized by an upper surface with high to medium amplitude, undulating, incoherent, and transparent reflectors, while, at the base of Unit 6, in some areas, a highly irregular, rugged reflector, which marks the transition from Unit 6 to the acoustic basement, has been observed.

The interpretation of the seismic stratigraphy revealed at least 4 major unconformities in nearly all basins suggesting that successive, major tectonic events have affected the entire area of Santorini-Amorgos Shear Zone (SASZ) during its evolution. They are named from top to bottom as U1, U2, U3, and U4. U1 is defined by a high amplitude and continuous reflector, and it is a relatively shallow unconformity, at roughly 30–50 msec depth below the seafloor that separates seismic Unit 1 above from seismic Unit 2 below. It has been mapped in the Amorgos South and Amorgos North basins, within the Astypalea North and South basins, in Anafi Basin, and in the western part of Anydros Basin (Figures 4.2.4, 4.2.5, 4.2.6, 4.2.7, 4.2.10).

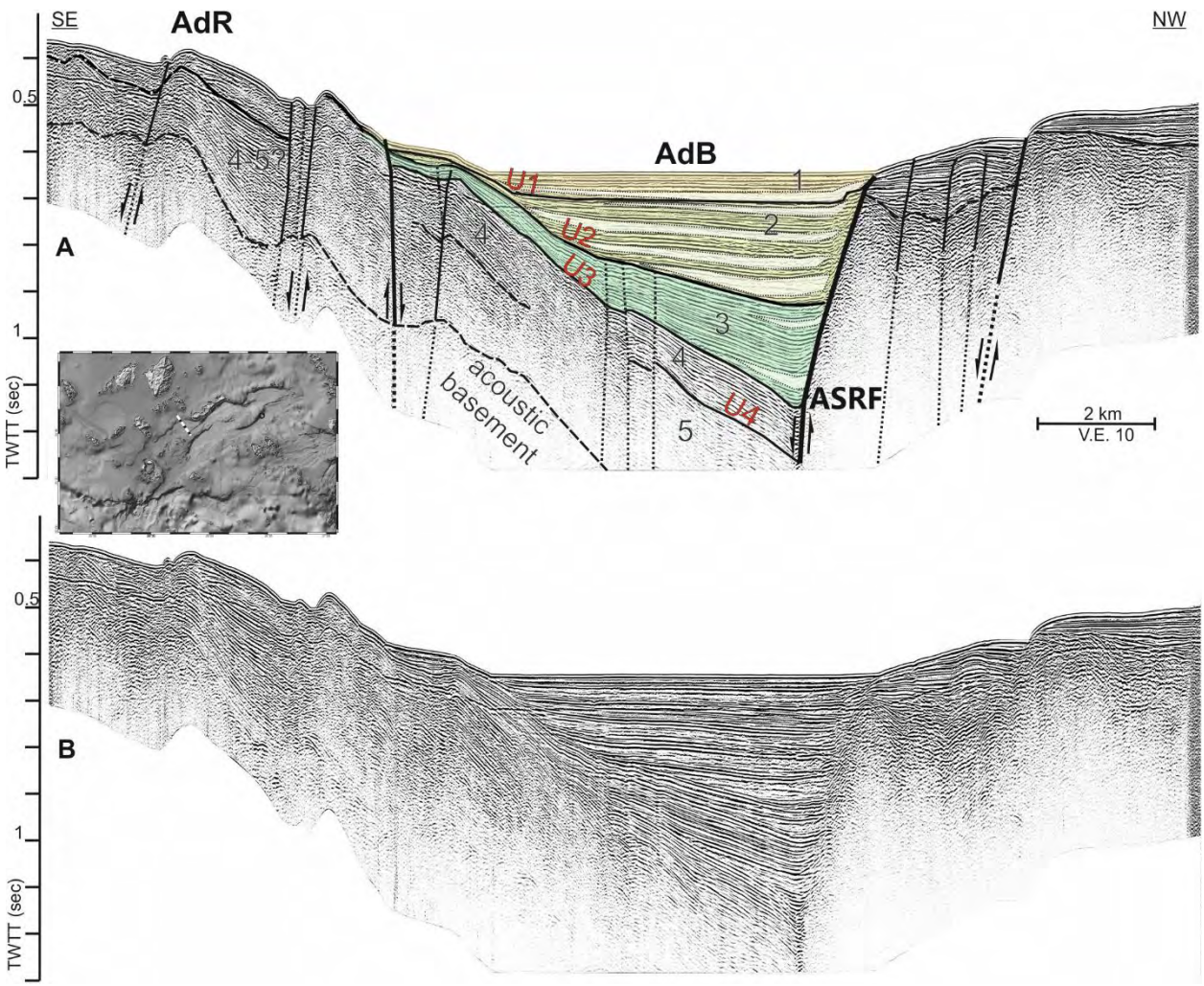

Figure 4.2.5: Airgun 40 ci seismic profile across the eastern part of Anydros Basin (AdB). AdR: Anydros Ridge, ASRF: Amorgos South Relay Fault. Terminology and symbols as in Figure 4.2.4.

Unconformity U2 is imaged as a high amplitude, erosional, undulating reflector that separates Unit 2 from Unit 3. It has been mapped in the Anydros, Anafi, Kinairos, Amorgos South, and Amorgos North basins and in the southwestern part of Amorgos South Basin (Figures 4.2.4, 4.2.5, 4.2.6, 4.2.7, 4.2.10). The internal reflectors of Unit 3 are truncated upwards by the Unconformity U2.

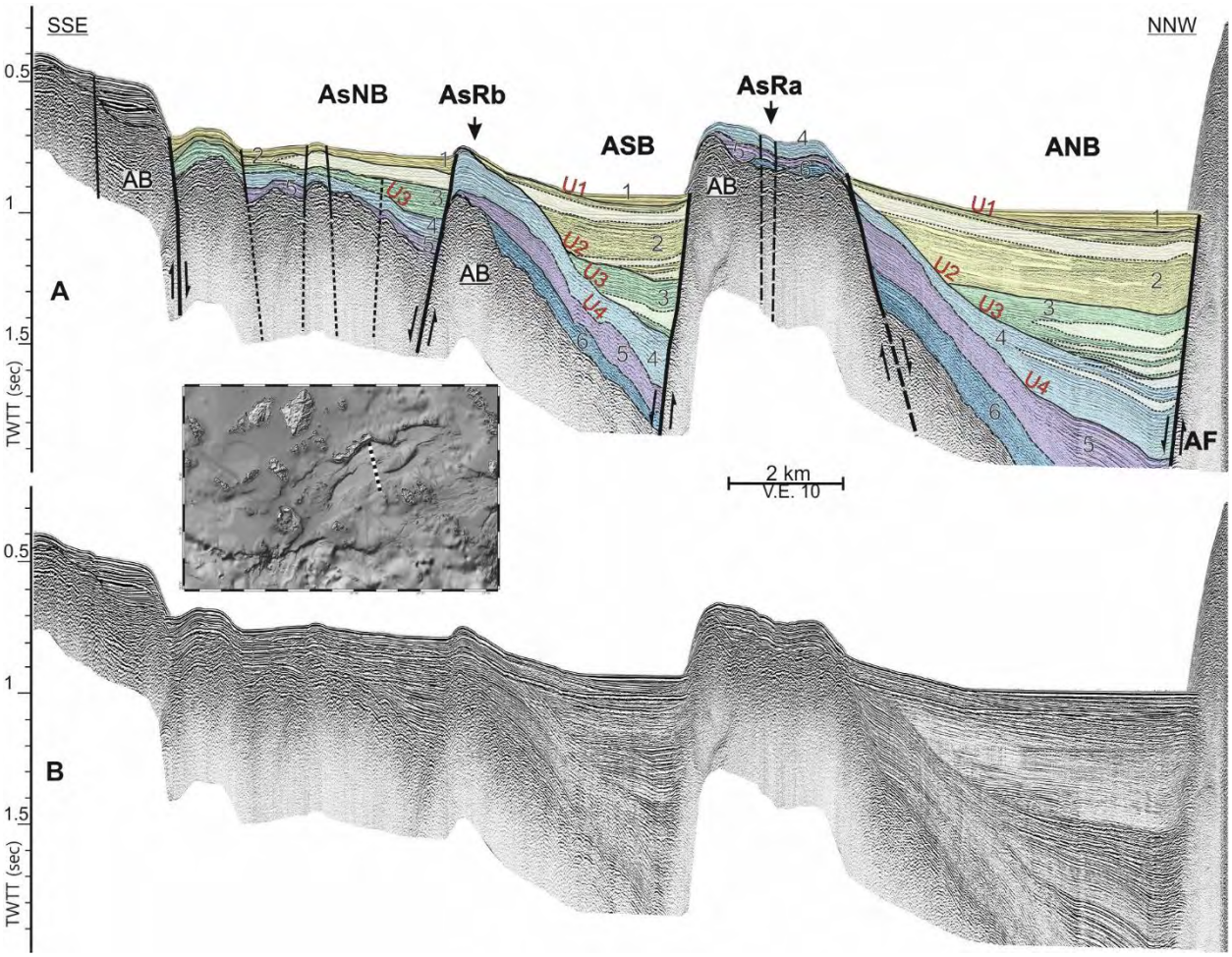

Figure 4.2.6: Airgun 40 ci seismic profile across the central part of Amorgos North Basin (ANB), the eastern part of Amorgos South Basin (ASB) and the western part of Astypalea North Basin (AsNB). Terminology and symbols as in Figure 4.2.4. AF: Amorgos Fault, AsRa: north splay of Astypalea Ridge and AsRb: south splay of Astypalea Ridge.

Unconformity U3 truncates the reflectors of the underlying Unit 4, while the reflectors of the overlying Unit 3 display onlap relationship. It has been mapped on the seismic profiles of all basins (Figures 4.2.4, 4.2.5, 4.2.6, 4.2.7, 4.2.10) and marks a major change in the evolution of the entire area. All units (4, 5, 6) below U3 display a roughly constant thickness across the basins;

they are tilted northwards, uplifted towards the south and occur on the uplifted ridges that separate the basins. The units above U3 (3, 2, 1) are deposited only within the basins and their thickness increases drastically towards the northern margins of the basins. Thus, Unconformity U3 marks the onset of enhanced tectonic activity along the present, major, basin-bounding faults that led to significant northward tilting of the lower parts of the sedimentary infill of the basins, enhanced subsidence close to northern margins of the basins, uplift and formation of the ridges along the southern margins. The tilting and uplifting of the basin's sediments has begun after the deposition of Unit 4 and has evolved simultaneously with the deposition of the sediments of

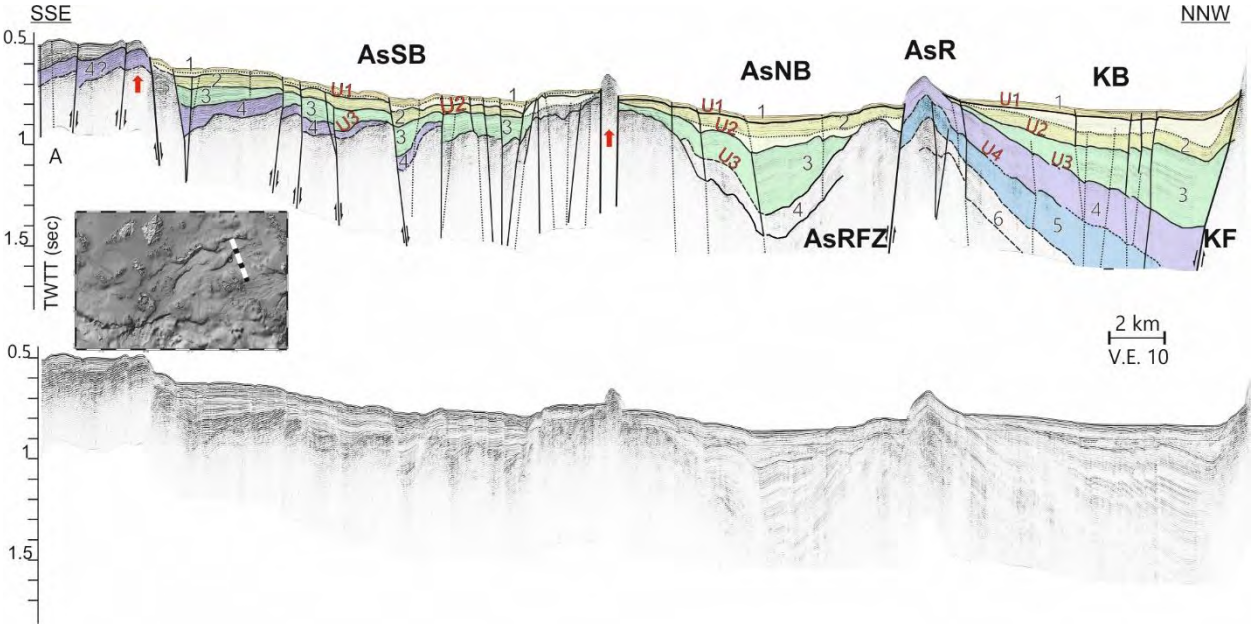

Figure 4.2.7: Airgun 40 ci seismic profile crossing the central part of Kinairos Basin (KB), the eastern part of Astypalea North Basin (AsNB), and Astypalea South Basin (AsSB). Terminology and symbols as in Figure 4.2.4. AsRF: Astypalea Ridge Fault, KF: Kinairos Fault.

Units 3, 2, and 1.

Unconformity U4 is a high amplitude and continuous reflector, which is mainly recognizable within the Amorgos North and Amorgos South basins, in the eastern part of Anydros Basin, in Anafi Basin and Kinairos Basin (Figures 4.2.4, 4.2.5, 4.2.6, 4.2.7, 4.2.10) and separates Unit 4 from Unit 5 below.

Table 4.2.2 presents the results obtained from the comparison of the analysis of the seismic stratigraphy of the current study with the results of previous studies.

Table 4.2.2. Seismic stratigraphic features in the current study and in the literature.

Current study	*Piper & Perissoratis (2003)*	*Nomikou et al. (2016*	*Nomikou et al. (2018)*
Unit 1	A1	AB-6	Amb6, Sab6, Ab6
Unconformity U1	UR3 (150–190 ka years) [66]	ab-5	
Unit 2	A2	AB-5	Amb5, Sab5, Ab5
Unconformity U2	UR2 and/or UA1 (Plio/Quaternary boundary) [66]		
Unit 3	B	AB-4 and/or AB-3, AB-2	Upper part of Amb4, Sab4, Ab4
Unconformity U3	UR2 and/or UA1 (Plio/Quaternary boundary) [66]		
Unit 4			
Unconformity U4			
Unit 5		AB-2 (?)	Sab3, Ab3
Unit 6		AB-1 (?)	Sab2, Ab2

4.2.5.2.1 Anafi Basin (AnB)

The seismic stratigraphy of AnB is very well illustrated in Figure 4. Sediments of about 700 msec thickness lie uncomfortably on the acoustic basement (AB) between the SW and NE faulted margins (Anafi and Anydros Ridge faults, respectively). The acoustic basement exhibits a high amplitude, undulating, discontinuous surface, which is not well distinguishable throughout the entire basin, with high amplitude, discontinuous internal reflectors. Units from 1 to 6 have been recognized within the sedimentary sequence.

Unit 1 shows a slight variation in the thickness along the south and north margins of the basin, of the order of magnitude of 20 msec. Unconformity U1, separates Unit 1 above from Unit 2 below. The upper part of Unit 2 is characterized by a chaotic layer of discontinuous, transparent, undulating, and high amplitude reflectors. The chaotic seismic reflections are interpreted as mass transport deposits, which are probably related to slope instability and gravitational sliding of material from the southern steep slopes of Anydros Ridge. The reflectors of Unit 2 onlap unconformity U2, that separates Unit 2 above from Unit 3 below. The latter shows a mean

thickness of about 100 msec across the basin, lies horizontally in the northern part of the basin and climbs up towards the southern margin. At least one layer with chaotic, undulating, and high amplitude reflectors has been mapped within Unit 3 and has been interpreted as a mass transport deposit, possibly related to enhanced tectonic activity along the northwestern margin of the basin. Despite the fact that the reflectors of this unit lie conformably on the following unit (Figure 4), unconformity U3 separates those two units, as stated below in the description of the seismic stratigraphy of the other basins. Unit 4 underlies Unit 3 and shows a maximum thickness of 100 msec at the center of the basin. Its internal reflectors display a divergent character close to the southeastern margin. The southeastern part of Unit 4, close to the SE faulted margin, lies unconformably on the eroded acoustic basement (AB).

Unit 5 shows a maximum thickness of about 250 msec close to the southeastern margin, indicating rapid subsidence of the basin during the deposition of this unit. Unconformity U4 that separates Unit 4 from Unit 5 can be traced only at the northwestern part of the basin. The chaotic character of Unit 5, which rests unconformably in the NW part, does not allow the separation of the top of Unit 5 from the base of Unit 4. On the central and the SE part of Anafi Basin (Figure 4.2.4), Unit 5 follows the inclination and the geometry of Unit 4 and is characterized by very well illustrated, high amplitude, continuous, closely spaced, and parallel reflectors.

Unit 6 can be mapped at a mean depth of 1400 msec. Due to the depth in which it is located and its acoustic seismic character, the interface between it and the presumable acoustic basement is not well discernible. Nevertheless, the undulating, discontinuous base of Unit 6 indicates that this seismic unit lies unconformably on the eroded basement.

4.2.5.2.2 Anydros Basin (AdB)

Anydros Basin is separated from Anafi Basin by the Anydros Ridge (Figures 4.2.2 and 4.2.4). The structure and seismic stratigraphy of the northeastern and southwestern parts of AdB are remarkably different (Figures 4.2.4 and 4.2.5). A well stratified sedimentary sequence with evident northward asymmetry characterizes the NE part of AdB (Figure 4.2.5). On the contrary, the sedimentary infill in the SW part of AdB indicates uniform subsidence and is intruded by multiple volcanic bodies that create cones and domes on the seafloor (Figure 4.2.4). The

subsidence of AdB has evolved between the Ios (IF) and Akrotiri-Anydros (AdF) faultzones. Interestingly, the volcanic activity in the Santorini-Amorgos area, which includes the volcanic complex of Santorini (Thera) and the Kolumbo volcanic chain, occurs exclusively within Anydros Basin, while the volcanic domes of Christiana Islets occur on the southwestern prolongation of AdB.

Only the three upper units (Units 1 to 3) have been recognized within the sedimentary infill in the SW part of AdB. Unit 1 (~20 msec thickness) rests unconformably on Unit 2 (Unconformity U1). The latter shows a maximum thickness of around 280 msec. Semichaotic facies of little coherent energy showing locally high amplitude, discontinuous reflectors within this unit suggests that they are mass transport deposits derived from the margins of the basin, or they are volcano-clastic deposits (pyroclastic flows, perhaps), originating from any of the adjacent volcanic centers. Figure 4.2.4 shows that Unit 2 thins out towards the northern faulted margin, while, towards the southern one, its thickness remains constant, at roughly 100 msec. A high amplitude, thick, and morphologically irregular reflector marks the erosional interface between Unit 2 and the underlying acoustic basement (AB), in the southern part of Anydros Basin (Figure 4.2.4). In the northwestern part of AdB, unconformity U2 separates Unit 2 (above) from Unit 3 (below). Unit 3 shows internal changes in amplitude characteristics and the reflectors close to the northern margin show a divergent character. Unit 3 lies unconformably (Unconformity U3) on the underlying layer.

The flat seafloor and the horizontal stratigraphic layering of the SW part of AdB, shown on the seismic profile of Figure 4.2.4, are interrupted by three vertical, elevated features. The two southernmost ones (V1 and V2) display a strongly reflective seafloor, internal chaotic seismic character, steep slopes, and sharp contacts with the surrounding sedimentary deposits. They coincide with two of the submarine volcanic domes of the Kolumbo chain, already mapped earlier (Nomikou et al., 2012, 2016). The third uplifted structure, north of the previous ones, has also been described by Nomikou et al. (2016). This structure displays flattened, strongly reflective top and internal layered seismic character, characterized by high amplitude, undulating, and semi-continuous reflectors. It is bounded towards NW and SE and uplifted by two, steep, opposite facing, high angle faults (~85^0 the northern one and ~70^0 the southern), pointing to a pop-up like,

compressional structure developed between two strike-slip faults. The downward flexure of the surrounding, subsiding sedimentary layers, close to both faults, supports the previous interpretation.

As mentioned above the NE part of AdB displays significant variations in the geometry and the seismic stratigraphy in respect to the SW part (Figure 4.2.5). A very well stratified sedimentary sequence with maximum thickness exceeding 600 msec characterizes the NE part of AdB. Units 1 to 5 have been mapped within its sedimentary infill. Unit 1 shows a mean thickness of 50 msec, while Unit 2 shows a maximum thickness of 230 msec close to the northern margin. At least five chaotic layers, with low coherent energy and internal high amplitude, discontinuous and irregular reflectors have been recognized within Unit 2. The highly disrupted seismic character, the recognizable toe region at the upper and lower part (Figure 4.2.5), and their proximity to the unstable faulted northern margin leads to the conclusion that they are MTDs related to slope failures (Frey-Martinez, 2007).

Unconformity U2 separates Unit 2 from Unit 3. The latter shows a maximum thickness of about 200 msec close to the northern margin (Amorgos South Relay Fault), which, similarly to Unit 2, thins out towards the southern margin. At least two, relatively small and thin MTDs have been mapped within this Unit close to the northern margin. This Unit lies unconformably on Unit 4 towards the northern margin (Unconformity U3). Unlike Units 2 and 3, Unit 4 displays a constant thickness of roughly 110 msec across the basin, indicating thus uniform subsidence during its deposition. Its geometry follows the one of its interface with the overlying Unit 3. The base of Unit 4 occurs at 1230 msec depth close to the northern margin. It ascents continuously towards the southern margin, the Anydros Ridge, and reaches minimum depth of roughly 500 msec or less below the top of the Ridge. Its seismic character becomes more undulating and discontinuous with depth. The lowermost recognizable unit is Unit 5, the reflections of which follow the geometry of Unit 4 and are tilted upwards on Anydros Ridge.

Hübscher et al. (2015) and Nomikou et al. (2016) recognize moat channels and mounded contourites on the NW part of the basin, in the lower part of the basin's infill. Their stratigraphic position corresponds to the lower half of unit 3 and the underling units, as defined in the current study.

4.2.5.2.3 Amorgos North (ANB) and Amorgos South (ASB) Basins

Amorgos North (ANB) and Amorgos South (ASB) Basins are described here in parallel because, as shown hereafter, they display remarkable seismic stratigraphic and structural similarities and can be considered as twin basins. They are separated from each other by the Northern Splay of Astypalea Ridge (AsRa), from the Anydros Basin to the North by the Anydros Ridge and from Astypalea Basin to the South by the Astypalea Ridge (AsR) and its Southern Splay (AsRb). The similitudes between the two basins are obvious on the seismic profile of Figure 4.2.6**.** The latter crosscuts the central, widest part of ANB (roughly 10 km width) and the eastern part of ASB with 5.5 km width.

Six different seismic units (Units from 1 to 6), that are significantly tilted towards the north, can be identified within the Amorgos North and Amorgos South basins, while the development of both basins is mainly controlled by the northern marginal faults. The sedimentary sequence lies on top of the acoustic basement, which shows a rugged surface topography. An elevation of the acoustic basement separates those basins and forms the North Splay of Astypalea Ridge (AsRa). Unit 1 lies on the seafloor and gradually thickens towards the north. The maximum thickness shown in the ANB is about 50–60 msec, and, in ASB, it is approximately 80–90 msec. Unit 1 onlaps unconformity U1, which separates it from the underlying Unit 2. The latter shows a maximum thickness exceeding 300 msec in the ASB and close to 300 msec in the ANB. Around 20–30 msec below the top of Unit 2, a chaotic layer with internal high amplitude, discontinuous and irregular reflectors, has been mapped in both basins, the thickness of which remains constant through the basins axis and is approximately 50 msec. This layer has been interpreted as MTD and is probably related to a rapid subsidence of the northern parts of the basins. In ASB, similar layers of smaller thickness have been mapped within the lowermost part of Unit 2.

Unconformity U2 separates Unit 2 above, from Unit 3 below, while, on the southern part of the basins, the reflectors of Unit 2 onlap unconformably (unconformity U3) on Unit 4. Unit 3 shows a maximum thickness of 170 msec in ASB and of 260 msec in ANB. Internal, chaotic layers at the lowermost part of Unit 3 have been interpreted as MTDs, associated with slope instabilities along the margins. Unit 4 lies below Unit 3 and close to the northern faulted margins of ASB and ANB shows its maximum thickness of 200 and 300 msec, respectively. Towards the southern

margins, it thins and pinches out on the uplifted acoustic basement, which forms the north and south splays of Astypalea Ridge (AsRa and AsRb). As aforementioned, the internal reflectors of Unit 2 and Unit 3 onlap the top of Unit 4 towards the south, while the reflectors of the latter are truncated by the angular unconformity U3.

Unconformity U4 separates Unit 4 from Unit 5. The distinction of Unit 5 from the Unit 6 is not easy, and the interface that separates them cannot be mapped in detail. However, following the geometry and morphology of the adjacent layers, the dashed line in Figure 4.2.6 attempts to define this surface. A highly irregular, rugged reflector marks the transition from Unit 6 to the acoustic basement. High amplitude and non-stratified internal reflectors occur on the upper part, while the lower part is acoustically transparent. It is worth noting that, like in the NE part of Anydros Basin, the lowermost parts of the sedimentary sequence in Amorgos North and in Amorgos South basins have been tilted and uplifted upwards, covering the north and south splays of Astypalea Ridge.

4.2.5.2.4 Astypalea North Basin (AsNB)

A SW-NE trending structural uplift of the acoustic basement and its sedimentary cover, which consists of Units 4, 5, and 6, forms the south splay of Astypalea Ridge and separates the Amorgos South Basin (ASB) from Astypalea North Basin (AsNB) (Figure 4.2.6). An elongated uplift of the acoustic basement separates Astypalea Basin into two sub-basins: a northern one (AsNB) and a southern one (AsSB). At least 4 seismic units have been mapped in the upper parts of the sedimentary sequences of the two sub-basins (Figure 4.2.7). The lower parts of the basins' infill have not been imaged properly due to rapid signal attenuation with depth. The westernmost part of AsNB displays northward asymmetry, similar to the previously described basins. Seismic units 1–5 have been mapped within AsNB. They show smaller thickness compared to the other basins which was to be expected, since the sedimentary infill of Astypalea Basin is slightly smaller. Seismic units 4 and 5 of ASB that have been uplifted on Astypalea Ridge, have also been mapped at the base of the sedimentary sequence of AsNB (Figure 4.2.6). Unit 5 has been deposited on the acoustic basement of AsNB. Therefore, Unit 6 observed in ASB, may not have been deposited in Astypalea Basin. Unit 1 is of constant thickness, while Units 2, 3, 4, and 5 show maximum

thickness close to the northern faulted margin. At the base of Unit 3, an undulating surface that truncates the underlying Unit 4 is related to unconformity U3.

The easternmost part of AsNB displays a more symmetric shape. Two faulted margins northwards (AsRF) and southwards define the basin. The seismic profile of Figure 4.2.7 shows a well stratified sedimentary infill in AsNB, whose thickness exceeds 600 msec at the center of the basin and thins out towards the margins. The lowermost part of the sedimentary sequence is not very well recorded, so only the upper seismic units (1 to 4) have been recognized.

4.2.5.2.5 Astypalea South Basin (AsSB)

Astypalea South Basin (AsSB) displays a more circular shape compared to the elongated shape of the AsNB. Apparently, normal faults bound the northern and southern margin, while the eastern slopes of Astypalea Island define the western margin of AsSB. Units from 1 to 4 have been recognized within the sedimentary sequence (Figure 4.2.7). Unit 1 is a thin layer, about 30 msec thick, of well stratified sediments. A thin layer with an irregular surface and high amplitude, undulating reflectors has been mapped at the base of Unit 1 and has been interpreted as MTD. Unit 2 underlies Unit 1 showing a mean thickness of 50 msec and Unit 3 below, showing a maximum thickness of 120 msec. The thickness of the following Unit 4 exceeds the 100 msec close to the southern margin and progressively decreases to the north. The base of Unit 4 shows a rugged morphology. Numerous high angle faults, running E-W, parallel to the basin axis, cross cut the sedimentary sequence of the AsSB. Units 3 and 4 display southward tilting due to the E-W faulting, while the basin as a whole displays maximum subsidence close to its northern margin.

4.2.5.2.6 Kinairos Basin (KB)

The northeastern part of the survey area is occupied by the Kinairos Basin (KB). The eastern prolongation of Astypalea Ridge separates Kinairos Basin to the North from AsNB to the South. The northern part of Figure 4.2.7 illustrates the central part of Kinairos Basin. Seismic Units from 1 to 6 have been mapped within the sedimentary sequence of KB. With the exception of Unit 1, all units show maximum thickness close to the northern faulted margin, indicating rapid subsidence to the north. The thickness of Unit 1 reaches the 30–40 msec. Unconformity U1 separates Unit 1 from the underlying seismic Unit 2. The maximum thickness of Unit 2 reaches

200 msec. A chaotic layer with internal variable amplitude, discontinuous reflectors has been mapped within Unit 2 and has been interpreted due to its geometric characteristics, as MTD. Unit 3 underlies Unit 2 and onlaps unconformity U3. Unit 4 displays seismic character similar to that of Unit 3. However, close to the southern margin, the reflectors become fuzzier and discontinuous. The interface that separates Unit 4 from Unit 5 is not very well illustrated. The attenuation of the seismic signal with depth prevents a detailed description of the nature of unit 6. However, an upper surface with high amplitude, undulating, discontinuous internal reflectors can be identified. Kinairos Basin displays a dual character. The lower half of the sedimentary sequence (mainly Units 4, 5, and 6) have been tilted and uplifted on the southern margin of the basin to form Astypalea Ridge. Tilting and uplift evolved in parallel with the deposition of the upper half of the basin's infill (Units 3, 2, and 1) and led to the shifting of the depocenter close to the northern faulted margin indicating northward asymmetry of the basin.

4.2.5.3 Seismic Stratigraphy: Ridges

The Anydros and Astypalea ridges with their splays (AdRa, AdRb, AsRa, and AsRb) as described above, separate the main basins that have been developed in the area. The following is a brief overview of the main features recognized through the interpretation of the seismic stratigraphy of each of them.

4.2.5.3.1 Anydros Ridge (AdRa, AdRb)

Anydros Ridge is characterized by the occurrence of the uplifted acoustic basement at the seafloor or at a shallow depth below the seafloor. The islet of Anydros, located on the ridge, marks the highest elevated part of the acoustic/alpine basement. The top of the basement displays rugged morphology pointing to subaerial/underwater erosion and faulting (Figures 4.2.4 and 4.2.5). Indeed, numerous faults cross-cut the southern part of the ridge, close to the margin of Anafi Basin and are responsible for the irregular seafloor. The northeastern part of the ridge is split into two branches (AdRa, AdRb) due to the prolongation of Amorgos Fault (Figure 4.2.2). The narrow-elongated valley in between the two branches is thinly sedimented. A narrow, faulted, SW-NE oriented depression occurs at the western part of the ridge and is filled up with sediments of roughly 250 msec thickness (Figure 4.2.4). A progadational sequence with

characteristic clinoforms occurs in the upper part of the sedimentary infill of the depression, indicating the development of a deltaic sequence, associated with a sea level roughly 400 msec (300 m) below the present one, during one of the low sea level stages of Quaternary. The sedimentary cover of the northeastern part of AdR mainly consists of sediments of the previously described Units 4 and 5 (Figure 4.2.5). Unconformity U3 marks the onset of the uplift of the lower units and the formation of the ridge. Active and apparently normal faults on this part of the ridge create local elevation of the seafloor and deform the sedimentary sequence.

4.2.5.3.2 Astypalea Ridge (AsRa, AsRb)

The formation of the tectonically controlled Astypalea Ridge (AsR), separates the Amorgos North from Amorgos South and Astypalea basins (Figure 4.2.6), the Amorgos South from Astypalea Basin (Figure 4.2.6), and the Kinairos from Astypalea Basin (Figure 4.2.7). It is divided to the west into two splays, the AsRa and the AsRb (Figure 4.2.2). The main body of the ridge is composed of the uplifted, northward tilted sediments of Units 4, 5, and 6 of Amorgos North Basin. Their thickness on the top of AsR exceeds 300 msec in the eastern part and decreases to less than 200 msec below the western part (AsRa, AsRb). As in the Anydros Ridge, Unconformity U3 indicates the onset of the uplift of the lower units of the basins and the formation of the ridge. The uplift of the main ridge and its splays has evolved on the footwall of SE-dipping faults.

4.2.5.3.3 Akrotiri Ridge (AkR)

The seismic profiles crossing Akrotiri Ridge show that the latter is free of sedimentary or volcano-sedimentary deposits (Figure 4.2.8). The acoustic basement occurs on the rugged seafloor of the ridge and is bounded by steep, SW-NE trending faults. The Akrotiri Fault (Figure 4.2.8) controls the northwestern flank of AkR and forms the tectonic boundary with the sedimentary infill of Christiana Basin (Tsampouraki-Kraounaki and Sakellariou, 2018). Perissa Fault forms the tectonic boundary of the ridge with Anafi Basin. Akrotiri Ridge is the physical prolongation of the southern part of the island of Santorini, where the alpine basement builds Profitis Elias Mountain and outcrops on the steep caldera walls at Athinios port. Therefore, a reasonable hypothesis is that the alpine basement extends southwards and forms the acoustic basement of Akrotiri Ridge.

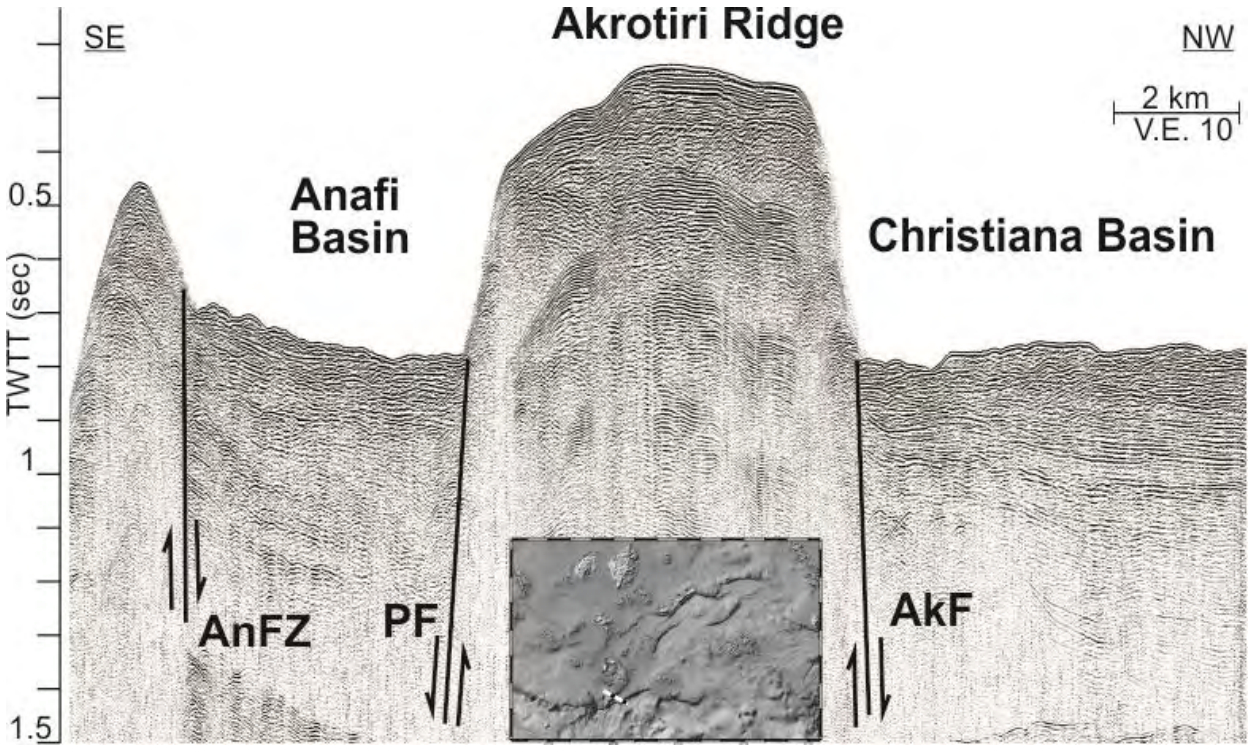

Figure 4.2.8: Airgun 40 ci seismic profile crossing the southwestern part of Anafi Basin, Akrotiri Ridge and the southeastern margin of Christiana Basin. AnFZ: Anafi Fault Zone, AkF: Akrotiri Fault, PF: Perissa Fault.

4.2.5.3.4 Anafi Ridge (AnR)

Anafi Ridge (AnR) is a 30-km long narrow ridge extending from the Island of Anafi towards the SW and forms the southern margin of Anafi Basin's western part. The ridge is not sedimented and the alpine basement that outcrops on the island occurs on the seafloor as acoustic basement.

4.2.5.4 Faulting

The processing and the interpretation of the seismic profiles, along with the swath bathymetry data, provide sufficient information for the reconstruction of the fault network in the Santorini-Amorgos Shear Zone in unprecedented detail, as well as for the understanding of their evolution and their impact on the evolution of the basins through time. Further on, detailed mapping of the tectonic network, along with the geological-geophysical data and interpretations, provide adequate information which enables the understanding of the style of long-term deformation and kinematics during the Plio-Quaternary.

The geometrical characteristics of each one of the major faults and fault zones are described in detail below, along with their impact on the evolution and structure of the relevant basins. The

complete fault network of the Santorini-Amorgos Shear Zone is shown on the tectonic map of Figure 4.2.9A. The active fault system indicates that the steep margins of the basins are controlled by mainly NE-SW trending, SE dipping faults and WNW- ESE to W-E trending, SSW- or S-dipping, step-over faults. With the exception of western Anydros Basin and Astypalea South Basin, all other basins display northward asymmetry. The maximum thickness of the basin infill, above Unconformity U3, occurs close to the northern marginal faults, while the older seismic units are tilted and uplifted to the South. The latter has resulted in the inversion of the basin's geometry and the formation of the Astypalea and Anydros ridges. Minor intra-basin faults deform the interior of the basins, while pop-up structures, observed in the basins and on the ridges, indicate significant deformation due to horizontal shearing. The proposed kinematics of the individual faults and fault zones and of the entire Santorini-Amorgos Shear Zone is shown on the map of Figure 4.2.9B.

4.2.5.4.1 Ios Fault Zone (IFZ) and Amorgos South Relay Fault (ASRF)

IFZ defines the northern margin of Anydros Basin. It consists of several, observed and possible segments that strike NE-SW, parallel to the long axis of Anydros Basin. It is a 50^0–65^0 SW-dipping fault zone that marks the offshore slopes south of Sikinos and Ios islands to the west and to the northeast terminates at the Amorgos South Relay Fault (ASRF). The southwestern and central parts of Anydros Basin are bounded by the IFZ to the North and the AdRNFZ to the South; they display no tectonic asymmetry and host the volcanic activity of the Christiana-Santorini-Kolumbo chain. The basin infill is cross-cut by SW-NE striking, high angle faults, which may or may not control the occurrence of the volcanic features. Such faults are the ones that create the SW-NE trending "graben" on the northeastern walls of the Santorini caldera and the nearly vertical faults with horizontal striations observed in the area of Koloumbo Cape on Santorini.

Amorgos South Relay Fault (ASRF) is a 15-km long, roughly W-E striking, roughly 60^0 S-dipping, apparently normal fault. The orientation of ASRF and its location between the northeastern tip of IFZ and Amorgos Fault indicate that it accommodates the transfer of strain between the SW-NE striking IFZ and AF. ARF marks the northern tectonic boundary of the northeastern part of Anydros Basin. Opposite to the southwestern and central parts, the

northeastern one displays northward tectonic asymmetry with ARF driving the enhanced subsidence of the basin floor in its hanging wall. The morphological scarp between the top of

South Amorgos Island on the footwall of ARF and the seafloor of the basin is roughly 1 km. The cumulative vertical offset, including the thickness of the basin infill reaches 1.5 km.

4.2.5.4.2 Akrotiri Fault (AkdF) and Anydros Ridge North Fault Zone (AdRNFZ)

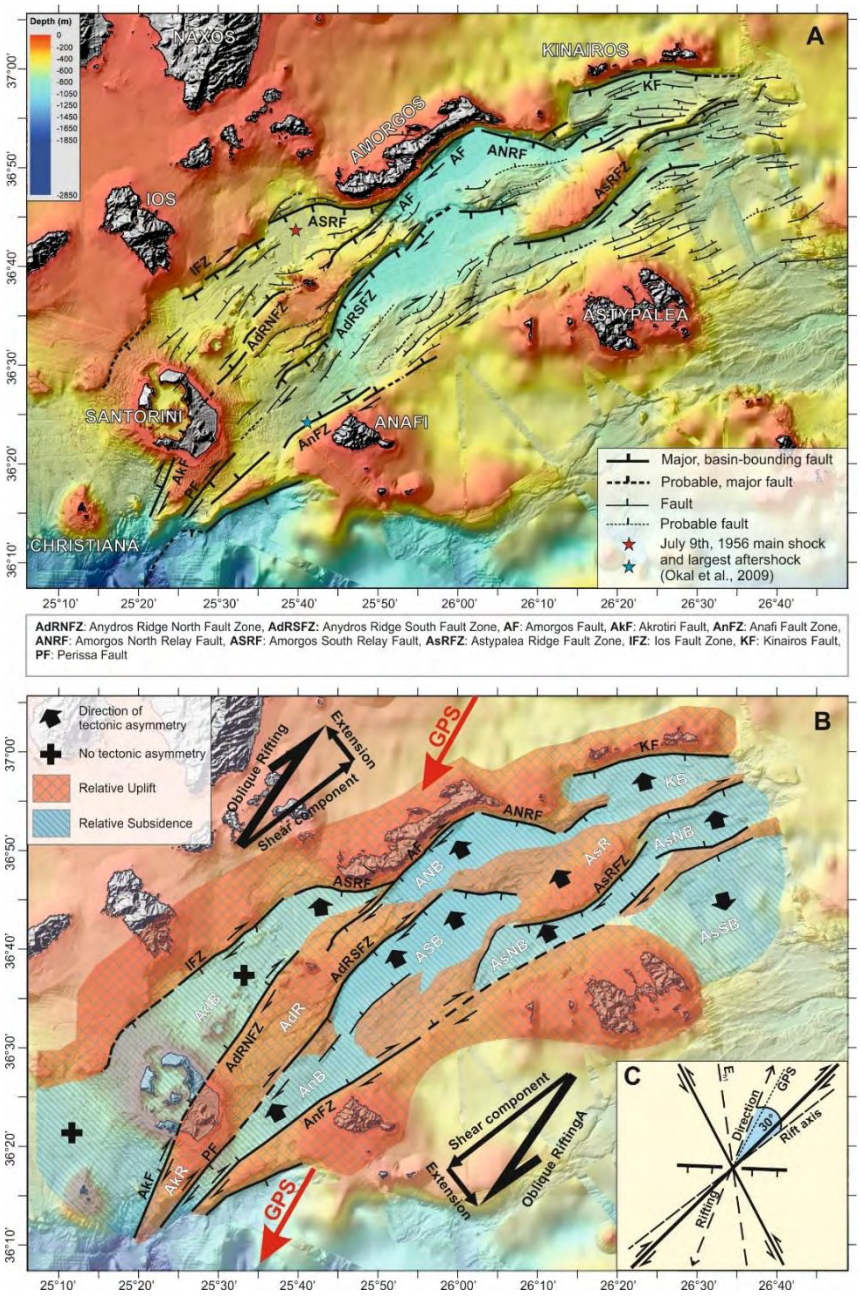

Figure 4.2.9: (**A**): Detailed map of the active fault network in Santorini-Amorgos Shear Zone. Teeth on the faults indicate the downthrown side. Half arrows show the sense of lateral motion. (**B**): Tectonic and kinematic map of Santorini-Amorgos Shear Zone. Dextral oblique rifting results from dextral strike-slip motion in NE-SW direction and extension in NW-SE direction. Red arrows show the direction of motion in respect to stable Eurasia, modified after Kreemer and Chamot-Rooke (2004). (**C**): Drawing explaining the kinematic of dextral oblique extension with the rift axis running at 30° in respect to the rifting direction (modified after Withjack and Jamison, 1986).

AkF and AdRNFZ constitute the southern tectonic margin of Anydros Basin to Anydros Ridge. They also mark the southern/southeastern limit of the volcanic activity in the Christiana-Santorini-Kolumbo volcanic chain.

Akrotiri Fault (AkF) is 13-km long, and its trace on the seafloor follows the foot of the northwestern slope of Akrotiri Ridge to the Christiana Basin. It strikes SW-NE and dips with a 50^0–55^0angle to the Northwest. Towards the SW, it terminates at the steep, south-facing margin of the deep Cretan Basin. The NE-ward prolongation of AkF's trace on the island of Santorini coincides with the possible fault that marks the northern limit of the occurrence of the alpine basement on the steep slopes of the caldera in the area of Athinios.

AdRNFZ follows further to the NE with the same SW-NE strike and NW dipping. The part of the fault zone between the eastern slope of Santorini and the islet of Anydros consists of three, en-echelon arranged, SW-NE striking segments. The total length of the three segments reaches 25 km. Further to the NE, the margin of Anydros Basin to Anydros Ridge is cross-cut by a series of E-W striking, N- and S-facing, normal faults. They are en-echelon arranged, each one is less than 5-km long, and they probably represent the NE-ward prolongation of AdRNFZ. The total length of AkF and AdRNFZ is roughly 70 km.

4.2.5.4.3 Perissa Fault (PF) and Anydros Ridge South Fault Zone (AdRSFZ)

PF defines the northwestern boundary of Anafi Basin to Akrotiri Ridge. It is a >15-km long, SW-NE striking fault that dips with a 50^0–55^0angle to the SE (Figure 4.2.8). The height of the morphological scarp, between the seafloor of Anafi Basin and the flat top of Akrotiri Ridge, exceeds 400 m. The cumulative vertical fault offset, including the thickness of the basin infill, exceeds 1 km. Towards the SW, both the fault and Akrotiri Ridge die out at the margin of the deeper Cretan Basin. Chaotic masses of unconsolidated sediments on its hanging wall indicate that the faulted slope has collapsed several times in the past.

AdRSFZ consists of at least three, SE-facing, SW-NE striking segments which mark the southeastern slope of Anydros Ridge and the tectonic and morphological boundary between the latter and the Anafi (AnF) and Amorgos South (ASB) Basins. The total length of AdRSFZ is 45–50 km and constitutes the northeastern prolongation of Perissa Fault. The two of them can be

considered segments of the same fault zone with roughly 80 km total length. The segments of AdRSFZ dip SE-wards with variable dip values. The southwestern segment dips with roughly 60^0, marks the northern margin of Anafi Basin and controls its evolution. The central and northeastern segments dip with 40^0–45^0 and 60^0, respectively, and form the northern tectonic boundary of Amorgos South Basin. They form a >500 m high morphological scarp between the central part of the ridge and the basin, which decreases towards the NE. The cumulative vertical fault offset, including the thickness of the basin infill, exceeds 1.2 km.

Maximum subsidence in the Amorgos South Basin occurs close to the AdRSFZ northeastern segments and is responsible for the tectonic asymmetry of the basin. The depocenter during the sedimentation of the younger basin infill, above the unconformity U3 (units 3, 2, 1), is located very close to the northern margin. The older units, 4, 5, and 6, below unconformity U3, display constant thickness across the basin and are tilted and uplifted to the south.

The northeastern terminal segment of AdRSFZ marks the boundary of the subsiding Amorgos South Basin with the tilted, uplifted, and inverted southern edge of the Amorgos North Basin, which resulted in the formation of the southern branch of Anydros Ridge. Total vertical offset of 600–700 m has been measured between the subsided lower units (4, 5, 6) of Amorgos South Basin and the equivalent units of Amorgos North Basin, which are uplifted on the ridge (Figure 4.2.6). The northern edge of AdRF terminates on a WNW-ESE trending normal fault, that controls the uplift of the northern splay of Astypalea Ridge and forms the northeastern boundary of Amorgos South Basin (Figure 4.2.9A).

4.2.5.4.4 Amorgos Fault (AF) and Amorgos North Relay Fault (ANRF)

AF is the most "famous" fault of the study area, as it is responsible for the impressive, steep, rocky, up to 700mhigh southeastern slopes of the island of Amorgos, which continue underwater for another 700 m before meeting the flat seafloor of Amorgos North Basin. It has been proposed in the literature that AF may has moved during the 9 July 1956, Amorgos earthquake (Okal et al., 2009 and references therein). The trace of AF runs along the foot of the subaerial-submarine southeastern slope of Amorgos for roughly 40 km. AF dips with 50^0 to $>65^0$ towards the SE, and its cumulative vertical offset, including the thickness of the infill of Amorgos North Basin (Figure

4.2.6), exceeds 2.2 km. The southwestern part of AF prolongs into the Anydros Ridge and divides it into the northern and southern branches. The northeastern part of AF constitutes the diachronic northern tectonic margin of Amorgos North Basin and is responsible for the tectonic asymmetry of the latter. The seismic Units 4, 5, and 6 of Amorgos North Basin display increasing thickness towards AF and are tilted and uplifted on the southern margin. Units 3, 2, and 1, above the Unconformity U3, are deposited unconformably on the previous basin infill; they are not tilted, and their depocenter is close to AF. This observation indicates rapid subsidence close to the northern margin throughout the evolution of ANB. Unconformity U3 marks a major event in the evolution of the basin and may indicate a dramatic change in the activity and/or the kinematics of AF.

Amorgos North Relay Fault (ANRF) starts from the northeastern tip of AF and prolongs for 15 km towards the ESE/SE. It dips with 45^0–50^0 SW-wards, defines the northeastern margin of ANB, and separates it through its uplifted footwall from the Kinairos Basin. The cumulative vertical offset of the faults reaches roughly 2.2 km.

Minor intra-basin faults have also been mapped within the basin, but their activity ceased before the deposition of Unit 2. Minor, NW-dipping active faults are observed along the southern margin of ANB to the north splay of Astypalea Ridge.

4.2.5.4.5 Kinairos Fault (KF)

The structural evolution of Kinairos Basin displays common characteristics with the ANB. The northern marginal fault, referred to as Kinairos Fault (KF), controls the development of the basin. KF is an almost W-E and south-dipping fault (40^0–50^0), with a length of about 25 km. Kinairos and Levitha islets occur on the top of the steep slopes on the footwall of KF. The morphological scarp, produced by the fault, exceeds 600 m, while its cumulative vertical offset of KF, including the thickness of the infill of KB (Figure 4.2.7), exceeds 1.5 km. With the exception of Unit 1, the seismic units that constitute the sedimentary infill of KB, display maximum thickness close to KF, indicating rapid subsidence to the north. Units 4 and 5 have been tilted and uplifted to the south on the prolongation of Astypalea Ridge, indicating basin inversion. High-angle faults (70^0–90^0)

cross-cut the sedimentary infill up to the seafloor. A secondary, N-dipping fault controls the southern margin of KB and contributes to the uplift of the easternmost part of Astypalea Ridge.

4.2.5.4.6 Anafi Fault Zone (AnFZ) and Astypalea Faulted Margin

AnFZ defines the southern margin of Anafi Basin and strikes NE-SW with 60_ NWdipping. It ends up on the termination of Anafi Ridge to the southwest, while, to the north-east, it is replaced by a series of minor faults that occur along and form the SWNE trending northern submarine slope off Astypalea Island. The lowermost parts of the sedimentary sequence of Anafi Basin show maximum thickness close to the AnFZ, indicating rapid subsidence during the deposition of Units 5 and 6. The depocenter of the Anafi Basin was gradually shifted to the North, and the maximum thickness of units 3, 2, and 1 occurs close to the northern tectonic margin (PF and AdRSFZ) of the basin (Figure 4.2.4).

Further to the northeast, the southern margin of ASB is controlled by synthetic to AnFZ, NW-dipping faults. These faults, along with high-angle faults that have been mapped on the south and southeastern parts of ASB, deform the oldest parts of the sedimentary sequence (Units 4, 5, and 6). The morphologically smooth transition from Anafi Basin to Amorgos South Basin becomes perceptible on the seismic profile of Figure 4.2.10**.** A small elevation of the acoustic basement separates those two basins. This elevation occurs between two secondary faults that appear inactive during the deposition of Unit 1.

4.2.5.4.7 Astypalea Ridge Fault Zone (AsRFZ)

AsRFZ is a 65–70-km long fault zone that originates from the Anafi-Astypalea margin, strikes SW-NE and defines the northern margin of Astypalea North Basin (AsNB) against the Amorgos South Basin in the SW, the Astypalea Ridge in the middle, and the Kinairos Basin (KB) in the NE.

The largest segment of AsRFZ controls the SE-facing, steep slope of Astypalea Ridge, is 28-km long, dips with 55^0 SE-ward, and marks the major tectonic boundary of Astypalea North Basin. As previously mentioned in Figure 4.2.6, the development of AsNB is mainly controlled by the AsRFZ and displays north-ward tectonic asymmetry.

The northeastern segments of AsRFZ are responsible for the uplift and formation of the eastern, narrow part of Astypalea Ridge, which separates AsNB from Kinairos Basin (Figure

4.2.7). The southern margin of AsNB is delineated by a N-facing marginal fault that controls the formation of a narrow structural up-lift of the basement and the seafloor that separates AsNB from Astypalea South Basin. The sedimentary infill of AsNB shows maximum thickness at the center of this part of the basin and thins out towards the northeastern and southeastern margin.

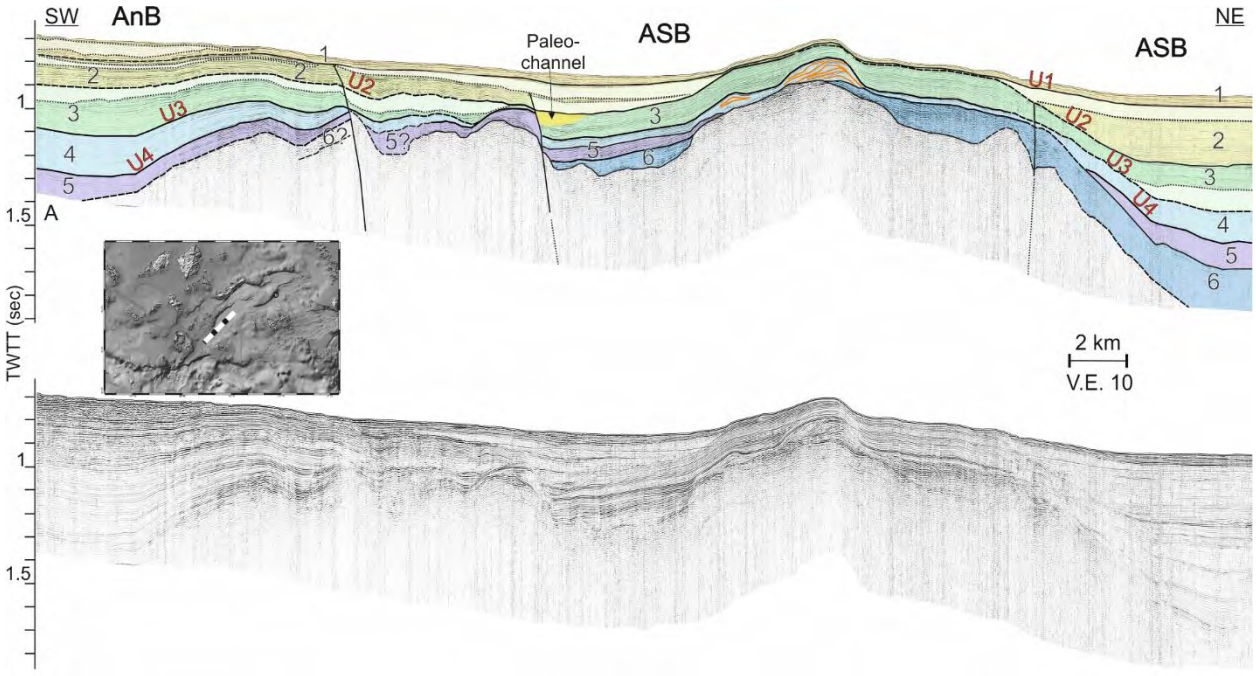

Figure 4.2.10: Airgun 40 ci seismic profile along Anafi Basin (AnB) and Amorgos South Basin (ASB) in SW-NE direction (along strike). Terminology and symbols as in Figure 4.2.4.

A high angle fault (>82^0) crosses the lower parts of the sedimentary sequence without affecting Units 1 and 2. Secondarily, NE-dipping (35^0) faults deform the sedimentary sequence close to the SE margin.

4.2.5.4.8 Astypalea South Basin Faults

The fault network in AsSB displays interesting differences in respect to the tectonic network of the other basins described so far. AsSB is cross cut by multiple, SW-NE to WSW-ENE striking, high-angle (>50^0) faults, which have deformed the sedimentary infill and led to S-ward tilting of the individual tectonic blocks (Figure 4.2.7). Within each tectonic block, the thickness of the lower Units 3 and 4 increases from North to South, while the upper Units 2 and 1 display constant more or less thickness with small variations.

This fact indicates rapid subsidence to the south during the deposition of Units 3 and 4, which was followed by a symmetrical subsidence during the deposition of units 2 and 1.

4.2.6 Discussion and Synthesis

The results described above provide insights into the Plio-Quaternary evolution, deformation, and kinematics of Santorini-Amorgos Shear Zone and, hitherto, into the evolution and structure of the South Aegean back arc area. The seismological characteristics of the 1956 Amorgos earthquake are discussed under the light of the present findings.

4.2.6.1 Basin evolution

Seven tectonically controlled basins have been mapped and described within Santorini-Amorgos Shear Zone, thus refining and completing our knowledge on the structure of the area. The new data presented here show that the Santorini-Anafi Valley of Perissoratis (1995), which has been renamed by Hooft et al. (2017) as Anafi Basin and by Nomikou et al. (2018) as Santorini-Anafi Basin, is not a single basin; it consists of two different basins, the Anafi Basin and Amorgos South Basin, which display opposite tectonic asymmetry and are separated from each other by a structural high.

Anydros Basin exhibits different geomorphological and geological features in its central-southwestern and northeastern parts, mainly due to active volcanic activity in the southwest and the northward tectonic asymmetry in the northeast. Amorgos North Basin and Amorgos South Basin can be considered as twin basins as they are characterized by identical stratigraphy and tectonic structure. Astypalea North Basin displays different characteristics between the western and eastern parts, with the western part showing northward asymmetry and the northeastern part showing a more symmetrical structure. The Astypalea South Basin on the other hand shows southward asymmetry with rapid subsidence of the lowermost parts of the sedimentary sequence close to the southern margin. Furthermore, the northeastern part of SASZ is occupied by the newly described Kinairos Basin, the stratigraphic and tectonic characteristics of which are very similar to the ones of ASB and ANB.

The new data presented here indicate a two-stage structural evolution of the area. The former, single basin has been fractured in Late Pliocene—Early Quaternary by younger, normal to oblique faults. Tectonic activity on the new faults has led to (i) enhanced subsidence on their hanging wall

and formation of the present basins and (ii) asymmetric uplift and tilting on their footwall, and creation of ridges that are topped by the uplifted older stratigraphic units of the previous basin. The analysis of the seismic stratigraphy revealed remarkable similarities, as well as certain differences in the sedimentary and tectonic evolution of the basins and ridges. Various minor and major events in the Plio-Quaternary tectonic activity in the area have been imprinted on the seismic stratigraphy as minor or major unconformities. Unconformity U3 is the most important among them, since it marks a major change in the evolution of the area, the formation of the ridges and the initiation of new basins.

Perissoratis et al. (1993) and Piper and Perissoratis (2003) proposed the occurrence of "basin inversion" (uplift of former basinal areas) in the South Aegean. Piper and Perissoratis (2003) suggest that "basin inversion" is the result of the change of the strike of the predominant faults from E-W to NE-SW, during the transition from the Pliocene to Quaternary. They also proposed that the deepest seismic units, eastwards of Santorini island, now form prominent ridges. The Unconformity U3 of the present study seems to be related to the transition from the status of a single basin to a complex regime of individual basins separated by uplifted shallow ridges.

The available data from SASZ do not allow a precise determination of the age of Unconformity U3. Chronological constraints of the post-Messinian infill of sedimentary basins in the Aegean Sea derives (i) either from the interpretation of low sea level prograding sequences and clinoforms or (ii) by comparison with the results of the Deep-Sea Drilling Project (DSDP) hole 378 in the Cretan Sea (Hsu et al., 1978). The latter penetrated 343.5 m below the seafloor and revealed two major unconformities: the top of the Messinian evaporites at roughly 305–310 m bsf and a younger one at roughly 130m bsf of an Early Quaternary approximate age (also see Tsampouraki-Kraounaki and Sakellariou, 2018, Figure 6, for a short section of a recent seismic profile through the 378 hole).

The seismic stratigraphy and structure of the sedimentary infill below and above the Early Quaternary unconformity in the Cretan Basin displays remarkable similarities with the seismic stratigraphy of the SASZ basins with the seismic units 6, 5, and 4 below the Unconformity U3 and the seismic units 3, 2, and 1 above it. A similar unconformity has been observed in the sedimentary infill of most of the basins in the South Aegean. It indicates a major change in the

tectonic regime with rearrangement and faulting of the Pliocene basins, onset of local subsidence and basin inversion (Bartole et al., 1983; Mascle and Martin, 1990; Piper and Perissoratis, 2003; Anastasakis and Piper, 2005). By comparison with the aforementioned data, it is proposed here that Unconformity U3 is equivalent to the Early Quaternary unconformity observed in DSDP hole 378.

The analysis and comparison of the seismic stratigraphy and structure of the seven basins of SASZ indicate that subsidence in the area initiated in the early Pliocene with the formation of one, single basin (Figure 4.2.11). The Pliocene basin included the Amorgos North, Amorgos South, Kinairos, the northeastern part of Anydros and probably Anafi basins. The seismic units 6, 5, and 4 represent the Pliocene deposits of the lower part of the sedimentary sequences, below Unconformity 3, in all these basins. The subsidence of the Pliocene basin was controlled predominantly by the northern, E-W to WSW-ENE striking, S-facing, marginal faults. They are the ancestors of the Perissa Fault, Amorgos Fault, and Kinairos Fault. The southern margin was controlled by the early Anafi Fault zone and probably by minor faulting further east.

The initial, single basin evolved into a significantly more complicated morphological and tectonic structure. Unconformity U3 marks the transition in Early Quaternary from the single basin to the present configuration with the multiple basins and ridges.

The seismic units 6, 5 and partly 4 are absent from the sedimentary sequence of the central and the south-western parts of Anydros Basin and of the Astypalea North and South basins. This evidence strongly suggests that these basins are more recent compared to the other basins of SASZ. Initiation of subsidence and formation of the Astypalea North, Astypalea South, and the central and southwestern part of Anydros Basin took place in the Early Quaternary. They are associated with the Unconformity U3 and are accompanied by tilting and uplift of the older basins and the formation of the Anydros and Astypalea Ridges (Figure 4.2.11).

Rifting of the southwestern and central parts of Anydros Basin occurred on the northern margin of the Pliocene basin and led to the formation of Anydros Ridge and its separation from the latter. Ios Fault Zone (IFZ) controls the northern margin, while Akrotiri Fault (AkF) and Anydros Ridge North Fault Zone (AdRNFZ) mark the southern boundary of the new basin. The

simultaneous initiation of the Anydros Ridge South Fault Zone (AdRSFZ) at the northeastern prolongation of the Perissa Fault (PF) accommodates the uplift of the Anydros Ridge.

Rifting in the Astypalea North Basin occurred in the southeastern part of the Pliocene single basin through the generation of the SE-facing Astypalea Ridge Fault Zone. Uplift of the footwall of the latter resulted to the formation of Astypalea Ridge.

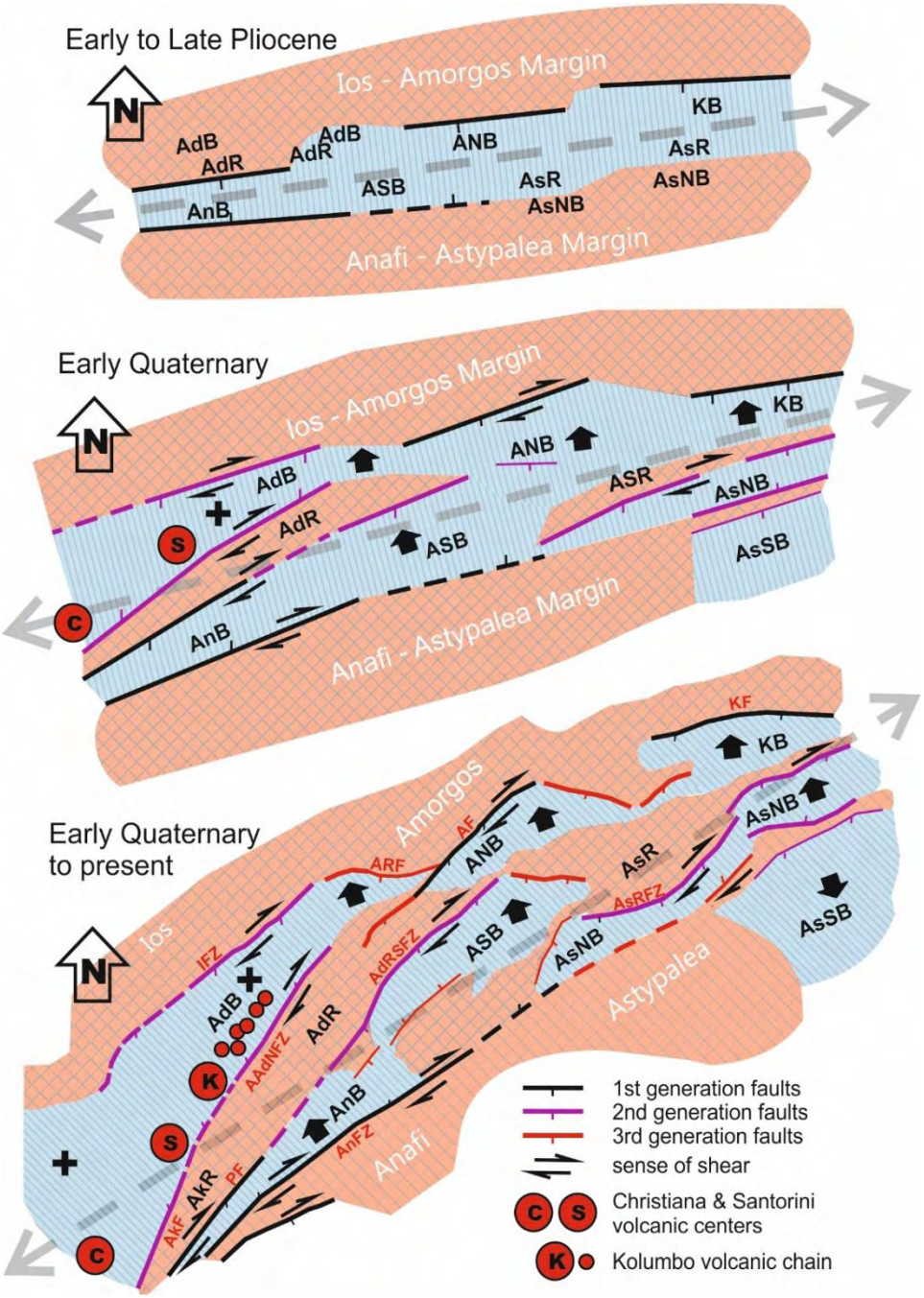

Figure 4.2.11: Schematic representation of the evolution of Santorini-Amorgos Shear Zone since Early Pliocene. See text for description and discussion.

The significant change of the geodynamic regime that led to the re-structuring of the Pliocene single basin and the rifting of new basins in the Early Quaternary, evolved further during the Quaternary and led to the present geological, geomorphological and tectonic configuration of the Santorini-Amorgos Shear Zone. Propagation and re-orientation of the older faults and initiation of new ones accommodated uplift and enlargement of the Anydros and Astypalea Ridges and preferential, localized subsidence in the new basins.

Propagation of the Amorgos Faults (AF) towards the SW and of the Anydros Ridge North and South Fault Zones (AdRNFZ, AdRSFZ) towards the NE resulted in the separation of Amorgos North Basin (ANB) from Amorgos South Basin (ASB) and in the separation of the northeastern part of Anydros Basin from the Amorgos North Basin. Initiation of the WNW-ESE striking Amorgos South Relay Fault (ASRF) led to the asymmetric subsidence in the northeastern part of Anydros Basin. Initiation of the WNW-ESE striking Amorgos North Relay Fault (ANRF), along with the progressive uplift of Astypalea Ridge, led to the separation of Kinairos Basin from Amorgos North Basin. Uplift and bi-directional propagation of the Astypalea Ridge, due to the Astypalea Ridge Fault Zone (AsRFZ), formed the boundary between the Astypalea Basin (AsB) and the Amorgos South Basin (ASB) and between AsB and Kinairos Basin (KB).

The basin evolution model presented above builds on older studies by Piper and Perissoratis (see Hsu et al., 1978 and Piper et al. 2007) in the area extending to the East of Santorini. They have observed a major change of the tectonic regime in the boundary between Pliocene and Quaternary that led from E-W normal faulting to NE strike-slip faulting. Different evolution has been proposed by Hübscher et al. (2015) and Nomikou et al. (2016). They have recognized multiple rift pulses in the area between Santorini and Amorgos islands with NE-SW striking normal faults controlling the evolution since Early Pliocene.

4.2.6.2 Deformation and Kinematics

The detailed map of the active fault network of SASZ is shown in Figure 4.2.9A, while the vertical and horizontal sense of movement along the individual faults, the tectonic asymmetry, and vertical movements of the basins and ridges and the kinematic interpretation of the entire structure is illustrated on the sketch-map of Figure 4.2.9B.

The fault network is dominated by NE-SW striking, SE-dipping faults and fault zones (IFZ, AF, KF, PF, AdRSFZ, AsRFZ) followed by NW-facing ones (AkF, AdRNFZ, AnFZ). These are the major faults which control the tectonic evolution, shape, subsidence and uplift of the multiple basins and ridges. They are accompanied by roughlyW-E (WSW-ENE to WNW-ESE) striking, S-facing normal faults (ASRF, ANRF), which seem to accommodate transfer of strain between the NE-SW striking fault zones.

The NE-SW striking faults are aligned subparallel or at low angle (<20^0) to the GPS vectors that show the direction of extension with respect to stable Eurasia (Kreemer and Chamot-Rooke, 2004). The direction of extension corresponds to the direction of rifting across the SASZ. However, the rifting direction displays angular relationship of roughly 30^0 with the orientation of the entire SASZ and with the orientation of the long axes of the basins and ridges that form the latter. The angular relationship between the orientation of SASZ and the rifting direction indicates significant obliquity with horizontal and vertical sense of displacement along the marginal, basin bounding faults and fault zones.

The mapped fault network of SASZ (Figure 4.2.9A) includes long, NE-SW striking, SE and NW-dipping, steep faults and short, WNW-ESE striking, S-dipping, moderate steep faults. This spatial configuration along with the obliquity between the orientation of SASZ and the rifting direction strongly suggests dextral to dextral oblique sense of movement along the major, NE-SW striking faults. The short WNW-ESE striking faults act as relay, normal faults that accommodate extension and transfer of strain between the former ones. Thus, the deformation of the basins and ridges in the SASZ since Early Quaternary evolved within a complex kinematic regime of dextral obliquity with a NE-SW trending, strike-slip motion associated with local subsidence (basins) and uplift (uplifted sediments, ridges) and extension in NW-SE direction (see Figure 4.2.9B). This interpretation is supported by new observations of the GPS velocity field of the Aegean by Briole et al. (2021), who recognized dextral transtensional movement of 4.5 mm yr^{-1} between the Amorgos and Astypalea islands.

The observed kinematic pattern coincides with the 30^0 oblique rifting model of Withjack and Jamison (1986), where the basin axis runs at 30^0 with respect to the rifting direction (Figure 4.2.9C). Their model foresees dextral, strike-slip faults running sub-parallel to the basin axis and normal

faults trending about 30^0 clockwise with respect to the rift axis. The results obtained from the current study blend in perfectly with this model. The NE-SW faults represent the strike-slip faults running sub-parallel to the basin axis and the WNW-ESE striking faults coincide to the extensional step over normal faults.

The interpretation of the style of deformation and the kinematic pattern in the Santorini-Amorgos Shear Zone, as described here above, takes advantage of and builds on previous studies that have contributed to the understanding of the structure and tectonics of this part of the Aegean Sea.

Dextral strike-slip faulting in NE-SW direction has been firstly proposed in the 90s by Mascle, Martin (1990) for the Santorini-Amorgos area and other areas in the Aegean. Papadopoulos and Pavlidis (1992) have suggested normal faulting with a significant right lateral, strike-slip component in the area. The conclusion of Stiros et al. (1994) was that Amorgos can be regarded as the uplifted and back-tilted footwall of a major normal fault or that the island marks the restraining (and uplifting) bend of the oblique-slip fault that controls its southeastern coast. Piper and Perissoratis (2003) and Piper et al. (2007) proposed that the style of the NE-SW faulting observed in the area east of Santorini Island, strongly suggest a strike-slip regime. The micro-seismicity data presented by Bohnhoff et al. (2006) have shown that the SW–NE Santorini—Amorgos zone is in the state of a right-lateral transtension. This observation has been reinforced by Dimitriadis et al. (2009). Sakellariou et al. (2017) proposed that both Thera and Kolumbo volcanic centers occur within the NE-SW-trending Anydros graben, which constitutes a negative flower structure related to a 40 km, possibly dextral, strike-slip zone, the Kameni-Kolumbo strike-slip, which can be extended SW-wards to the Christiana volcanic island. Analysis and relocation of the 2011–2012 seismic crisis in Santorini Caldera by Papadimitriou et al. (2015) showed that the seismicity was NE-SW oriented with focal mechanisms, indicating dextral strike-slip faulting. Tsampouraki-Kraounaki and Sakellariou (2017) suggested that the NE-SW-trending, morphologically complex area northeast of Thera until the islands of Amorgos, Astypalea and Kalymnos, which encompasses Anydhros Basin and the six sub-basins of Amorgos Basin undergoes dextral transtensional deformation accommodated by NE-SW strike slip to oblique faults and E-W normal step-over faults. Sakellariou and Tsampouraki- Kraounaki (2019) have

refined the offshore fault network and the kinematics of the Aegean Sea. They proposed that deformation is dominated by dextral shear zones in the northern, central, and southwestern Aegean and by sinistral shear zones in the southeastern Aegean. The Santorini-Amorgos Shear Zone displays a dextral sense of movement and marks the boundary between the dextral and sinistral shearing.

Opposite to the dextral sense of shearing described above, Hübscher et al. (2015), Nomikou et al. (2016,2018), and Hooft et al. (2017) have suggested that normal faulting is the main tectonic mechanism controlling the formation and evolution of the Anydhros Basin and the Thera-Amorgos area. Nomikou et al. (2016) stated that normal NE-SW striking, SE-dipping faulting is the superior mechanism forming the present horst and graben structures in the Santorini-Amorgos area, even though they have recognized an additional strike-slip component. A different interpretation has been recently proposed by Tzanis et al. (2020). The authors studied the kinematic regime of the Santorini area by using gravity, magnetotelluric, and DGPS data. According to their interpretation, the kinematic regime in that area is characterized by NW-SE dextral strike slip faults and NE-SW normal to sinistral faults generated by N-S oriented $\sigma 1$ and E-W oriented $\sigma 3$. However, the marine geophysical data presented here, as well as the seismological data available in previous studies, do not support sinistral sense of slip along the NE-SW striking faults of the area. In addition, the dextral transtensional movement of 4.5 mm yr-1 between the Amorgos and Astypalea islands, observed by Briole et al. (2021), strongly support significant dextral sense of horizontal slip along the SASZ, as proposed in the current work.

4.2.6.3 The Amorgos 1956 Earthquake

The focal mechanism, epicenter, and magnitude of the 9 July 1956, "Amorgos Earthquake", the largest seismic event in the Aegean Sea in the 20th century, have been the subject of many studies with contradicting results. The magnitude of the earthquake varies between M: 7.5 (Galanopoulos, 1957; Ambraseys, 1960; Papazachos and Delibasis, 1969; Papazachos et al., 1985; Papadopoulos et al., 2014), M: 7.6 (Konstantinou, 2010), and M: 7.8 (Okal et al., 2009), while the magnitude of the largest aftershock, that followed 12 min after the main shock, has been estimated to M: 7.2 (Okal et al., 2009). The focal mechanisms proposed so far are different from each other. Papazachos and Delibassis (1969) and Ritsema (1974) have suggested strike-slip movement along

NE-SW striking, SE-dipping fault, while Shirokova (1972) proposed a normal faulting geometry. Konstantinou (2010) and Okal et al. (2009) proposed normal faulting on a fault dipping gently to the SSE (see Okal et al., 2009 for a thorough discussion). Brüstle et al. (2014) proposed that the focal mechanism of the first event indicates normal slip with minor dextral motion on a SW-NE striking SE dipping fault plane ($\phi = 36^0$, $\delta = 62^0/67^0$, $\lambda = -96^0/-108^0$) at a depth of 25 ± 5 km. They also confirm that the focal mechanism is consistent with the location of the epicenter on the northern flank of the Santorini–Amorgos graben. It is commonly accepted (but not proved with field data) that the Amorgos Fault is related with and moved during the 1956 earthquake.

The epicenters calculated by the various studies for the main shock fall within an area a few tens of kilometers wide, west and southwest of the island of Amorgos. The epicenters of the main shock and of the largest aftershock, with the coordinates calculated by Okal et al. (2009) are shown on the map of Figure 4.2.9A. The epicenter of the main shock (Okal et al., 2009) falls within the northeastern part of Anydros Basin, on the footwall of Amorgos Fault and roughly 8–9 km northwest from its trace. If the location of the epicenter and the normal-slip focal mechanism are correct, it is highly unlikely that the earthquake moved the SE-dipping Amorgos Fault, as in this case it should be located on the hanging wall of the fault. In that case, the main shock may be associated with one of the faults that define the northern margin of Anydhros Basin. Alternatively, if the strike-slip focal mechanism on the NE-SW striking plane is the correct one for the main shock, it may fit with dextral slip on Amorgos Fault.

4.2.6.4 Implications for the Plio-Quaternary Evolution of the South Aegean bak-arc

It has been previously shown that the change in the mode of deformation is related with the Unconformity U3, which marks the transition from the extensional, Pliocene single basin to the Quaternary multi-basin dextral shear zone, and that U3 can be correlated with the Early Quaternary unconformity observed in DSDP hole 378 in the Cretan Sea (Hsu et al., 1978).

Several seismic profiling surveys conducted in the South Aegean Sea since the 80s (see Bartole et al., 1983; Rossi et al., 1986; Mascle and Martin, 1990; Piper and Perissoratis, 2003; Anastasakis and Piper, 2005; Tsampouraki-Kraounaki and Sakellariou, 2018 and others) have provided significant information on the evolution and structure of the sedimentary basins (Myrtoon, Maleas, Chania, Heraklion, Christiana, Kamilonissi, Karpathos Basins, Figure 4.2.1). A major

unconformity M marks the top of Messinian occurrences throughout the South Aegean. It represents the erosional surface of the exposed basement below the margins and the top of the Messinian evaporites below the basins. A second, widespread unconformity has been observed in the sedimentary infill of most of the basins in the South Aegean and has been correlated with the Early Quaternary unconformity observed in the DSDP 378 drill hole in the Cretan Basin (Hsu et al., 1978). It marks a major change in the tectonic regime, which led to rearrangement and faulting of the Pliocene basins, tilting of the basins' infill, local subsidence, and/or uplift and the development of the present morphological structure (see Bartole et al., 1983; Rossi et al., 1986; Mascle and Martin, 1990; Piper and Perissoratis, 2003; Anastasakis and Piper, 2005; Tsampouraki-Kraounaki and Sakellariou, 2018 and others).

The similarities between the structural characteristics of the South Aegean basins with the SASZ basins presented in this work are sound and point to a comparable structural evolution during the Plio-Quaternary. The evolution of SASZ from a single, E-W oriented, extensional basin in the Pliocene to the present, SW-NE striking, structurally complicated zone of dextral shearing and oblique rifting, composed of multiple basins and ridges, follows the progressive stretching of the South Aegean back-arc area towards SSW. The presumably Early Quaternary age of Unconformity U3 provides chronological constrains for the transition from N-S directed extension to NE-SW oriented dextral shearing.

A similar change in the style of deformation and basin evolution in the South Aegean Sea is strongly indicated by the available literature data described previously. Consequently, it is proposed here that the entire South Aegean back arc area has been affected in the Early Quaternary by a major change of the geodynamic regime that led to the formation of the present geomorphological configuration and structure. Large, mostly W-E oriented basins may have dominated the area between the Cyclades Plateau to the North and the Hellenic Arc to the South during the Pliocene. The Early Quaternary unconformity observed in most of the basins marks the transition from N-S extension, accommodated by mostly W-E normal faulting, to a new kinematic pattern composed mainly of NESW and NW-SE conjugate, strike-slip to oblique faulting and secondary W-E faults (see Mascle and Martin, 1990; Sakellariou and Tsampouraki-Kraounaki, 2019). Subsequent deformation and fracturing of the Pliocene large basins led to

enhanced subsidence in smaller basins, uplift and inversion of the previous basin infill and creation of new structural highs and ridges.

Back arc extension in the Aegean initiated in the Middle Eocene and is since then driven by the roll-back of the subducting East Mediterranean slab and the advancement of the trench towards the south (Royden, 1993; Jolivet and Faccena, 2000; Faccena et al., 2003; Brun and Faccena, 2008; Jolivet and Brun, 2008; Brun and Sokoutis, 2010; Jolivet et al., 2013; Faccena et al., 2014). The velocity of the trench retreat was less than 1 cm/y until the Middle Miocene and accelerated progressively to reach 3.2 cm/y in the Plio-Quaternary (Brun et al., 2016), while, according to Beniest et al. (2016), it accelerated by a factor of 5 after the Pliocene. Roll back and trench retreat led to a progressive increase of the curvature of the Hellenic Arc, re-organization of the crustal extension in the South Aegean back-arc area, re-orientation of older faults and initiation of new ones that deformed the older basins and led to extensive new basin and ridge formation.

The arrival and propagation of the North Anatolian Fault (NAF) in the North Aegean added one more factor of complexity. It is not yet adequately understood if and how the NAF interacts with the roll back and the trench retreat and how their interplay affects the evolution and deformation of the Aegean back arc since the arrival of the former. Armijo et al. (1996, 1999) were the first to propose that NAF propagated in the North Aegean in Late Miocene to Early Pliocene, at roughly 5 Ma BP and triggered the initiation and development of the major grabens in the Corinth, North Evia, and Thermaikos Gulfs. However, more recent studies propose that NAF may have arrived in the Aegean in the Early Pleistocene, at 2 Ma BP (Le Pichon et al., 2016) or Early to Middle Pleistocene (Beniest et al., 2016) or even earlier, at 430 ka BP (Ferentinos et al., 2018). Beniest et al. (2016) suggested that the establishment of NAF in the North Aegean Sea in the Lower to Middle Pleistocene may be responsible for the acceleration of the trench retreat and increase of its curvature after the Pliocene.

The presumably Early Quaternary in age Unconformity U3 in the SASZ and its correlation with the equivalent unconformity observed in the basins of the South Aegean indicate a drastic change in the basin evolution and mode of deformation. Enhanced shearing and oblique rifting along the SASZ and probably widely in the South Aegean are the results of the change in the

angular relationship between the orientation of the rifted basins and the kinematic regime. It is proposed here that the establishment of the Early Quaternary to present kinematic regime has been triggered by the gradual propagation in the North Aegean and the onset of interaction between the NAF and the trench retreat.

To confirm the above hypothesis and to gain reliable chronological constraints on the evolution and style of the deformation in the South Aegean Sea back arc area, further systematic swath bathymetry and seismic profiling surveys are needed. As already stated, most of the South Aegean Sea is either not surveyed at all or covered by sparse and old data of limited use. The significant lack of data leaves many open questions on the basin evolution, the style of deformation, and the kinematic regime.

4.2.7 Conclusions

Processing, analysis, and interpretation of systematic swath bathymetry and seismic profiling data obtained during several cruises on the R/V AEGAEO of the Hellenic Center for Marine Research between 2001 and 2017 in the broader area between Santorini, Amorgos, Kalymnos, Astypalea, and Anafi Islands in the South Aegean Sea, Greece, lead to the following major conclusions.

Santorini-Amorgos Shear Zone (SASZ) is a NE-SW striking, dextral shear, and oblique rifting zone. It includes seven, actively subsiding, elongated or spindle-shaped basins (Anydros, Anafi, Amorgos South, Amorgos North, Kinairos, Astypalea North and Astypalea South Basins), two actively uplifting, shallow ridges (Anydros and Astypalea Ridges), and several branches formed in the prolongations of the ridges. Dextral shearing and oblique rifting are accommodated by NE-SW oblique faults and fault zones, running at a low angle with respect to the NNE-SSW oriented kinematic vectors, and by roughly W-E striking, normal, transfer faults. The active fault pattern and kinematics is compatible with dextral oblique rifting across a rift zone oriented at roughly 30_ in respect to the rifting direction. The axis of SASZ strikes $N50^0$–55^0 E, while the GPS derived kinematic vectors that indicate the rifting direction are oriented at $N25^0$–30^0 E.

The SASZ initiated in the Early Pliocene as a single, W-E oriented, extensional basin developed within a N-S directed extensional regime. The sediments deposited during Pliocene represent the lower part of the sedimentary sequences of the Anafi, Amorgos South, Amorgos North, and

Kinairos basins, which were united into a single basin. A major reorganization of the geodynamic and kinematic regime took place sometime in the Early Quaternary and was imprinted in the seismic stratigraphy of the above basins with the Unconformity U3. It led to reorientation of the older faults and initiation of new ones striking NE-SW, disruption of the former single basin with local subsidence creating four new depocenters (basins) and local uplift, and rifting of the northern and southern Pliocene margins, formation of the Anydros, Astypalea North, and Astypalea South basins and of the Anydros and Astypalea ridges.

The apparent discrepancy between the dip-slip normal focal mechanism modeled for the 9 July 1956, Amorgos earthquake and the dextral shearing kinematics attributed to the SASZ is being discussed. It is proposed here that the normal faulting focal mechanism on a fault dipping to the SSE, proposed by Okal et al. (2009), is compatible with the geometry and kinematic characteristics of the W-E striking Amorgos South Relay Fault (ASRF) and can be explained within the dextral strike-slip regime of the SASZ.

Comparison of the seismic stratigraphy, evolution and structure of SASZ and of the basins of the South Aegean, indicates that the entire area has been affected by a major change of the kinematic regime. Enhanced shearing and oblique rifting along the SASZ and probably in the entire South Aegean back arc area is the result of the change of the angular relationship between the orientation of the rifted basins and the kinematic regime. It is proposed here that the establishment of the Early Quaternary to present kinematic regime has been triggered by the gradual propagation of the North Anatolian Fault in the North Aegean and the onset of interaction with the trench retreat since the Early Quaternary.

Acknowledgments

This work uses swath bathymetry and seismic profiling data acquired during several cruises of R/V AEGAEO between 2001 and 2017 and funded partly by THERA (2006) and Eurofleets2 LGT-AMORGOS-56 international projects and partly by national (HCMR) funds. The authors are grateful to the colleagues and technicians who contributed to the acquisition of the data. The crew and the captain of R/V AEGAEO are particularly acknowledged for their continuous support and smooth collaboration during the cruises. We would like to thank Emeritus Professor J. Mascle for

the valuable discussions we had with him at the early stage of the preparation of the manuscript. Last but not least, we are grateful to the reviewers for the critical and constructive review of the manuscript.

References

Alexandri, M.; Papanikolaou, D.; Nomikou, P.; Ballas, D. Santorini Volcanic Field–New Insights Based on Swath Bathymetry; Abstracts IUGG: Saporo, Japan, 2003.

Ambraseys, N.N. The seismic sea wave of July 9, 1956, in the Greek archipelago. J. Geophys. Res. Space Phys. 1960, 65, 1257–1265. https://doi.org/10.1029/JZ065i004p01257

Anastasakis, G.; Piper, D.J. Late Neogene evolution of the western South Aegean volcanic arc: Sedimentary imprint of volcanicity around Milos. Mar. Geol. 2005, 215, 135–158. https://doi.org/10.1016/j.margeo.2004.11.014

Angelier, J.; Lybéris, N.; Le Pichon, X.; Barrier, E.; Huchon, P. The tectonic development of the hellenic arc and the sea of crete: A synthesis. Tectonophysics 1982, 86, 159–196. https://doi.org/10.1016/0040-1951(82)90066-X

Armijo, R.; Meyer, B.; King, G.C.P.; Rigo, A.; Papanastassiou, D. Quaternary evolution of the Corinth Rift and its implications for the Late Cenozoic evolution of the Aegean. Geophys. J. Int. 1996, 126, 11–53. https://doi.org/10.1111/j.1365-246X.1996.tb05264.x

Armijo, R.; Meyer, B.; Hubert, A.; Barka, A. Westward propagation of the North Anatolian fault into the northern Aegean: Timing and kinematics. Geology 1999, 27, 267–270. https://doi.org/10.1130/0091-7613(1999)027<0267:WPOTNA>2.3.CO;2

Bartole, R.; Catani, G.; Lenardon, G.; Vinci, A. Tectonics and sedimentation of the Southern Aegean Sea. Boll. Oceanol. Teor. Appl. 1983, 4, 319–340.

Beniest, A.; Brun, J.-P.; Gorini, C.; Crombez, V.; Deschamps, R.; Hamon, Y.; Smit, J. Interaction between trench retreat and Anatolian escape as recorded by neogene basins in the northern Aegean Sea. Mar. Pet. Geol. 2016, 77, 30–42. https://doi.org/10.1016/j.marpetgeo.2016.05.011

Billiris, H.; Paradissis, D.; Veis, G.; England, P.; Featherstone, W.; Parsons, B.; Cross, P.; Rands, P.; Rayson, M.; Sellers, P.; et al. Geodetic determination of tectonic deformation in central Greece from 1900 to 1988. Nat. Cell Biol. 1991, 350, 124–129. https://doi.org/10.1038/350124a0

Bohnhoff, M.; Rische, M.; Meier, T.; Becker, D.; Stavrakakis, G.; Harjes, H.-P. Microseismic activity in the Hellenic Volcanic Arc, Greece, with emphasis on the seismotectonic setting of the Santorini–Amorgos zone. Tectonophysics 2006, 423, 17–33. https://doi.org/10.1016/j.tecto.2006.03.024

Bornovas, J.; Rondoyanni, T. Geological map of Greece, scale 1:500.000. Inst. Geol. Min. Explor. Greece 1984.

Briole, P.; Rigo, A.; Lyon-Caen, H.; Ruegg, J.C.; Papazissi, K.; Mitsakaki, C.; Balodimou, A.; Veis, G.; Hatzfeld, D.; Deschamps, A. Active deformation of the Corinth rift, Greece: Results from repeated Global Positioning System surveys between 1990 and 1995. J. Geophys. Res. Space Phys. 2000, 105, 25605–25625. https://doi.org/10.1029/2000JB900148

Briole, P.; Ganas, A.; Elias, P.; Dimitrov, D. The GPS velocity field of the Aegean. New observations, contribution of the earthquakes, crustal blocks model. Geophys. J. Int. 2021, 226, 468–492. https://doi.org/10.1093/gji/ggab089

Brun, J.-P.; Faccenna, C. Exhumation of high-pressure rocks driven by slab rollback. Earth Planet. Sci. Lett. 2008, 272, 1–7. https://doi.org/10.1016/j.epsl.2008.02.038

Brun, J.-P.; Sokoutis, D. 45 m.y. of Aegean crust and mantle flow driven by trench retreat. Geology 2010, 38, 815–818. https://doi.org/10.1130/G30950.1

Brun, J.-P.; Faccenna, C.; Gueydan, F.; Sokoutis, D.; Philippon, M.; Kydonakis, K.; Gorini, C. The two-stage Aegean extension, from localized to distributed, a result of slab rollback acceleration. Can. J. Earth Sci. 2016, 53, 1142–1157. https://doi.org/10.1139/cjes-2015-0203

Brüstle, A.; Friederich,W.; Meier, T.; Gross, C. Focal mechanism and depth of the 1956 Amorgos twin earthquakes from waveform matching of analogue seismograms. Solid Earth 2014, 5, 1027–1044. https://doi.org/10.5194/se-5-1027-2014, 2014

Chatzipetros, A.; Kiratzi, A.; Sboras, S.; Zouros, N.; Pavlides, S. Active faulting in the north-eastern Aegean Sea Islands. Tectonophysics 2013, 597–598, 106–122. https://doi.org/10.1016/j.tecto.2012.11.026

Clarke, P.J.; Billiris, H.; Paradissis, D.; Veis, G.; Cross, P.A.; Denys, P.H.; Ashkenazi, V.; Kahle, H.-G.; Muller, M.-V.; Davies, R.R.; et al. Crustal strain in central Greece from repeated GPS measurements in the interval 1989–1997. Geophys. J. Int. 1998, 135, 195–214. https://doi.org/10.1046/j.1365-246X.1998.00633.x

Cocard, M.; Kahle, H.-G.; Peter, Y.; Geiger, A.; Veis, G.; Felekis, S.; Paradissis, D.; Billiris, H. New constraints on the rapid crustal motion of the Aegean region: Recent results inferred from GPS measurements (1993–1998) across the West Hellenic Arc, Greece. Earth Planet. Sci. Lett. 1999, 172, 39–47. https://doi.org/10.1016/S0012-821X(99)00185-5

Davies, R.; England, P.; Parsons, B.; Billiris, H.; Paradissis, D.; Veis, G. Geodetic strain of Greece in the interval 1892–1992. J. Geophys. Res. Space Phys. 1997, 102, 24571–24588. https://doi.org/10.1029/97JB01644

Dewey, J.F.; ¸Sengor, A.M.C. Aegean and surrounding regions: Complex multiplate and continuum tectonics in a convergent zone. Geol. Soc. Am. Bull. 1979, 90, 84–92. https://doi.org/10.1130/0016-7606(1979)90<84:AASRCM>2.0.CO;2

Dimitriadis, I.; Karagianni, E.; Panagiotopoulos, D.; Papazachos, C.; Hatzidimitriou, P.; Bohnhoff, M.; Rische, M.; Meier, T. Seismicity and active tectonics at Coloumbo Reef (Aegean Sea, Greece): Monitoring an active volcano at Santorini Volcanic Center using a temporary seismic network. Tectonophysics 2009, 465, 136–149. https://doi.org/10.1016/j.tecto.2008.11.005

Dimitriadis, I.; Papazachos, C.; Panagiotopoulos, D.; Hatzidimitriou, P.; Bohnhoff, M.; Rische, M.; Meier, T. P and S velocity structures of the Santorini–Coloumbo volcanic system (Aegean Sea, Greece) obtained by non-linear inversion of travel times and its tectonic implications. J. Volcanol. Geotherm. Res. 2010, 195, 13–30. https://doi.org/10.1016/j.jvolgeores.2010.05.013

Faccenna, C.; Jolivet, L.; Piromallo, C.; Morelli, A. Subduction and the depth of convection in the Mediterranean mantle. J. Geophys. Res. Space Phys. 2003, 108. https://doi.org/10.1029/2001JB001690

Faccenna, C.; Becker, T.W.; Auer, L.; Billi, A.; Boschi, L.; Brun, J.P.; Capitanio, F.A.; Funiciello, F.; Horvàth, F.; Jolivet, L.; et al. Mantle dynamics in the Mediterranean. Rev. Geophys. 2014, 52, 283–332. https://doi.org/10.1002/2013RG000444

Ferentinos, G.; Georgiou, N.; Christodoulou, D.; Geraga, M.; Papatheodorou, G. Propagation and termination of a strike slip fault in an extensional domain: The westward growth of the North Anatolian Fault into the Aegean Sea. Tectonophysics 2018, 745, 183–195. https://doi.org/10.1016/j.tecto.2018.08.003

Frey-Martinez, J. 3D Seismic Interpretation of Mass Transport Deposits: Implications for Basin Analysis and Geohazard Evaluation. Submar. Mass Mov. Conseq. 2007, 28, 553–568. https://doi.org/10.1007/978-90-481-3071-9_45

Fytrolakis, N.; Papanikolaou, D. Stratigraphy and structure of Amorgos Island, Aegean Sea. Ann. Geol. Pays Hellen. 1981, 30, 455–472.

Galanopoulos, A.G. The seismic sea wave of 9 July 1956. Prakt. Akad. Athens 1957, 32, 90–101.

Goldsworthy, M.; Jackson, J.; Haines, J. The continuity of active fault systems in Greece. Geophys. J. Int. 2002, 148, 596–618. https://doi.org/10.1046/j.1365-246X.2002.01609.x

Heath, B.A.; Hooft, E.E.E.; Toomey, D.R.; Papazachos, C.B.; Nomikou, P.; Paulatto, M.; Morgan, J.V.; Warner, M.R. Tectonism and Its Relation to Magmatism Around Santorini Volcano from Upper Crustal P Wave Velocity. J. Geophys. Res. Solid Earth 2019, 124, 10610–10629. https://doi.org/10.1029/2019JB017699

Hooft, E.E.; Nomikou, P.; Toomey, D.R.; Lampridou, D.; Getz, C.; Christopoulou, M.-E.; O'Hara, D.; Arnoux, G.M.; Bodmer, M.; Gray, M.; et al. Backarc tectonism, volcanism, and mass wasting shape seafloor morphology in the Santorini-Christiana-Amorgos region of the Hellenic Volcanic Arc. Tectonophysics 2017, 712–713, 396–414. https://doi.org/10.1016/j.tecto.2017.06.005

Hsu, K.J.; Montadert, L.; Bernouilli, D.; Bizon, G.; Cita, M.; Erickson, A.; Fabricius, F.; Garrison, R.E.; Kido, R.B.; Mellieres, F.; et al. Site 378: Cretan basin. Init. Rep. Deep-Sea Drill. Proj. 1978, 42, 321–357.

Hübscher, C.; Ruhnau, M.; Nomikou, P. Volcano-tectonic evolution of the polygenetic Kolumbo submarine volcano/Santorini (Aegean Sea). J. Volcanol. Geotherm. Res. 2015, 291, 101–111. https://doi.org/10.1016/j.jvolgeores.2014.12.020

İşcan, Y.; Tur, H.; Göka¸san, E. Morphologic and seismic features of the Gulf of Gökova, SW Anatolia: Evidence of strike-slip faulting with compression in the Aegean extensional regime. Geo-Mar. Lett. 2012, 33, 31–48. https://doi.org/10.1007/s00367-012-0307-x

Jackson, J. Active Tectonics of the Aegean Region. Annu. Rev. Earth Planet. Sci. 1994, 22, 239–271. https://doi.org/10.1146/annurev.ea.22.050194.001323

Jackson, J.; McKenzie, D. Rates of active deformation in the Aegean Sea and surrounding regions. Basin Res. 2007, 1, 121–128. https://doi.org/10.1111/j.1365-2117.1988.tb00009.x

Jolivet, L.; Faccenna, C. Mediterranean extension and the Africa-Eurasia collision. Tectonics 2000, 19, 1095–1106. https://doi.org/10.1029/2000TC900018

Jolivet, L.; Brun, J.-P. Cenozoic geodynamic evolution of the Aegean. Acta Diabetol. 2008, 99, 109–138. https://doi.org/10.1007/s00531-008-0366-4

Jolivet, L.; Faccenna, C.; Huet, B.; Labrousse, L.; Le Pourhiet, L.; Lacombe, O.; Lecomte, E.; Burov, E.; Denèle, Y.; Brun, J.-P.; et al. Aegean tectonics: Strain localisation, slab tearing and trench retreat. Tectonophysics 2013, 597–598, 1–33. https://doi.org/10.1016/j.tecto.2012.06.011

Kahle, H.-G.; Müller, M.V.; Geiger, A.; Danuser, G.; Mueller, S.; Veis, G.; Billiris, H.; Paradissis, D. The strain field in northwestern Greece and the Ionian Islands: Results inferred from GPS measurements. Tectonophysics 1995, 249, 41–52. https://doi.org/10.1016/0040-1951(95)00042-L

Kahle, H.-G.; Cocard, M.; Peter, Y.; Geiger, A.; Reilinger, R.; McClusky, S.; King, R.; Barka, A.; Veis, G. The GPS strain rate field in the Aegean Sea and western Anatolia. Geophys. Res. Lett. 1999, 26, 2513–2516. https://doi.org/10.1029/1999GL900403

Kahle, H.-G.; Cocard, M.; Peter, Y.; Geiger, A.; Reilinger, R.; Barka, A.; Veis, G. GPS-derived strain rate field within the boundary zones of the Eurasian, African, and Arabian Plates. J. Geophys. Res. Space Phys. 2000, 105, 23353–23370. https://doi.org/10.1029/2000JB900238

Kassaras, I.; Kapetanidis, V.; Ganas, A.; Tzanis, A.; Kosma, C.; Karakonstantis, A.; Valkaniotis, S.; Chailas, S.; Kouskouna, V.; Papadimitriou, P. The New Seismotectonic Atlas of Greece (v1.0) and Its Implementation. Geosciences 2020, 10, 447. https://doi.org/10.3390/geosciences10110447

Kilias, S.P.; Nomikou, P.; Papanikolaou, D.; Polymenakou, P.N.; Godelitsas, A.; Argyraki, A.; Carey, S.; Gamaletsos, P.; Mertzimekis, T.J.; Stathopoulou, E.; et al. New insights into hydrothermal vent processes in the unique shallow-submarine arc-volcano, Kolumbo (Santorini), Greece. Sci. Rep. 2013, 3, 1–13. https://doi.org/10.1038/srep02421

Kiratzi, A. Focal mechanisms of shallow earthquakes in the Aegean Sea and the surrounding lands determined by waveform modelling: A new database. J. Geodyn. 2003, 36, 251–274. https://doi.org/10.1016/S0264-3707(03)00050-4

Kokkalas, S.; Xypolias, P.; Koukouvelas, I.; Doutsos, T. Postcollisional contractional and extensional deformation in the Aegean region. In Post-Collisional Tectonics and Magmatism in the Mediterranean Region and Asia: Geological Society of America Special Paper; Dilek, Y., Pavlides, S., Eds.; Geological Society of America: Boulder, CO, USA,2006; Volume 409, pp. 97–123. https://doi.org/ 10.1130/2006.2409(06)

Konstantinou, K. Crustal rheology of the Santorini–Amorgos zone: Implications for the nucleation depth and rupture extent of the 9 July 1956 Amorgos earthquake, southern Aegean. J. Geodyn. 2010, 50, 400–409. https://doi.org/10.1016/j.jog.2010.05.002

Kreemer, C.; Chamot-Rooke, N.; Lepichon, X. Constraints on the evolution and vertical coherency of deformation in the Northern Aegean from a comparison of geodetic, geologic and seismologic data. Earth Planet. Sci. Lett. 2004, 225, 329–346. https://doi.org/10.1016/j.epsl.2004.06.018

Le Pichon, X.; Angelier, J. The hellenic arc and trench system: A key to the neotectonic evolution of the eastern Mediterranean area. Tectonophysics 1979, 60, 1–42. https://doi.org/10.1016/0040-1951(79)90131-8

Le Pichon, X.L.; Angelier, J.; Osmaston, M.F.; Stegena, L. The Aegean Sea. Philos. Trans. R. Soc. London. Ser. A, Math. Phys. Sci. 1981, 300, 357–372. https://doi.org/10.1098/rsta.1981.0069

Le Pichon, X.; Angelier, J.; Sibuet, J.-C. Plate boundaries and extensional tectonics. Tectonophysics 1982, 81, 239–256. https://doi.org/10.1016/0040-1951(82)90131-7

Le Pichon, X. Land-locked oceanic basins and continental collision: The Eastern Mediterranean as a case example. In Symposium on Mountain Building; Hsu, K.J., Ed.; Academic Press: San Diego, CA, USA, 1983; pp. 201–211.

Le Pichon, X.; Chamot-Rooke, N.; Lallemant, S.; Noomen, R.; Veis, G. Geodetic determination of the kinematics of central Greece with respect to Europe: Implications for eastern Mediterranean tectonics. J. Geophys. Res. Space Phys. 1995, 100, 12675–12690. https://doi.org/10.1029/95JB00317

Le Pichon, X.; ¸Sengör, A.C.; Kende, M.J.; Imren, C.; Henry, P.; Grall, C.; Karabulut, H. Propagation of a strike-slip plate boundary within an extensional environment: The westward propagation of the North Anatolian Fault. Can. J. Earth Sci. 2016, 53, 1416–1439. https://doi.org/10.1139/cjes-2015-0129

Mascle, J.; Martin, L. Shallow structure and recent evolution of the Aegean Sea: A synthesis based on continuous reflection profiles. Mar. Geol. 1990, 94, 271–299. https://doi.org/10.1016/0025-3227(90)90060-W

McClusky, S.; Balassanian, S.; Barka, A.; Demir, C.; Ergintav, S.; Georgiev, I.; Gurkan, O.; Hamburger, M.; Hurst, K.; Kahle, H.; et al. Global Positioning System constraints on plate kinematics and dynamics in the eastern Mediterranean and Caucasus. J. Geophys. Res. Space Phys. 2000, 105, 5695–5719. https://doi.org/10.1029/1999JB900351

McKenzie, D. Active Tectonics of the Mediterranean Region. Geophys. J. Int. 1972, 30, 109–185. https://doi.org/10.1111/j.1365-246X.1972.tb02351.x

McKenzie, D. Active tectonics of the Alpine–Himalayan belt: The Aegean Sea and surrounding regions. Geophys. J. Int. 1978, 55, 217–254. https://doi.org/10.1111/j.1365-246X.1978.tb04759.x

McKenzie, D.; Jackson, J. A block model of distributed deformation by faulting. J. Geol. Soc. 1986, 143, 349–353. https://doi.org/10.1144/gsjgs.143.2.0349

Melidonis, N.G. The Geology of Anafi island. Ph.D. Thesis, Aristotle University of Thessaloniki, Boulder, CO, USA, 1964; 308p.

Müller, M.; Geiger, A.; Kahle, H.-G.; Veis, G.; Billiris, H.; Paradissis, D.; Felekis, S. Velocity and deformation fields in the North Aegean domain, Greece, and implications for fault kinematics, derived from GPS data 1993–2009. Tectonophysics 2013, 597–598, 34–49. https://doi.org/10.1016/j.tecto.2012.08.003

Nomikou, P.; Papanikolaou, D. Extension of active fault zones on Nisyros volcano across the Yali-Nisyros Channel based on onshore and offshore data. Mar. Geophys. Res. 2011, 32, 181–192. https://doi.org/10.1007/s11001-011-9119-z

Nomikou, P.; Carey, S.; Papanikolaou, D.; Bell, K.C.; Sakellariou, D.; Alexandri, M.; Bejelou, K. Submarine volcanoes of the Kolumbo volcanic zone NE of Santorini Caldera, Greece. Glob. Planet. Chang. 2012, 90-91, 135–151 https://doi.org/10.1016/j.gloplacha.2012.01.001

Nomikou, P.; Hubscher, C.; Ruhnau, M.; Bejelou, K. Tectono-stratigraphic evolution through successive extensional events of the Anydros Basin, hosting Kolumbo volcanic field at the Aegean Sea, Greece. Tectonophysics 2016, 671, 202–217. https://doi.org/10.1016/j.tecto.2016.01.021

Nomikou, P.; Hübscher, C.; Papanikolaou, D.; Farangitakis, G.; Ruhnau, M.; Lampridou, D. Expanding extension, subsidence and lateral segmentation within the Santorini–Amorgos basins during

Quaternary: Implications for the 1956 Amorgos events, central–south Aegean Sea, Greece. Tectonophysics 2018, 722, 138–153. https://doi.org/10.1016/j.tecto.2017.10.016

Noomen, R., Ambrosius, B.A.C., Wakker, K.F. Crustal motions in the Mediterranean region determined from Laser Ranging to LAGEOS. In: Smith, D.E., Turcotte, D.L. (Eds.), Contributions of Space Geodesy to Geodynamics : Crustal Dynamics. AGU, Washington, DC 1993, pp. 331–346, doi:10.1029/GD023

Nyst, M.; Thatcher, W. New constraints on the active tectonic deformation of the Aegean. J. Geophys. Res. Space Phys. 2004, 109, 1–23. https://doi.org/10.1029/2003JB002830

Ocakoğlu, N.; Nomikou, P.; I¸scan, Y.; Loreto, M.F.; Lampridou, D. Evidence of extensional and strike-slip deformation in the offshore Gökova-Kos area affected by the July 2017 Mw6.6 Bodrum-Kos earthquake, eastern Aegean Sea. Geo-Mar. Lett. 2018, 38, 211–225. https://doi.org/10.1007/s00367-017-0532-4

Okal, E.A.; Synolakis, C.E.; Uslu, B.; Kalligeris, N.; Voukouvalas, E. The 1956 earthquake and tsunami in Amorgos, Greece. Geophys. J. Int. 2009, 178, 1533–1554. https://doi.org/10.1111/j.1365-246X.2009.04237.x

Papadimitriou, P.; Kapetanidis, V.; Karakonstantis, A.; Kaviris, G.; Voulgaris, N.; Makropoulos, K. The Santorini Volcanic Complex: A detailed multi-parameter seismological approach with emphasis on the 2011–2012 unrest period. J. Geodyn. 2015, 85, 32–57. https://doi.org/10.1016/j.jog.2014.12.004

Papadopoulos, G.A.; Pavlides, S.B. The large 1956 earthquake in the South Aegean: Macroseismic field configuration, faulting, and neotectonics of Amorgos Island. Earth Planet. Sci. Lett. 1992, 113, 383–396. https://doi.org/10.1016/0012-821X(92)90140-Q

Papadopoulos, G.A.; Gràcia, E.; Urgeles, R.; Sallares, V.; De Martini, P.M.; Pantosti, D.; González, M.; Yalciner, A.C.; Mascle, J.; Sakellariou, D.; et al. Historical and pre-historical tsunamis in the Mediterranean and its connected seas: Geological signatures, generation mechanisms and coastal impacts. Mar. Geol. 2014, 354, 81–109. https://doi.org/10.1016/j.margeo.2014.04.014

Papanikolaou, D. Tectonostratigraphic models of the Alpine terranes and subduction history of the Hellenides. Tectonophysics 2013, 595–596, 1–24. https://doi.org/10.1016/j.tecto.2012.08.008

Papazachos, B.; Delibasis, N. Tectonic stress field and seismic faulting in the area of Greece. Tectonophysics 1969, 7, 231–255. https://doi.org/10.1016/0040-1951(69)90069-9

Papazachos, B.; Koutitas, C.; Hatzidimitriou, P.; Karacostas, B.; Papaioannou, C. Source and short-distance propagation of the July 9, 1956 southern Aegean tsunami. Mar. Geol. 1985, 65, 343–351. https://doi.org/10.1016/0025-3227(85)90064-7

Papazachos, C.B.; Kiratzi, A.A. A detailed study of the active crustal deformation in the Aegean and surrounding area. Tectonophysics 1996, 253, 129–153. https://doi.org/10.1016/0040-1951(95)00047-X

Papazachos, B.C.; Papadimitriou, E.E.; Kiratzi, A.A.; Papazachos, C.B.; Louvari, E.K. Fault plane solutions in the Aegean Sea and the surrounding area and their tectonic implication. Boll. Geofis. Teor. Appl. 1998, 39, 199–218.

Pavlides, S.; Tranos, M. Structural characteristics of two strong earthquakes in the North Aegean: Ierissos (1932) and Agios Efstratios (1968). J. Struct. Geol. 1991, 13, 205–214. https://doi.org/10.1016/0191-

8141(91)90067-S

Pe-Piper, G.; Piper, D.J.; Perissoratis, C. Neotectonics and the Kos Plateau Tuff eruption of 161 ka, South Aegean arc. J. Volcanol. Geotherm. Res. 2005, 139, 315–338. https://doi.org/10.1016/j.jvolgeores.2004.08.014

Perissoratis, C.; Andrinopoulos, A.; Zacharaki, P.; Zimianitis, E. Sedimentological and geological studies in the middle part of the South Aegean Arc: Preliminary results. Bull. Geol. Soc. Greece 1993, 28, 511–531.

Perissoratis, C. The Santorini volcanic complex and its relation to the stratigraphy and structure of the Aegean arc, Greece. Mar. Geol. 1995, 128, 37–58. https://doi.org/10.1016/0025-3227(95)00090-L

Pérouse, E.; Chamot-Rooke, N.; Rabaute, A.; Briole, P.; Jouanne, F.; Georgiev, I.; Dimitrov, D. Bridging onshore and offshore present-day kinematics of central and eastern Mediterranean: Implications for crustal dynamics and mantle flow. Geochem. Geophys. Geosyst. 2012, 13, 1–25. https://doi.org/10.1029/2012GC004289

Piper, D.; Perissoratis, C. Quaternary neotectonics of the South Aegean arc. Mar. Geol. 2003, 198, 259–288. https://doi.org/10.1016/S0025-3227(03)00118-X

Piper, D.J.W.; Pe-Piper, G.; Perissoratis, C.; Anastasakis, G. Distribution and chronology of submarine volcanic rocks around Santorini and their relationship to faulting. Geol. Soc. Lond. Spec. Publ. 2007, 291, 99–111. https://doi.org/10.1144/SP291.5

Reilinger, R.E.; McClusky, S.C.; Oral, M.B.; King, R.W.; Toksoz, M.N.; Barka, A.A.; Kinik, I.; Lenk, O.; Sanli, I. Global Positioning System measurements of present-day crustal movements in the Arabia-Africa-Eurasia plate collision zone. J. Geophys. Res. Space Phys. 1997, 102, 9983–9999. https://doi.org/10.1029/96JB03736

Reilinger, R.; McClusky, S.; Vernant, P.; Lawrence, S.; Ergintav, S.; Cakmak, R.; Ozener, H.; Kadirov, F.; Guliev, I.; Stepanyan, R.; et al. GPS constraints on continental deformation in the Africa-Arabia-Eurasia continental collision zone and implications for the dynamics of plate interactions. J. Geophys. Res. Space Phys. 2006, 111, 1–26. https://doi.org/10.1029/2005JB004051

Reilinger, R.; McClusky, S.; Paradissis, D.; Ergintav, S.; Vernant, P. Geodetic constraints on the tectonic evolution of the Aegean region and strain accumulation along the Hellenic subduction zone. Tectonophysics 2010, 488, 22–30. https://doi.org/10.1016/j.tecto.2009.05.027

Ritsema, A.R. Earthquake mechanisms of the Balkan region, Kon. Ned. Meteor. Inst. Repts. 1974, 74, 36.

Rossi, S.; Got, H.; Taviani, M.; Martin, L. Elements structuraux de la mer de Crete orientale et du Golfe d'Antalya (Mediterranee orientale). Mem. Soc. Geol. It. 1986, 36, 153–164.

Royden, L.H. The tectonic expression slab pull at continental convergent boundaries. Tectonics 1993, 12, 303–325. https://doi.org/10.1029/92TC02248

Sakellariou, D.; Sigurdsson, H.; Alexandri, M.; Carey, S.; Rousakis, G.; Nomikou, P.; Georgiou, P.; Ballas, D. Active Tectonics in the Hellenic Volcanic Arc: The Kolumbo Submarine Volcanic Zone. Bull. Geol. Soc. Greece 2017, 43, 1056. https://doi.org/10.12681/bgsg.11270

Sakellariou, D.; Tsampouraki-Kraounaki, K. Plio-Quaternary Extension and Strike-Slip Tectonics in the Aegean. In Transform Plate Boundaries and Fracture Zones; Elsevier: Amsterdam, The Netherlands,

2019; pp. 339–374.

Shirokova, E.I. Napryazheniya i Razryvy v Ochagakh Zemletryasenii Sredizemnomorskovo-Aziatskovo Seismicheskovo Poyasa, in Polye upRugikh Napryazhenii Zemli i Mekhanizm Ochagov Zemletryasenii; Balakina, L.M., Vvedenskaya, A.V., Golubeva, N.V., Misharina, L.A., Shirokova, E.I., Eds.; Akad. Nauk SSSR: Moskow, Russia, 1972; pp. 112–148. (In Russian)

Sigurdsson, H.; Carey, S.; Alexandri, M.; Vougioukalakis, G.; Croff, K.L.; Roman, C.; Sakellariou, D.; Anagnostou, C.; Rousakis, G.; Ioakim, C. Marine investigations of Greece's Santorini volcanic field. Eos 2006, 87, 337–339. https://doi.org/10.1029/2006EO340001

Smith, P.E.; York, D.; Chen, Y.; Evensen, N.M. Single crystal40Ar-39Ar dating of a Late Quaternary paroxysm on Kos, Greece: Concordance of terrestrial and marine ages. Geophys. Res. Lett. 1996, 23, 3047–3050. https://doi.org/10.1029/96GL02759

Soukis, K.; Papanikolaou, D. Contrasting geometry between alpine and late- to post- alpine tectonic structures in Anafi Island (Cyclades). Bull. Geol. Soc. Greece 2004, 36, 1688–1696. https://doi.org/10.12681/bgsg.16575

Stiros, S.C.; Marangou, L.; Arnold,M. Quaternary uplift and tilting of Amorgos Island (Southern Aegean) and the 1956 earthquake. Earth Planet. Sci. Lett. 1994, 128, 65–76. https://doi.org/10.1016/0012-821X(94)90135-X

Straub, C.; Kahle, H.-G. Global Positioning System (GPS) estimates of crustal deformation in the Marmara Sea region, Northwestern Anatolia. Earth Planet. Sci. Lett. 1994, 121, 495–502. https://doi.org/10.1016/0012-821X(94)90086-8

Taymaz, T.; Jackson, J.; McKenzie, D. Active tectonics of the north and central Aegean Sea. Geophys. J. Int. 1991, 106, 433–490. https://doi.org/10.1111/j.1365-246X.1991.tb03906.x

Tsampouraki-Kraounaki, K.; Sakellariou, D. Strike-slip deformation behind the Hellenic subduction: The Amorgos Shear Zone, South Aegean Sea. In Proceedings of the 8th Internation-al INQUA Meeting on Paleoseismology, Active Tectonics and Archeoseismology, Blenheim, New Zeeland, 13–16 November 2017; Clark, K.J., Upton, P., Langridge, R., Kelly, K., Hammond, K., Eds.; pp. 392–395. doi:10.21420/G2H061

Tsampouraki-Kraounaki, K.; Sakellariou, D. Seismic stratigraphy and geodynamic evolution of Christiana Basin, South Aegean Arc. Mar. Geol. 2018, 399, 135–147. https://doi.org/10.1016/j.margeo.2018.02.012

Tur, H.; Yaltırak, C.; Elitez, I.; Sarıkavak, K.T. Pliocene–Quaternary tectonic evolution of the Gulf of Gökova, southwest Turkey. Tectonophysics 2015, 638, 158–176. https://doi.org/10.1016/j.tecto.2014.11.008

Tzanis, A.; Chailas, S.; Sakkas, V.; Lagios, E. Tectonic deformation in the Santorini volcanic complex (Greece) as inferred by joint analysis of gravity, magnetotelluric and DGPS observations. Geophys. J. Int. 2020, 220, 461–489. https://doi.org/10.1093/gji/ggz461

Uluğ, A.; Duman, M.; Ersoy, ¸S.; Özel, E.; Avcı, M. Late Quaternary sea-level change, sedimentation and neotectonics of the Gulf of Gökova: Southeastern Aegean Sea. Mar. Geol. 2005, 221, 381–395. https://doi.org/10.1016/j.margeo.2005.03.002

Van Hinsbergen, D.J.; Krijgsman,W.; Langereis, C.G.; Cornée, J.-J.; Duermeijer, C.E.; Van Vugt, N. Discrete Plio-Pleistocene phases of tilting and counterclockwise rotation in the southeastern Aegean arc (Rhodos, Greece): Early Pliocene formation of the south Aegean left-lateral strike-slip system. J. Geol. Soc. 2007, 164, 1133–1144. https://doi.org/10.1144/0016-76492006-061

Withjack, M.O.; Jamison, W.R. Deformation produced by oblique rifting. Tectonophysics 1986, 126, 99–124. https://doi.org/10.1016/0040-1951(86)90222-2

4.3. Plio-Quaternary extension and strike-slip tectonics in the Aegean

https://doi.org/10.1016/B978-0-12-812064-4.00014-1

4.3.1 Abstract

Detailed review and integrated re-interpretation of geological, seismological and geodetic data indicate a major change in the style of deformation of the Aegean microplate since the Early Pliocene. Widespread, arc-perpendicular, back-arc extension in the Miocene has been replaced by extensive shearing along strike-slip zones in the Plio-Quaternary. The Aegean crust "flows" toward SSW, confined between its northern (North Anatolian and Kephallinia Faults) and southern boundaries (East Hellenic Trench). It undergoes extension predominantly accommodated by strike-slip tectonics. Dextral shearing along major NE-SW strike-slip zones associated with conjugate NW-SE sinistral and WNW-ESE normal faults dominates over most of the Aegean Region and creates a complex pattern of localized transtensional features and the formation of new basins, along with local transpressional deformation and local uplift. Sinistral NE-SW to ENE-WSW trending shearing prevails in the southeastern Aegean, parallel to the sinistral shear zones of the Pliny and Strabo Trenches. The formation of the various Plio-Quaternary basins, the kinematic characteristics of individual faults and the spatial distribution of volcanoes of the Volcanic Arc can be adequately explained in the frame of the proposed deformation and kinematic pattern.

4.3.2. Introduction

Post-Miocene extension in the Aegean is related to the subduction of the African lithosphere beneath the Aegean, which initiated already in the Eocene (Jolivet et al., 2013; Brun et al., 2016 and references therein) and its interaction with the westward motion of Anatolia along the North Anatolian Fault since Late (?) Miocene to Pliocene (Armijo et al., 1996, 1999; Reilinger et al., 2010 and references therein). Although the outline of this overarching geotectonic framework is in general adequately described and understood, after decades of geological, geophysical, seismological and geodetic research, discussion still goes on and many aspects of the observed complex deformation pattern within the Aegean and along its boundaries are not yet convincingly explained. Very early, in the 70s, Le Pichon & Angelier (1979, 1981) first proposed that extension in the Aegean results from the retreat of the NNE-wards subducting East

Mediterranean slab. The first plate kinematic models described the Neogene to Quaternary tectonic evolution as the result of the interaction between slab retreat, back-arc extension and westward displacement of Anatolia along the dextral strike-slip North Anatolian Fault (NAF) (McKenzie, 1972, 1978; Dewey & Şengör, 1979; Le Pichon & Angelier, 1981). Before the 80s it was already evident that the Aegean is a deforming microplate bounded by two major strike-slip fault-zones with opposite sense of shear (Figure 4.3.1A): the westward prolongation of the dextral NAF in the North Aegean Trough (NAT) (Dewey & Şengör, 1979) represents the northern, transform-type boundary (Mercier et al., 1976; Brunn, 1976; Tapponnier, 1977); the Strabo and Pliny Trenches on the Levantine (eastern) segment of the Hellenic Trench mark the southern boundary of the deforming Aegean with sinistral sense of shear (Le Pichon & Angelier, 1979).

At that time, many of the key geodynamic features were not well recognized yet: The Hellenic Trench was considered as the front of the subduction and the Mediterranean Ridge (MR) was not yet interpreted as an accretionary prism. Compressional structures were already recognized in the 70s (Finetti, 1976) but the first solid geological evidence on the nature and development of the MR as an accretionary prism were only later presented by Chaumillon & Mascle (1995), Chaumillon et al. (1996) and Chaumillon & Mascle (1997). Shortly after, Mascle et al. (1999) provided new data supporting incipient continental collision with the Libyan promontory south of Crete. The high obliquity of the plate velocities in respect to the Hellenic Arc led Le Pichon et al. (1995) to propose that strain partitioning occurs, explaining thus the already observed separation of the Hellenic Trench in two branches with different kinematic characteristics: the western one (Matapan or Ionian Trench) characterized by frontal compression accompanied by dextral lateral motion (Huchon et al., 1982; Lyberis et al., 1982) and the eastern branch (Pliny and Strabo Trenches) displaying oblique compression with sinistral strike-slip component (Huchon et al., 1982; Mascle et al., 1982; Mascle et al., 1986).

In the following years, numerous surveys were conducted with the aim of defining the major tectonic elements and their kinematic setting in the Aegean Region. The majority of these surveys focused on seismological and broad scale geological data (Angelier et al., 1982; Le Pichon, 1982; Le Pichon et al., 1982; McKenzie & Jackson, 1986; Jackson and McKenzie, 1988; Taymaz et al., 1991; Jackson, 1994; Armijo et al., 1996; Papazachos and Kiratzi, 1996; Papazachos et al., 1998;

Armijo et al., 1999; Goldsworthy et al., 2002; Kiratzi & Louvari, 2003; Kokkalas et al., 2006; Chatzipetros et al., 2013) and GPS campaigns (Billiris et al., 1991; Noomen et al., 1993; Straub & Kahle, 1994; Kahle et al., 1995; Le Pichon et al., 1995; Davies et al., 1997; Reilinger et al., 1997; Clarke et al., 1998; Cocard et al., 1999; Briole et al., 2000; Kahle et al., 2000; McClusky et al., 2000; Kreemer & Chamot-Rooke, 2004; Nyst & Thatcher, 2004; Reilinger et al., 2006, 2010; Perouse et al., 2012). They led to a tremendous improvement of our understanding on the kinematic regime and deformation pattern of the Aegean.

During all these years, the progress in studying the seismological and kinematic pattern was much faster than the systematic mapping and detailed study of the offshore geological structure. Compared to the structural complexity of the Aegean, very few systematic marine geological surveys were conducted, thus the state of knowledge is still far from complete (Figure 4.3.2.). Consequently, the hypotheses and models proposed so far for the geodynamic evolution of the Aegean were based mostly on seismological and kinematic data. The poorly mapped seafloor morphology as well as the scattered data on the offshore geological and tectonic structure were taken into consideration only subordinately. A second, equally important factor to be taken into consideration is the huge difference between the short time interval (tens of years) covered by the seismological observations and GPS data and the long time periods (hundreds of thousands to millions of years) over which geological processes have evolved and led to the formation of the present geological structure in the Aegean.

A thorough analysis and comparison of the proposed kinematic models with the observed and mapped geological structures does reveal inconsistencies between them. Reilinger et al. (2010) already discussed the discrepancy between the geophysical and geological evidence for widespread Quaternary extension in the Peloponnese and South Aegean and the geodetic observations, which indicate very little internal deformation throughout this region (Kahle et al., 2000; McClusky et al., 2000; Reilinger et al., 2006; Perouse et al., 2012). This inconsistency may deviate from the general agreement between GPS and geologic estimates of plate motions and fault slip rates within the E. Mediterranean region (McClusky et al., 2000, 2003; Allen et al., 2004;

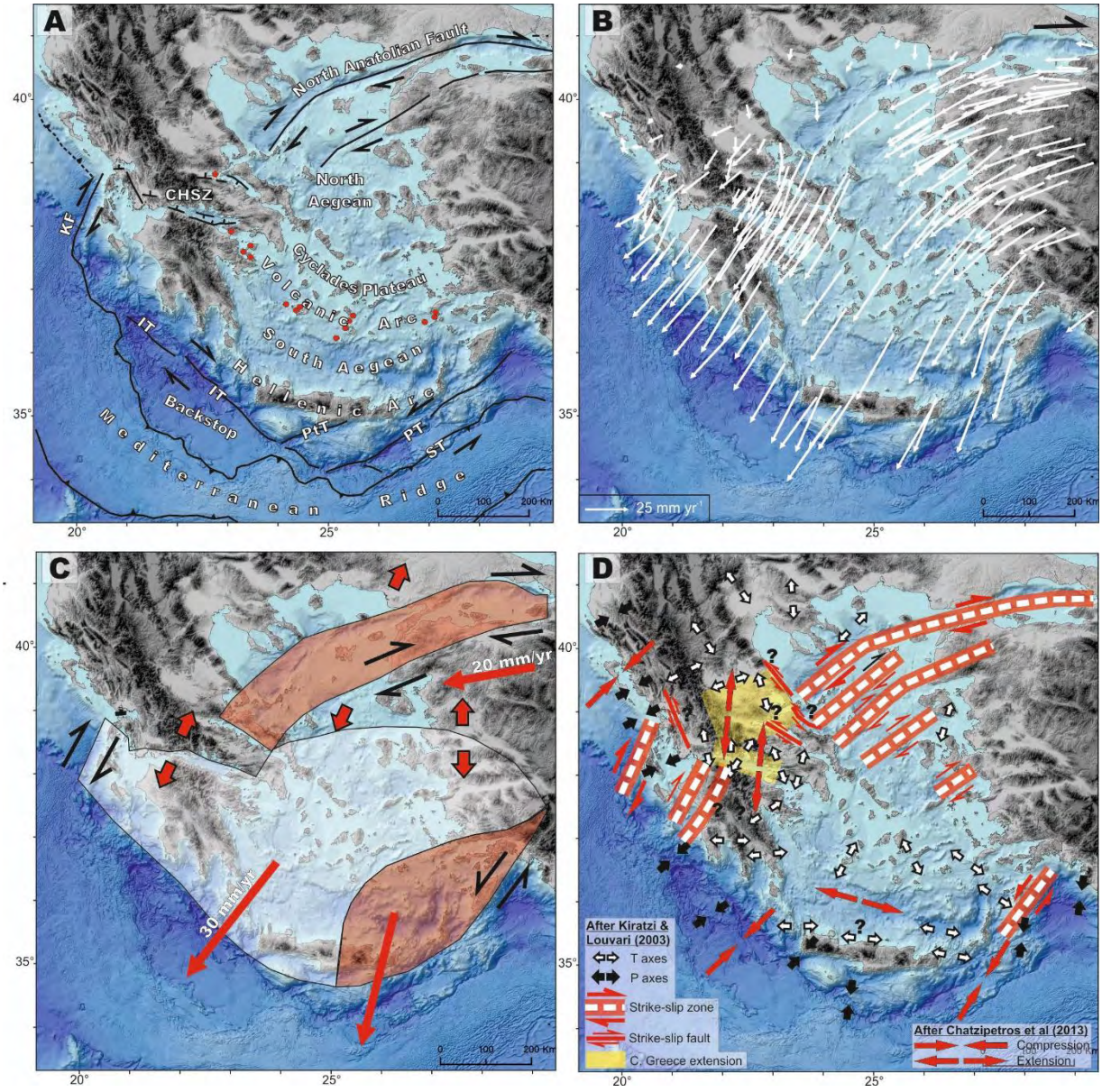

Figure 4.3.1: (**A**): Major geodynamic elements of the Aegean Region. White circles represent volcanoes of the Volcanic Arc (VA). Bathymetry and Topography extracted from Brossolo et al. (2012). A= Anatolia, B= Backstop, CG= Corinth Gulf, CHSZ= Central Hellenic Shear Zone, CP= Cyclades Plateau, IT= Ionian Trench, KF= Kephallinia Fault, MR= Mediterranean Ridge, MS= Marmara Sea, NA= North Aegean, NAF= North Anatolian Fault, P= Peloponnese, PT= Pliny Trench, PtT= Ptolemy Trench, RB= Rhodes Basin, SA= South Aegean, ST= Strabo Trench. (**B**): GPS velocities modified after Kreemer & Chamot-Rooke (2004). Note that velocities increase from 18-20 mm/yr towards West in the Western Anatolia to 33-34 mm/yr towards S24°W in the South Aegean relative to Eurasia. (**C**): Schematic illustration of present-day tectonics after Reilinger et al. (2010). The white shaded area shows the central Aegean and Peloponnese translating towards SW as coherent block with little deformation. The dark shaded areas show deformation zones in the SE Aegean and between the north and south branches of the NAF in the N. Aegean. The sense of motion across major tectonic structures is shown by the thick and the half arrows. The long arrows indicate the rates of motion relative to Eurasia. (**D**): Map of P (compression) and T (extension) axes and major geotectonic elements as derived from earthquake focal mechanisms, modified after Kiratzi & Louvari (2003) and Chatzipetros et al. (2013). NE-SW dextral strike-slip prevails over North Aegean (north of Cyclades Plateau), in the Ionian Island (KF) and NW Peloponnese. E-W extension on Crete and S. Peloponnese is replaced by arc-perpendicular extension in the South Aegean and by oblique compression and left-lateral strike slip along Pliny and Strabo Trenches.

Reilinger et al., 2006). We will show later on that it is not the only case within the Aegean where geodetic and geologic motions are not directly compatible.

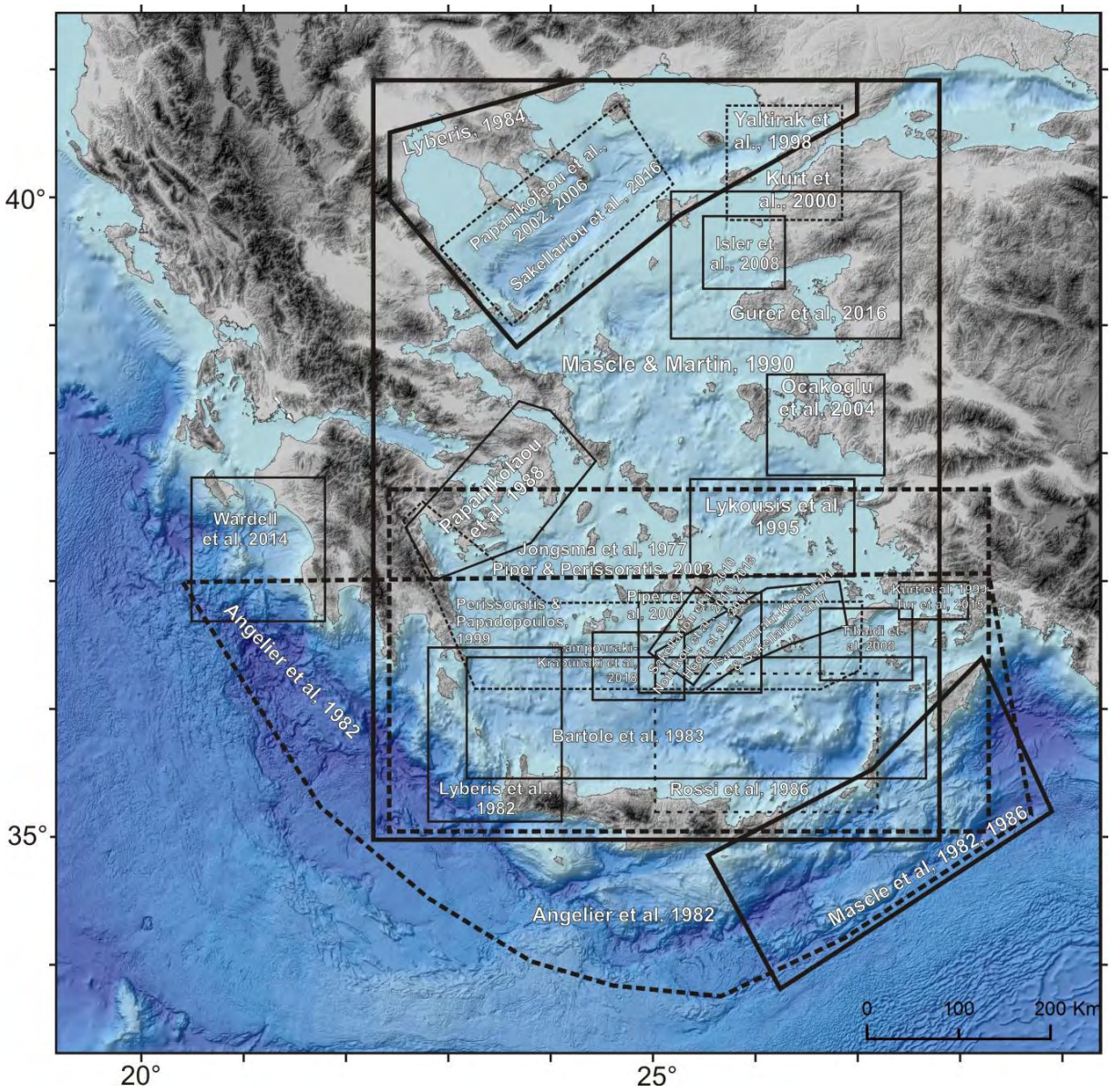

Figure 4.3.2: Geographic coverage of marine geophysical and structural surveys in the Aegean Region. The list of surveys is not exhaustive.

The first systematic effort to create a comprehensive map of offshore faulting and to understand the geologic structure of the entire Aegean Sea (Mascle & Martin, 1990) was based on the interpretation of industrial, widely spaced, multi-channel, seismic reflection profiles. They proposed that the Aegean Sea has been progressively affected by NE-SW trending strike-slip zones after the Miocene. It can be considered as a stretching continental domain cut into several

NE-SW trending, elongated crustal blocks, which move progressively towards the southwest. Opposing that model, Armijo et al. (1996, 1999) proposed that fast extension is localized in the NW Aegean (NAT) and Central Greece (Corinth Gulf) at the termination of NAF, while only slow extension occurs across distinct, arc-parallel zones in the South Aegean and SW Anatolia. Both regional scale analyses were predated by a number of local surveys in the North and South Aegean Sea. Needham et al. (1973) and Brooks & Ferentinos (1980) provided the first data from the North Aegean Trough (NAT) while the first comprehensive description of the offshore fault network and structure of the entire NAT was provided by Lyberis (1984). Jongsma et al. (1977), Huchon et al. (1982), Bartole et al. (1983) and Rossi et al. (1986) were the first who surveyed the South Aegean Sea by means of seismic profiling and bathymetric data. Le Quellec et al. (1980) and Lyberis et al. (1982) studied the western branch of the Hellenic Arc and Trench while Mascle et al. (1982, 1986) surveyed the eastern part of the Hellenic Arc. Angelier et al. (1982) provided a comprehensive synthesis of the South Aegean Sea and the Hellenic Arc, explained the subsidence of the Sea of Crete in terms of uniform stretching of the lithosphere and discussed the implications of the opening of the Sea of Crete on the tectonic evolution of the straits to the West and East of Crete.

Since the 90s and until recently, dozens of marine geological and geophysical cruises and surveys have been conducted by various national and international research teams and contributed to a significant improvement of our knowledge on the present geological structure and to our understanding of the geodynamic evolution of the Aegean in the recent geological period. Despite the huge progress during the last decade, there are still many areas either not surveyed or with insufficient data, which prevent a robust understanding of the geological and geodynamic processes which evolved through the time and led to the formation of the present complex structure in the Aegean Region.

The aim of this paper is to provide an overview of the current state of knowledge on the geological structure, active tectonics and the seismological regime in the Aegean, to compare them and finally to discuss the different kinematic models proposed so far. Recent progress in swath bathymetry coverage and seismic profiling data is also presented. New evidence is provided showing that, along with the northern and southern strike-slip boundaries, strike-slip

faulting and transtensional/transpressional deformation within the deforming Aegean has played a significant role in its geodynamic evolution during the Plio-Quaternary. Finally, this paper aims to highlight the still existing gaps in the current knowledge and to identify open questions and challenges for future research.

4.3.3. North Aegean Sea / North Aegean Trough (NAT) / North Anatolian Fault (NAF)

4.3.3.1. Seafloor Morphology - Sedimentary Basins - Fault Network

The North Aegean Sea (NAS), as described here, includes the marine area between Northern Greece (Macedonia and Thrace) to the North, Anatolia to the West, Central Greece to the East and the Cyclades Plateau to the South. It is characterized by two NE-SW to ENE-WSW trending troughs, the North Aegean Trough and the North Skyros - Edremit Trough, as well as a series of variably shaped basins and shallows between the latter, the Cyclades Plateau, the eastern coast of Evia and the western coast of NW Anatolia (Figure 4.3.3).

The NAT has, from early research, been associated with the prolongation of the dextral strike-slip NAF in the Aegean Sea (Dewey and Şengor, 1979) and marks the northern boundary of the actively deforming "Aegean microplate" to the relatively not deforming, stable Eurasia continent (McKenzie, 1970, 1972, 1978; Brunn, 1976; Dewey and Sengor, 1979; Sengor, 1979; Le Pichon and Angelier, 1979, 1981; McKenzie and Jackson, 1986; Taymaz et al., 1991; Armijo et al., 1999). The NAT is a 300-km-long morphological feature composed of two parts with distinct morphological and structural characteristics. The western NAT (Sporadhes Basin in Lyberis 1984), between Pelion Peninsula and Lemnos Island, trends N40°E and consists of a series of variably shaped basins, including the 1600-m-deep Sporadhes Basin, separated by structural highs and shallower ridges. The eastern NAT (Saros Trough in Lyberis, 1984) trends N70°E and extends between North of Lemnos Island and Saros Gulf. It displays elongate morphology and consists of the 1500-m-Lemnos deep and the narrow, up to 1000-m-deep basin, between

Samothraki and Gokceada Islands (Imbros Depression in Mascle and Martin, 1990), which continues eastward into the Saros Gulf.

The westernmost segments of the NAF have been correlated with the N40°E trending, steep-faulted escarpment which marks the southern margin of the western NAT already by Lyberis

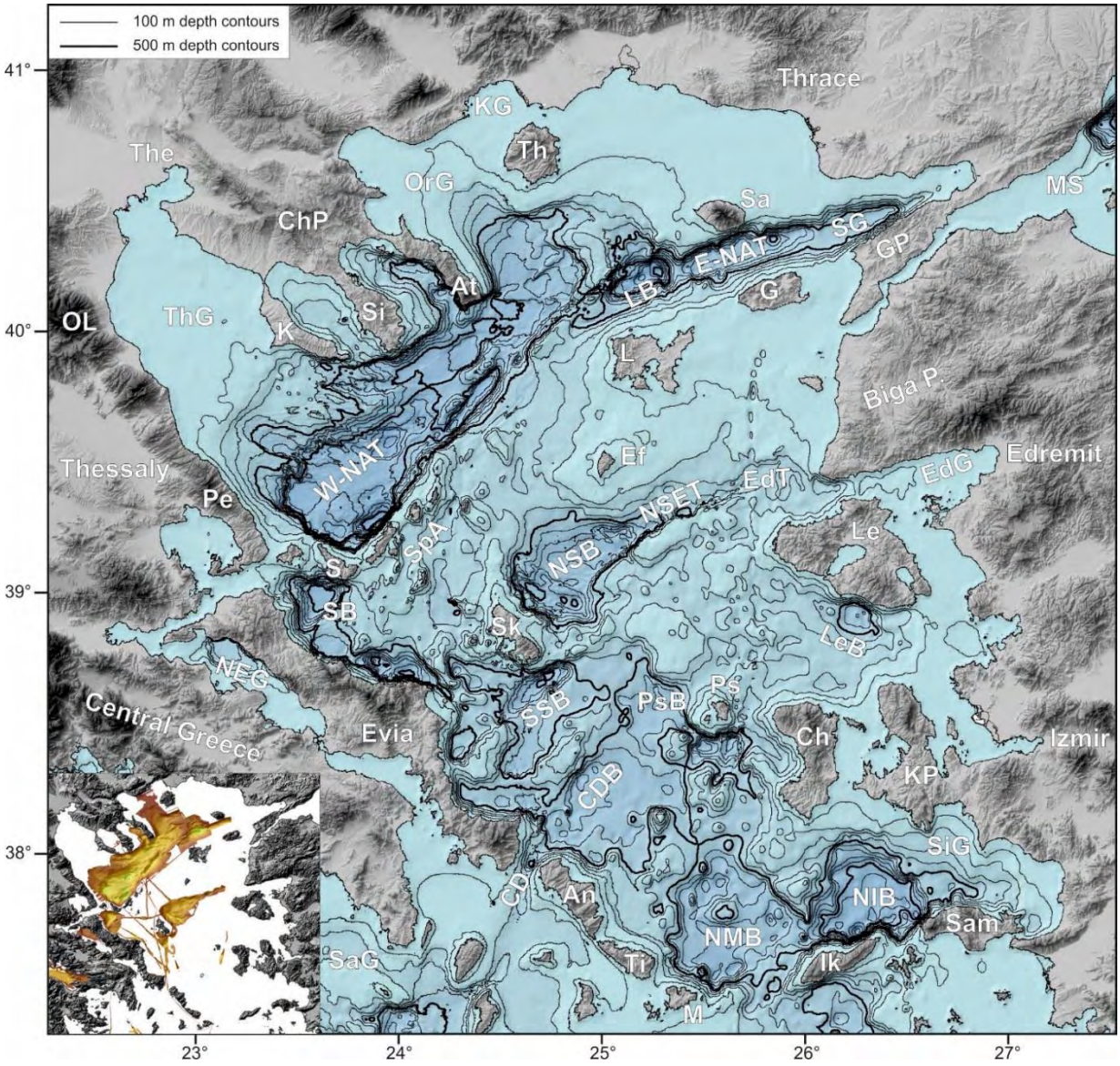

Figure 4.3.3: Updated bathymetry of the North Aegean Sea, derived from GEBCO and swath bathymetry data processed at 250m grid (Drakopoulou and Kyriakidou, 2016; Sakellariou and Tsampouraki-Kraounaki, 2016; https://emodnet. eu/bathymetry). Inset map: swath bathymetry coverage in the North Aegean. An, Andros; At, Athos; Ch, Chios; CD, Cavo Doro strait; CDB, Cavo Doro Basin; ChP, Chalkidiki Peninsula; CG, Corinth Gulf; EdG, Edremit Gulf; EdT, Edremit Trough; Ef, Agios Efstratios; E-NAT, Eastern NAT; G, Gokceada; GP, Gelibolu Peninsula; Ik, Ikaria; K, Kassandra; KG, Kavala Gulf; L, Lemnos; LB, Lemnos Basin; Le, Lesvos; LeB, Lesvos Basin; MS, Marmara Sea; NEG, North Evia Gulf; NIB, North Ikaria Basin; NMB, North Mykonos Basin; NSB, North Skyros Basin; NSET, North Skyros-Edremit Trough; OL, Olympos; OrG, Orfanou Gulf; Pe, Pelion; Ps, Psarra; PsB, Psarra Basin; S, Skopelos; SB, Skopelos Basin; Sa, Samothrace; SaG, Saronic Gulf; Sam, Samos; SG, Saros Gulf; Si, Sithonia; SpA, Sporadhes Archi- pelago; Sk, Skyros; SSB, South Skyros Basin; Th, Thassos; The, Thessaloniki; ThG, Thermaikos Gulf; Ti, Tinos; W-NAT, Western NAT.

(1984) and Mascle and Martin (1990). Their systematic marine geophysical survey of the NAT led to comprehensive interpretations of its structure and fault network and along with Roussos and Lyssimachou (1991), provided solid marine geophysical evidence on the strike-slip character of this fault zone. The seismic stratigraphy of NAT's infill indicates up to 6-km-thick middle or late Miocene and Plio-Quaternary sediments including evaporite-bearing strata, with the thickest deposits located below the Thermaikos-Sporadhes Basin, at the southwestern end of the NAT, and below the Kavala-Orphanos Basin, East of Athos Peninsula (Needham et al., 1973; Lalechos and Savoyat, 1979; Brooks and Ferentinos, 1980; Lyberis, 1984; Mascle and Martin, 1990; Beniest et al., 2016; Brun et al., 2016). Brun and Sokoutis (2007), Kydonakis et al. (2015), and Brun et al. (2016) suggested that the western NAT initiated as a sinistral transtensional basin under NE-SW extension during the exhumation of the Southern Rhodope Core Complex in the Paleogene-Oligocene, to laterally accommodate the dextral rotation of the Chalkidiki block. A shift in the direction of extension from NE-SW to N-S may have occurred in the Pleistocene and has been documented onshore as well (Mercier et al., 1987, 1989; Lyberis, 1984). According to Mascle and Martin (1990), NW-SE extension prevailed in the middle or Late Miocene and shifted to NE-SW extension or transtension in the Plio-Quaternary, when the NAF broke into the NAS (Armijo et al., 1996, 1999; Papanikolaou et al., 2002, 2006). Two major fault groups seem to control the development of the western NAT: NE-SW dextral strike-slip faults and NW-SE to NNW-SSE normal faults, with the latter forming the western boundaries of the main depocenters.

Swath bathymetric data and shallow seismic profiles in the western NAT led Papanikolaou et al. (2002, 2006) to associate the observed structures with oblique opening accommodated by NE-SW marginal and E-W intrabasin strike-slip faults and NW-SE normal faults along the Pelion and Athos margins. Strike-slip deformation dominates in the eastern part of the West- ern NAT, while vertical movements increase toward its western end. The main N40°E trending, strike-slip fault zone along its southern margin consists of over 12 fault segments with restraining and releasing bends between them (Sakellariou et al., 2016). It has resulted in the creation of the structurally composite southern margin with the main escarpment accompanied by pressure ridges and transtensional small basins. The overall structure of the western NAT, with the numerous, curved faults and fault splays initiating from the marginal fault zone, crosscut the basin toward the west

and the northwest and divide it into uplifting and subsiding slices. It has been interpreted as the horsetail structure developed at the western termination of the NAF (Sakellariou et al., 2016). The N70°E oriented eastern part of the NAT consists of three main narrow basins. The 1500-m spindle-shaped Lemnos Basin has developed at the junction between the western and the eastern NAT. It contains thin Messinian evaporites and displays a complex structural pattern characterized by main faulting running ENE-WSW accompanied by secondary NW-SE and minor NNE-SSW faults (Mascle and Martin, 1990). Its location at the bending point between the N40°E marginal faults of the west- ern NAT and the N70°E faults of the eastern NAT may indicate that it has been formed as a transtensional or pull-apart basin. Further east, the narrow and elongate 1000-m-deep basin between Samothrace and Gokceada Islands is bounded by ENE-WSW steep faulted scarps (Lyberis, 1984) and is separated from the 600-m-deep Saros Trough by a shallow NNE-SSW trending ridge. The Ganos fault, a main segment of the northern strand of the NAF, is the major feature forming the Gulf of Saros and the homonymous Trough (Yaltirak et al., 1998; Kurt et al., 2000; Yaltirak and Alpar, 2002). The fault network in the Gulf includes strike-slip faults with normal components, which bound the Saros trough to the north and south, and normal faults located within the trough. The Saros trough has been interpreted as a negative flower structure developed along the major Ganos fault zone (Kurt et al., 2000).

The fault network of Lemnos Island reflects the deformation pattern of the NAT (Koukouvelas and Aydin, 2002; Pavlides and Tranos, 1991; Pavlides et al., 1990; Roussos, 1993; Tranos, 2009). The Lemnos Island, located on the southern shoulder of theNAT, is crosscut by NE-SW to ENE-WSW dextral strike-slip faults with or without normal component (Chatzipetros et al., 2013). Similarly to Lemnos, the Agios Efstratios Island is crosscut by an almost purely dextral N36° trending strike-slip fault, which moved during the 1968 Ms.:7.1 earthquake (Pavlides et al., 1990; Kiratzi et al., 1991). The fault pattern on the island, with the main NE-SW dextral strike-slip fault and a conjugate, NW-SE sinistral fault along the northeastern coast, is in agreement with the general transtensional regime (Chatzipetros et al., 2013).

The NSET is a 200-km-long composite morphological feature consisting of the North Skyros Basin (NSB) in the west and the Edremit Trough (EdT) and Gulf (EdG) in the east (Figure 4.3.3). The 1200-m-deep NSB is an equilateral triangle with its NW-SE trending base parallel to the

eastern coastline of Skyros Island and its top at 70km toward ENE (Papanikolaou et al., 2015), where it continues in the narrower and shallower ENE-WSW trending EdT. The NSB is an asymmetric graben with several subbasins bounded by a major southern marginal fault and an antithetic northern fault and crosscut by E-W trending strike-slip fault zones. Maximum depths occur close to the faulted western margin of the NSB off the Skyros Island (Papanikolaou et al., 2015). The EdT is described as an asymmetric graben by Mascle and Martin (1990) bounded by major southern faults and displaying strike-slip deformation of the sedimentary infill. The eastern part of EdT displays a structural complexity with clear strike-slip faulting. Isler et al. (2008) have shown that a major ENE-WSW strike-slip runs along the northern margin. A second WNW-ESE trending SSW-facing normal fault marks the releasing bend between the previous fault and the one controlling the Edremit Gulf basin (Yaltirak et al., 2012). The latter is a lens-shaped pull-apart basin bounded by two right-lateral strike-slip fault zones, the Edremit fault zone along the southern coast of Biga Peninsula and the Balıkesir-Havran fault zones along the southern side of the Gulf (Gurer et al., 2016). Further west, but still on the southern margin of Edremit Gulf and Trough, Lesvos island displays two main fault groups: a NNE-SSW trending one, represented by the dextral strike- slip Agia Paraskevi fault zone that is associated with the 1867 earthquake and a WNW- ESE group of normal or oblique faults, which control the south-western coast of the island (Chatzipetros et al., 2013).

Very few marine geophysical data are available for the area extending between the Skyros-Edremit Trough to the north and the Cyclades Archipelago to the south and our knowledge on the offshore structure is only based on the regional work of Mascle and Martin (1990), who describe this area as composed of alternatively uplifted basement blocks (islands and shallow banks) and subsiding extensional depressions, subject to NE-SW directed extension. The Lesvos Basin (LeB, Figure 4.3.3), up to 700m deep, is a thickly sedimented and complex Plio- Quaternary basin southwest of Lesvos Island, bounded by NW-SE trending faults. The NNE-SSE trending Psarra Ridge separates the LeB to the east from the Psarra Basin to the west. The latter is an extensional structure affected by active strike-slip and normal faulting. Further south, the Cavo Doro (CD) Basin (SE Evia Basin of Mascle and Martin, 1990), north of Andros Island, is a wide depression bounded toward the NW by a NE-SW trending ridge, which separates it from the

South Skyros Basin (SSB). To the east, the North Mykonos (NM) Basin is a thickly sedimented depression divided into two subbasins by a NE-SW trending horst. The northern subbasin displays half-graben structural configuration and deepens toward SE while the southern basin is bordered by actively tilting basement blocks. Despite the lack of systematic seismic profiling data, this structural configuration strongly suggests that the NM Basin has been affected by NE-SW trending strike-slip faulting.

The North Ikaria Basin (NIB, Figure 4.3.3) consists of a Plio-Quaternary, wide, asymmetric depression bounded to the south by major en echelon arranged faults, which imply a transcurrent component (Mascle and Martin, 1990). A strike-slip character for these faults has also been suggested by Lykousis et al. (1995). Strike-slip deformation is evident on the Samos Islands, on the southern margin of the NIB. NNE-SSW-directed extension has resulted in the creation of E-W faults and the reactivation of older NW-SE and NE-SW faults as strike-slip ones (Chatzipetros et al., 2013). On the northern margin of the NIB, the Sigacik Gulf along with the Karaburun Peninsula and the Izmir area undergo intense deformation along N-S and NE-SW strike-slip faults (Ocakoglu et al., 2004, 2005). As no further data are available from the NIB, it is not known how the southern marginal faults interact with the ones observed to the north.

Finally, a series of basins has developed between the eastern coast of Evia and the Sporadhes Archipelago and Skyros Island. The SSB (Figure 4.3.3) results from the interaction of NW-SE and NE-SW faults. Its southern margin is controlled by an important, apparently normal, active fault, which is associated with very narrow and asymmetric trough-like features suggesting the existence of transcurrent fractures. Sakellariou et al. (2013) interpret the SSB as the westernmost segment of the North Skyros-Edremit fault zone, the final termination of the southern branch of the NAF. The Skopelos Basin (SB, Figure 4.3.3), between Skopelos Island and the northeast coasts of Evia, is a complex extensional structure controlled by WNW-ESE major faults and secondary NNE-SSW trending ones.

4.3.3.2 Seismological and Geodetic Constraints

The NAS is one of the seismically most active areas in the region and is regarded as an area of typical right lateral strike-slip faulting regime (e.g., Taymaz et al., 1991; Pavlides and Tranos, 1991; Kiratzi and Louvari, 2003) associated with the activity of the NAF (Figure 4.3.1D). The NAF

has been recognized very early as the northern boundary of the deforming Aegean (Figure 4.3.1A) with the NAT representing the morphological expression of this boundary (McKenzie, 1972, 1978; Dewey and Şengör, 1979; Le Pichon and Angelier, 1981). GPS measurements (Figure 4.3.1B and 4.3.1C) have confirmed and quantified the strike-slip motion across the NAF to about 23mm/year (Kahle et al., 2000; McClusky et al., 2000; Kreemer and Chamot- Rooke, 2004; Nyst and Thatcher, 2004; Reilinger et al., 2006, 2010; Perouse et al., 2012; Müller et al., 2013).

Seismological data indicate that the NAF splits into a number of branches in the North Aegean. They are distributed between the NAT to the north and the CP to the south; they extend up to the coasts of Evia and stop abruptly against Central Greece (Kiratzi, 2002; Kiratzi and Louvari, 2003). Fault plane solutions indicate dextral shearing, with the majority of the earthquakes occurring along the NAT and secondarily along the NSET, while two more seismically less distinct zones between Psara and Lesvos and north of Ikaria Island show off (Kiratzi and Louvari, 2003). Within the dominant NE-SW dextral shear regime, the Mw=6.4 Skyros 2001 earthquake ruptured a NNW-SSE trending sinistral strike-slip fault north of Skyros Island (Melis et al., 2001; Benetatos et al., 2002; Karakostas et al., 2003; Ganas et al., 2005). This fault has been interpreted as a conjugate fault in respect to the NE-SW dextral strike-slip faults and is compatible with the N-S to NNE-SSW extension of the North Aegean (Ganas et al., 2005). Sinistral strike-slip faulting has been also proposed by Kiratzi and Louvari (2003) for the eastern coasts of Evia and may contribute to the transferring of the motion from the NAF into the Aegean mainland.

Recent GPS campaigns confirm that the prevailing deformation style in the NAS is dextral shear and suggest that it is mostly localized in two well-confined regions, the NAT and the NSET (Müller et al., 2013). Dextral strike-slip motion along the NAT decreases from 21.2mm/year along the Saros basin to 12.5mm/year south of the Chalkidiki peninsula and about 7mm/year at the southwestern corner of the Sporadhes basin. Less than 5mm/year is transferred from the Sporadhes islands/Pelion toward Northern Evia. Strike-slip motion of about 10mm/year in total is attributed to the Skyros-Edremit fault and the Agios Efstratios fault, while the Psara-Lesvos fault with rates of 4mm/year is kinematically a less distinct structure (Müller et al., 2013). The strain analysis based on the above GPS data is in agreement with the seismological observations along the Evia coasts and north of Skyros and suggests a sinistral strike-slip component on all

NNW-SSE trending faults along the western shoreline of the NAS (Müller et al., 2013). Moreover, they are compatible with the NW-SE trending faults along the eastern margins of Pelion/Olympos and Athos mapped by Lyberis (1984) and Mascle and Martin (1990), in the NAS south of the NAT (Mascle and Martin, 1990) and on the NE Aegean islands (Chatzipetros et al., 2013). These faults have been interpreted as sinistral strike-slip or normal faults.

The suggested localization of strain along the NAT and the NSET (Müller et al., 2013) coincides largely with the spatial distribution of the seismicity and with the fact that these two elements are the most striking morphological and geotectonic structures in the NAS. Besides that, geomorphological and geological-geophysical data indicate that a considerable amount of deformation must have affected and may actively affect larger areas of the NAS.

The updated offshore morphology of Figure 4.3.3 shows a tectonically controlled relief with many depressions, up to 1000–1200m deep and with various shapes, bounded by steep faulted slopes and separated from each other by shallow elongate or variably shaped structural highs. The 1200-m-deep NIB, for example, initiated in the Miocene (Beniest et al., 2016) and evolved in the Plio-Quaternary while bounded to the South by a strike-slip fault zone (Mascle and Martin, 1990) with evident dextral movement (Kiratzi and Louvari, 2003). Active strike-slip faulting along with extensional tectonics has been observed on its northern margin, in the Sigacik Gulf, the Karaburun Peninsula, and the Izmir area (Ocakoglu et al., 2004, 2005; Benetatos et al., 2006; Uzel et al., 2013; Yolsal-Cevikbilen et al., 2014; Cirmik et al., 2017). The 1000-m-deep SSB and SB, along with the less deep but structurally similar basins off the Evia coasts, bear evidence of significant Plio-Quaternary and ongoing deformation at the western termination of the southern branches of the NAF. The structurally complex area southwest of Lesvos Island, including the LeB, which has hosted the recent M=6.3 normal fault earthquake in June 2017 (Ganas et al., 2017), shows also significant evidence of geologically recent and ongoing deformation.

In addition to the geomorphological constraints, the available sparse geophysical data (e.g., Mascle and Martin, 1990) indicate that dextral strike-slip faulting in NE-SW direction and sinistral strike-slip to normal faulting in NW-SE direction has been active throughout the Plio-Quaternary and is still active in the entire North Aegean area.

In regard to the limited transfer of strain from the North Aegean toward the eastern part of Central Greece proposed by Müller et al. (2013), seismological observations indicate strike slip motions crossing the central and southern part of the Evia Island reaching the tip of the southern Evoikos Gulf (Kiratzi, 2002). In addition, NW-SE trending strike-slip faults have been mapped in the North Evia Gulf and have played a role in the development of its spindle shaped 400-m-deep basin (Sakellariou et al., 2007), while left-lateral slip along them has been confirmed with seismological data (Ganas et al., 2016).

4.3.4. South Aegean Sea/Volcanic Arc

4.3.4.1 Seafloor Morphology—Sedimentary Basins—Fault Network

The South Aegean Sea, as described here, includes the CP to the north and extends between the western coast of Anatolia to the east, the eastern coast of Peloponnese to the west, and the Hellenic arc (Crete, Rhodes Islands) to the south (Figure 4.3.1A).

For decades, the shallow marine CP has been considered as a tectonically inactive area extending from Central Greece to the west until the western coast of Anatolia to the east. Therefore, very few data are available from this area and very little is known on its offshore structure. However, a more thorough look at the updated bathymetry of the CP reveals some interesting geomorphological observations (Figure 4.3.4). Its northern edge is marked by (i) a NW-SE running ridge consisting of the South Evia, Andros (An), Tinos (Ti), and Mykonos (M) Islands and (ii) a ENE-WSW running ridge delineated by the Ikaria (Ik) and Samos (Sam) Islands. Both directions coincide with the major tectonic trends recognized in the NAS. The 500-m-deep CD strait separates South Evia from the Andros Island and extends further SSW-ward as a narrow, deep depression, between Kea (Ke) and the Kythnos (Ky) Islands. A similar, narrow and deep, NE-SW running strait separates the Serifos and Sifnos Islands and terminates in the Myrtoon Basin (MB). The 700m deep, NW-SE elongate, South Ikaria Basin (SIB) separates the wide shelf of Anatolia from the central part of the CP. Interestingly, the main morphological elements of the seafloor and of the nonvolcanic islands are aligned along the two main trends of the major tectonic elements described so far: NW-SE and NE-SW. The southern margin of the CP hosts the Hellenic volcanic arc (Figure 4.3.1A). Its outward (toward SW, S, and SE) outline

displays a complex morphology and coincides with the tectonically controlled margins of important basins (Myrtoon, Christiana, Heraklion, and Amorgos Basins).

The western sector of the South Aegean seafloor (Figure 4.3.4) is marked by the Argolic Gulf (ArB) and Maleas (MaB) Basins, two NW-SE elongate 1000–1200-m-deep basins that developed along the western flanks of the Peloponnese and Kithyra-Antikythera Ridge. A narrow ridge

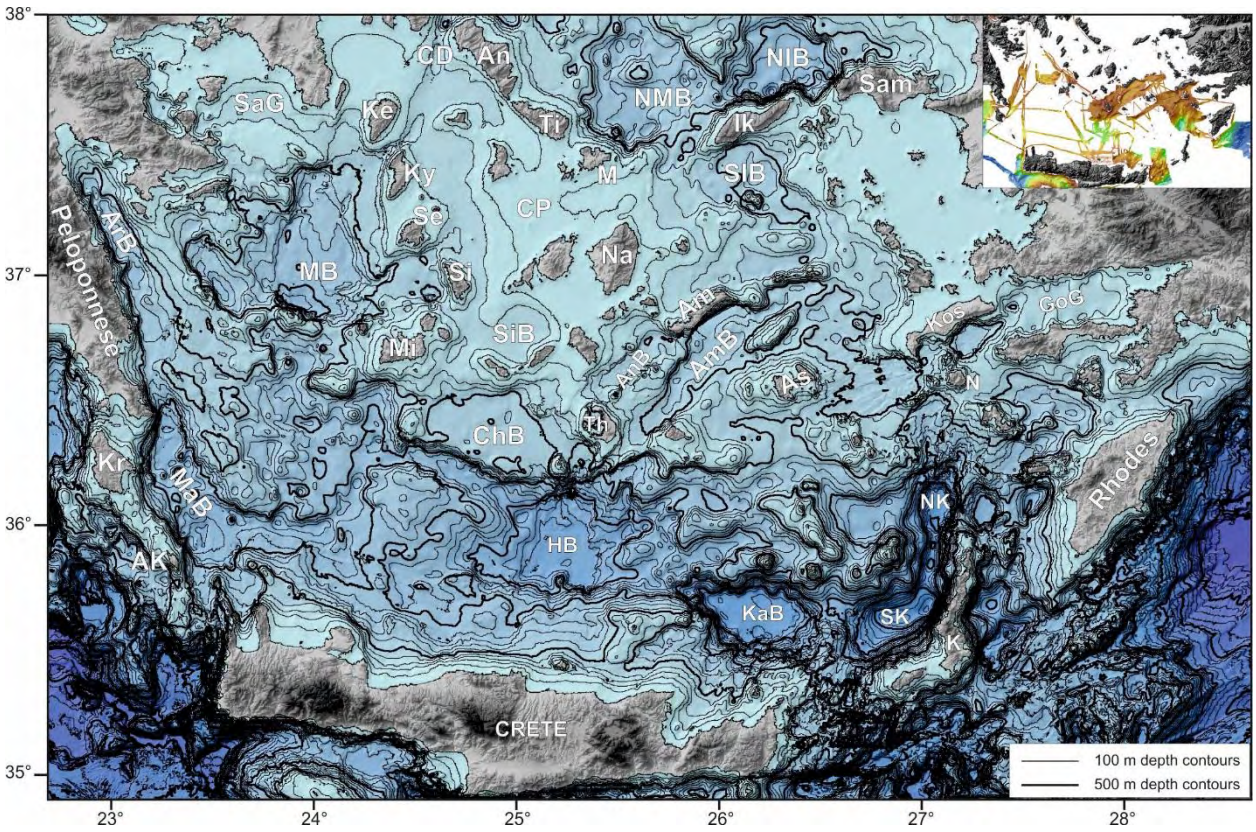

Figure 4.3.4: Updated bathymetry of the South Aegean Sea, derived from GEBCO and swath bathymetry data processed at 250m grid (Drakopoulou and Kyriakidou, 2016; Sakellariou and Tsampouraki-Kraounaki, 2016; https://emodnet. eu/bathymetry). Inset map: swath bathymetry coverage in the South Aegean. AK, Antikythera; Am, Amorgos; AmB, Amorgos Basin; An, Andros; AnB, Anydhros Basin; ArB, Argolic Basin; As, Astypalaea; CD, Cavo Doro Strait; ChB, Christiana Basin; CP, Cyclades Plateau; GoG, Gulf of Gökova; HB, Heraklion Basin; Ik, Ikaria; K, Karpathos; KaB, Kamilonissi Basin; Ke, Kea; Kr, Kythera; Ky, Kythnos;M, Mykonos;MaB, Maleas Basin;MB, Myrtoon Basin; Mi, Milos; N, Nisyros; Na, Naxos; NIB, North Ikaria Basin; NK, North Karpathos Basin; NMB, North Mykonos Basin; SaG, Saronic Gulf; Sam, Samos; Se, Serifos; Si, Sifnos; SiB, Sikinos Basin; SIB, South Ikaria Basin; SK, South Karpathos Basin; Th, Thera; Ti, Tinos.

separates the ArG from the composite 1100-m-deep MB and the MaB from a morphologically "chaotic" area extending southwest of Milos Island (Mi). The south and southeastern part of the South Aegean displays an even more complex morphology. The entire area encompassing the 500-m-deep flat Christiana Basin (ChB) in the west and the 400–500-m-deep Anydhros (AnB) and

the 700m deep, composite Amorgos (AmB) elongate Basins in the east, hosts the volcanic group of Thera Island (Santorini) and displays two main trends: NE-SW in the AnB and AmB andWNW-ESE to NW-SE in the ChB. The NE-SW trend matches the orientation of the steep slopes bounding the AmB and the distribution of the volcanic centers in the AnB. Further south, the almost 2000-m-deep Heraklion Basin (HB) displays a rhomboid to irregular shape. NE-SW to ENE-WSW trending shallow ridges and narrow depressions separate the HB from the >2000-m-deep rhomboid Kamilonissi Basin (KaB). The southeast corner of the South Aegean is marked by the lazy-S shaped >2500-m-deep South and North Karpathos Basins (SK and NK), which constitute a negative, mirror-image, of the Karpathos and Kassos Islands landscape.

Unlike the CP, a relatively large amount of data, most of it acquired in the 1980s and 1990s, is available for the deeper, southern part of the South Aegean Sea. Jongsma et al. (1977), Angelier et al. (1982), Lyberis et al. (1981, 1982), Bartole et al. (1983), and Rossi et al. (1986) were the first who surveyed the Cretan Sea by means of seismic profiling. In addition, the DSDP Hole 378 (Hsü et al., 1978) was drilled in the western edge of the Heraklion Basin (HK) and provided valuable sedimentological and chronological constraints for the seismic stratigraphic interpretation of the geophysical data. Jongsma et al. (1977) observed strong vertical tectonic movements on normal faults as responsible for the formation of the "Cretan Trough," with extensional tectonics dominating this area since at least 10Ma. According to Lyberis et al. (1981), the observed pattern of normal faulting is consistent with the expansion of the Sea of Crete as a result of the uniform stretching of the underlying lithosphere. Bartole et al. (1983) suggest that the birth of all deep basins located south of the CP dates back to the Tortonian or even the Serravalian (see also Angelier et al., 1982) and that strong vertical differential tectonic movements in the Plio-Quaternary are responsible for the present-day morphology. NE-SW and N-S trending faults with a significant sinistral strike-slip component are, according to Rossi et al. (1986), the two main fault groups responsible for the structural evolution of the Kamilonissi (KaB) and Karpathos Basins (SK and NK) along with the broader area of the southeast Aegean and the adjacent part of the Hellenic Trench.

Mascle and Martin (1990) have provided a comprehensive description and synthesis of the structure and evolution of the South Aegean Sea. The Argolic Gulf and the Maleas Basins in the

west display an asymmetric structure controlled by the NNW-SSE trending, E-facing faults. NW-SE to N-S faulting in the Argolic Gulf, along with some distinct ENE-WSW faults have been reported by Papanikolaou et al. (1988). The HB is described as a roughly E-W oriented, almost flat, basin showing two dominant directions (Mascle and Martin, 1990): a NW-SE one prevailing in the western side and a NE-SW one characterizing the eastern part of the basin. The rhomboid Kamilonissi Basin (KaB) is surrounded by steep slopes, contains a 2s (roughly 2km) thick infill and seems to result from NW-SE directed extension. It is separated from the "Astypalea platform" by a strongly deformed area cut into several NE-SW trending elongate half grabens indicating shearing associated with strike-slip fault zones. The SK and NK Basins are bounded by NW-SE and NNE-SSW faults. In general, Mascle and Martin (1990) suggested that most of the South Aegean has resulted from the interaction of faults trending ENE-WSW and NNW-SSE.

Perissoratis and Papadopoulos (1999) studied the Argolic Gulf, Christiana, and Amorgos Basins mostly for their sedimentary infill and slope stability and provided important data on the major faults of these areas, while Piper and Perissoratis (2003) provided a synthetic map of the offshore faulting and structure in the South Aegean Sea. They propose that E-W faulting dominated the central part of the South Aegean area in the Pliocene. It was followed by N-S and NE-SW faults north and south of Milos and mainly NE-SW faults in Amorgos and Santorini region. In the entire region, from Kos throughAmorgos to Santorini (Thera), the style of NE-SW faulting, the narrow basement ridges and the basin inversions strongly suggest a strike-slip regime (Piper and Perissoratis, 2003; Piper et al., 2007).

The spatial distribution of the volcanoes along the volcanic arc and its relationship with tectonic elements have been discussed extensively. Papazachos and Panagiotopoulos (1993) suggested that the epicenters of shallow and intermediate depth earthquakes in the Aegean volcanic arc can be grouped into five, well defined, linear clusters trending about N60E; they are associated with normal faulting and coincide with the five volcanic groups (Sousaki, Methana, Milos, Santorini, and Nisyros).

According to Pe-Piper and Piper (2005) and Piper et al. (2007) faulting appears to be important in localizing the distribution of volcanoes. Milos is located at the intersection of N-S and NE-SW-trending fault systems (Piper and Perissoratis, 2003). In the area around and east of Thera

volcanism appears to be localized along dextral NE-SW-trending faults, which show major seafloor offsets near the Kolumbo volcanic chain. Sakellariou et al. (2010) proposed that both Thera and Kolumbo volcanic centers occur within the NE-SW-trending Anydros graben, which constitutes a negative flower structure related to a 40km, possibly dextral, strike-slip zone, the Kameni-Kolumbo strike-slip, which can be extended SW-wards to the Christiana volcanic island. Similarly, Tsampouraki-Kraounaki and Sakellariou (2017) suggest that the NE-SW-trending, morphologically complex area northeast of Thera until Amorgos, Astypalea, and Kalymnos Islands, which encompasses Anydhros Basin and the six subbasins of Amorgos Basin undergoes dextral transtensional deformation accommodated by NE-SW strike-slip to oblique faults and E-W normal step-over faults. Opposite to that, Hübscher et al. (2015), Nomikou et al. (2016, 2018), and Hooft et al. (2017) recognize normal faulting as the main tectonic mechanism controlling the formation and evolution of the Anydhros Basin and the Thera-Amorgos area.

Further east, Pe-Piper et al. (2005) have shown that volcanism at Kos and Nisyros is strongly influenced by sinistral ENE-WSW trending strike-slip faults causing extension on older N-S or NE-SW trending faults while Tibaldi et al. (2008) and Nomikou and Papanikolaou (2011) characterized the same fault system as normal faults. Iscan et al. (2013), Ulug et al. (2005), Tur et al. (2015), and Ocakoglu et al. (2018) provided solid evidence for strike-slip tectonics prevailing in the Gulf of G€okova (GG), east of Kos Island. Moreover, Tur et al. (2015) interpreted this area as part of a lazy-S shaped structure, which encompasses the Kamilonissi Basin (KaB), the SK and NK Basins, and the GG and has developed within the sinistral strike-slip regime of the southeastern sector of the Hellenic arc.

4.3.4.2. Seismological and Geodetic Constrains

Instrumental seismicity indicates that the earthquake focal mechanisms south of the volcanic arc are either pure normal faulting, or normal faulting combined with considerable strike-slip motions (Kiratzi and Louvari, 2003). In fact, within the entire area from Peloponnese to the West to Rhodes to the East, the direction of the T-axis is more or less stable and trends WNW-ESE, irrespective of the orientation of the kinematic character of faulting (Kiratzi, 2013). This corresponds with a mainly trench-parallel extension, as has been documented by Angelier et al. (1982), Mercier et al. (1989), Armijo et al. (1992), Benetatos et al. (2004), Kreemer and Chamot-

Rooke (2004), Lyon-Caen et al. (1988), and Shaw and Jackson (2010). Armijo et al. (1992) suggested that the change from the older, N-S, arc-perpendicular extension to the E-W, arc-parallel extension took place in the Pliocene (2-4 Ma) and implies that the Aegean started to collide with the northern African margin. A slightly different perspective for the distribution of strain in the South Aegean Sea has been provided by Kokkalas et al. (2006). According to these authors, ENE-WSW extension accommodated by sinistral strike-slip, NE-SW faults and N-S to NNE-SSW extensional faults prevails in the southeastern part. The central part is characterized by NNE-SSW extension accommodated by NE-SW to ENE-WSW and NW-SE extensional faults and minor NNE-SSW- trending dextral strike-slip faults. Finally, the western part of the South Aegean, along with Peloponnese, is dominated by WSW-ENE extension accommodated by NNW-SE faults.

Until recently, it was believed that extension in the South Aegean is concentrated in the western and eastern parts (Benetatos et al., 2004; Shaw and Jackson, 2010). The 2012 sequence provided the first instrumental evidence for the operation of the previously mentioned young active N-S faults in the central part of the south Aegean Sea, at the edge of the Cretan Basin, accommodating extension within the overriding Aegean plate. In January 2012, a moderate size earthquake sequence (Mw5.0 and Mw5.3 were the two strongest events) occurred in the South Aegean Sea, southwest of Thera, and close to the northern slope of the HB (Kiratzi, 2013). The distribution of the epicenters shows that two structures were activated simultaneously: a dextral N-S strike-slip fault and a second NE-SW trending one. Kiratzi (2013) states that this earthquake is a significant evidence that WNW-ESE extension is active throughout the South Aegean area. The 2012 earthquake sequence is not the only one in the South Aegean associated with dextral strike-slip faulting. Bohnhoff et al. (2006) analyzed over 2000 earthquakes between 2002 and 2004 in the central part of the volcanic arc. They concluded that the highest activity was identified along the SW-NE striking Santorini (Thera)-Amorgos zone that is in the state of right-lateral transtension. Similar observations have been described by Dimitriadis et al. (2009, 2010) for the seismic activity of the Santorini-Kolumbo zone. In addition, focal mechanisms of the 2011-12 seismicity in the caldera of Santorini indicate strike slip faulting along approximately NE-SW faults (Papadimitriou et al., 2015).

Despite the relatively low seismicity in this area, the largest earthquake (M:7.8) in the last century in the entire Aegean Sea occurred in July 1956 southwest of Amorgos Island. The proposed focal mechanisms vary between dextral strike-slip and dip-slip movement on a NE-SW-trending SE dipping fault (Okal et al., 2009 and references therein). A NE-SW normal faulting mechanism agrees with the observations of Nomikou et al. (2016, 2018) and Hooft et al. (2017), while the data provided by Mascle and Martin (1990), Piper and Perissoratis (2003), Piper et al. (2007), and Tsampouraki-Kraounaki and Sakellariou (2017) indicate dextral transtension in this area. Further east, Yolsal-Cevikbilen et al. (2014) observed in the GG mostly N-S extension accommodated by E-W faults with a relatively small amount of sinistral strike-slip component.

GPS data show that N-S-oriented extensional strain rates accompanied by normal faulting dominate in the western Anatolia and central and southern Greece. Kahle et al. (1999) suggest that N-S extension results from transtensional-type active processes in the Aegean, which are possibly associated with back-arc spreading and rollback of the subducting slab. The kinematic model proposed by Kreemer and Chamot-Rooke (2004) shows that the extension direction of the overriding Aegean plate is oriented in a roughly NW-SE direction. These authors state that a large part of the South Aegean and of the backstop of the MR form one single relatively rigid block, which moves at 33–34mm/year in the direction of S24W±1 toward stable Nubia. They recognize that the two main characteristics of the kinematics of the southern Aegean are the SSW-ward motion of the rigid Aegea and the motion of up to 10mm/year of the southeastern Aegean away from stable Aegea (McClusky et al., 2000). Reilinger et al. (2010) explain that the sequential propagation of deformation associated with the NAF across the N. Aegean during the past 1-4Ma resulted in the concentration of extensional deformation associated with the Africa slab retreat in the N. Aegean and allowed the South Aegean and Peloponnese to translate SW-wards with little deformation.

4.3.5. The Hellenic Arc and Trench

4.3.4.1. Seafloor Morphology—Fault Network

The southward convex Hellenic Arc encompasses from west to east the Ionian Islands, the southwestern and southern part of the Peloponnese, Kythera and Antikythera Ridge, Gavdos, Crete, Kassos, Karpathos, and Rhodes Islands (Figures 4.3.1A and 4.3.7). It displays variable

morphology with high altitude mountainous blocks (e.g., on the Peloponnese and Crete) alternating with low plains, deep gulfs (south Peloponnese) and deep and steep marine straits [west and east Cretan straits, Karpathos-Rhodes].

The Hellenic Trench surrounds the outward side of the arc and displays three distinct sectors: The northwestern sector marks the steep escarpment and the >3000 deep, NNE-SSW elongate, asymmetric basin parallel to the western slope of Kephallinia Island. The western sector, known as IT or Matapan Trench (Mascle and Le Quellec, 1980), trends NW-SE and extends from the Ionian Islands to the south of Gavdos Island. It is a composite morphological feature characterized by small, discontinuous, NW-SE elongate, or spindle-shaped basins with depths exceeding 4000–5000m and separated by shallower ridges. The NW slopes of the Trench are steep and irregular, with N-S trending ridges advancing toward south. The SW slopes of the Trench toward the MR are less steep. The eastern sector is delineated by three striking features: the WSW-ENE trending Ptolemy Trench south of central Crete, and the WSW-ENE to SW-NE trending Pliny and Strabo Trenches. Complex seafloor topography with shallow ridges and NW-SE trending linear deeps prevails in the areas between the Ptolemy and Pliny Trenches and between the Pliny and Strabo Trenches. The Ptolemy Trench terminates eastward at the NNE-SSW trending Ierapetra graben while the Pliny and Strabo Trenches extend up to the 4000-m-deep Rhodes Basin.

In the 1970s, Le Pichon et al. (1979) provided for the first time “multinarrow beam” bathymetric data along the Hellenic Trench. They observed that the IT is divided into small basins that are deformed by compressional stress acting roughly perpendicularly to the trench. The Pliny and Strabo Trenches display narrow en echelon slots oriented obliquely to the trend of the main trenches. Le Pichon et al. (1979) came to the conclusion that the Hellenic Trench represents a subduction trench dominated by arc-perpendicular compression along the IT and sinistral transform motion along the Pliny and Strabo trenches. Huchon et al. (1982) concluded that the Hellenic Trench is the boundary between the Aegean continental extensional domain and the Mediterranean compressional domain. The structure of the trench is controlled by the kinematics of the subduction. Thus, fracturing along the IT occurs perpendicular to the main compressional stress and at about 35° along the eastern segment of the trench.

Lyberis et al. (1982) were led to a new interpretation of the active deformation between southeastern Peloponnese and western Crete. According to them, the subsidence of the western Cretan strait results from E-W extension accommodated by oblique, en echelon normal faults indicating significant dextral strike-slip deformation. Thus, the Kythera-west Crete strait is an example of complex dextral strike-slip and extensional deformation.

The southern Hellenic Arc, according to Angelier et al. (1982), undergoes radial extension and motions along north-south strike-slip faults during mid-Pleistocene to recent. However, Lyon-Caen et al. (1982) and Armijo et al. (1992) stated that at present the Peloponnesus and Crete are dominated by approximately E-W extension and dip-slip movements along approximately N-S-oriented faults.

On Crete Island, the basin of Heraklion initiated in the Late Messinian as an expression of arc parallel extension (Fassoulas, 2001). Since the Middle Pliocene, fault development resumed in two normal directions, NW-SE and NE-SW, as a result of a pure multidirectional extension, an arc-normal extension induced by the slab rollback and an arc-parallel stretching due to the westward Anatolian extrusion. Van Hinsbergen and Meulenkamp (2006) have shown that from approximately 10Ma onward, the southward migration of the area that presently covers Crete was accompanied by E-W extension, and the opening of the Sea of Crete to the north. During the Pliocene, Crete emerged and tilted to the NNW, probably as a result of left-lateral transpression.

Ten Veen and Meier (1998), by quantifying and modeling geological observations on Crete, suggested that ENE-WSW left lateral shearing along N070E-N075E trending faults associated with N020E oversteps and NW-SE normal faults prevails during the Plio-Quaternary. This is in agreement with the observations of Ten Veen and Kleinspehn (2003) in the Messara Basin (southern Central Crete) according to which the deformation of the basin since the Pliocene has been dominated by N070E sinistral faults developed in a transtensional regime.

Further east, Mascle et al. (1982) and Leite and Mascle (1982) observed that the Strabo Trench displays a complex deformation pattern with areas of extension, areas of compression, and probable strike-slip deformation. Mascle et al. (1986) proposed that the Strabo area reflects crustal shortening together with complex strike-slip fault rearrangement, as suggested by Jackson and McKenzie (1988) and Jackson (1994). They concluded that the en-echelon arrangement of both the

Pliny and Strabo trenches indicates a recent readjustment in response to a general southwest motion of the stretched Aegean domain, locked to the south and laterally ejected toward the Ionian Basin. Ten Veen and Kleinspehn (2002) recognized in the island of Rhodes two neotectonic deformation phases separated by a kinematic change in the Early Pliocene, after which the inner forearc started to experience sinistral transtension. Ten Veen and Kleinspehn (2003) suggest that both the onshore and offshore areas of the eastern Hellenic arc, from Crete to Rhodes, are characterized by a series of c. N070E wrench dominated zones and extensional, N020E striking zones, which act as secondary oversteps. This deformation pattern was initiated in the Early Pliocene and led to the fast uplift of Crete and Karpathos as postulated by the widespread occurrence of mass transport deposits (Zachariasse et al., 2008 and references therein). In addition, Pliocene uplift in Crete was accompanied by enhanced subsidence and relative deepening of offshore tectonic troughs south of Crete accommodated by WSW-ENE transtentional fault sets (Alves et al., 2007).

4.3.4.2 Seismological and Geodetic Constraints

The Hellenic Trench is a major bathymetric and morphological feature of the Hellenic subduction zone. However, the Hellenic Trench is not the expression of an oceanic trench in the usual sense and does not constitute the surface expression of the main subduction interface. Taymaz et al. (1990) and Meier et al. (2004) have shown that the earthquakes directly beneath the trench represent low-angle thrusts at 20-40km depth and are associated with the interface between the overriding Aegean and the subducting African plates. Arc-parallel extension accommodated mostly by N-S normal faulting prevails in the overriding plate in the area of Crete (Taymaz et al., 1990). According to Kiratzi and Louvari (2003), low-angle thrusting and reverse faulting prevails along the Hellenic arc, from southwest of Zakynthos island up to the northeast of Rhodes island and is attributed to the northward motion of Africa and the subduction below the Hellenic arc.

Recent mapping of the downgoing slab below the IT and Peloponnese by using teleseismic receiver function analysis on a dense two-dimensional (2D) seismic array revealed a segmentation into dipping panels by along-dip faults (Sachpazi et al., 2016a, b). These faults display a striking correlation with the occurrence of large earthquakes in the upper and lower

plate and at the interplate boundary and imply that the slab rollback occurs in a differential piecewise manner imposing its specific stress and deformation pattern onto the overriding Aegean plate. It is worth noting that the segmentation of the downgoing slab is an idea suggested much earlier. Flemming (1978) studied the Holocene eustatic changes and coastal tectonics in the northeast Mediterranean and reached the conclusion that the quasilinear sections of the subduction zone, the Ionian and Strabo branches, are interrupted by short tear faults and abrupt changes of strike at intervals of 50-100km along their length.

Meier et al. (2004) have shown that the Hellenic Trench system is part of the Aegean lithosphere and observed notable differences in the seismicity between the IT south of western Crete and the Ptolemy Trench south of central Crete. The latter is characterized by high seismic activity occurring within a vertical zone extending from the upper crust down to the plate interface at about 30km depth. A strong correlation between seafloor morphology and transtensional movements south of Crete has also been observed by Kokinou et al. (2012).

Toward the NW, the IT terminates at the steep NNE-SSW-trending bathymetric escarpment along the NW edge of the Ionian Islands. This escarpment marks the surface expression of the Kephallinia transform fault (KF) that is associated with NE-SW right-lateral strike-slip faulting seismicity (Baker et al., 1997; Louvari et al., 1999; Sachpazi et al., 2000; Kiratzi and Louvari, 2003; Kokinou et al., 2006). Louvari et al. (1999) suggested that the KF consists of two segments with different strikes: a southern, 90-km-long segment that trends NE, and a northern, 40-km-long segment striking NNE. The Kephallinia fault marks the change from oceanic subduction below Peloponnese to the southeast to continent-continent collision to the northwest (Van Hinsbergen et al., 2006; Brun and Sokoutis, 2010; Royden and Papanikolaou, 2011). Shaw and Jackson (2010) have shown that NE-SW right-lateral shear at the western end of the subduction is not restricted to the KF, but is distributed on several strike-slip faults in the area between the KF and NW Peloponnese.

Two main types of faulting have been proposed for the eastern sector of the Hellenic Arc and Trench by Shaw and Jackson (2010): (i) low-angle, northward dipping thrust earthquakes on the main subduction interface with slip vectors parallel to the Africa-Aegean convergence but oblique to the strike of the eastern arc and (ii) NE-SW left-lateral strike-slip faulting in the

overriding plate. Özbakır et al. (2013) have shown that the region of the Pliny and Strabo "trenches" obeys the mechanics of a sinistral shear zone model (Tchalenko, 1970). These authors interpret the seismic anomaly off the southeast coast of Rhodes as a tear between the Hellenic and Cyprus subduction zones. The Pliny-Strabo shear zone represents the surface expression of this tearing process in the form of the development of a shear zone between the Aegean lithosphere in the NW and the African lithosphere in the SE. The Pliny and Strabo "trenches" themselves most likely correspond to linked Riedel shears (Özbakır et al., 2013).

Results of GPS campaigns show that the direction of shortening is almost constant along the Hellenic Arc, from the Ionian Islands to the island of Rhodes (Kahle et al., 1999, 2000). Maximum shortening trends N27°E, in fairly good agreement with the seismic results, while in the southern Ionian Islands compression occurs in a N34°E direction. Maximum sinistral shear strain rates are observed along the Strabo-Pliny trench system, which seems to act as a transform fault system clearly defining the southeastern boundary of the Aegean microplate (Kahle et al., 1999, 2000). Kreemer and Chamot-Rooke (2004) and Perouse et al. (2012) have highlighted the presence of active shear partitioning within the MR that leads to 19–23mm/ year of dextral motion at the wedge-backstop contact along the IT; whereas the Pliny and Strabo trenches in the eastern Hellenic Trench accommodate 21–23mm/year of sinistral motion. According to these observations, the backstop of the western MR is kinematically part of the southern Aegean. The latter moves as a single block at 33–34mm/year toward S24° W, while a clear divergence between the western and eastern Hellenic Arc is evident. The south- eastern Aegean moves at a rate of up to 10mm/year away from the stable south Aegean (McClusky et al., 2000; Kreemer and Chamot-Rooke, 2004; Reilinger et al., 2006; Perouse et al., 2012). Finally, the velocity field modeled by Perouse et al. (2012) indicates that both ends of the Hellenic subduction zone coincide with two crustal toroidal patterns, a clockwise one at the NW end and a counterclockwise one at the eastern end. The authors suggest that both toroidal flows are related to slab tears detaching the Hellenic slab from the Apulian platform to the west and the continental fragments off Anatolia to the east.

4.3.6. New Offshore Morphology and Fault Network

Figures 4.3.3 - 4.3.5 show the most up-to-date bathymetric relief of the Aegean Sea and Hellenic Trench (Drakopoulou and Kyriakidou, 2016; Sakellariou and Tsampouraki-Kraounaki, 2016),

produced in the framework of EMODNET Bathymetry project (https://emodnet. eu/bathymetry). Literally all available, former and recent, swath bathymetry data, GEBCO bathymetry, and single beam echo soundings have been reprocessed and gridded to 250m cell-size resolution to create a digital elevation model of the seabed. The inset maps in Figures 4.3.3 and 4.3.4 show the swath bathymetry coverage in the Northern and Southern Aegean, respectively. Further processing and analysis of the bathymetric data have led to the precise map- ping of the flat-bottomed basins, the shallow ridges, banks and plateaus and the steep slopes, which are potentially associated with active faults.

Figure 4.3.5 shows the spatial distribution of morphological basins in the Aegean Sea and the Hellenic Trench, categorized according to their depth. Most of the basins display a rhomboid, elliptical, trapezoid, or spindle shape, their dimensions do not exceed a few tens of kilometers and are aligned predominantly in NE-SW to ENE-WSW, and secondarily in NW-SE to WNW-ESE, directions. The latter two directions prevail over the entire Aegean Sea and coincide with the orientation of the steep, submarine slopes that bound the basins.

The majority of the morphological basins in the Aegean are shallower than 1000m.Numerous, small, and larger basins occur in the NAS. The 1600-m-deep NAT is the deepest among them, followed by the North Ikarian Basin and the small basins off the northeastern coast of Evia, which are slightly deeper than 1000m. The southern margin of the CP displays a complex relief with small and larger islands and shallow ridges alternating with NE-SW and NW-SE elongate, <1000-m-deep basins. Maximum depths, between 2000 and 2500m, occur only at the southeastern edge of the Aegean, west of the Karpathos Island, and north of eastern Crete. The rest of the South Aegean is characterized by variable-shaped basins (elongate, rhomboid, and spindle shaped)

with bottom depths ranging between 1000 and 2000m, and separated from each other by shallow ridges.

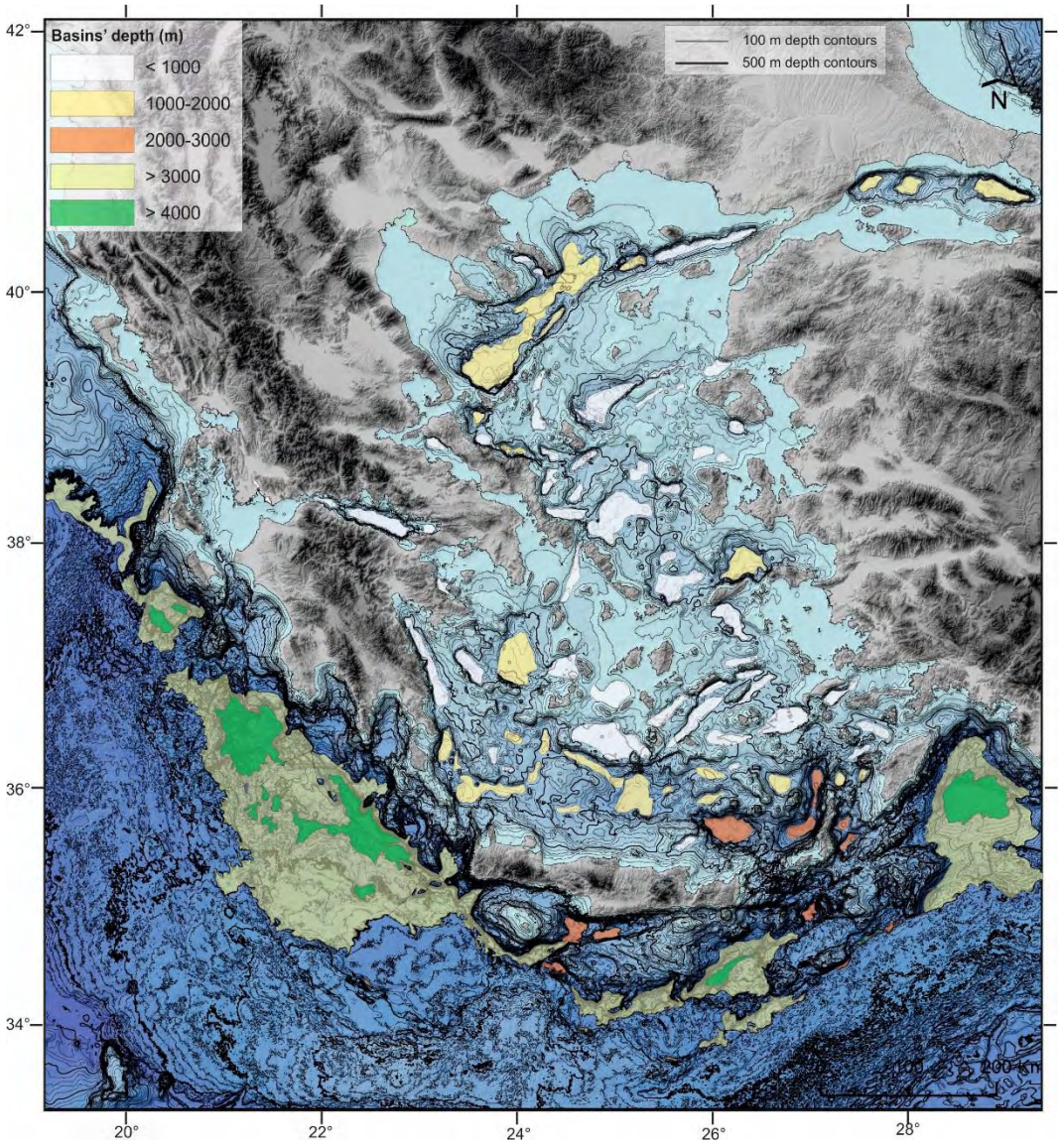

Figure 4.3.5: Morphological basins in the Aegean Sea and the Hellenic Trench categorized according to their depth. The Aegean Sea is characterized by variably shaped, isolated basins bounded by steep slopes, shallow banks, ridges, and islands. The distribution of the basins is rather random and the maximum basin depth does not exceed 2500m. The basins of the Hellenic Trench are aligned along the major Ptolemy, Pliny, Strabo trenches, and the IT and their depths range between 2500 and 5000m.

The three sectors of the Hellenic Trench (the Kephallinia fault, IT, and Pliny-Strabo Trenches) display distinct morphological characteristics. A narrow, NNE-SSW-trending, 3000–3500-m-deep elongate trough occurs along the steep escarpment of the Kephallinia fault west of the Ionian

Islands. The IT consists of a series of isolated troughs or irregularly shaped basins with depths exceeding 4000–5000m, aligned in the NW-SE direction. Finally, the three main NE-SW-trending morphological features of the eastern sector, the Ptolemy, Pliny, and Strabo Trenches, show up as linear elements consisting of several smaller troughs and basins, separated from each other by ridges and structural highs.

Old and recent, multi- and single-channel, analog and digital, seismic reflection profiles available at the Hellenic Center for Marine Research (Inset map in Figure 4.3.6) have been or are in the process of being reprocessed and reinterpreted. The old analog profiles have been digitized and many of them have been transformed into SEG-Y format. Reinterpretation of these profiles combined with the new high-resolution bathymetry led to significantly improved localization and better tracing of the faults imaged within them. The aim of this effort is to produce an updated map of the offshore fault network and geological structure and contribute to a better understanding of the dominant deformation mechanism of the Aegean after the Messinian.

Along with the available seismic profiles, a significant amount of information on the offshore faults of various areas of the Aegean is included in the existing literature. The major results of the most relevant works have been presented and briefly discussed in the previous chapters while the respective survey areas are visualized on the map of Figure 4.3.2**.** The offshore faults and other structural data that are available in the literature have been taken into consideration during the creation of the offshore faulting map. The traces of the published faults have been redrawn on the updated bathymetric relief by taking into consideration the de- tailed morphology while maintaining their geometrical and kinematic characteristics.

Almost three decades after the first map of offshore faults in the Aegean published in the benchmark paper by Mascle and Martin (1990), the map presented here (Figure 4.3.6) visualizes the most up-to-date information and the current state of knowledge on the offshore faults and the Plio-Quaternary basins. This map and the elements shown on it have derived from the interpretation of the available, old and recent seismic profiling data, the integration of structural data extracted from the existing literature and from the structural analysis of the new bathymetric relief. Faults shown on the map have been either imaged on seismic profiles or extracted from the literature or inferred from the bathymetry. Faults inferred only from seismological observations,

with no surface expression, are not included in this map. The accuracy of the mapped structural elements is directly related to the density and resolution of the available bathymetric and seismic profiling data. A rather small part of the Aegean has been systematically surveyed by means of swath bathymetry and seismic profiling. For the rest, only low-resolution GEBCO bathymetry and widely spaced, scattered seismic profiles are available. Therefore, this map serves as a visualization of the current state of knowledge, which is still far from being complete. It will be continuously updated as new data and information will become available in the future.

A first observation, which derives from the comparison of the morphological and structural maps of Figures 4.3.5 and 4.3.6, is that the morphological basins coincide largely with the main Plio-Quaternary basins. This leads to the rather obvious conclusion that the present morphological configuration is the result of the geodynamic processes that have been active during the last 5Ma. A second observation is that most of the volcanoes are aligned parallel to the main fault directions and are thus spatially associated with major faults. This is in good agreement with the previously suggested control of the active tectonic elements on the spatial distribution and surface expression of volcanism along the arc (e.g., Papazachos and Panagiotopoulos, 1993; Piper and Perissoratis, 2003; Pe-Piper and Piper, 2005; Piper et al., 2007; Sakellariou et al., 2010).

A third observation is that the faults tend to group in two main directions: (i) NE-SW to ENE-WSW and (ii) NW-SE to WNW-ESE. The NE-SW to ENE-WSW faults run either parallel to or at low angle with respect to the kinematic vectors (Figure 4.3.1B) derived from the GPS data (Kahle et al., 1999, 2000; Kreemer and Chamot-Rooke, 2004; Reilinger et al., 2010). The NW-SE to WNW-ESE faults are oriented perpendicular to or at high angle with respect to the GPS vectors. As it will be discussed below, the value of the angle between the GPS vectors and the fault direction seems to be important for the kinematic character of the latter. Faults oriented parallel to the GPS vectors are expected to display predominantly strike-slip character (dextral or sinistral), while faults oriented at higher angles may display normal to oblique sense of motion.

Geological, seismological, and geodetic data discussed previously clearly indicate that dextral strike-slip along the NE-SW to ENE-WSW trending faults and fault zones is the dominant deformation mechanism in the NAS, between the NAT to the north and the CP to the south

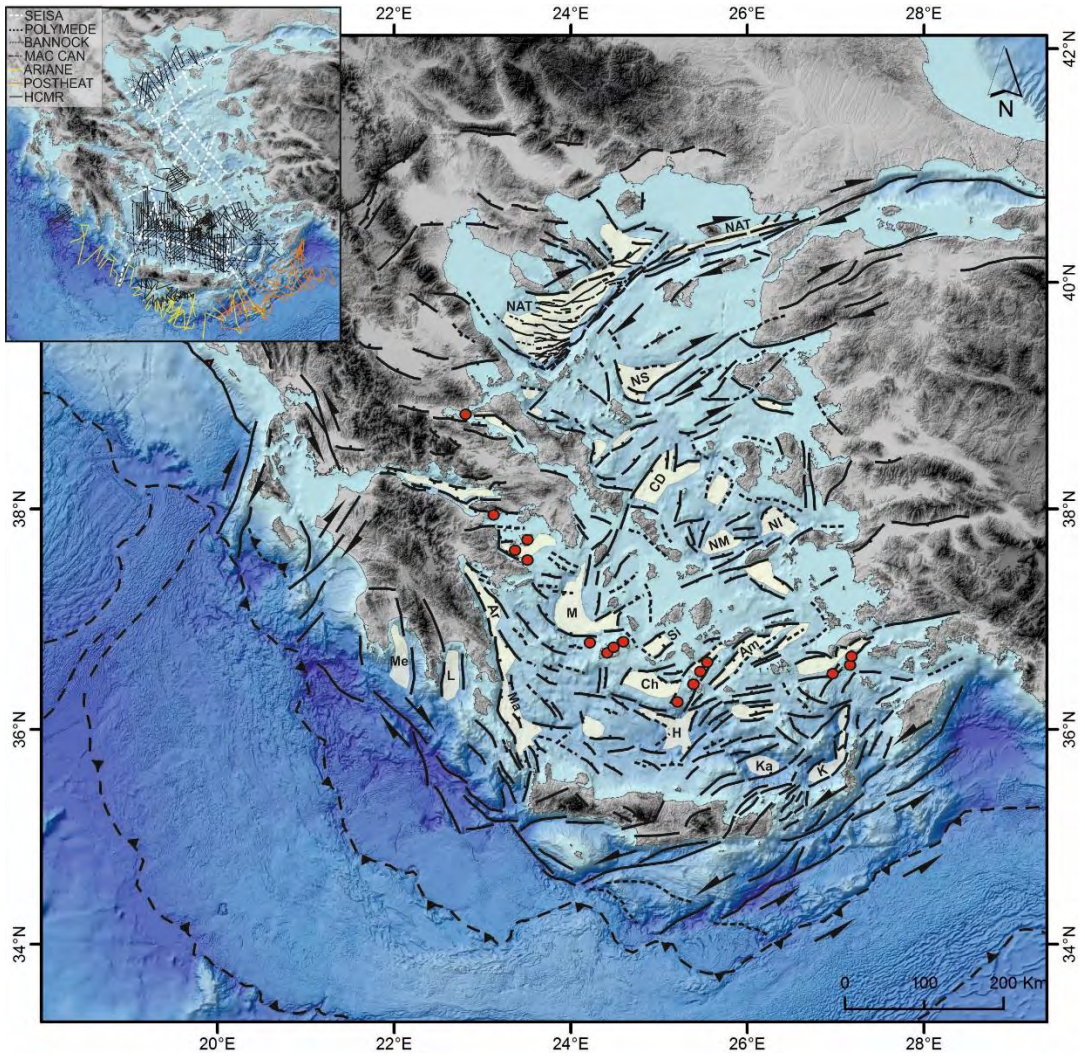

Figure 4.3.6: Active fault network and distribution of the main Plio-Quaternary basins in the Aegean. Inset map: seismic profiles available in the Aegean Sea. Red dots show the main volcanoes of the Volcanic Arc. Yellow areas indicate Plio- Quaternary basins with sediment thickness >500m. Black lines show active faults; dashed black lines indicate possible/ inferred faults. Ticks on the faults mark the hanging wall. Halfarrows show the sense of strike-slip motion. Basins: Am, Amorgos; Ar, Argolic; CD, Cavo Doro; Ch, Christiana; H, Heraklion; K, Karpathos; Ka, Kamilonissi; L, Lakonikos; M, Myrtoon; Me, Messiniakos; NAT, North Aegean Trough; NI, North Ikarian; NM, North Mykonos; NS, North Skyros; Si, Sikinos.

(Kiratzi and Louvari, 2003; Kahle et al., 2000; Kreemer and Chamot-Rooke, 2004; Reilinger et al., 2006, 2010; Perouse et al., 2012; Chatzipetros et al., 2013; Müller et al., 2013). These faults and fault zones terminate toward the SW before the coastline of Central Greece (Evia) and are associated with NW-SE to WNW-ESE running, conjugate, sinistral strike-slip to oblique faults (Kiratzi and Louvari, 2003; Ganas et al., 2005 and references therein; Müller et al., 2013). These two fault groups control the development of the Plio- Quaternary basins in the NAS as transtensional

basins (Beniest et al., 2016). West of the NAS, in Central Greece (North Evia Gulf, Corinth Gulf, Trichonis Lake), the fault network consists of WNW-ESE to NW-SE normal faults with or without significant sinistral horizontal component. NE-SW dextral strike-slip faults are absent from Central Greece and occur again further west, in NW Peloponnese.

The NE-SW trending fault zone that runs along the western margin of CD Basin and between SE Evia and the Cyclades Archipelago (CD Strait) is the first one (from North to South) that extends southwestwards beyond the eastern coastline of Central Greece. It breaks through the CP and reaches the Myrtoon Basin (M) west of it. Similarly, the NE-SW fault zone running along the southern margin of North Ikaria (NI) and North Mykonos Basins continues toward SW, south of Mykonos, and is in line with the NE-SW faults between Milos and Serifos Islands. Both aforementioned fault zones seem to be involved in the creation and evolution of the MB, along with the WNW-ESE to NW-SE faults that control its southwestern margin.

The eastern half of the South Aegean Sea and the eastern sector of the Hellenic Trench, from the CP to the Pliny and Strabo Trenches, are dominated by NE-SW to ENE-WSW trending strike-slip to oblique faults and fault zones. Seismological and geological data indicate dextral transtension for the Santorini to Amorgos area and dextral oblique rifting along the Amorgos shear zone (Bohnhoff et al., 2006; Sakellariou et al., 2010; Piper et al., 2007; Tsampouraki-Kraounaki and Sakellariou, 2017, 2018). Geological and geodetic data show that south of the Amorgos shear zone the sense of shear changes from dextral to sinistral toward southeast. Interestingly, the change in the sense of shear coincides with the southeastern boundary between the “rigid” Central Aegean and the deforming Southeast Aegean blocks (Fig. 4.3.1C) as defined by Reilinger et al. (2010). Sinistral strike-slip character has been proposed for the NE-SW to ENE-WSW faults in the southeastern corner of the Aegean, including the GG, Kos and Nisyros areas, Karpathos and Kamilonissi Basins, Rhodes, and Eastern Crete (Mascle and Martin, 1990; ten Veen and Kleinspehn, 2002, 2003; Pe-Piper et al., 2005; Ulug et al., 2005; Tur et al., 2015; Ocakoglu et al., 2018). The sinistral, strike-slip faulting in the SE Aegean coincides with the sinistral strike-slip character of Pliny and Strabo Trenches. According to Kreemer and Chamot-Rooke (2004), the Pliny and Strabo Trenches accommo- date 21–23mm/year of sinistral motion between the Aegean plate and the MR.

The western half of the South Aegean Sea displays NNW-SSE to WNW-ESE faulting predominantly. Geodetic data indicate that this part of the Aegean behaves as a single block, which translates toward SSW without significant internal deformation (McClusky et al., 2000; Kreemer and Chamot-Rooke, 2004; Reilinger et al., 2006, 2010; Perouse et al., 2012). The latter seems to be supported by the absence of upper plate seismicity (Kiratzi and Louvari, 2003) but is in apparent contrast to the morphological and geological structure of the area (see Reilinger et al., 2010 for discussion). The digital elevation model (DEM) of the western South Aegean Sea shows many, smaller and larger, elongate to irregularly shaped basins. Most of the mare deeper than 1000m and are bounded by steep NNW-SSE to WNW-ESE and NE-SW-trending slopes, separated from each other by shallow ridges and banks. The structural data indicate enhanced basin subsidence and sedimentary unconformities attributed to active tectonic processes throughout the Plio-Quaternary. Further west, the South Peloponnese is fractured by NNW-SSE trending faults, which control the formation of horst and graben structure detected in the Messiniakos (Me) and Lakonikos (L) Gulfs. Despite the absence of detailed bathymetric and seismic profiling data south of Peloponnese, these faults seem to extend southwards and terminate at the IT. Dextral motion of 19–23mm/year has been modeled by Kreemer and Chamot-Rooke (2004) along the contact of the MR to the backstop and the IT. It is therefore possible that the NNW-SSE trending extensional faulting in South Peloponnese may be kinematically related to the dextral motion along the NW-SE trending IT.

4.3.7. Geodynamic Synthesis and Open Questions

The analysis of the new offshore morphology, the results of the reprocessing and interpretation of the available, old and recent, seismic profiles and the published geological data has allowed a new, detailed mapping of the offshore fault network and a better understanding of the geological structure of the Aegean region (Figure 4.3.6). The integration of the newly described geological structures with the available seismological and geodetic information allows a re-evaluation and reinterpretation of the major geodynamic elements and of the regional and local deformation pattern and kinematic regime (Figure 4.3.7).

The Kephallinia fault (KF) and the prolongation of the NAF in the NAT constitute the northern dextral, strike-slip boundary of the deforming Aegean crust, as suggested very early on and

confirmed repeatedly with various data sets (McKenzie, 1972, 1978; Dewey and Sengör 1979; Le Pichon and Angelier, 1981; Taymaz et al., 1991; Kahle et al., 2000; McClusky et al., 2000; Kiratzi

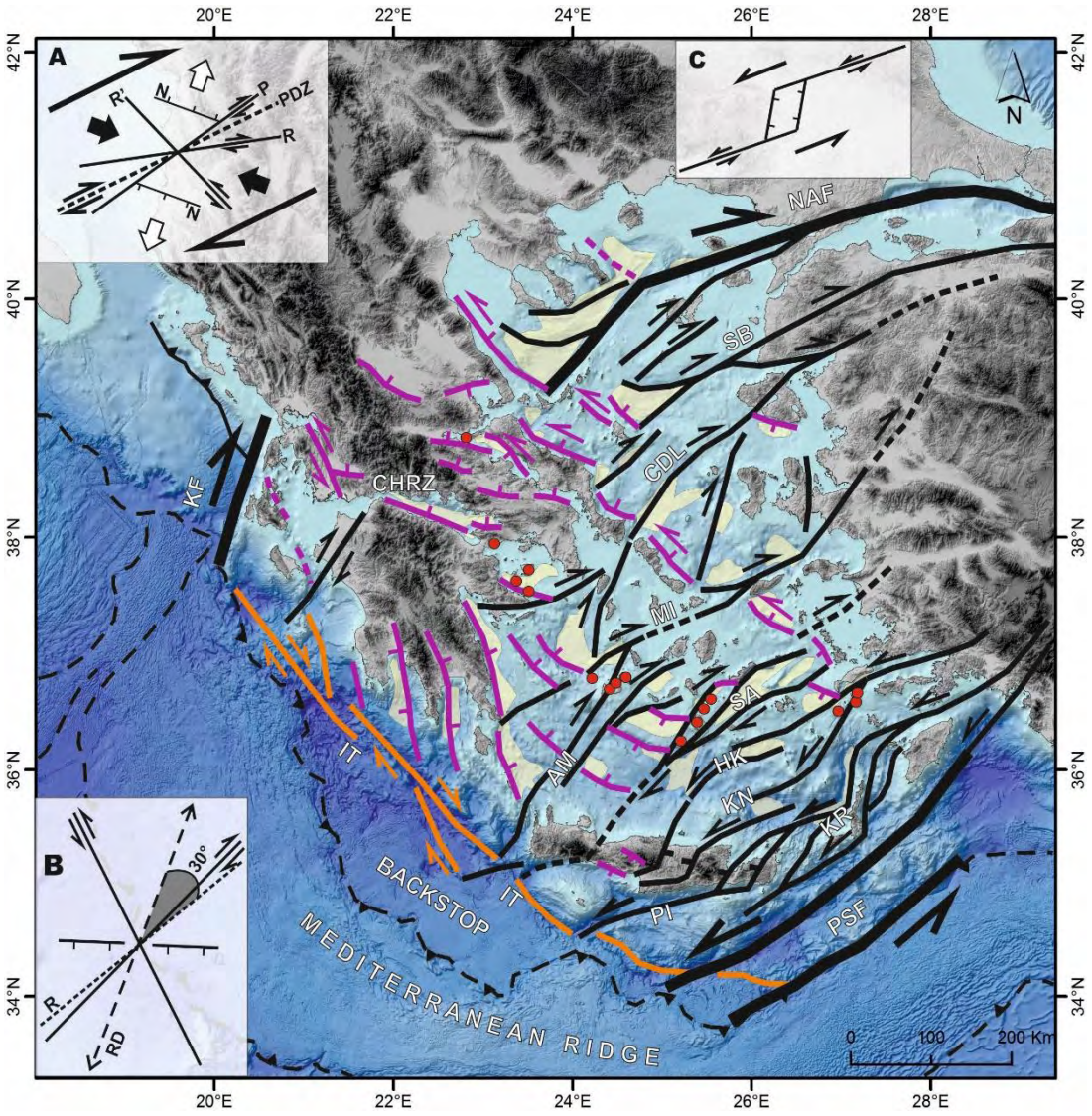

Figure 4.3.7: Plio-Quaternary deformation pattern in the overriding Aegean crust. Red dots show volcanoes of the Vol- canic Arc. Yellow areas show Plio-Quaternary basins with sediment thickness>500m. The North Anatolian (NAF), the Central Hellenic Relay Zone (CHRZ) and the Kephallinia fault (KF) mark the dextral, northern boundary of the deforming Aegean. The Pliny-Strabo fault zone (PSF) marks the sinistral, southern boundary. Between them, major and minor, NE-SW shear-zones split the Aegean in elongate crustal blocks. Between the NAF and the Santorini- Amorgos (SA) fault zone they display dextral shear and are associated with NW-SE to N-S sinistral strike-slip to oblique faults and W-E to WNW-ESE normal faults. South of SA the NE-SW shear zones display sinistral sense of motion and are associated with N-S to NNE-SSW extensional step-over faults and WNW-ESE to NW-SE normal faults. The formation of the Plio-Quaternary basins obeys the principles of basin formation along strike-slip fault zones (Riedel, 1929; Mann et al., 1983; Christie-Blick and Biddle, 1985; Mann, 2007) and oblique rifting (Withjack and Jamison, 1986). Major fault zones: AM, Antikythera-Milos; CDL, Cavo Doro-Lesvos; HK, Heraklion-Kos; KN, Kasteli-Nisyros; KR, Karpathos-Rhodes; MI, Myrtoon-Ikaria; PI, Ptolemy-Ierapetra; SA, Santorini-Amorgos; SB, Skyros-Biga. Inset A: diagram showing the orientation of Riedel shears (P, R, R′, N) and of the principal displacement zone (PDZ) in a dextral strike-slip deformation zone. R, P, and R′ are strike-slip faults, N are normal faults (Riedel, 1929). Inset B: drawing explaining the kinematic of dextral oblique extension. R: rift trend; RD: relative displacement direction between opposite sides of the rift (Withjack and Jamison, 1986). Inset C: simplified drawing explaining the kinematic pattern in the southeastern Aegean and East Crete.

and Louvari, 2003; Kreemer and Chamot-Rooke, 2004; Nyst and Thatcher, 2004; Reilinger et al., 2006, 2010; Perouse et al., 2012; Müller et al., 2013). Central Greece is located between the opposite tips of the KF and the NAF, and acts as an extensional relay zone, the Central Hellenic Relay Zone (CHRZ), between the two, left stepping, dextral strike-slip fault zones (KF and NAF), as already proposed by Shaw and Jackson (2010), and coincides with the Central Hellenic Shear Zone proposed by Papanikolaou and Royden (2007). The Pliny and Strabo Trenches (PSF) form the eastern NE-SW-trending sector of the Hellenic Trench and represent the southern, sinistral transform-type boundary of the overriding Aegean crust to the MR (Le Pichon and Angelier, 1979; Kahle et al., 1999; Kreemer and Chamot-Rooke, 2004, Reilinger et al., 2006, 2010; Shaw and Jackson, 2010; Perouse et al., 2012; Özbakır et al., 2013).

Between these two plate boundaries, the dextral northern one (KF-CHRZ-NAF) and the sinistral southern one (PSF), the overriding Aegean crust "flows" toward SW to SSW and is being internally deformed. The resultant SW- to SSW-ward extension is accommodated by major and minor dextral NE-SW to ENE-WSW-oriented shear zones and conjugate sinistral strike-slip, oblique, and normal faults. These various shear zones create local extension and transtension evolving at rates and following trends which, locally, may differ from the overall extension rate and orientation of the Aegean crust as a whole.

NNE-SSW extension in the North Aegean south of NAT is predominantly accommodated by the NE-SW to ENE-WSW-trending dextral strike-slip Skyros-Biga (SB), Cavo Doro-Lesvos (CDL) fault zones and several other minor ones along with NW-SE sinistral to oblique, conjugate faults, and WNW-ESE normal faults. This kinematic pattern is compatible with the Riedel shears model as expected in dextral strike-slip zones (Inset A in Figure 4.3.7): the dextral strike-slip, NE-SW, and ENE-WSW faults represent the P and R shears, the NW-SE sinistral faults the R' shears and the WNW-ESE faults the N faults. Note that the fault pattern in the CHRZ coincides with the N faults.

Further south, the dextral CDL and the Myrtoon-Ikaria (MI) fault zones break through the CP and extend until the MB and the eastern margin of Peloponnese (see also Figure 4.3.6 of Brun et al., 2016). Similarly, to the NAS structure, they are associated with NW-SE and WNW-ESE faults. It is worthy to note that the two main tectonic directions, NE-SW and NW-SE, can be recognized

on the main morphological elements of the Aegean Sea including the orientation of the Cyclades and Dodecanese Islands. The Antikythera-Milos (AM) fault zone is probably a splay of the MI Zone and can be followed until the western Cretan strait. The volcanic centers on and around Milos Island are located on the MI Zone. According to the available geological and seismological data, the Santorini-Amorgos (SA) fault zone is the last one toward south displaying dextral sense of motion. It extends southwestwards through the central South Aegean and western Crete to the ENE-WSW trending trench between the latter and Gavdos block. The SA Zone hosts the Santorini volcanic province, which includes the Christiana is- lets, Santorini, and the Kolumbo volcanic chain. All these volcanic centers are arranged in NE-SW direction (Kameni-Kolumbo Line) and occur in the Anydhros Basin, one of the sub- basins developed along the SA fault zone.

All aforementioned zones are sinuous or curved shear zones. Releasing or restraining bends, depending on the local kinematic pattern, form in the areas where the shear zones change direction, creating transtensional and transpressional structures locally. The Plio- Quaternary basins have developed either in a transtensional regime on releasing bends, or as pull-apart basins, or at the junction between the NE-SW dextral strike-slip and the NW-SE sinistral strike-slip to oblique faults and in horsetail structures. Oblique rifting along the NE-SW fault zones (see Inset B in Figure 4.3.7) is another mechanism explaining basin formation in the Aegean, in particular along the SA fault zone. The submarine shallow ridges and banks, as well as the islands, represent uplifted blocks, possibly associated with restraining bends. This deformation mechanism can explain the creation of the "Aegean puzzle" consisting of areas of enhanced local subsidence alternating rapidly spatially with uplifted blocks.

Southeast of the SA fault zone, in the southeastern Aegean, the sense of shear changes from dextral to sinistral. The Heraklion-Kos (HK), Kasteli-Nisyros (KN), Ptolemy-Ierapetra (PI), and KR fault zones display sinistral sense of shear and follow the kinematic character of the Pliny and Strabo fault zones. They are associated with NNE-SSW oriented normal to oblique faults, including the spectacular, predominantly normal faults, which crosscut eastern Crete and link the ENE-WSW strike-slip zones in southeastern Aegean to the ones running along the troughs south of Crete and east of Gavdos (see Inset C in Figure 4.3.7) (ten Veen and Kleinspehn, 2003). The spindle-shaped Kamilonissi and the lazy-S shaped Karpathos Basins (Ka and K in Figure

4.3.6), the deepest basins of the Aegean Sea, have developed as pull-apart basins along the KN and KR sinistral shear zones, respectively.

The IT represents a complex NW-SE-trending geodynamic element. Geodetic data (Kreemer and Chamot-Rooke, 2004) show that the backstop, southwest of the trench, belongs to the overriding Aegean crust. Thus the IT, which accommodates a considerable amount of dextral strike-slip motion, does not coincide with the outer limit of the Aegean crust. The southeastern part of the IT is offset in en-echelon arranged segments by the three ENE- WSW shear zones (Ptolemy, Pliny, and Strabo). The characteristics of the northwestern part of the trench, west of Crete until the Kephallinia fault, are less well constrained. It probably represents the surface expression of a diffuse dextral strike-slip zone developed within the upper plate, between the backstop and the arc and may be associated with SW-ward thrusting in the lower upper plate. The NNW-SSE trending normal faults in South Peloponnese may also be related with the kinematics of the IT.

The geodynamic configuration presented above and in Figure 4.3.7. accommodates the deformation of the Aegean microplate during the Plio-Quaternary. Widespread, arc-perpendicular, back-arc extension presumably prevailing in Miocene has been progressively replaced in the Plio-Quaternary by extensive shearing along NE-SW strike-slip zones imposing a complex pattern of localized transtension and formation of new basins along with local transpression, uplift, and creation of structural highs. Whereas the rollback of the East Mediterranean slab remains the driving mechanism for the extension of the overriding Aegean crust, the reasons for the progressive change in the style of deformation in the Plio-Quaternary can be found in: (i) the incipient collision of the Aegean crust with the Libyan promontory south of Crete in Late Miocene-Early Pliocene, which may have led to the partitioning of strain along the Hellenic arc; (ii) the initiation of the Kephallinia fault as a dextral, strike-slip boundary between the Apulia- NW Greece continent-continent collision to the NW and the ongoing subduction of the Ionian slab to the SE; (iii) the westward motion of Anatolia and the advance of the NAF and its branches in the Aegean Sea; (iv) the recently observed segmentation of the subducting Ionian slab into dipping panels by along-dip faults and the suggested mechanical coupling between the lower and the upper plate (Sachpazi et al., 2016a, b).

However, backarc extension in the Aegean was initiated already in the Middle Eocene and was driven by the rollback of the subducting East Mediterranean slab (Royden, 1993; Jolivet and Faccenna, 2000; Faccenna et al., 2003, 2014; Brun and Faccenna, 2008; Brun and Sokoutis, 2010, Jolivet and Brun, 2010, Jolivet et al., 2013). The velocity of the trench retreat was <1cm/ year until Middle Miocene and the slow rate of extension was associated with the exhumation of the metamorphic core complexes. The trench retreat accelerated progressively since Middle Miocene to reach 3.2cm/year in the Plio-Quaternary, the crustal extension became distributed and led to the formation of Neogene basins in the Aegean (Brun et al., 2016). Therefore, it should not be excluded that some of the faults and fault zones active in the Plio-Quaternary may have exploited preexisting zones of mechanical discontinuity or may be inherited from older, Middle to Upper Miocene tectonic elements, which became themselves deformed, rotated or changed their kinematic character as the deformation of the Aegean crust was progressing and the curvature of the Hellenic arc was increasing.

As already stated, systematic swath bathymetry and seismic profiling data are available only from limited offshore areas in the Aegean and the Hellenic Trench. Most parts of them are either not surveyed or covered by sparse data, thus their structure is not known in detail. This leaves many open questions on the evolution and the style of deformation of individual areas as well as on the precise location of major and minor faults and fault zones. The deformation pattern of the entire Aegean as described above will be continuously updated and refined in the future, as new data will be made available.

Acknowledgements

This work results from the integration of numerous surveys conducted by the Institute of Oceanography of HCMR aboard R/V Aegaeon during the last decades in the Aegean Sea, combined with previous data. We are grateful to our colleagues and the crew of R/V Aegaeon for their contribution in the acquisition of the seismic data. We particularly wish to thank Dr. V. Lykousis and Dr. G. Rousakis for their valuable collaboration and support. The work of Emeritus Professor J. Mascle in the Aegean has been the inspiration for our work. We would like to thank him for providing us with the old seismic profiles, for the repeated discussions with him and for his valuable suggestions and comments during the preparation of the manuscript. Ass. Prof. H.

Kranis is greatly acknowledged for reading the earlier version of the manuscript and sharing with us his thoughts on the tectonics of the Aegean Sea. Last but not least, we are grate- ful to Prof. J.-P. Brun for the critical and constructive review of the manuscript. His comments and suggestions helped us to improve significantly the final paper.

References

Allen, M., Jackson, J., Walker, R., 2004. Late Cenozoic reorganization of the Arabia–Eurasia collision and the compar- ison of short term and long term deformation rates. Tectonics. 23. https://doi.org/10.1029/2003TC001530.

Alves, T.M., Lykousis, V., Sakellariou, D., Alexandri, S., Nomikou, P., 2007. Constraining the origin and evolution of con- fined turbidite systems: southern Cretan margin, eastern Mediterranean Sea (34°30–36°N). Geo-Mar. Lett. 27, 41–61.

Angelier, J., Lyberis, N., Le Pichon, X., Barrier, E., Huchon, P., 1982. The tectonic development of the Hellenic arc and the sea of Crete: a synthesis. Tectonophysics 86, 159–196.

Armijo, R., Lyon-Caen, H., Papanastasiou, D., 1992. East-west extension and Holocene normal-fault scarps in the Hel- lenic arc. Geology 20, 491–494.

Armijo, R., Meyer, B., King, G.C.P., Rigo, A., Papanastassiou, D., 1996. Quaternary evolution of the Corinth rift and its implications for the late Cenozoic evolution of the Aegean. Geophys. J. Int. 126, 11–53.

Armijo, R., Meyer, B., Hubert, A., Barka, A., 1999. Westward propagation of the north Anatolian into the northern Aegean: timing and kinematics. Geology 27 (3), 267–270.

Baker, C., Hatzfeld, D., Lyon-Caen, H., Papadimitriou, E., Rigo, A., 1997. Earthquake mechanisms of the Adriatic Sea and western Greece: implications for the oceanic subduction-continental collision transition. Geophys. J. Int. 131, 594–599.

Bartole, R., Catani, G., Lenardon, G., Vinci, A., 1983. Tectonics and sedimentation of the southern Aegean Sea. Boll. Oceanol. Teor. App. 1, 319–340.

Benetatos, C., Roumelioti, Z., Kiratzi, A., Melis, N., 2002. Source parameters of the M 6.5 Skyros island (north Aegean Sea) earthquake July 26. Ann. Geophys. 45 (3), 513–526.

Benetatos, C., Kiratzi, A., Papazachos, C., Karakaisis, G., 2004. Focal mechanisms of shallow and intermediate depth earthquakes along the Hellenic trench. J. Geodyn. 37, 253–296.

Benetatos, C., Kiratzi, A., Ganas, A., Ziazia, M., Plessa, A., Drakatos, G., 2006. Strike-slip motions in the Gulf of Sigˇac¸ik (western Turkey): properties of the 17 October 2005 earthquake seismic sequence. Tectonophysics 426, 263–279.

Beniest, A., Brun, J.P., Gorini, C., Crombez, V., Deschamps, R., Hamon, Y., Smit, J., 2016. Interaction between trench retreat and Anatolian escape as recorded by neogene basins in the northern Aegean Sea. Mar. Pet. Geol. 77, 30–42.

Billiris, H., Paradisis, D., Veis, G., England, P., Featherstone, W., Parsons, B., Cross, P., Rands, P., Rayson,

M., Sellers, P., Ashkenazi, V., Davison, M., Jackson, J., Ambraseys, N., 1991. Geodetic determination of tectonic de- formation in Central Greece from 1900 to 1988. Nature 350, 124–129.

Bohnhoff, M., Rische, M., Meier, T., Becker, D., Stavrakakis, G., Harjes, H.-P., 2006. Micro-seismic activity in the Hel- lenic volcanic arc, Greece, with emphasis on the seismotectonic setting in the Santorini-Amorgos zone. Tectonophysics 423, 17–33.

Briole, P., Rigo, A., Lyon-Caen, H., Ruegg, J.C., Papazissi, K., Mitsakaki, C., Balodimou, A., Veis, G., Hatzfeld, D., Deschamps, A., 2000. Active deformation of the Corinth rift, Greece: results from repeated Global Positioning Sys- tem surveys between 1990 and 1995. J. Geophys. Res. 105, 25 605–25 625.

Brossolo, L., Mascle, J., Loubtrieu, B., 2012. Morpho-Bathymetric Map of the Mediterranean Sea (scale 1:4,000,000), first ed. CGMW/UNESCO.

Brooks, M., Ferentinos, G., 1980. Structure and evolution of the Sporadhes basin of the north Aegean trough, northern Aegean Sea. Tectonophysics 68, 15–30.

Brun, J.-P., Faccenna, C., 2008. Exhumation of high-pressure rocks driven by slab rollback. Earth Planet. Sci. Lett. 272, 1–7. https://doi.org/10.1016/j.epsl.2008.02.038.

Brun, J.-P., Sokoutis, D., 2007. Kinematics of the southern Rhodope core complex. Int. J. Earth Sci. 96, 1079–1099. https://doi.org/10.1007/s00531-007-0174-2.

Brun, J.P., Sokoutis, D., 2010. 45 m.Y. Of Aegean crust and mantle flow driven by trench retreat. Geology 38 (9), 815–818. https://doi.org/10.1130/G30950.1.

Brun, J.P., Faccenna, C., Gueydan, F., Sokoutis, D., Philippon, M., Kydonakis, K., Gorini, C., 2016. The two-stage Ae- gean extension, from localized to distributed, a result of slab rollback acceleration. Can. J. Earth Sci. 53, 1142–1157. (2016). https://doi.org/10.1139/cjes-2015-0203.

Brunn, J.H., 1976. L'arc concave Zagro-taurique et les arcs convexes tauriques et egéen: collision des arcs induits. Bull. Soc. Géol. Fr. 18, 553–567.

Chatzipetros, A., Kiratzi, A., Sboras, S., Zouros, N., Pavlides, S., 2013. Active faulting in the north-eastern Aegean Sea islands. Tectonophysics 597–598, 106–122.

Chaumillon, E., Mascle, J., 1995. Variations laterales des fronts de deformation de la Ride Mediterraneenne. Bull. Soc. Geol. Fr. 5, 463–478.

Chaumillon, E., Mascle, J., 1997. From foreland to forearc domains: new multichannel seismic reflection survey of the Mediterranean ridge accretionary complex (eastern Mediterranean). Mar. Geol. 138 (237–259), 1997.

Chaumillon, E., Mascle, J., Hoffmann, J., 1996. Deformation of the western Mediterranean ridge: Importance of Messinian evaporitic formations. Tectonophysics 263, 163–190.

Christie-Blick, N., Biddle, K.T., 1985. Deformation and basin formation along strike-slip faults. In: Biddle, K.T., Christie-Blick, N. (Eds.), Strike-slip deformation, Basin Formation and Sedimentation. 37, SEPM Spec. Publ., pp. 1–34

Çırmık, A., Pamukçu, O., Gonenç, T., Kahveci, M., Salk, M., Herring, T., 2017. Examination of the kinematic structures in Izmir (western Anatolia) with repeated GPS observations (2009, 2010 and

2011). J. Afr. Earth Sci. 126, 1–12.

Clarke, P.J., Davies, R.R., England, P.C., Parsons, B., Billiris, H., Paradissis, D., Veis, G., Cross, P.A., Denys, P.H., Ashkenazi, V., Bingley, R., Kahle, H.-G., Muller, M.-V., Briole, P., 1998. Crustal strain in Central Greece from re- peated GPS measurements in the interval 1989–1997. Geophys. J. Int. 135, 195–214.

Cocard, M., Kahle, H.G., Peter, Y., Geiger, A., Veis, G., Felekis, S., Paradissis, D., Billiris, H., 1999. New constraints on the rapid crustal motion of the Aegean region: recent results inferred from GPS measurements (1993–1998) across the west Hellenic arc, Greece. Earth Planet. Sci. Lett. 172, 39–47.

Davies, R., England, P., Parsons, B., Biliris, H., Paradissis, D., Veis, G., 1997. Geodetic strain of Greece in the interval 1892–1992. J. Geophys. Res. 102, 24 571–24 588.

Dewey, J.F., Şengör, A.M.C., 1979. Aegean and surrounding regions: complex multiplate and continuumtectonics in a convergent zone. Geol. Soc. Am. Bull. 90, 84–92.

Dimitriadis, I., Karagianni, E., Panagiotopoulos, D., Papazachos, C., Hatzidimitriou, P., Bohnhoff, M., Rische, M., Meier, T., 2009. Seismicity and active tectonics at Coloumbo reef (Aegean Sea, Greece): Monitoring an active vol- cano at Santorini volcanic center using a temporary seismic network. Tectonophysics 465, 136–149.

Dimitriadis, I., Papazachos, C., Panagiotopoulos, D., Hatzidimitriou, P., Bohnhoff, M., Rische, M., Meier, T., 2010. P and S velocity structures of the Santorini–Coloumbo volcanic system (Aegean Sea, Greece) obtained by non- linear inversion of travel times and its tectonic implications. J. Volcanol. Geotherm. Res. 195, 13–30.

Drakopoulou, P., Kyriakidou, C., 2016. Morphological map of the Hellenic and adjacent regions. Institute of Ocean- ography, Hellenic Centre for Marine Research.

Faccenna, C., Jolivet, L., Piromallo, C., Morelli, A., 2003. Subduction and the depth of convection in the Mediterranean mantle. J. Geophys. Res. 108, 2099. https://doi.org/10.1029/2001JB001690.

Faccenna, C., Becker, T.W., Auer, L., Billi, A., Boschi, L., Brun, J.-P., Capitanio, F.A., Funiciello, F., Horvath, F., Jolivet, L., Piromallo, C., Royden, L., Rossetti, F., Serpelloni, E., 2014. Mantle dynamics in the Mediterranean. Rev. Geophys. 52. https://doi.org/10.1002/2013RG000444.

Fassoulas, C., 2001. The tectonic development of a Neogene basin at the leading edge of the active European margin: the Heraklion basin, Crete, Greece. J. Geodyn. 31, 49–70.

Finetti, I., 1976. Mediterranean Ridge: a young submerged chain associated with the Hellenic Arc. Bolletino Geofis Tdor Applied XIII, 31–65.

Flemming, N.C., 1978. Holocene Eustatic Changes and Coastal Tectonics in the Northeast Mediterranean: Implica- tions for Models of Crustal Consumption. In: Mathematical and Physical Sciences.Philosophical Transactions of the Royal Society of London, Series A, 289, pp. 405–458. No. 1362 (Jun. 22, 1978).

Ganas, A., Drakatos, G., Pavlides, S.B., Stavrakakis, G.N., Ziazia, M., Sokos, E., Karastathis, V.K., 2005. The 2001 mw¼6.4 Skyros earthquake, conjugate strike-slip faulting and spatial variation in stress within the central Aegean Sea. J. Geodyn. 39 (1), 61–77.

Ganas, A., Mouzakiotis, E., Moshou, A., Karastathis, V., 2016. Left-lateralshearinsidethenorthgulfofEvia

rift, Central Greece, evidenced by relocated earthquake sequences and moment tensor inversion. Tectonophysics 682, 237–248.

Ganas, A., Elias, P., Briole, P., Valkaniotis, S., Kassaras, I., Foumelis, M., Moshou, A., Kourkouli, P., Papathanassiou, G., Rogier, M., Chouliaras, G., Argyrakis, A., Parcharidis, I., 2017. In: The June 12, 2017 M6.3 Lesvos offshore earthquake sequence (Aegean Sea, Greece): fault model and stress analysis from seismic and geo- detic observations. Book of Abstracts, 15th Congress of the RCMNS, Athens, Greece 2017, p. 161.

Goldsworthy, M., Jackson, J., Haines, J., 2002. The continuity of active faults in Greece. Geophys. J. Int. 148, 596–618. G€urer, O.F., Sangu, E., €Ozburanb, M., G€urb€uz, A.,

Gürer, A., Sinir, H., 2016. Plio-quaternary kinematic development and paleostress pattern of the Edremit Basin, western Turkey. Tectonophysics 679, 199–210.

Hooft, E.E.E., Nomikou, P., Toomey, D.R., Lampridou, D., Getz, C., Christopoulou, M.-E., O'Hara, D., Arnoux, G.M., Bodmer, M., Gray, M., Heath, B.A., VanderBeek, B.P., 2017. Backarc tectonism, volcanism, and mass wasting shape seafloor morphology in the Santorini-Christiana-Amorgos region of the Hellenic volcanic arc. Tectonophysics 712–713, 396–414.

Hsü, K.J., Montadert, L., Bernouilli, D., Bizon, G., Cita, M., Erickson, A., Fabricius, F., Garrison, R.E., Kido, R.B., Mellieres, F., Muller, C., Wright, R.C., 1978. Site 378: cretan basin. Initial Rep. Deep Sea Drill. Proj. 42 (1), 321–357.

Hübscher, C., Ruhnau, M., Nomikou, P., 2015. Volcano-tectonic evolution of the polygenetic Kolumbo submarine volcano/Santorini (Aegean Sea). J. Volcanol. Geotherm. Res. 291, 101–111.

Huchon, P., Lyberis, N., Angelier, J., Le Pichon, X., Renard, V., 1982. Tectonics of the Hellenic trench: a synthesis of Seabeam and submersible observations. Tectonophysics 86, 69–112.

Işcan, Y., Tur, H., G€okaşan, E., 2013. Morphologic and seismic features of the Gulf of G€okova, SW Anatolia: evidence of strike-slip faulting with compression in the Aegean extensional regime. Geo-Mar. Lett. 33 (1), 31–48.

Işler, E.B., Aksu, A.E., Yaltırak, C., Hiscott, R.N., 2008. Seismic stratigraphy and quaternary sedimentary history of the northeast Aegean Sea. Mar. Geol. 254, 1–17.

Jackson, J., 1994. Active tectonics of the Aegean region. Annu. Rev. Earth Planet. Sci. 22, 239–271. Jackson, J., McKenzie, D., 1988. Rates of active deformation in the Aegean Sea and surrounding regions. Basin Res. 1, 121–128.

Jolivet, L., Brun, J.-P., 2010. Cenozoic geodynamic evolution of the Aegean. Int. J. Earth Sci. 99, 109–138. https://doi. org/10.1007/s00531-008-0366-4.

Jolivet, L., Faccenna, C., 2000. Mediterranean extension and the Africa–Eurasia collision. Tectonics 19, 1095–1106.

Jolivet, L., Faccenna, C., Huet, B., Labrousse, L., Le Pourhiet, L., Lacombe, O., Lecomte, E., Burov, E., Denèle, Y., Brun, J.P., Philippon, M., Paul, A., Salaün, G., Karabulut, H., Piromallo, C., Monié, P., Gueydan, F., Okay, A.I., Oberhänsli, R., Pourteau, A., Augier, R., Gadenne, L., Driussi, O., 2013. Aegean tectonics: strain localisation, slab tearing and trench retreat. Tectonophysics 597, 1–33. https://doi.org/10.1016/j.tecto.2012.06.011.

Jongsma, D., Wissman, G., Hinz, F., Garde, S., 1977. Seismic studies in the Cretan Sea. The southern Aegean Sea: an extensional marginal basin without sea floor spreading? Results of R.V. "Meteor" and R.R.S. "Shackleton" cruises. "Meteor" Forschungsergeb. Geol. Geophys., C 27, 3–30.

Kahle, H.G., Mueller, M.V., Geiger, A., Danuser, G., Mueller, S., Veis, G., Billiris, H., Paradissis, D., 1995. The strain field in NW Greece and the Ionian islands: results inferred from GPS measurements. Tectonophysics 249, 41–52.

Kahle, H.G., Cocard, R., Peter, Y., Geiger, A., Reilinger, R., McClusky, S., King, R., Barka, A., Veis, G., 1999. The GPS strain rate field in the Aegean Sea and western Anatolia. Geophys. Res. Lett. 26 (16), 2513–2516. https://doi.org/ 10.1029/1999GL900403.

Kahle, H.-G., Cocard, M., Peter, Y., Geiger, A., Reilinger, R., Barka, A., Veis, G., 2000. GPS-derived strain rate field within the boundary zones of the Eurasian, African, and Arabian plates. J. geophys. Res. 105, 23 353–23 370.

Karakostas, V.G., Papadimitriou, E.E., Karakaisis, G.F., Papazachos, C.B., Scordilis, E.M., Vargemezis, G., Aidona, E., 2003. The 2001 Skyros, northern Aegean, Greece, earthquake sequence: off-fault aftershocks, tectonic implications, and seismicity triggering. Geophys. Res. Lett. 30(1). https://doi.org/10.1029/2002GL015814.

Kiratzi, A.A., 2002. Stress tensor inversion along the westernmost north Anatolian fault zone and its continuation into the north Aegean Sea. Geophys. J. Int. 151 (2), 360–376.

Kiratzi, A., 2013. The January 2012 earthquake sequence in the Cretan Basin, south of the Hellenic volcanic arc: focal mechanisms, rupture directivity and slip models. Tectonophysics 586, 160–172.

Kiratzi, A., Louvari, E., 2003. Focal mechanisms of shallow earthquakes in the Aegean Sea and the surrounding lands determined by waveform modelling: a new database. J. Geodyn. 36 (1–2), 251–274.

Kiratzi, A., Wagner, G., Langston, C., 1991. Source parameters of some large earthquakes in northern Aegean deter- mined by body waveform inversion. Pure Appl. Geophys. 135, 515–527.

Kokinou, E., Papadimitriou, E., Karakostas, V., Kamberis, E., Vallianatos, F., 2006. The Kefalonia transform zone (off- shore western Greece) with special emphasis to its prolongation towards the Ionian abyssal plain. Mar. Geophys. Res. 27, 241–252.

Kokinou, E., Tiago, A., Kamberis, E., 2012. Structural decoupling in a convergent forearc setting (southern Crete, east- ern Mediterranean). GSA Bull. https://doi.org/10.1130/B30492.1.

Kokkalas, S., Xypolias, P., Koukouvelas, I., Doutsos, T., 2006. Postcollisional contractional and extensional deforma- tion in the Aegean region. In: Dilek, Y., Pavlides, S. (Eds.), Post-collisional tectonics and magmatism in the Med- iterranean region and Asia: geological Society of America Special Paper. 409, pp. 97–123. https://doi.org/ 10.1130/2006.2409(06). Koukouvelas, I.K., Aydin, A., 2002. Fault structure and related basins of the north Aegean Sea and its surroundings. Tectonics 21, 1046.

Kreemer, C., Chamot-Rooke, N., 2004. Contemporary kinematics of the southern Aegean and the Mediterranean ridge. Geophys. J. Int. 157, 1377–1392.

Kurt, H., Demirbag, E., Kuşçu, I˙., 1999. Investigation of the submarine active tectonism in the Gulf of G€okova, south- west Anatolia–southeast Aegean Sea, by multi-channel seismic reflection data.

Tectonophysics 305, 477–496.

Kurt, H., Demirbag, E., Kuşçu, I., 2000. Active submarine tectonism and formation of the Gulf of Saros, northeast Ae- gean Sea, inferred from multi-channel seismic reflection data. Mar. Geol. 165, 13–26.

Kydonakis, K., Moulas, E., Chatzitheodoridis, E., Brun, J.-P., Kostopoulos, D., 2015. First-report on Mesozoic eclogite- facies metamorphism preceding Barrovian overprint from the western Rhodope (Chalkidiki, northern Greece). Lithos 220, 147–163. https://doi.org/10.1016/j.lithos.2015.02.007.

Lalechos, N., Savoyat, E., 1979. In: La sedimentation Neogene dans le Fosse Nord Egeen.Proc. 6th Colloquium on the Geology of the Aegean region, 1977. v2, pp. 591–603.

Le Pichon, X., 1982. Land-Locked Oceanic Basins and Continental Collision: The Eastern Mediterranean as a Case Example. In: Hsu, K.J. (Ed.), Mountain Building Processes. San Diego, Academic Press, pp. 201–211.

Le Pichon, X., Angelier, J., 1979. The Hellenic arc and trench system: a key to the neotectonic evolution of the eastern Mediterranean area. Tectonophysics 60, 1–42.

Le Pichon, X., Angelier, J., 1981. The Aegean Sea. Philos. Trans. R. Soc. Lond. 300, 357–372.

Le Pichon, X., Angelier, J., Aubouin, J., Lyberis, N., Monti, S., Renard, V., Got, H., Hsu, K., Mart, Y., Mascle, J., Matthews, D., Mitropoulos, D., Tsoflias, P., Chronis, G., 1979. From subduction to transform motion: a seabeam survey of the Hellenic trench system. Earth Planet. Sci. Lett. 44, 441–450.

Le Pichon, X., Angelier, J., Sibuet, J.-C., 1982. Plate boundaries and extensional tectonics. Tectonophysics 81, 239–256. Le Pichon, X., Chamon-Rooke, N., Lallemant, S., Noomen, R., Veis, G., 1995. Geodetic determination of the kinematics of Central Greece with respect to Europe: implications for eastern Mediterranean tectonics. J. Geophys. Res. 100, 12675–12690.

Le Quellec, P., Mascle, J., Got, H., Vittori, J., 1980. Seismic structure of Southwestern peloponnesus continental mar- gin. Am. Assoc. Petr. Geol. Bull. 64 (2), 242–263.

Leite, O., Mascle, J., 1982. Geological structures on the south Cretan continental margin and Hellenic trench (eastern Mediterranean). Mar. Geol. 49, 199–223.

Louvari, E., Kiratzi, A.A., Papazachos, B.C., 1999. The Cephalonia transform fault and its extension to western Lefkada Island (Greece). Tectonophysics 308 (1–2), 223–236.

Lyberis, N., 1984. Tectonic evolution of the north Aegean trough. In: The Geological Evolution of the Eastern Med- iterranean. 17, Spec. Publ. Geol. Soc., pp. 709–725

Lyberis, N., Angelier, J., Huchon, P., Le Pichon, X., Renard, V., 1981. La mer de Crete: Extension et subsidence. Proceedings, HEAT symposium. Vol. 1, pp. 364–382. Athens 1981.

Lyberis, N., Angelier, J., Barriert, E., Lallemant, S., 1982. Active deformation of a segment of arc: the strait of Kythera, Hellenic arc, Greece. J. Struct. Geol. 4 (3), 299–311.

Lykousis, V., Anagnostou, C., Pavlakis, P., Rousakis, G., Alexandri, M., 1995. Quaternary sedimentary history and neotectonic evolution of the eastern part of the central Aegean Sea, Greece. Mar. Geol. 128, 59–71.

Lyon-Caen, H., Armijo, R., Barrier, E., Lallemant, S., 1982. Active deformation of a segment of arc: the

strait of Ky- thera, Hellenic arc. Greece. J. Struct. Geol. 4, 299–311.

Lyon-Caen, H., Armijo, R., Drakopoulos, J., Baskoutas, J., Delibasis, N., Gaulon, R., Kouskouna, V., Latoussakis, J., Makropoulos, N., Papadimitriou, P., Papanastasiou, D., Pedotti, G., 1988. The 1986 Kalamata (South Peloponne- sus) earthquake: detailed study of a normal fault, evidences for east-west extension in the Hellenic arc. J. Geophys. Res. 93, 14967–15000.

Mann, P., 2007. Global catalogue, classification, and tectonic origin of restraining- and releasing bends on active and ancient strike-slip fault systems. In: Cunningham, W.D., Mann, P. (Eds.), Tectonics of Strike-Slip Restraining and Releasing Bends. 290. Geological Society Lond., Special Publications, pp. 13–142.

Mann, P., Hempton, M.R., Bradley, D.C., Burke, K., 1983. Development of pull-apart basins. J. Geol. 91, 529–554. Mascle, J., Le Quellec, P., 1980. The Matapan trench (Ionian Sea): example of trench disorganization? Geology 8, 77–88. Mascle, J., Martin, L., 1990. Shallow structure and recent evolution of the Aegean Sea: a synthesis based on continuous reflection profiles. Mar. Geol. 94, 271–299.

Mascle, J., Jongsma, D., Campredon, R., Dercourt, J., Glacon, G., Lecleach, A., Lyberis, N., Malod, J.A., Mitropoulos, D., 1982. The Hellenic margin from eastern Crete to Rhodes: preliminary results. Tectonophysics 86, 133–147.

Mascle, J., Le Cleach, A., Jongsma, D., 1986. The eastern Hellenic margin from Crete to Rhodes: example of progres- sive collision. Mar. Geol. 73, 145–168.

Mascle, J., Huguen, C., Benkhelil, J., Chamot-Rooke, N., Chaumillon, E., Foucher, J.-P., Griboulard, R., Kopf, A., Lamarche, G., Volkonskaia, A., Woodside, J., Zitter, T., 1999. Images may show start of European-African plate collision. EOS Trans. AGU 80, 421–428.

McClusky, S., Balassanian, S., Barka, A., Demir, C., Ergintav, S., Georgiev, I., Gurkan, O., Hamburger, M., Hurst, K., Kahle, H., Kastens, K., Kekelidze, G., King, R., Kotzev, V., Lenk, O., Mahmoud, S., Mishin, A., Nadariya, M., Ouzounis, A., Paradissis, D., Peter, Y., Prilepin, M., Reilinger, R., Sanli, I., Seeger, H., Tealeb, A., Toks€oz, M.N., Veis, G., 2000. Global positioning system constraints on plate kinematics and dynamics in the eastern Mediterra- nean and Caucasus. J. Geophys. Res. 105, 5695–5719.

McClusky, S., Reilinger, R., Mahmoud, S., Ben Sari, D., Tealeb, A., 2003. GPS constraints on Africa (Nubia) and Arabia plate motion. Geophys. J. Int. 155, 126–138.

McKenzie, D., 1970. Plate tectonics of the Mediterranean region. Nature 226, 239–248. McKenzie, D., 1972. Active tectonics of the Mediterranean region. Geophys. J. Roy. Astr. Soc. 30, 109–185. McKenzie, D.P., 1978. Active tectonics of the alpine Himalayan Belt, the Aegean Sea and surrounding regions. Geophys. J. Roy. Astr. Soc. 55, 217–252.

McKenzie, D., Jackson, J., 1986. A block model of distributed deformation by faulting. J. Geol. Soc. Lond. 143, 349–353. Meier, T., Rische, M., Endrun, B., Vafidis, A., Harjes, H.-P., 2004. Seismicity of the Hellenic subduction zone in the area of western and Central Crete observed by temporary local seismic networks. Tectonophysics 383, 149–169.

Melis, N.S., Stavrakakis, G.N., Zahradnik, J., 2001. A study of the focal properties of the Skyros earthquake (MW¼ 6.5/July 26, 2001), Aegean Sea. Greece Orfeus Newslett. 3, 11.

Mercier, J.L., Carey, E., Philip, H., Sorel, D., 1976. La ne`otectonique plio-quaternaire de l'arc ?eg?een externe et de la mer ?eg?ee et ses relations avec la seismicit?e. Bull. Soc. G?eol. Fr. 18 (2), 355–372.

Mercier, J.-L., Sorel, D., Simeakis, K., 1987. Change in the state of stress in the overriding plate of a subduction zone: the Aegean arc from the Pliocene to the present. Annales Tectonicae 1, 20–39.

Mercier, J.-L., Sorel, D., Vergely, P., Simeakis, K., 1989. Extensional tectonic regimes in the Aegean basins during the Cenozoic. Basin Res. 2, 49–71. https://doi.org/10.1111/j.1365-2117.1989.tb00026.x.

Müller, M.D., Geiger, A., Kahle, H.-G., Veis, G., Billiris, H., Paradissis, D., Felekis, S., 2013. Velocity and deformation fields in the north Aegean domain, Greece, and implications for fault kinematics, derived from GPS data 1993–2009. Tectonophysics 597–598, 34–49.

Needham, H.D., Le Pichon, X., Melguen, M., Pautot, G., Renard, V., Avedik, F., Carre, D., 1973. North Aegean Sea trough: 1972 Jean Charcot cruise. Bull. Geol. Soc. Greece 10, 152–153.

Nomikou, P., Papanikolaou, D., 2011. Extension of active fault zones on Nisyros volcano across the Yali-Nisyros Channel based on onshore and offshore data. Mar. Geophys. Res. https://doi.org/10.1007/s11001-011-9119-z.

Nomikou, P., Hübscher, C., Ruhnau, M., bejelou, K., 2016. Tectono-stratigraphic evolution through successive exten- sional events of the Anydros Basin, hosting Kolumbo volcanic field at the Aegean Sea, Greece. Tectonophysics 671, 202–217.

Nomikou, P., H€ubscher, C., Papanikolaou, D., Farangitakis, G.P., Ruhnau, M., Lampridou, D., 2018. Expanding ex- tension, subsidence and lateral segmentation within the Santorini—amorgos basins during quaternary: implica- tions for the 1956 Amorgos events, central—south Aegean Sea, Greece. Tectonophysics 722, 138–153.

Noomen, R., Ambrosius, B.A.C., Wakker, K.F., 1993. Crustal motions in the Mediterranean region determined from Laser Ranging to LAGEOS. In: Smith, D.E., Turcotte, D.L. (Eds.), Contributions of Space Geodesy to Geodynamics : Crustal Dynamics. AGU, Washington, DC, pp. 331–346.

Nyst, M., Thatcher, W., 2004. New constraints on the active tectonic deformation of the Aegean. J. Geophys. Res. 109 (B11406), 2004. https://doi.org/10.1029/2003JB002830.

Ocakoglu, N., Demirbag, E., Kuşçu, I., 2004. Neotectonic structures in the area offshore of Alacati, Doganbey and Kusadasi (western Turkey): evidence of strike-slip faulting in the Aegean extensional province. Tectonophysics 391, 67–83.

Ocakoğlu, N., Demirbag, E., Kuşçu, I., 2005. Neotectonic structures in Izmir gulf and surrounding regions (western Turkey): evidences of strike-slip faulting with compression in the Aegean extensional regime. Mar. Geol. 219, 155–171.

Ocakoğlu, N., Nomikou, P., Işcan, Y., Loreto, M.F., Lampridou, D., 2018. Evidence of extensional and strike-slip de- formation in the offshore G€okova-Kos area affected by the July 2017 Mw6.6 Bodrum-Kos earthquake, eastern Ae- gean Sea. Geo-Mar. Lett. https://doi.org/10.1007/s00367-017-0532-4. published online 11 Jan. 2018.

Okal, E.A., Synolakis, C.E., Uslu, B., Kalligeris, N., Voukouvalas, E., 2009. The 1956 earthquake and tsunami in Amorgos, Greece. Geophys. J. Int. 178, 1533–1554.

Özbakır, A.D., Şeng€or, A.M.C., Wortel, M.J.R., Govers, R., 2013. The Pliny–Strabo trench region: a large

shear zone resulting from slab tearing. Earth Planet. Sci. Lett. 375, 188–195. Papadimitriou, P., Kapetanidis, V., Karakonstantis, A., Kaviris, G., Voulgaris, N., Makropoulos, K., 2015. The Santorini volcanic complex: a detailed multi-parameter seismological approach with emphasis on the 2011–2012 unrest period. J. Geodyn. 85, 32–57.

Papanikolaou, D.J., Royden, L.H., 2007. Disruption of the Hellenic arc: late Miocene extensional detachment faults and steep Pliocene-quaternary normal faults—or what happened at Corinth? Tectonics 26, TC5003. https:// doi.org/10.1029/2006TC002007.

Papanikolaou, D., Lykousis, V., Chronis, G., Pavlakis, P., 1988. A comparative study of neotectonic basins across the Hellenic arc: the Messiniakos, Argolikos, Saronikos and southern Evoikos gulfs. Basin Res. 1, 167–176.

Papanikolaou, D., Alexandri, M., Nomikou, P., Ballas, D., 2002. Morphotectonic structure of the western part of the north Aegean Basin based on swath bathymetry. Mar. Geol. 190, 465–492.

Papanikolaou, D., Alexandri, M., Nomikou, P., 2006. Active faulting in the north Aegean basin. Geol. Soc. America, Sp Paper 409, 189–209. https://doi.org/10.1130/2006.2409(11).

Papanikolaou, D., Nomikou, P., Livanos, I., Papantoniou, G., Rousakis, G., Lampridou, D., 2015. Oblique opening of Skyros Basin in the North Aegean Sea, based on Morphotectonic Analysis. Geoph. Res. 17, Abstracts. EGU2015–3465, EGU General Assembly 2015.

Papazachos, C.B., Kiratzi, A.A., 1996. A detailed study of active crustal in the Aegean and surrounding region, 1996. Tectonophysics 253, 129–153.

Papazachos, B.C., Panagiotopoulos, D.G., 1993. Normal faults associated with volcanic activity and deep rupture zones in the southern Aegean volcanic arc. Tectonophysics 220, 301–308.

Papazachos, B.C., Papadimitriou, E.E., Kiratzi, A.A., Papazachos, C.B., Louvari, E.K., 1998. Fault plane solutions in the Aegean Sea and the surrounding area and their tectonic implication. Boll. Geofis. Teor. Appl. 39, 199–218.

Pavlides, S., Tranos, M., 1991. Structural characteristics of two strong earthquakes in the north Aegean: Ierissos (1932) and AgiosEfstratios (1968). J. Struct. Geol. 13, 205–214.

Pavlides, S., Mountrakis, D., Kilias, A., Tranos, M., 1990. The role of strike–slip movements in the extensional area of northern Aegean (Greece). A case of transtensional tectonics. Annales Tectonicae 4, 196–211.

Pe-Piper, G., Piper, D.J.W., 2005. The south Aegean active volcanic arc: relationships between magmatism and tec- tonics. Dev. Volcanol. 7, 113–133.

Pe-Piper, G., Piper, D.J.W., Perissoratis, C., 2005. Neotectonics and the Kos plateau tuff eruption of 161 ka, south Ae- gean arc. J. Volcanol. Geotherm. Res. 139, 315–338.

Perissoratis, C., Papadopoulos, G.A., 1999. Sediment instability and slumping in the southern Aegean Sea and the case history of the 1956 tsunami. Mar. Geol. 161, 287–305.

Perouse, E., Chamot-Rooke, N., Rabaute, A., Briole, P., Jouanne, F., Georgiev, I., Dimitrov, D., 2012. Bridging onshore and offshore present-day kinematics of central and eastern Mediterranean: Implications for crustal dynamics and mantle flow, Geochem. Geophys. Geosyst. 13, Q09013. https://doi.org/10.1029/2012gc004289.

Piper, D.J.W., Perissoratis, C., 2003. Quaternary neotectonics of the south Aegean arc. Mar. Geol. 198, 259–288. Piper, D.J.W., Pe-Piper, G., Perissoratis, C., Anastasakis, G., 2007. Distribution and chronology of submarine volcanic rocks around Santorini and their relationship to faulting. Geol. Soc. Lond., Spec. Publ. 291, 99–111.

Reilinger, R.E., McClusky, S.C., Oral, M.B., King, R.W., Toksoz, M.N., Barka, A.A., Kinik, I., Lenk, O., Sanli, I., 1997. Global positioning system measurements of present-day crustal movements in the Arabia-Africa-Eurasia plate collision zone. J. Geophys. Res. 102, 9983–9999.

Reilinger, R., McClusky, S., Vernant, P., Lawrence, S., Ergintav, S., Cakmak, R., Ozener, H., Kadirov, F., Guliev, I., Stepanyan, R., Nadariya, M., Hahubia, G., Mahmoud, S., Sakr, K., ArRajehi, A., Paradissis, D., Al-Aydrus, A., Prilepin, M., Guseva, T., Evren, E., Dmitrotsa, A., Filikov, S.V., Gomez, F., Al-Ghazzi, R., Karam, G., 2006. GPS constraints on continental deformation in the Africa–Arabia–Eurasia continental collision zone and implications for the dynamics of plate interactions. J. Geophys. Res. BO5411. doi:https://doi.org/10.1029/2005JB004051.

Reilinger, R., McClusky, S., Paradissis, D., Ergintav, S., Vernant, P., 2010. Geodetic constraints on the tectonic evolu- tion of the Aegean region and strain accumulation along the Hellenic subduction zone. Tectonophysics 488, 22–30.

Riedel, W., 1929. Zur Mechanik geologischer Brucherscheinungen. Zentralblatt f€ur Mineralogie, Geologie und Paleontologie 1929B, 354–368.

Rossi, S., Got, H., Taviani, M., Martin, L., 1986. Elements structuraux de la mer de Crete orientale et du Golfe d'An- talya (Mediterranee orientale). Mem. Soc. Geol. It. 36, 153–164.

Roussos, N., 1993. Geological map of Greece, Lemnos Island sheet. Inst. Geol. Mineral Exploration Greece, scale 1, 50.000.

Roussos, N., Lyssimachou, T., 1991. Structure of the central north Aegean trough: an active strike-slip deformation zone. Basin Res. 3, 39–48.

Royden, L.H., 1993. The tectonic expression slab pull at continental convergent boundaries. Tectonics 12, 629–638. Royden, L.H., Papanikolaou, D.J., 2011. Slab segmentation and late Cenozoic disruption of the Hellenic arc. Geochem. Geophys. Geosyst. 12, Q03010. https://doi.org/10.1029/2010GC003280.

Sachpazi, M., Hirn, A., Clement, C., Haslinger, F., Laigle, M., Kissling, E., Charvis, P., Hello, Y., Lepine, J.-C., Sapin, M., Ansorge, J., 2000. Western Hellenic subduction and Cephalonia transform: local earthquakes and plate transport and strain. Tectonophysics 319, 301–319.

Sachpazi, M., Laigle, M., Charalampakis, M., Diaz, J., Kissling, E., Gesret, A., Becel, A., Flueh, E., Miles, P., Hirn, A., 2016a. Segmented Hellenic slab rollback driving Aegean deformation and seismicity. Geophys. Res. Lett. 43. https://doi.org/10.1002/2015GL066818.

Sachpazi, M., Laigle, M., Charalampakis, M., Sakellariou, D., Flueh, E., Sokos, E., Daskalaki, E., Galvé, A., Petrou, P., Hirn, A., 2016b. Slab segmentation controls the interplate slip motion in the SW Hellenic subduction: new insight from the 2008 Mw 6.8 Methoni interplate earthquake. Geophys. Res. Lett. 43. https://doi.org/ 10.1002/2016GL070447.

Sakellariou, D., Tsampouraki-Kraounaki, K., 2016. Offshore faulting in the Aegean Sea: a synthesis based on bathy- metric and seismic profiling data. Bull. Geol. Soc. Greece L (1), 124–133.

Sakellariou, D., Rousakis, G., Kaberi, H., Kapsimalis, V., Georgiou, P., Kanellopoulos, T., Lykousis, V., 2007. Tectono- sedimentary structure and late quaternary evolution of the north Evia gulf basin, Central Greece: preliminary re- sults. Bull. Geol. Soc. Greece XXXVII (1), 451–462.

Sakellariou, D., Sigurdsson, H., Alexandri, M., Carey, S., Rousakis, G., Nomikou, P., Georgiou, P., Ballas, D., 2010. Active tectonics in the Hellenic volcanic arc: the Kolumbo submarine volcanic zone. Bull. Geol. Soci. Greece XLIII (2), 1056–1063.

Sakellariou, D., Mascle, J., Lykousis, V., 2013. Strike slip tectonics and transtensional deformation in the Aegean Re- gion and the Hellenic Arc: preliminary results. Bul. Geol. Soc. Greece XLVII (2), 647–656.

Sakellariou, D., Rousakis, G., Vougioukalakis, G., Ioakim, C., Panagiotopoulos, I., Morfis, I., Zimianitis, E., Athanasoulis, K., Tsampouraki-Kraounaki, K., Mpardis, D., Karageorgis, A.P., 2016. Deformation pattern in the western North Aegean trough: preliminary results. Bull. Geol. Soc. Greece L (1), 134–143.

Sengör, A.M.C., 1979. The north Anatolian transform fault: Its age, offset and tectonic significance. J. Geol. Soc. Lond. 136, 269–282.

Shaw, B., Jackson, J.A., 2010. Earthquake mechanisms and active tectonics of the Hellenic subduction zone. Geophys. J. Int. 181 (2), 966–984.

Straub, C., Kahle, H.G., 1994. Global positioning estimates of crustal deformation in the Marmara Sea region, north- western Anatolia, earth planet. Sci. Lett. 121, 495–502.

Tapponnier, P., 1977. Evolution tectonique du systéme alpin en méditerranée: poinconnement et écrasement rigide-plastique Bull. Soc. Géol. Fr., 19, 437-460.

Taymaz, T., Jackson, J., Westaway, R., 1990. Earthquake mechanisms in the Hellenic trench near Crete. Geophys. J. Int. 102, 695–731.

Taymaz, T., Jackson, J., McKenzie, D., 1991. Active tectonics of the north and central Aegean Sea. Geophys. J. Int. 106, 433–490.

Tchalenko, J.S., 1970. Similarities between shear zones of different magnitudes. Bull. Geol. Soc. Am. 81, 1625–1639.

Ten Veen, J.H., Kleinspehn, K.L., 2002. Geodynamics along an increasingly curved convergent plate margin: late Miocene-Pleistocene Rhodes, Greece. Tectonics 21(3). https://doi.org/10.1029/2001TC001287.

Ten Veen, J.H., Kleinspehn, K.L., 2003. Incipient continental collision and plate-boundary curvature: Late Pliocene– Holocene transtensional Hellenic forearc, Crete, Greece. J. Geol. Soc. London 160, 161–181.

Ten Veen, J.H., Meijer, P.T., 1998. Late Miocene to recent tectonic evolution of Crete (Greece): geological observations and model analysis. Tectonophysics 298, 191–208.

Tibaldi, A., Pasquare, F.A., Papanikolaou, D., Nomikou, P., 2008. Tectonics of Nisyros Island, Greece, by field and offshore data, and analogue modeling. J. Struct. Geol. 30, 1489–1506.

Tranos, M.D., 2009. Faulting of Lemnos Island; a mirror of faulting of the north Aegean trough (northern Greece). Tectonophysics 467, 72–88.

Tsampouraki-Kraounaki, K., Sakellariou, D., 2017. Strike-slip deformation behind the Hellenic

subduction: The Amorgos shear zone, south Aegean Sea. In: Clark, K.J., Upton, P., Langridge, R., Kelly, K., Hammond, K. (Eds.), Proceedings of the 8th International INQUA Meeting on Paleoseismology, Active Tectonics and Archeoseismology.In: GNS Science (GNS Science miscellaneous series 110), pp. 392–395. https://doi.org/ 10.21420/G2H061.

Tsampouraki-Kraounaki, K., Sakellariou, D., 2018. Seismic stratigraphy and geodynamic evolution of Christiana Ba- sin. South Aegean Arc. Mar. Geology 399, 135–147.

Tur, H., Yaltirak, C., Elitez, I., Sarikavak, K.T., 2015. Pliocene–quaternary tectonic evolution of the Gulf of G€okova, Southwest Turkey. Tectonophysics 638, 158–176.

Uluğ , A., Duman, M., Ersoy, Ş., Özel, E., Avcı, M., 2005. Late Quaternary Sea-level change, sedimentation and neotectonics of the Gulf of G€okova: southeastern Aegean Sea. Mar. Geol. 221, 381–395.

Uzel, B., Sozbilir, H., Ozkaymak, C., Kaymakcı, N., Langereis, C.G., 2013. Structural evidence for strike-slip deforma- tion in the Izmir–Balıkesir transfer zone and consequences for late Cenozoic evolution of western Anatolia (Turkey). J. Geodyn. 65, 94–116.

van Hinsbergen, D.J.J., Meulenkamp, J.E., 2006. Neogene supradetachment basin development on Crete (Greece) dur- ing exhumation of the south Aegean core complex. Basin Res. 18, 103–124 (2006).

van Hinsbergen, D.J.J., van der Meer, D.G., Zachariasse, W.J., Meulenkamp, J.E., 2006. Deformation of western Greece during Neogene clockwise rotation and collision with Apulia. Int. J. Earth Sci. 95 (3), 463–490.

Wardell, N., Camera, L., Mascle, J., Nicolich, R., Marchi, M., Barison, E., 2014. The structural framework of the Pel- oponnese continental margin from Zakynthos to Pylos from seismic reflection and morpho-bathymetric data. B. Geofis. Teor. Appl. 55 (2), 343–367.

Withjack, M.O., Jamison, W.R., 1986. Deformation produced by oblique rifting. Tectonophysics 126, 99–124. Yaltirak, C., Alpar, B., 2002. Kinematics and evolution of the northern branch of the north Anatolian fault (Ganos fault) between the sea of Marmara and the Gulf of Saros. Mar. Geol. 190, 351–366.

Yaltırak, C., Alpar, B., Yűce, H., 1998. Tectonic elements controlling the evolution of the Gulf of Saros (northeastern Aegean Sea, Turkey). Tectonophysics 300, 227–248.

Yaltırak, C., Işler, E.B., Aksu, A.E., Hiscott, R.N., 2012. Evolution of the Bababurnu Basin and shelf of the Biga pen- insula: western extension of the middle strand of the north Anatolian fault zone, northeast Aegean Sea. Turkey. J. Asian Earth Sci. 57, 103–119.

Yolsal- Çevikbilen, S., Taymaz, T., Helvacı, C., 2014. Earthquake mechanisms in the gulfs of G€okova, Sıgˇacık, Kuşadası, and the Simav region (western Turkey): neotectonics, seismotectonics and geodynamic implications. Tectonophysics 635, 100–124.

Zachariasse, W.J., van Hinsbergen, D.J.J., Fortuin, A.R., 2008. Mass wasting and uplift on Crete and Karpathos during the early Pliocene related to initiation of south Aegean left-lateral, strike-slip tectonics. GSA Bull. 120 (7/8), 976–993. https://doi.org/10.1130/B26175.1.

5. Conclusions-Discussion

The conclusions arising from this study, confirm the complicated pattern of deformation governing not only the southern Aegean but the entire Aegean as a whole. The main results that emerged from the three published papers are presented in detail in subchapters **4.1.7**, **4.2.7** and **4.3.7**. This chapter is an attempt to summarize and synthesize these results as well as to highlight the hitherto unanswered questions concerning the kinematics and deformation of the Aegean.

The seismic stratigraphy of Christiana has been compared with the seismic stratigraphy of the neighboring Myrtoon Basin as presented by Anastasakis and Piper (2005) to enable a chronostratigraphic approach to the basin's sedimentary processes. Plio-Quaternary sediments constitute the Christiana Basin's infill. On the basin's margins the sedimentary formations overly the Messinian erosion surface, while in the basin, they have been deposited above the Messinian evaporites. A prominent dome observed in the central part of the basin has been interpreted as a probable salt dome intruding the lower part of the basin infill. Seven distinct seismic units have been recognized within the basin's infill. At least three thick, chaotic layers, with irregular morphology have been mapped on the eastern part of the basin and have been associated with volcanoclastic deposits derived from Santorini volcanic center. The youngest of them (deposit I) is associated with the Early Bronze Age (Minoan) eruption, while the next (deposit II) is slightly younger than 0,42 Ma and may be related to the Peristeria volcano. The lowest recognizable thick deposit (III) is the thickest and widest distributed pyroclastic flow deposit in the basin and most probably the biggest in the entire South Aegean. It has been deposited shortly after 1.2 Ma and may be linked with an eruption of the early volcanic centers of Akrotiri.

The structural analysis of Christiana Basin indicates that the post-Miocene evolution of the basin displays two main stages. During the early stage, subsidence of the three main depocenters in the NW, W and SE part of the basin has been controlled by E-W to ESE- WNW trending faults, with a significant horizontal component of movement. The end of the early stage is marked by the cessation of activity on the southern marginal fault and the migration of the northern faults towards the north where the basin expanded significantly towards the south and north. New deposits covered the old, southern tectonic margin and draped unconformably the Christiana Ridge which separates Christiana Basin from Cretan Basin to the south. The ridge has undergone

southward tilting as has been evidenced by the southward slopping of the top of the alpine basement and its sedimentary cover. The southern margin marks the transition from the early, fault-controlled basin boundary to the present, not faulted margin. The old northern margin has also been covered by new deposits while the present margin is located much closer to Folegandros and Sikinos Islands and trends WSW-ENE. The current picture of Christiana suggests that it continues to be at the second stage of development, while the first stage lasted until the Lower or Middle Pleistocene.

On the offshore area between Santorini and Amorgos Islands, the processing and the interpretation of swath bathymetry and seismic data, reveal the existence of seven morphological basins (Anydros, Anafi, Amorgos South, Amorgos North, Kinairos, Astypalea North and Astypalea South basins) and four ridges (Astypalea and Anydros ridges with their splays and Akrotiri and Anafi ridges). The basins display a spindle or elongate shape and trend NE-SW. Six distinct seismic units have been mapped within the sedimentary infill of the basins, while Astypalea and Anydros Ridges are covered by uplifted, tilted sediments of the lowermost parts of the neighboring basins. At least four major unconformities have been recognized in all basins suggesting that major tectonic events have affected the entire area. They are named from top to bottom as U1, U2, U3 and U4. The description and stratigraphic position of unconformities U1, U2 and U3 allow their correlation with UR3, UR2 and/or UA1 respectively of Piper and Perissoratis (2003) which led to a chronological estimation where U1 dated at 150-190 ka years, while U3 probably indicate the boundary between sediments of Pliocene and Quaternary age and is proposed here as equivalent to the Early Quaternary unconformity observed in DSDP hole 378 (Hsu et al., 1978).

The formation of the basins is mainly controlled by NE-SW trending, SE dipping faults and WNW-ESE to W-E trending, SSW-or S-dipping step-over faults. The basins display northward asymmetry, except Anydros and Astypalea South basins. The unconformity U3 marks the onset of enhanced tectonic activity along with the present, marginal faults which led to a significant northward tilting of the lower parts of the sedimentary infill of the basins and led to the uplift and formation of the ridges along the southern margins. Pop-up structures that have formed within the basins and on the ridges indicate deformation due to horizontal shearing.

The SASZ initiated as a single and E-W oriented single basin in the Early Pliocene, composed of the ancestors of Anafi, Amorgos South, Amorgos North and Kinairos basins. In the Early Quaternary it has been evolved into a more complex structure of seven elongated NE-SW trending basins, separated by shallow ridges. Unconformity U3 marks this transition which evolved further during Quaternary and led to the present geotectonic configuration of SASZ. It is proposed here that the deformation of the area has been controlled by dextral shearing and oblique rifting which is accommodated by NE-SW strike-slip to highly oblique faults and fault zones, running at a low angle with respect to the NNE-SSW oriented kinematic vectors, and by roughly W-E striking, normal, transfer faults. The dip-slip normal focal mechanism, modeled for the 9th of July, 1956 Amorgos earthquake, can be compatible with the dextral shearing kinematics of SASZ as it fits perfectly with the geometry and kinematic characteristics of the W-E striking Amorgos South Relay Fault (ASRF).

The focused research on the two neighboring areas of the South Aegean (Christiana Basin and SASZ) yielded a series of interesting observations and results. The observations of Perissoratis (1995) and Piper and Perissoratis (2003) on the change in the strike of the faults from E-W to NE-SW, during the Early Pleistocene, are in contrast with the result arising for Christiana Basin from the current dissertation. The direction of the marginal faults throughout its evolution in two stages remains constant. On the other hand, further east, in the area between Santorini, Amorgos and Astypalea Islands, there is a change in the morphology, where an initially E-W oriented, single basin, evolves into a more complex structure of SW-NE trending, multiple basins and ridges in Early Quaternary. The limited and sparse data do not allow a clear interpretation of why this is happening. This apparent discrepancy may be explained by various interpretations. The extensional kinematic regime, expressed by E-W trending faults during Pliocene, has been changed to a new kinematic pattern composed mainly of NE- SW oblique faulting during Early Quaternary. This change, which affected mainly the Santorini-Amorgos Shear Zone, may have reactivated Christiana Basin as an extensional structure at the termination of a dextral shear zone (a sort of horsetail structure) in its later stage of evolution. Another possible interpretation is related to the changes in curvature between the central, and the eastern and western parts of the Hellenic Arc. The Hellenic plate boundary has stepped southward and its curvature increased,

forcing plate convergence vectors to evolve with changes most strongly expressed along the easternmost and westernmost Hellenic subduction zone (Ten Veen and Kleinspehn, 2002 and references therein). This can be reflected in the different kinematic patterns that have been observed in the South Aegean, with rapidly evolving extensional areas and areas whose deformation is the result of a more complex and oblique displacement pattern.

The evolution of the area south of Amorgos from one single basin to a more complex structure of asymmetric basins seems to be chronologically related to the transition of Christiana basin from the first to the second stage of development. Unconformity U3, which is dated as an Early Quaternary unconformity and marks this change in the geodynamic configuration, is related to several major unconformities described by previous literature data for the entire South Aegean (Bartole et al., 1983; Mascle and Martin, 1990; Perissoratis, 1995; Piper and Perossoratis, 2003; Piper et al., 2007).

Bartole et al. (1983) suggested that the present-day morphology of the South Aegean is the result of very strong differential tectonic movements during the Early Quaternary. Figure 5.1 illustrates old, analog seismic profiles acquired by Bartole et al., (1983), from the western and central part of the South Aegean. The reflector Q has been mapped in the Iraklion Basin (Figure 3A of Bartole) and Akrotiri Basin (Figure 3B) and according to the authors corresponds to the Lower-Middle Quaternary unconformity found at the ODP site 378 (Hsu et al., 1978). They also mentioned that the Pliocene sediments filled mainly the basinal areas, while the structural highs were covered mostly by sediments of Quaternary age. The seismic character of the Q horizon and its geometrical relationship with the underlying and overlying seismic units coincides very well with the unconformity U3 in the Santorini-Amorgos area. This unconformity marks the onset of a new geodynamic regime where the N-S oriented extension accommodated by W-E normal faults changes to a more complicated pattern of transpression and transtension zones accommodated by NE- SW and NW-SE conjugate, strike-slip to oblique faulting and secondary W-E faults (see also Perissoratis, 1995; Piper and Perissoratis, 2003). This is in agreement with the observation of Briole et al. (2021) who recognized dextral transtensional movement of 4.5 mm yr^{-1}

between the Amorgos and Astypalea islands. All of the above, suggest that a major change during the Plio-Quaternary led to a complete reconstruction of several areas of the South Aegean Sea.

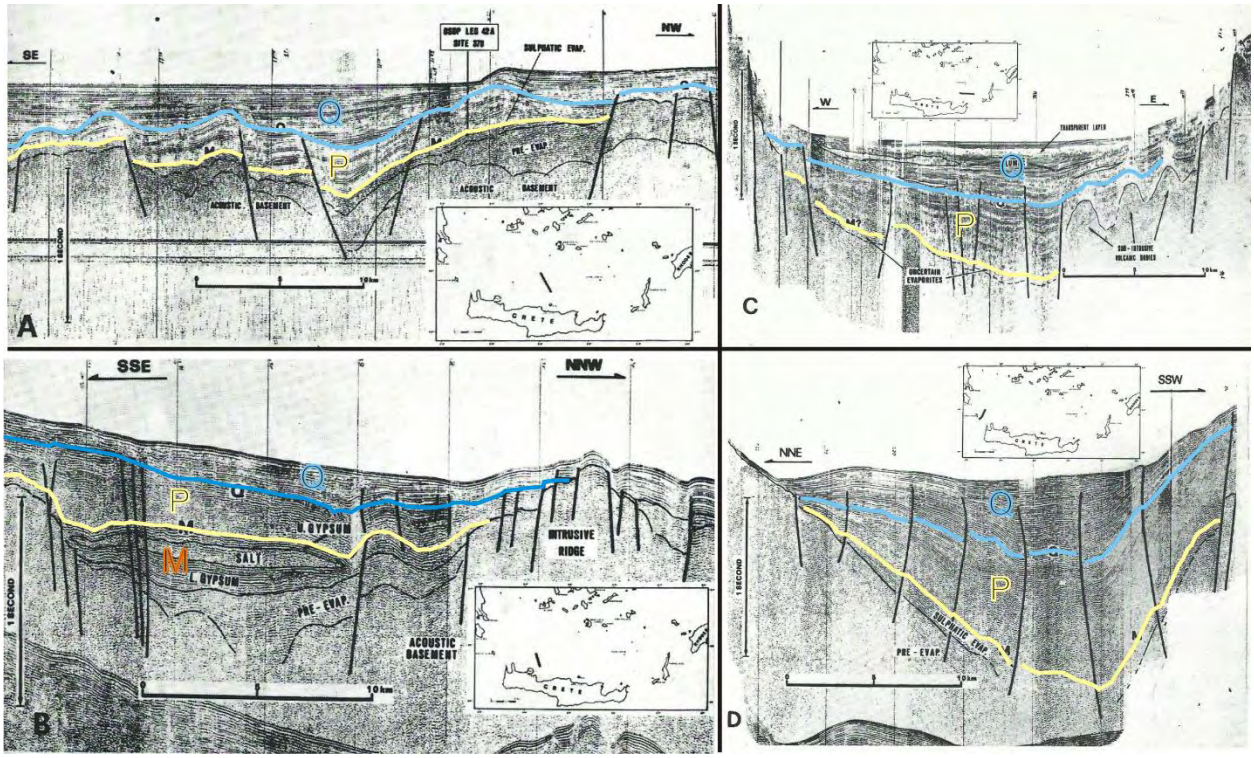

Figure 5.1: Seismic profiles acquired by Bartole et al. (1983). Q: Quaternary sediments, P: Pliocene sediments, M: Messinian evaporites

Interesting observations also emerged by the analysis of the offshore fault network and the offshore morphology, in combination with the re-evaluation of the results arise from the seismic interpretation and re-interpretation of old and new seismic profiles and previous literature data. Most of the morphological basins in the Aegean Sea, which are aligned in NE-SW to ENE-WSW and secondarily in NW-SE to WNW-ESE directions, coincide with the main Plio-Quaternary basins indicating that the present morphological configuration resulted from the geodynamic processes that have been active during the last 5 Ma. The spatial distribution of volcanos along the arc has been controlled mainly by active tectonic mechanisms. NE-trending faults control the NE-alligment of the volcanic features and the development of the volcanic centers has been associated with transtensional deformation (Kokkalas and Aydin, 2013). The Aegean crust flows to the SSW between its northern dextral boundary (defined by the Kefallonia Fault, the Central Hellenic Relay Zone and the North Anatolian Fault) and its sinistral southern boundary (defined

by Pliny and Strabo fault zone). Extensive shearing along NE-SW strike-slip zones in Plio-Quaternary replaces the Miocene, arc-perpendicular, back-arc extension. The complex pattern of the internal Aegean domain accommodates a complex pattern of localized transpressional and transtentional features and is resulted from the extensional deformation in combination with strike-slip tectonics.

The cause of these enlarged changes in the geodynamic configuration of the South Aegean Sea, around, is not yet clear. The complicated deformation pattern within the Aegean "microplate" has not been systematically described or is poorly understood. Many offshore areas in the Aegean are still not surveyed thus the questions on its intraplate deformation and kinematics remain largely unanswered. It is widely accepted that the propagation of the North Anatolian Fault in the North Aegean resulted in the geodynamic framework of the entire Aegean Sea. Armijo et al. (1996-1999) proposed that NAF propagated in the North Aegean in Late Miocene to Early Pliocene, at roughly 5 Ma BP. More recent studies propose that NAF may have arrived in the Aegean in the Early Pleistocene, at 2 Ma BP (Le Pichon et al., 2015), or Early to Middle Pleistocene (Beniest et al., 2016). The latter coincides largely with the observed changes in the geodynamic processes and on the morphological configuration of the South Aegean. This strongly indicates that the gradual propagation of the North Anatolian Fault in the North Aegean may trigger the Early Quaternary to present deformation.

6. Strategy Plan for Future Research

The processing and reprocessing of old and recent seismic profiles and swath bathymetry data, and the integration of previous literature data on the interpretation have contributed to the understanding of the geodynamic evolution of the South Aegean Sea. However, the analysis of the present-day kinematics requires a detailed geological study for the entire South Aegean. As mentioned in previous chapters, many areas are either unexplored or covered with poor quality, older or sparse, data. The detailed mapping of the offshore faulting and the geomorphological configuration is necessary to clearly define the geodynamic framework under which the deformation that governs the Aegean takes place.

Tectonic deformation governing the Aegean back-arc domain involves complex geodynamic processes. The results obtained from the current study deviate from the prevailing theory of Armijo et al. (1996) with the arc-parallel zones of extension. It is proposed here that the deforming Aegean flows towards SW, between the two plate boundaries of the dextral North Anatolian Fault and the sinistral Pliny and Strabo Fault Zone. The randomly distributed basins and ridges associated with NW-SE and NE-SW strike-slip to oblique faults and W-E or WNW-ESE to NW-SE normal faults indicate local zones of extension and transtension accommodated by strike-slip to oblique faults and by normal faults.

A thorough geological study of the Central and South Aegean could answer the long-standing questions on the deformation that prevails in back-arc areas. Very few studies have been conducted in the Central Aegean and their results provide information mainly for the local deformation processes. The systematic survey of this area which is considered until today as a rigid block can reveal very interesting observations about its internal deformation.

The available seismic data in the South Aegean Sea are mainly old, analog seismic profiles or single-channel profiles with limited coverage. It is crucial to improve our knowledge on the geological structure and the evolution of that area to understand the geodynamic framework and kinematics prevailing in the area. The Santorini-Amorgos Shear Zone constitutes the southernmost area in which dextral sense of motion is observed. South of that area the kinematics change from dextral to sinistral. The same area also coincides with the southeastern boundary of

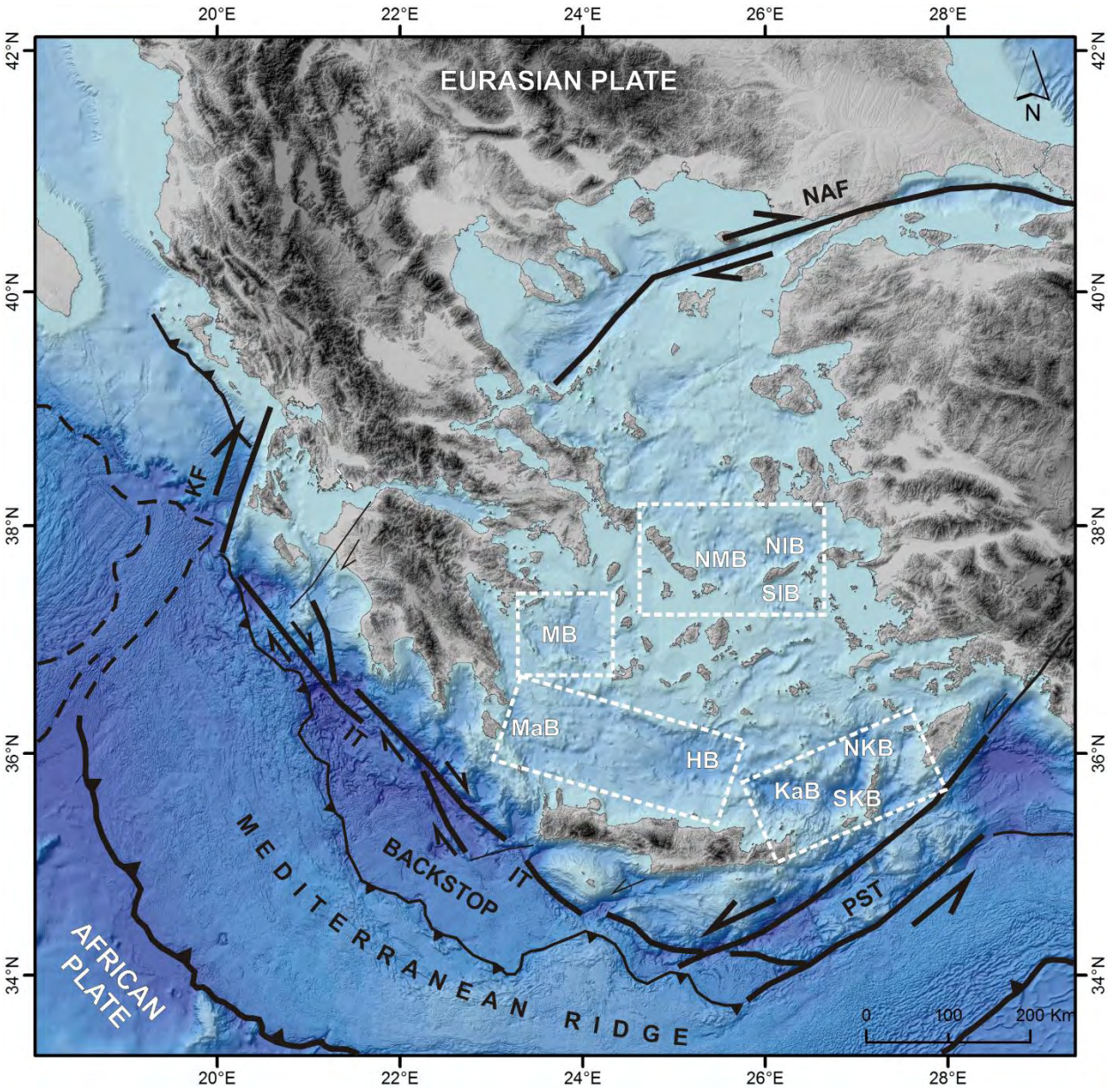

Figure 6.1. Bathymetric map of the Aegean. The white dotted squares illustrate areas for suggested future research. NIB: Borth Ikaria Basin, SIB: South Ikaria Basin, NMB: North Mykonos Bsin, MB: Myrtoon Basin, MaB: Maleas Basin, HB: Heraklion Basin, KaB: Kamilonissi Basin, NKB: North Karpathos Basin, SKB: South Karpathos Basin.

the Central Aegean Block, which displays little internal stretching as defined by Reilinger et al. (2010). What is changing in the geodynamic context and the Santorini-Amorgos Shear Zone illustrates the boundary between a dextral and a sinistral sense of movement? The geomorphological configuration and orientation of the major basins of the South Aegean (e.g. Maleas Basin, Heraklion Basin, Kamillonisi Basin, Karpathos basin e.t.c.) resulted only from extensional normal faulting mechanisms or includes a more complex mechanism of strike-slip to

oblique faulting? What is the correlation between the observed Plio-Quaternary unconformity and the overall deformation that affects the entire Aegean? Is the change in the faulting direction and which is expressed also and by this unconformity, related to the propagation of the North Anatolian Fault on the North Aegean?

The map in Figure 6.1: illustrates suggested areas for future research. Better coverage in swath bathymetry and digital seismic profiles acquired from these areas can contribute to the understanding of the geological background while leading to a better assessment of potential future geological hazards. In addition, the installation of a denser network of GPS stations in various Aegean islands could provide information for the smaller scale movements. The detailed mapping of the fault network and the geomorphological structures, as well as the systematic recording of the directions and velocities of the individual displacements, can provide answers to hitherto unanswered questions about the evolution and the style of deformation of the Aegean domain.

References

Anastasakis, G., Piper, D.J.W., 2005. Late Neogene evolution of the western South Aegean volcanic arc: sedimentary imprint of volcanicity around Milos. Mar. Geol. 215, 135–158.

Angelier, J., Lybeeris, N., Le Pichon, X., Barrier, E., Huchon, P., 1982. The tectonic development of the Hellenic arc and the sea of Crete: a synthesis. Tectonophysics 86, 159–196.

Armijo, R., Meyer, B., King, G.C.P., Rigo, A., Papanastassiou, D., 1996. Quaternary evolution of the Corinth rift and its implications for the late Cenozoic evolution of the Aegean. Geophys. J. Int. 126, 11–53. Armijo, R., Meyer, B., Hubert, A., Barka, A., 1999. Westward propagation of the north Anatolian into the northern Aegean: timing and kinematics. Geology 27 (3), 267–270.

Armijo, R., Meyer, B., Hubert, A., Barka, A., 1999. Westward propagation of the north Anatolian into the northern Aegean: timing and kinematics. Geology 27 (3), 267–270.

Bartole, R., Catani, G., Lenardon, G., Vinci, A., 1983. Tectonics and sedimentation of the southern Aegean Sea. Boll. Oceanol. Teor. App. 1, 319–340.

Beniest, A., Brun, J.P., Gorini, C., Crombez, V., Deschamps, R., Hamon, Y., Smit, J., 2016. Interaction between trench retreat and Anatolian escape as recorded by neogene basins in the northern Aegean Sea. Mar. Pet. Geol. 77, 30–42.

Billiris, H., Paradisis, D., Veis, G., England, P., Featherstone, W., Parsons, B., Cross, P., Rands, P., Rayson, M., Sellers, P., Ashkenazi, V., Davison, M., Jackson, J., Ambraseys, N., 1991. Geodetic determination of tectonic de- formation in Central Greece from 1900 to 1988. Nature 350, 124–129.

Bonev N, Burg JP, Ivanov Z (2006) Mesozoic-tertiary structural evolution of an extensional gneiss dome—the Kesebir-Kardamos dome, eastern Rhodope (Bulgaria, Greece). Int J Earth Sci 95:318–340. doi:10.1007/s00531-005-0025-y

Briole, P., Rigo, A., Lyon-Caen, H., Ruegg, J.C., Papazissi, K., Mitsakaki, C., Balodimou, A., Veis, G., Hatzfeld, D., Deschamps, A., 2000. Active deformation of the Corinth rift, Greece: results from repeated Global Positioning Sys- tem surveys between 1990 and 1995. J. Geophys. Res. 105, 25 605–25 625.

Brun JP, Sokoutis D (2007) Kinematics of the Southern Rhodope Core Complex (North Greece). Int J Earth Sci doi: 10.1007/s00531-007-0174-2

Brun, J.-P., and Sokoutis, D. 2010. 45 m.y. ofAegean crust and mantle flow driven by trench retreat. Geology, 38: 815–818. doi:10.1130/G30950.1.

Brun, J.-P., Gueydan, F., Kydonakis, K., Philippon, M., Sokoutis, D., Beniest, A., Gorini, C., 2015. The two-stage Aegean extension, slow-localized vs fast- distributed. In: European Geoscience Union General Assembly 2015.

Brun, J.-P., Faccenna, C., Gueydan, F., Sokoutis, D., Philippon, M., Kydonakis, K., Gorini, C., 2016. The two-stage Aegean extension, from localized to distributed, a result of slab rollback acceleration. Can. J. Earth Sci. 53 (999), 1e16.

Burchfiel BC, Nakov R, Tzankov T (2003) Evidence from the Mesta half-graben, SW Bulgaria, for the Late Eocene beginning of Aegean extension in the Central Balkan Peninsula. Tectono- physics 375:61–76. doi:10.1016/j.tecto.2003.09.001

Caputo, M., Panza, G.F. and Postpischl, D., 1970. Deep structure of the Mediterranean Basin. J. Geophys. Res., 75: 4919-4923.

Clarke, P.J., Davies, R.R., England, P.C., Parsons, B., Billiris, H., Paradissis, D., Veis, G., Cross, P.A., Denys, P.H., Ashkenazi, V., Bingley, R., Kahle, H.-G., Muller, M.-V., Briole, P., 1998. Crustal strain in Central Greece from re- peated GPS measurements in the interval 1989–1997. Geophys. J. Int. 135, 195–214.

Cocard, M., Kahle, H.G., Peter, Y., Geiger, A., Veis, G., Felekis, S., Paradissis, D., Billiris, H., 1999. New constraints on the rapid crustal motion of the Aegean region: recent results inferred from GPS measurements (1993–1998) across the west Hellenic arc, Greece. Earth Planet. Sci. Lett. 172, 39–47.

Davies, R., England, P., Parsons, B., Biliris, H., Paradissis, D., Veis, G., 1997. Geodetic strain of Greece in the interval 1892–1992. J. Geophys. Res. 102, 24 571–24 588.

Dewey, J.F., and Sengör, A.C. 1979. Aegean and surrounding regions: complex mul- tiplate and continuum tectonics in a convergent zone. Geological Society of America Bulletin, 90: 84–92. doi:10.1130/0016-7606(1979)90%3C84:AASRCM% 3E2.0.CO;2.

Fytikas M, Innocenti F, Manetti P, Mazzuoli R, Peccerillo A, Villari L (1984) Tertiary to Quaternary evolution of volcanism in the Aegean region. In: Dixon EJ, Robertson AHF (eds) The geological evolution of the Eastern Mediterranean. Geol. Soc. Spec. Pb., vol 17. Geological Society, London, pp 687–699

Gautier P., J.-P. Brun, R. Moriceau, D. Sokoutis, J. Martinod, and L. Jolivet (1999), Timing, kinematics and cause of Aegean extension: a scenario based on a comparison with simple analogue experiments, Tectonophysics, 315, 31–72.

Goldsworthy, M., Jackson, J., Haines, J., 2002. The continuity of active faults in Greece. Geophys. J. Int. 148, 596–618. Jackson, J., 1994. Active tectonics of the Aegean region. Annu. Rev. Earth Planet. Sci. 22, 239–271.

Jackson, J., 1994. Active tectonics of the Aegean region. Annu. Rev. Earth Planet. Sci. 22, 239–271.

Jackson, J., McKenzie, D., 1988. Rates of active deformation in the Aegean Sea and surrounding regions. Basin Res. 1, 121–128.

Jolivet, L., Brun, J.P., 2010. Cenozoic geodynamic evolution of the Aegean. Int. J. Earth Sci. 99, 109–138. https://doi.org/10.1007/s00531-008-0366-4.

Jolivet, L., Faccenna, C., Huet, B., Labrousse, L., Le Pourhiet, L., Lacombe, O., Lecomte, E., Burov, E., Dene`le, Y., Brun, J.P., Philippon, M., Paul, A., Sala€un, G., Karabulut, H., Piromallo, C., Moni?e, P., Gueydan, F., Okay, A.I., Oberh€ansli, R., Pourteau, A., Augier, R., Gadenne, L., Driussi, O., 2013. Aegean tectonics: strain localisation, slab tearing and trench retreat. Tectonophysics 597, 1–33. https://doi.org/10.1016/j.tecto.2012.06.011.

Jongsma, D., Wissman, G., Hinz, F., Garde, S., 1977. Seismic studies in the Cretan Sea. The southern Aegean Sea: an extensional marginal basin without sea floor spreading? Results of R.V. "Meteor" and R.R.S. "Shackleton" cruises. "Meteor" Forschungsergeb. Geol. Geophys., C 27, 3–30.

Kahle, H.G., Mueller, M.V., Geiger, A., Danuser, G., Mueller, S., Veis, G., Billiris, H., Paradissis, D., 1995. The strain field in NW Greece and the Ionian islands: results inferred from GPS measurements.

Tectonophysics 249, 41–52.

Kahle, H.-G., Cocard, M., Peter, Y., Geiger, A., Reilinger, R., Barka, A., Veis, G., 2000. GPS-derived strain rate field within the boundary zones of the Eurasian, African, and Arabian plates. J. geophys. Res. 105, 23 353–23 370.

Kárník, V.. 1972. A note on the morphology and activity of seismic zones in the Aegean region. Nature. 239: 72-73.

Kiratzi, A., Louvari, E., 2003. Focal mechanisms of shallow earthquakes in the Aegean Sea and the surrounding lands determined by waveform modelling: a new database. J. Geodyn. 36 (1–2), 251–274

Kokkalas, S., Xypolias, P., Koukouvelas, I., Doutsos, T., 2006. Postcollisional contractional and extensional deforma- tion in the Aegean region. In: Dilek, Y., Pavlides, S. (Eds.), Post-collisional tectonics and magmatism in the Med- iterranean region and Asia: geological Society of America Special Paper. 409, pp. 97–123. https://doi.org/ 10.1130/2006.2409(06).

Kokkalas, S., & Aydin, A., 2013. Is there a link between faulting and magmatism in the south-central Aegean Sea? *Geological Magazine*, *150*(2), 193–224. https://doi.org/10.1017/S0016756812000453

Kounov A, Seward D, Bernoulli D, Burg JP, Ivanov Z., 2004 Thermotectonic evolution of an extensional dome: the Cenozoic Osogvo-Lists core complex (Kraishte zone, western Bulgaria). Int J Earth Sci 93:1008–1024. doi:10.1007/s00531-00004- 00435-00532

Kreemer, C., Chamot-Rooke, N., 2004. Contemporary kinematics of the southern Aegean and the Mediterranean ridge. Geophys. J. Int. 157, 1377–1392.

Le Pichon, X., Angelier, J., 1979. The Hellenic arc and trench system: a key to the neotectonic evolution of the eastern Mediterranean area. Tectonophysics 60, 1–42.

Le Pichon, X., and Angelier, J. 1981. The Aegean Sea. Philosophical Transactions of the Royal Society, London, Series A, 300: 357–372.

Le Pichon, X., 1982. Land-Locked Oceanic Basins and Continental Collision: The Eastern Mediterranean as a Case Example. In: Hsu, K.J. (Ed.), Mountain Building Processes. San Diego, Academic Press, pp. 201–211.

Le Pichon, X., Chamon-Rooke, N., Lallemant, S., Noomen, R., Veis, G., 1995. Geodetic determination of the kinematics of Central Greece with respect to Europe: implications for eastern Mediterranean tectonics. J. Geophys. Res. 100, 12675–12690.

Lyberis, N., Angelier, J., Huchon, P., Le Pichon, X., Renard, V., 1981. La mer de Crete: Extension et subsidence.Pro- ceedings, HEAT symposium. Vol. 1, pp. 364–382. Athens 1981.

Lyberis, N., Angelier, J., Barriert, E., Lallemant, S., 1982. Active deformation of a segment of arc: the strait of Kythera, Hellenic arc, Greece. J. Struct. Geol. 4 (3), 299–311.

Lykousis, V., Anagnostou, C., Pavlakis, P., Rousakis, G., Alexandri, M., 1995. Quaternary sedimentary history and neotectonic evolution of the eastern part of the central Aegean Sea, Greece. Mar. Geol. 128, 59–71

Mascle, J., Martin, L., 1990. Shallow structure and recent evolution of the Aegean Sea: a synthesis based

on continuous reflection profiles. Mar. Geol. 94, 271–299.

McClusky, S., Balassanian, S., Barka, A., Demir, C., Georgiev, I., Hamburg, M., Hurst, K., Kahle, H., Kastens, K., Kekelidze, G., King, R., Kotzev, V., Lenk, O., Mahmoud, S., Mishin, A., Nadariya, M., Ouzounis, A., Paradissis, D., Peter, Y., Prilepin, M., Reilinger, R., Sanli, I., Seeger, H., Tealeb, A., Toksoz, M.N., Veis, G., 2000. Global Positioning System constraints on plate kinematics and dynamics in the eastern Mediterranean and Caucasus. J. Geophys. Res. 105, 5695–5720.

McKenzie, D., 1972. Active tectonics of the Mediterranean region. Geophys. J. R. Astr. Soc. 30, 109–185.

McKenzie, D., 1978. Active tectonics of the Alpine-Himalayan belt: the Aegean Sea and surrounding regions. Geo- phys. J. R. Astr. Soc. 55, 217–254.

McKenzie, D., Jackson, J., 1986. A block model of distributed deformation by faulting. J. Geol. Soc. Lond. 143, 349–353.

Nomikou, P., Papanikolaou, D., Alexandri, M., Sakellariou, D., Rousakis, G., 2013. Subma- rine volcanoes along the Aegean volcanic arc. Tectonophysics 597:123–146. http://dx.doi.org/10.1016/j.tecto.2012.10.001.

Noomen, R., Ambrosius, B.A.C., Wakker, K.F., 1993. Crustal motions in the Mediterranean region determined from Laser Ranging to LAGEOS. In: Smith, D.E., Turcotte, D.L. (Eds.), Contributions of Space Geodesy to Geodynamics : Crustal Dynamics. AGU, Washington, DC, pp. 331–346.

Nyst, M., Thatcher, W., 2004. New constraints on the active tectonic deformation of the Aegean. J. Geophys. Res. 109 (B11406), 2004. https://doi.org/10.1029/2003JB002830.

Papadopoulos. G.A.. 1982. Contribution to the study of the active deep tectonics of the Aegean and the surrounding areas. Sci. D. Thests. Univ. of Thessaloniki. 176 pp. (in Greek with Engl. abstr.).

Papadopoulos, G. A., Kondopoulou, D. P., Leventakis, G. A., Pavlides, S. B., 1986. Seismotectonics of the Aegean region, Tectonophysics, 124, 1–2,pp 67-84

Papadopoulos, G.A.; Pavlides, S.B., 1992. The large 1956 earthquake in the South Aegean: Macroseismic field configuration, faulting, and neotectonics of Amorgos Island. Earth Planet. Sci. Lett., 113, 383–396. [CrossRef]

Papazachos. B.C. and Comninakis. P.E.. 1969. Aftershock sequences and crustal structure in the region of Greece. Natl. Ohs.. Seismol. Inst.. Final Sci. Rep. June 1969.

Papazachos. B.C. and Comninakis. P.E.. 1971. Geophysical and tectonic features of the Aegean arc. J. Geophys.Res.. 76: 8517--8533.

Papazachos, C.B., Kiratzi, A.A., 1996. A detailed study of active crustal in the Aegean and surrounding region, 1996. Tectonophysics 253, 129–153.

Papazachos, B.C., Papadimitriou, E.E., Kiratzi, A.A., Papazachos, C.B., Louvari, E.K., 1998. Fault plane solutions in the Aegean Sea and the Athens surrounding area and their tectonic implication. Boll. Geof. Teor. App. 39, 199–218.

Papazachos, B.C., Papaioannou, C.A., Papazachos, C.B., Savvaidis, A.S., 1999. Rupture zones in the Aegean region. Tectonophysics 308, 205–221.

Pe-Piper G, Piper DJW (2002) The igneous rocks of Greece. The anatomy of an orogen, p 573, Gebru¨der

Borntraeger, Berlin

Pe-Piper G, Piper DJW (2006) Unique features of the Cenozoic igneous rocks of Greece. In: Dilek Y, Pavlides S (eds) Postcollisional tectonics and magmatism in the Mediterranean region and Asia, doi:210.1130/2006.2409(1114), Geological Society of America, pp 259–282

Pe-Piper G, Piper DJW (2007) Neogene back-arc volcanism of the Aegean: new insights into the relationship between magmatism and tectonics. In: Beccaluva L, Bianchini G (eds) Cenozoic volcanism in the Mediterranean area. doi:10.1130/2007. 2418(1102), Geological Society of America, pp 17–31

Perissoratis, C., 1995. The Santorini volcanic complex and its relation to the stratigraphy and structure of the Aegean arc, Greece. Mar. Geol., 128, 37–58. [CrossRef]

Perouse, E., Chamot-Rooke, N., Rabaute, A., Briole, P., Jouanne, F., Georgiev, I., Dimitrov, D., 2012. Bridging onshore and offshore present-day kinematics of central and eastern Mediterranean: Implications for crustal dynamics and mantle flow, Geochem. Geophys. Geosyst. 13, Q09013. https://doi.org/10.1029/2012gc004289.

Philippon, M., Brun, J.-P., Gueydan, F., and Sokoutis, D. 2014. The interaction between Aegean back-arc extension and Anatolia escape since Middle Mio- cene. Tectonophysics, 631: 176–188. doi:10.1016/j.tecto.2014.04.039.

Piper, D.; Perissoratis, C., 2003. Quaternary neotectonics of the South Aegean arc. Mar. Geol. , 198, 259–288.

Piper, D.J.W., Pe-Piper, G., Perissoratis, C., Anastasakis, G., 2007. Distribution and chronology of submarine volcanic rocks around Santorini and their relationship to faulting. Geol. Soc. Lond., Spec. Publ. 291, 99–111.

Ranguelov, B., 2005. A model of the Aegean geodynami zone. In South Aegean Volcanic Arc Present Knowledge and Future Perspectives; Elsevier: Amsterdam, The Netherlands, 2005, pp 11-17.

Reilinger, R.E., McClusky, S.C., Oral, M.B., King, R.W., Toksoz, M.N., Barka, A.A., Kinik, I., Lenk, O., Sanli, I., 1997. Global positioning system measurements of present-day crustal movements in the Arabia-Africa-Eurasia plate collision zone. J. Geophys. Res. 102, 9983–9999

Reilinger, R., McClusky, S., Vernant, P., Lawrence, S., Ergintav, S., Cakmak, R., Ozener, H., Kadirov, F., Guliev, I., Stepanyan, R., Nadariya, M., Hahubia, G., Mahmoud, S., Sakr, K., ArRajehi, A., Paradissis, D., Al-Aydrus, A., Prilepin, M., Guseva, T., Evren, E., Dmitrotsa, A., Filikov, S.V., Gomez, F., Al-Ghazzi, R., Karam, G., 2006. GPS constraints on continental deformation in the Africa–Arabia–Eurasia continental collision zone and implications for the dynamics of plate interactions. J. Geophys. Res. BO5411. doi:https://doi.org/10.1029/2005JB004051.

Reilinger, R., McClusky, S., Paradissis, D., Ergintav, S., Vernant, P., 2010. Geodetic constraints on the tectonic evolu- tion of the Aegean region and strain accumulation along the Hellenic subduction zone. Tectonophysics 488, 22–30.

Ring, U., Glodny, J., Will, T., Thomson, S., 2010. The Hellenic subduction system: high- pressure metamorphism, exhumation, normal faulting, and large-scale extension. Annual Review of Earth and Planetary Sciences 38, 45–76. http://dx.doi.org/ 10.1146/annurev.earth.050708.170910.

Rossi, S., Got, H., Taviani, M., Martin, L., 1986. Elements structuraux de la mer de Crete orientale et du Golfe d'An- talya (Mediterranee orientale). Mem. Soc. Geol. It. 36, 153–164.

Sakellariou, D.; Tsampouraki-Kraounaki, K. Plio-Quaternary Extension and Strike-Slip Tectonics in the Aegean. In Transform Plate Boundaries and Fracture Zones; Elsevier: Amsterdam, The Netherlands, 2019; pp. 339–374.

Sengör, A.M.C., Tüysüz, O., Imren, C., Sakınç, M., Eyidogan, H., Görür, N., et al. 2005. The North Anatolian Fault: A New Look. Annual Review of Earth and Planetary Sciences, 33: 37–112. doi:10.1146/annurev.earth.32.101802.120415.

Shaw, B., and J. Jackson (2010), Earthquake mechanisms and active tectonics of the Hellenic subduction zone, Geophys. J. Int., 181(2), 966–984.

Straub, C., Kahle, H.G., 1994. Global positioning estimates of crustal deformation in the Marmara Sea region, north- western Anatolia, earth planet. Sci. Lett. 121, 495–502.

Taymaz, T., Jackson, J., McKenzie, D., 1991. Active tectonics of the north and central Aegean Sea. Geophys. J. Int. 106, 433–490

Ten Veen, J.H., Kleinspehn, K.L., 2002. Geodynamics along an increasingly curved convergent plate margin: late Miocene-Pleistocene Rhodes, Greece. Tectonics 21(3). https://doi.org/10.1029/2001TC001287.